Metal Interactions with the Sulfur Cycle in Modern and Ancient Environments

Amanda Margaret Jessie Galsworthy

Submitted in accordance with the requirements for the degree of Doctor of Philosophy

The University of Leeds

School of Earth and Environment

September 2014

The candidate confirms that the work submitted is her own, except where work which has formed part of jointly authored publications has been included. The contribution of the candidate and the other authors to this work has been explicitly indicated below. The candidate confirms that appropriate credit has been given within the thesis where reference has been made to the work of others.

The work in Chapter 5 of this thesis has appeared in the following publication:

Mortimer, R.J.G., Galsworthy, A.M.J., Bottrell, S.H., Wilmot, L.E., Newton, R.J., 2011. Experimental evidence for rapid biotic and abiotic reduction of Fe(III) at low temperatures in salt marsh sediments: a possible mechanism for formation of modern sedimentary siderite concretions. Sedimentology v.58: 15114-1529.

I was responsible for the elemental sulfur core extractions.

Acknowledgments

First and foremost I would like to thank Professors, Robert Mortimer and Simon Bottrell for being fantastic supervisors. Indeed, they have tolerated my general panics and field-work temper tantrums which were usually brought about by oversized flies at Thorne Moors and hungry probe-eating crabs at Warham. Most importantly, they have managed to work around me and my work commitments even though they are extremely busy themselves. Thank you so much for everything!

I would like to thank both Natural England and English Heritage for allowing me to use their field sites; this project would not have been possible otherwise. Thanks to David Ashley and Sam Allshorn (University of Leeds) for assistance with the Ion Chromatography analyses; Bob Knight (University of Hull) for ICP-MS analysis of the trace metal solid-phase and Hao Cheng (DGT Research) for ICP-MS analysis of the trace metal pore-water samples. Thanks to Nick Rukin (collection) and Dave Hatfield (analysis) who obtained the Shales-with-Beef Member data many, many moons ago! In fact I was 9 years old when the samples were collected, I am now 35, feel old Simon?

Thank you to Getech Plc, which is the company I have worked for during the duration of my degree, who have been sympathetic for the (very) short notice of a week's 'holiday'. I would especially like to thank my direct line manager Simon Campbell for just being a good manager, and Dr Nykky Allen for assisting me when I took my little foray to the dark-side of organic geochemistry! Thanks to Dr Sheona Masterton for her bed time reading!

Thanks to my knee for dislocating in the year that I needed to submit. I can say with some confidence that without the injury I wouldn't have been sat in a darkened room writing, instead I would have had lots of fun doing all the outdoor activities that I shouldn't have been!

Last of all, thanks to my family, namely, Belinda and Victoria Galsworthy (and small ones) and Dickie Brown; just because they are a great bunch and I adore them.

Abstract

Modelling global biogeochemical cycles requires an understanding of processes at a range of scales. Small-scale redox processes are often modelled as a succession of successively less energy efficient reactions which are predominantly mediated by bacteria. This thesis is a series of discrete studies which examine early diagenetic processes in a peatbog, saltmarsh and an ancient marine sequence.

In an ombrotrophic peat bog at Thorne Moors, redox horizons, which influence the behaviour of sulfur and iron, are complex because they are impacted by abiotic and biotic processes, roots, lateral flows and potentially “hotspots” of organic matter (OM) degradation. In these systems the long-term fate of trace metals was found to be predominantly controlled by dust deposition suggesting that they are immobile; this was confirmed by the DET and DGT data.

Warham salt marsh results show that due to the rapid sedimentation rates, more reactive iron is buried which then partially oxidises sulfide to elemental sulfur in the deeper sediment and to sulfate in the near-surface.

The ancient site (Shales-with-Beef Member) has concretionary horizons that coincide with partial oxidation of sulfide to elemental sulfur and a change in iron chemistry, whilst the organic matter input and anoxic conditions remained the same. The changes in diagenetic conditions arose from slow sedimentation rates which cause the less reactive iron to remain longer in the biogeochemical zone.

This study shows that redox zones are much more complex than the series of cascading reactions which successively yield less energy and are predominantly mediated by bacteria.

Contents

Figure Listing

Table Listing

List of Abbreviations

ANC	Acid Neutralising Capacity
BSR	Bacterial Sulfate Reduction
CPI	Carbon Preference Index
CIE	Carbon Isotope Excursion
DET	Diffusive Equilibration in Thin Films
DGT	Diffusive Gradient in Thin Films
DOP	Degree of Pyritization
EPA	Environmental Protection Agency
ICP-MS	Inductively Coupled Plasma Mass Spectrometry
MSR	Microbial Sulfate Reduction
OM	Organic Matter
K	Permeability
Ø	Porosity
SRB	Sulfate Reducing Bacteria
TEAP	Terminal Electron Accepting Process
TOC	Total Organic Carbon

Chapter 1 Introduction

1.1 Introduction

This thesis is concerned with metal interactions with the sulfur cycle in aquatic sediments. The work has been carried out in both modern and ancient environments and as a consequence has been undertaken as discrete studies, each with a separate literature review. This chapter introduces the rationale behind the research and provides a basic understanding of biogeochemical cycles, and rudimentary interactions between sulfur and metals in aquatic sediments.

1.2. Overview of biogeochemical cycles

The interaction between biogeochemical cycles is the key link to understanding many earth surface processes over geological time (e.g. Berner, 1989; Falkowski et al., 1998; Zachos et al., 2008). At the highest level, geochemical systems can be broken down into reservoirs and fluxes (e.g. Schimel, 1995). Reservoirs are often grouped into: atmosphere, hydrosphere, biosphere, sediments, and rocks (Figure 1.1), although they are much more complex in reality (e.g. Hedges, 1991; Schimel, 1995; Jickells et al., 2005). As biogeochemical cycles are known to be intrinsically linked, then changes to one geochemical reservoir can affect another, which could then impact on another and so forth (e.g. Berner, 1982; Ku et al., 1999; Friedl and Wüest, 2002; Jickells et al., 2005). For instance, an increase of bioavailable Fe by a factor of 2 to the global oceans could cause a decrease in atmospheric CO_2 by 13-30 ppm (Lefevre and Watson, 1999).

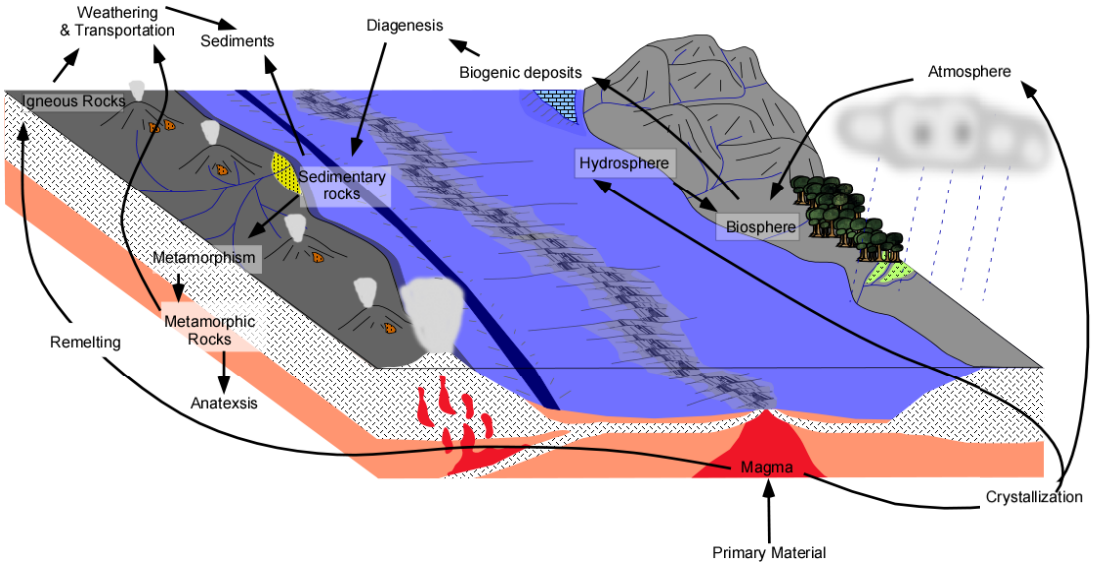

Figure 1.1 Interactions between global fluxes and large-scale reservoirs. *This schematic diagram represents the basic fluxes between large-scale reservoirs and fluxes. The interactions between reservoirs are complex and the biogeochemical cycles are intrinsically linked, thus it is important to understand how the fluxes and reservoirs interact both on a global and local scale.*

Earth system modelling can predict the consequences of changing one or more variables of the geochemical cycles (e.g. Cox and Kwaitkowski, 2013; Hopkins et al., 2014). However, to achieve this robustly the detail needs to be incorporated into the models, with refinements made as our knowledge-base increases. Clearly, we need to be able to understand the impacts of the changes to the big-scale reservoirs, but also understand the fine detail of each reservoir and fluxes, as well as the interactions between them (Muraoka et al., 2010). Moreover, as carbon is one of the biogeochemical cycles, this has clear implications of understanding and modelling the effects of CO_2 and CH_4 on greenhouse warming and future climate change (e.g. Clauseen et al., 2002; Cox and Kwaitkowski, 2013; Hopkins et al., 2014).

1.3 Redox reactions: small-scale interactions within biogeochemical cycles

Redox reactions illustrate how global geochemical cycles are intrinsically linked on a small-scale (e.g. Berner, 1982; Ku et al., 1999). Redox zones are a series of characteristic changes within sediments that are directly related to a cascade of microbial respiration reactions (although they can be abiotic) that successively yield less energy in the presence of organic matter (e.g. Froelich et al., 1979; Burdige, 2006 and references therein; Sevenson et al., 1997 and references therein). The energy yielded from highest to lowest is: oxygen reduction; nitrate reduction; manganese reduction; iron reduction; sulfate reduction and finally the formation of methane (Figure 1.2; Table 1.1: Froelich et al., 1979). Importantly, oxygen is added to the atmospheric reservoir when organic matter accumulates in marine sediments and rocks (e.g. Berner, 1982).

Process	Chemical Reaction	ΔG° (kJ mol Glucose $^{-1}$)	Eq.
Aerobic respiration	$C_6H_{12}O_6 + 6O_2 \rightarrow 6CO_2 + 6H_2O$	-2.82	1.1
Denitrification	$5C_6H_{12}O_6 + 24NO_3^- \rightarrow 12N_2 + 24HCO_3^- + 6CO_2 + 18H_2O$	-2.66	1.2
Manganese reduction	$C_6H_{12}O_6 + 18CO_2 + 6H_2O + 12\ \delta\text{-}MnO_2 \rightarrow 12Mn^{2+} + 24HCO_3^-$	-2.38	1.3
Iron reduction	$C_6H_{12}O_6 + 42CO_2 + 24Fe(OH)_3 \rightarrow 24Fe^{2+} + 48HCO_3^- + 18H_2O$	-0.79	1.4
Sulfate reduction	$C_6H_{12}O_6 + 6SO_4^{2-} \rightarrow 6H_2S + 12HCO_3^-$	-0.45	1.5
Methanogenesis	$2C_6H_{12}O_6 \rightarrow 6CH_4 + 6CO_2$	-0.30	1.6

Table 1.1 Microbially mediated reactions using OM as an energy source. *This table show which reactions yield more energy (using glucose as an example) and therefore which species are more favourable for*

bacteria. Aerobic respiration yields the most and methanogenesis yields the least energy (Burdige, 2006 and references therein).

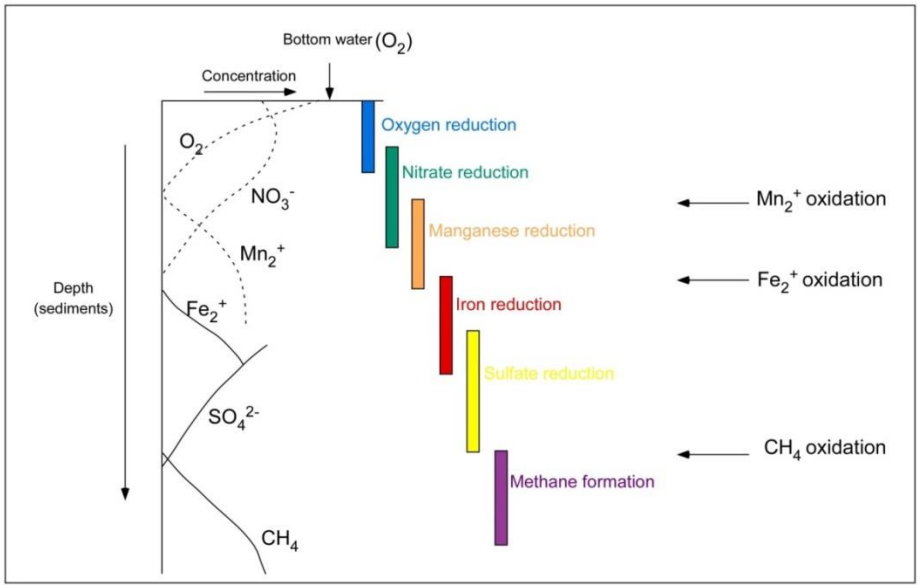

Figure 1.2 The relationship between depth and redox reactions.
This figure shows the same as Table 1.1; the successive dominate use of TEAPs by bacteria during the remineralisation of OM in marine sediments. The figure, however, relates the reactions to depth showing that aerobic respiration is the most dominate reaction by bacteria in the very near shallow and methanogenesis is the most dominate reaction in the deeper part of the sediment (modified from Burdige, 2006 and references therein). This is oversimplified however as there are more variables which have an impact on the way bacteria use species for terminal electron transfer (modified from Froelich et al, 1979; Burdige, 2006).

Figure 1.2 and Table 1.1 would suggest that these initial redox reactions happen in an ordered fashion down through the sediment profile. In reality, this model is oversimplified as it does not include a whole range of variables that impact the natural environment. For example, burrowing organisms introduce O_2 into previously anoxic sediment causing lateral variability of redox zones across the sediment. Nor does it include the complex nature of bacteria, for instance, sulfate reducing bacteria (SRB) can reduce sulfate, oxygen, nitrate and nitrite, and oxidise

different states of sulfur, e.g. zerovalent sulfur (Fuseler et al., 1996). Additionally, abiotic reactions have an influence over the redox zones in sediments, for example:

$$2FeOOH + H_2S \rightarrow 2Fe^{2+} + S^0 + 4OH^- \quad (1.7),$$

$$MnO_2 + H_2S \rightarrow Mn^{2+} + S^0 + 2OH^- \quad (1.8),$$

$$MnO_2 + 2Fe^{2+} + 2H20 \rightarrow Mn^{2+} + 2FeOOH + H^+ \quad (1.9),$$

(Thamdrup et al., 1994 and references therein).

Sediments will vary with regards to the concentration of chemical species within the pore-waters, for instance in euxinic basins where the bottom waters are H_2S rich. In this instance O_2 reduction cannot occur in the upper part of the sediment.

1.3.1 Redox reactions between sulfur and metals in natural aquatic sediments

Equation 1.5 shows how bacteria use sedimentary organic matter (OM) as a reducing agent and energy source to produce H_2S from SO_4^{2-}. Sulfate is unstable in the presence of organic matter in reduced environments, leading to microbial sulfate reduction (MSR). The products of MSR are stable, including the neutralisation of acidity, as long as the conditions remain anoxic and the reduced sulfur species produced are not re-oxidized (e.g. Giblin et al., 1990; Morgan, 1995; Chapman, 2001). Once sulfide is formed it has two (major) ultimate sinks; binding with metals or with organic matter (e.g. Peters et al., 2005). In most aquatic sedimentary systems, sulfide will react with Fe to form metastable monosulfides,

$$2H^+ + SO_4^{2-} + 2CH_2O \rightarrow H_2S + 2CO_2 + 2H_2O \quad (1.10).$$

Sulfur may go through many cycles of oxidation and reduction before final burial as pyrite (or organo-sulfur). Additionally, trace metals can often be incorporated into

the crystal lattice during formation of sulfide minerals, (e.g. Bousiquot et al., 2002; Mullet et al., 2004).

Redox reactions mediate transfer of material between reservoirs and can therefore exert control on important fluxes between reservoirs in biogeochemical cycles. Large systems for example, marine systems, clearly play a substantial role in global biogeochemical cycles. As do the cumulative effect of many small reservoirs, for example, peatbogs. Residence times, however, are also important in factoring how sensitive a system will be to either contributing to or reacting to global biogeochemical changes. The shorter the residence time the more sensitive they will be (e.g. Morris and Waddington, 2011), for example, chemical species in rocks will have significantly longer residence times than chemical species in a wetland ecosystem. Indeed, wetlands are good examples of aquatic sediment systems, with relatively short residence times that have large stocks of organic carbon, thus they are of global importance for carbon storage (Moore et al., 2013; Scharlemann et al., 2014), as well as being important ecosystems in their own right.

1.4 The importance of understanding wetland environments

Wetlands are notoriously difficult to define as there is not one definition that encompasses every type. The Environmental Protection Agency (EPA) uses a definition that was taken from the U.S. Army Corps of Engineers and defines wetlands as “areas that are inundated or saturated by surface or groundwater at a frequency and duration sufficient to support, and that under normal circumstances do support, a prevalence of vegetation typically adapted for life in saturated soil conditions” (USACE, 1987). Cowardin et al. (1979) use a similar definition which is widely accepted in the scientific community: “land where an excess of water is the

dominant factor determining the nature of soil development and the types of animals and plant communities living at the soil surface. It spans a continuum of environments where terrestrial and aquatic systems integrate".

The largest constituent of the terrestrial carbon pool are wetlands, with much focus on northern peatlands, which are estimated to sequester 20-30 g CO_2 m^{-2} yr^{-1} (Roulet, 2000) and salt marshes which are thought to sequester 210g CO_2 m^{-2} yr^{-1}, thus these environments play an important role in the global carbon cycle (Chmura et al., 2003). Not only can changes in anthropogenic activity potentially turn these carbon sinks into sources, but they can also have detrimental consequences to the local environment. For example, if sulfide minerals are oxidised, due to the instability of the wetland then this adds acidity to the surrounding pore-waters (generating Acid Sulfate Soils; e.g. Powell and Martens 2005) (equation 1.11), and releases trace metals which were incorporated in the crystal lattice of the sulfide minerals. The trace metals can be toxic (Bousiquot et al., 2002; Mullet et al., 2004) and in some cases (due to anthropogenic activities) radioactive (Livens et al., 2004).

$$FeS_2 + 3.5\ O_2 \rightarrow Fe^{2+} + 2SO_4^{2-} + 2H^+ \quad (1.11)$$

The study outlined in this thesis focuses on two major types of wetlands; peatlands and saltmarshes. Peatlands can be separated into two major types depending on how they are fed; ombrotrophic, where they receive all their nutrients from the atmosphere (e.g. Damman, 1978); and minerotrophic, where they receive nutrients from the atmosphere but are also fed from waters which have been in contact with the bedrock (e.g. Verhoeven, 1986). This study deals with ombrotrophic peatbogs. Peatbogs are a carbon sink (e.g. Turunen et al., 2002; Holden, 2005; Belyea and

Baird, 2006) and are estimated to have stored enough carbon to reduce global temperatures by 1.5° to 2° C over the last 10,000 years (Holden, 2005). Extraction of peatbogs and fires, for example, reduces the ability of peatbogs to sequester carbon and may ultimately cause them to become a source of carbon (Holden, 2005; Novak et al., 2008; Clark et al., 2010; Silvola et al., 1996). Peatbog preservation is therefore an important factor in climate change. Additionally, peatbogs and saltmarshes are important in ecology, providing niche environments for plants, animals and insects, including being an important stop-over for migrating birds (e.g. English Nature, 2002) and in salt marshes, shellfish and fish (e.g. Natural England, 2014).

1.5 Linking the past to the present

Understanding any type of depositional system is useful for understanding past environments. This is especially so for the energy industry as costs associated with extracting sour crude oil and coal with large amounts of S are high. More information and models during the early stages of the exploration process could potentially reduce production costs. This is because models could better constrain S-content within oil or coal, but only if the depositional and diagenetic processes are fully understood. Understanding modern day processes, however, cannot include large temporal variations, including Earth's positive or negative feedback systems. The rock record can identify global-scale changes within the biogeochemical cycles. The Palaeocene-Eocene boundary, for example, shows a major change in atmospheric composition, preserved in the rock records as carbon isotope excursions (CIE) (Kurtz et al., 2003; Moore and Kurtz, 2008; Cui et al., 2011). Typical carbon isotope signatures have been identified from processes that occur today, thus understanding isotope excursions are relating modern day signatures with the past. In

the case of the Late Palaeocene Thermal Maximum, it has been postulated that there was a loss of peat via burning that was a contributing factor to the CIE (e.g. Kurtz et al., 2003; Cui et al., 2011), although certainly not proven (Moore and Kurtz, 2008). Therefore, elucidating the intrinsic workings of depositional systems that store significant amounts of C will help understand present day systems, but also serve as an analogue for both past and future systems in Earth System Modelling.

1.6. Approach of this work

1.6.1 Rationale / approach

Metal and sulfur cycling in different aquatic environments is complex. Higher resolution geochemical studies and comparison of modern and ancient environments will advance our understanding of these cycles and how they interact with other chemical species (e.g. trace metals, carbon).

1.6.2 Aims and objectives

Redox reactions in sediments tend to occur over small vertical distances and are expected to control most of the fate of sulfur and metal within the sediments. In modern day aquatic sediment studies the methodology needs to have sufficiently high resolution to pick up the detail in the pore-waters.

To identify the redox zones within the upper 40 cm of a peat bog in order to understand the chemical evolution of the peat.

- To understand the (small scale) heterogeneity.
- To understand the geochemical gradients that may be important loci of biogeochemical activity.
- To link the hydrology, ecology and biogeochemistry.

- To determine if the diplotelmic model is consistent with the small-scale processes.

After the redox zones within the peat bog have been evaluated then undertake a metals study.

- To understand potential sources of trace metals.
- To evaluate metal mobility within this system.
- To understand the relative mobility of different metals.
- To determine if using Pb dating in these sediments is suitable.
- To relate the redox zones with trace metal mobility.

To understand iron and sulfur cycling within a salt marsh.

- To elucidate the redox zones.
- To understand early diagenesis.
- To link the unusual geochemistry to the depositional system.

To use the knowledge learnt from the previous sub-set of modern day studies and apply this to an ancient rock to elucidate the processes occurring during early diagenesis.

- To identify differences in geochemistry and relate to sedimentary horizons.
- To elucidate the changing redox state(s) of the environment during early diagenesis.

1.7 Site details

Three differing sites were identified to test the hypothesis. Thorne Moors in the Humberhead Levels is a raised peatbog that has been used prior to this study to determine peat atmospheric archives (e.g. Novak et al., 2008a). Warham salt marsh in Norfolk is a well-studied salt marsh that shows peculiar geochemistry (Pye et al., 1990). The Shales-with-Beef Member (Jurassic) is a test case for applying modern day observations and relating them to understand the depositional systems.

1.7.1 Warham Salt Marsh, Norfolk

Warham Salt Marsh is located on the North Norfolk Coast, England (Figure 1.3) and is separated into an upper marsh (c. 2000 to 400 years old) and a lower marsh (post-1850). These are separated by aeolian sands on a low beach ridge (Pye et al., 1990; Penthick, 1980). Underlying the salt marshes are eroded boulder clay and chalk (Funnell and Pearson, 1984). The lower salt marsh has developed quickly. Aerial photography taken in 1948 shows that the area was poorly vegetated with a limited creek system; and by 1960 there was a well-defined creek system on a well vegetated salt marsh.

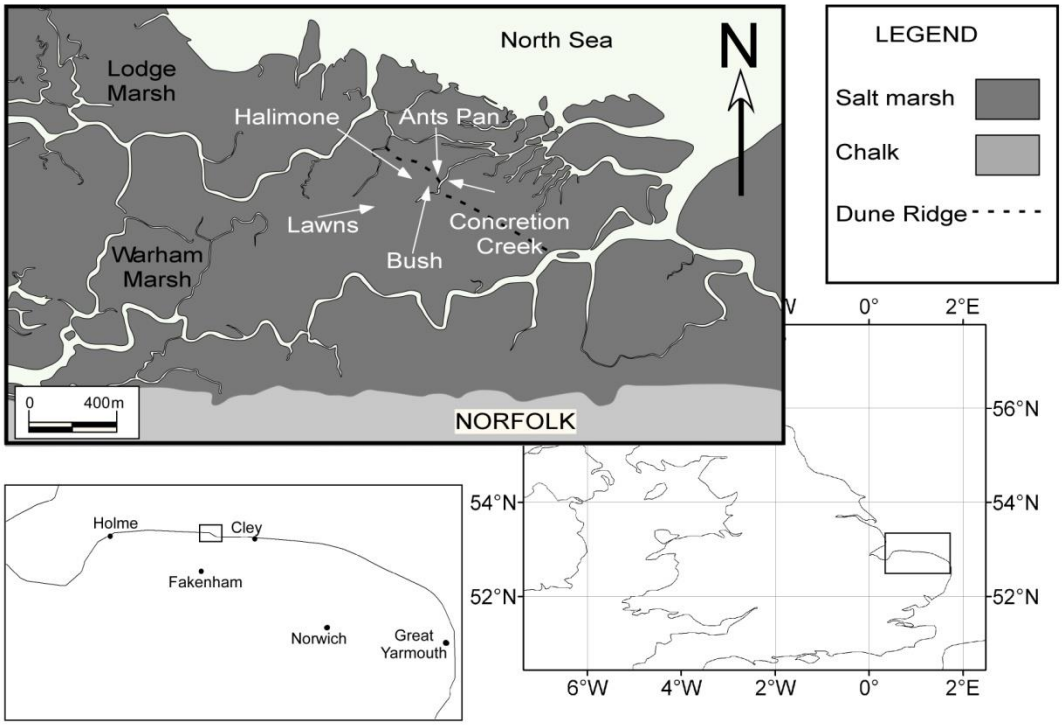

Figure 1.3 Warham Salt Marsh, North Norfolk Coast.
Warham site is an accreting salt marsh located in North Norfolk, U.K. The aim of using this site was to understand the iron and sulfur cycling within these sediments. Image modified from Google Maps (2010).

There are two main sites used at Warham, one is a permanent water pan which has developed on the lower, younger marsh (Ant's Pan), while the other site, also located on the younger lower marsh is well-developed grasses found between permanent pans (Lawns Site). Two other sites were used, one mainly comprising predominantly 'bush' vegetation and one comprising predominantly *Halimone* vegetation; these are located near the main sites (Figures 1.3 and 1.4).

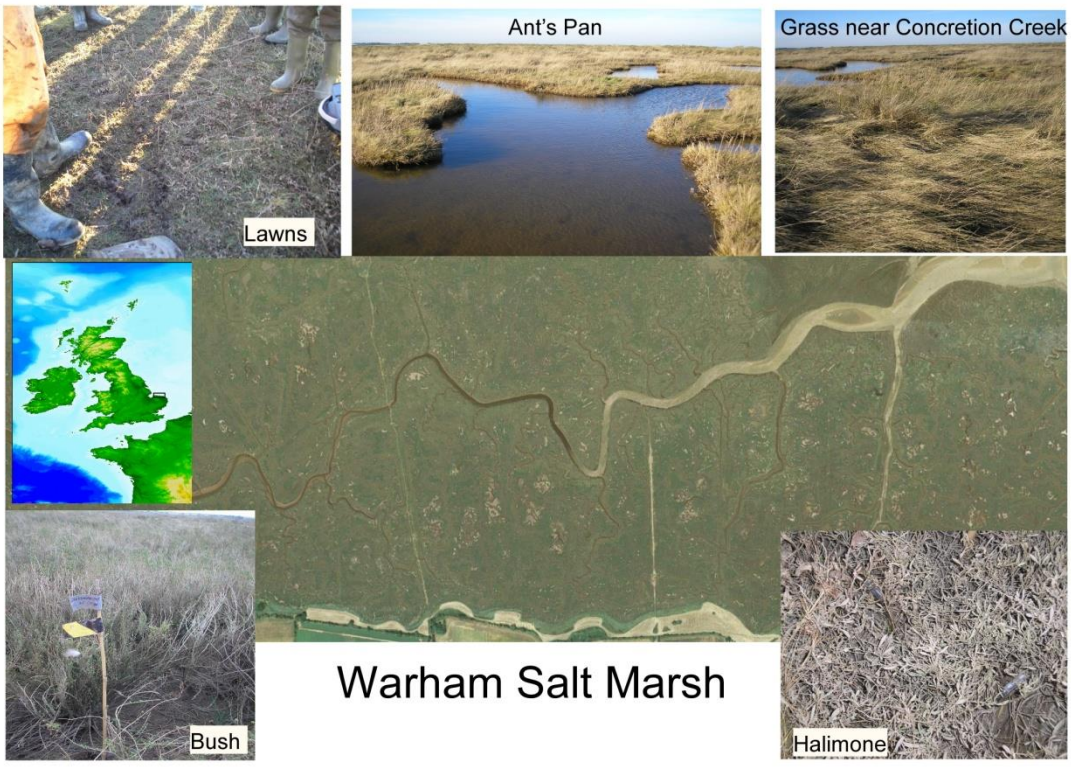

Figure 1.4 Warham sites.
These are the differing sediments types that were sampled at Warham, which are; a water pan (Ant's Pan), grass which is located close to a major creek, three sites that are dominated by Halimone, bushes, and grass vegetation respectively. Warham Salt Marsh image taken from Google Maps (2010) and photographs taken during field trips.

1.7.2 Thorne Moors, Humberhead Levels

Thorne Moors (Figure 1.5) is a raised ombrotrophic peatland located in the Humberhead Levels, Northern England, which covers 1909 hectares and its approximate central point is 53° 38' 17" N, 00° 53' 51" W. The central area was chosen because this it has been managed as a National Nature Reserve, and here the shallow (2.5 m) *Sphagnum* and *Eriophorum* dominated peat bog has developed in previously cut bays that have not been disturbed since pre-1920. Additionally, the peatland water table has been stabilized for over a decade as a result of a pro-active conservation programme (Roworth, 2000). Pollution at this site is derived from coal burning industries and power generation in industrialized northern England; acid

sulfate deposition at this site peaked in the 1970s and has declined ever since (Novak et al., 2005). Within the cut bay, six sites were chosen for sampling approximately 5 m apart. Site 1 was an area of flat *Sphagnum* 'lawn' close to the water table with small, very shallow open pools and minor *Eriophorum*; site 2 was a hummocky area (hummocks up to 150 mm high above water table) and comprised of a more equal mix of *Sphagnum* and *Eriophorum*. Site 3 was an open pool whilst sites 4, 5 and 6 were also *Sphagnum* 'lawns'.

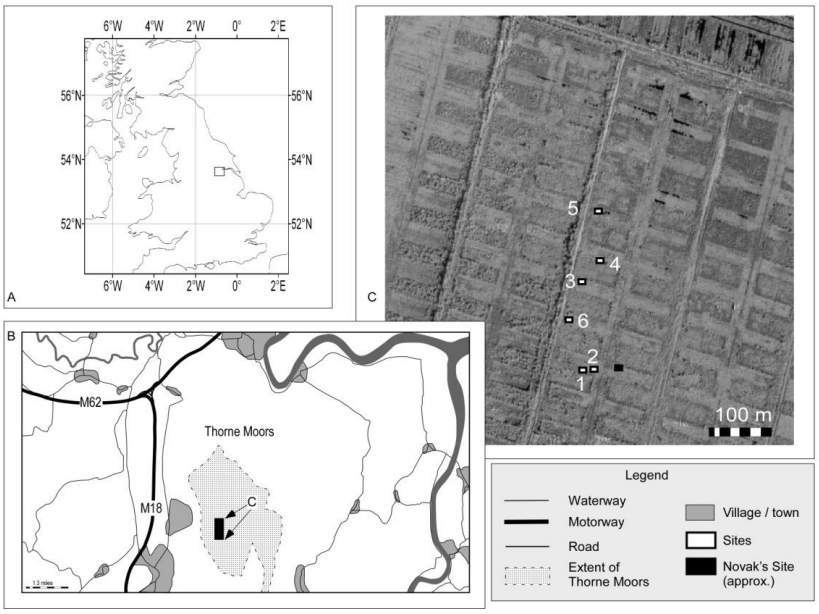

Figure 1.5 Thorne Moor site.
Thorne Moors is an ombrotrophic peat bog located in the Humberhead Levels, UK. The aim of visiting this site was to understand where the redox zones were located and the behaviour of metals in these sediment types. Maps modified from Google Map (2010). Site locations were obtained by GPS data (Garmin Forerunner 410).

1.7.3 Charmouth Beach, Dorset

Much of the cliff outcrops in this area are Jurassic in age. At that time much of Britain was under shallow marine conditions (Bradshaw et al., 1992; Evans et al.,

2003; Ziegler, 1990). Although there were eustatic sea-level fluctuations (Hallam, 2001), the (Present Day) Dorset Coast stayed sub-aqueous (Figure 1.6).

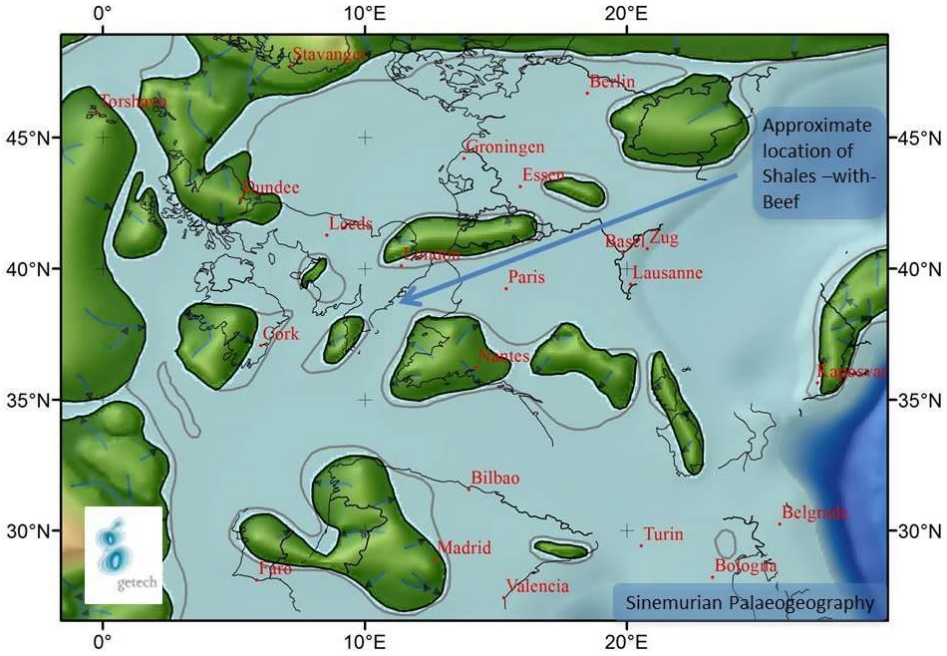

Figure 1.6 Palaeogeography of the British Isles and surrounding area. *This is the palaeotopography for (what is now) Europe during the Sinemurian (Lower Jurassic). The light blues are shallow marine and the dark blues are deeper; the darker greens are low lying land and the lighter greens are topographically higher. The aim of this study is to elucidate the changing redox states(s) of the environment during early diagenesis. Image courtesy of Getech (2013).*

During the Sinemurian, the Shales-with-Beef Member was deposited, a 28-30m thick basal member of the Charmouth Mudstone Formation. The member comprises fossiliferous marine paper shales, with limestone beds and interbedded seams of "beef", fibrous calcite separated by clay parting (Lang et al., 1923; Gallois, 2008; Paul et al., 2008; Page, 2009). This formation also contains concretions which have been studied by Wolff et al. (1991) who undertook a chemical analysis of them and noted that they comprised of a calcitic core, dolomitic zone and calcitic outer rim. The zones represent the different bacterial processes during the time of carbonate formation which show that the environment was reduced throughout. This is

consistent with the overlying Birchi Beds, which show $\delta^{13}C$ values between -10 to -14‰ in the carbonate concretions, suggesting an important contribution of carbonate derived sulfate reduction, and associated reducing environment. Additionally, the shales are finely laminated with no evidence of benthic activity (Marshall, 1982). This member has been well studied (Lang et al., 1923; Marshall, 1982; Wolff et al., 1991; Parkinson, 1996; Gallois, 2008; Paul et al., 2008; Page, 2009) and the formation of concretions highlight a change in the pore-water chemistry during burial. Thus it should be a good test case to see if there are any preserved changes between sulfur species and metals.

1.8 Bulk properties of peatbogs and saltmarshes

To ensure that the appropriate sampling method is used we need to understand the bulk properties of the types of sediments used in this study.

1.8.1 Peatbogs

Peats are formed from decomposing plants, and are often dominated by one or two species, which in part dictates the internal structure of the peat which can range from fibrous to amorphous (Shotyk, 1988). The plant types also have some control on the peat shear strength which may be elevated if there are root zones (Waldron et al., 1981). For instance *Sphagnum* does not have roots whilst *Eriophorum* has roots and a high root turnover (Gebauer et al., 1995; Tolvanen et al., 2004; Currey et al., 2011), leading to a well-developed "root mat" layer (thus *Eriophorum* contributes to higher peat strength where there are roots). At Thorne Moors *Sphagnum* and *Eriophorum* are the predominant species (Novak et al., 2008). The seasonal variation in plant growth and subsequent decay, internal structure, amount of OM and depth mainly determine the permeability (K) and porosity ($ø$) of peat bogs

(Brown et al, 2000; Aldrich and Feng, 2000; Ma and Tobin, 2004). These changes are important as they can modify lateral and vertical water flows either via creating new channels, changing the size of the channels, or a change in direction of channels. Such changes to channels will ultimately introduce oxygen into new areas of the peat thus changing the redox chemistry of the surrounding area. Clearly peatbogs cannot be seen as a homogenous system, however they are often described as a two layered system; the acrotelm, which has high hydraulic conductivity and a fluctuating water table, and catotelm, the inert permanently saturated layer. The latter is the main body of the peatbog. Importantly, this two layered approach is regularly used in peatbog modelling for both ecohydrology and carbon budgeting (e.g. Holden and Burt, 2003; Holden, 2005).

1.8.2 Saltmarshes

Salt marshes form on accreting intertidal zones in areas of low energy. The sediments comprise muddy silts with a low organic matter and low *ø* and *K*, however, if the sand content increases then so do *ø* and *K* (Boorman, 2009). As with peat bogs, there is a reduction in ø and K in the deeper sediments compared to the surface, due to compaction and more decomposed states of organic matter. Salt marshes have high rates of microbial respiration, thus oxygen diffusion is limited to the shallow parts of the sediment (Teal and Kanwisher, 1966). Therefore, bacteria will use other chemical species, which yield less energy when used in their respiration (Figure 1.2 and Table 1.1), which should be stable; this results in high amounts of H_2S in these sediments (e.g. Alongi, 1998; Howes et al., 1981). Split-cores at Warham salt marsh illustrate the change in redox by a change in sediment colour from the surface to the deeper parts of the peat (from lighter orange/brown colours at the top of the sediment, to predominantly very dark grey/black coloured

sediments over a short vertical distance). However, although lateral-water flows are uncommon at this site and burrowing is common in the shallower parts of the sediment, there are clear lighter brown coloured horizons deeper in the sediments, suggesting that the conditions become less reduced (Watts, 2006; Wilmot, 2007). The reasons for this are not well understood but it is suggested that rapid burial rates at this site, due to the high sedimentation rates, could have initiated conditions which favour the reduction of iron more than sulfate, which may have allowed SRB to reduce iron (Pye, 1981; Coleman et al., 1993).

1.9 Thesis outline

This aim of this chapter was to introduce the project and sampling sites; Chapter 2 covers the methodology and the rationale for choosing the sampling methods. Chapter 3 identifies redox zones, specifically the reduction of nitrate and sulfate, at Thorne Moors using pore-water and other complimentary data. Whilst Chapter 4 looks at iron and selected trace metals (both solid-phase and pore-waters) profiles from the same site to determine their mobility. Pore-water data (iron, sulfate, chloride and nitrate) and solid-phase data collected (elemental sulfur) from Warham Salt marsh are discussed in Chapter 5. The final data chapter covers the environmental conditions under which the Jurassic Shales-with-Beef Member was deposited (Chapter 6). The discussion and conclusions (Chapter 7) synthesises key findings from this study and identify where it fits in with current scientific understanding.

Chapter 2 Methodology

2.1 Pore-water sampling: theory and applications

There are numerous methods to measure pore-waters in aquatic sediments, and many studies require high resolution sampling because element mobilisation typically occurs over mm scales (e.g. Docekalova et al., 2002; Davison et al., 1991; Davison et al., 1994; Devries and Wang, 2003; Teasdale et al., 1995; Chapman et al., 2002; Xu et al., 2012). The methods used, however, depend on the research question proposed, with the most appropriate method (or combination of methods) depending on factors such as the chemical species determined, the nature of the sediment, and the vertical, spatial and temporal sampling resolution required.

In this study, the key driver for the method of pore-water sampling is the need to obtain vertical depth data for $\sum$Fe, Cl^-, NO_3^-, SO_4^{2-}, Zn, Cu, Co, Cd, Pb and Ni at high resolution (mm). Limited disturbance of the sediment was also vital; especially at the sediment-water interface (SWI) as this is often where the key redox reactions occur and steep gradients result (e.g. Fones et al., 2001; Docekalova et al., 2002; Devries and Wang, 2003; Davison et al., 1991; Fones et al., 1998; Xu et al., 2012). These methods need to be compatible with both a peatbog and a saltmarsh, which are both difficult to sample. Evaluating the methods for pore-water sampling has been an integral part of the study. Although there are more pore-water sampling methods than discussed below, these are usually modified versions of the main samplers or have been designed for a particular site in mind, thus they have been omitted.

2.1.1 Coring, slicing and centrifuging

Coring is one of the simplest and cheapest procedures for obtaining interstitial pore-waters and solid-phase chemistry, and as a consequence it is a long-established method (e.g. LaForce et al., 1998; Blomqvist, 1991 and references therein; Jezequel et al., 2007; van Oploo et al., 2008). Additionally, any unused samples can easily be preserved as long as the sample remains frozen. As this method is not in-situ, the integrity of the data can be compromised during sample collection from compaction, due to mechanical disturbance (Blomqvist, 1991), and the introduction of oxygen (Bufflap and Allen, 1995 and references therein; Bender, 1983), with the latter altering the pore-water redox state (Davison et al., 1982; Mortimer et al., 1998 Bufflap and Allen, 1995 and references therein). Additional problems may arise (mainly sample oxidation) from transportation of the cores from the field to the laboratory (LaForce et al., 1998). Moreover, it is not always possible to retrieve enough pore-water when centrifuging the sample (note that this process can also induce changes in chemistry), allowing for only cm scale resolution (Carignan et al., 1985; Davison et al., 1982; Jezequel et al., 2007), which could give rise to critical geochemistry being missed resulting in erroneous geochemical interpretations.

Summary: this method is cheap and simple, with the main advantage being that both the solid-phase and pore-water chemistry data come from the same core. However, potential problems include compaction, oxygenation, contamination and low spatial resolution.

2.1.2 Well-type suction methods

2.1.2.1 Suction lysimeters / sediment sippers

Sediment sippers are an array of different length PVC tubes which have porous bases that are commonly used in coarser grained sediments (Montgomery et al., 1979; Berg and McGlathery, 2001; Balistrieri et al., 2007). Equilibration takes between one day and one week, although some workers have modified the design so that pore-waters equilibrate within hours (Fourqurean et al., 1992). Retrieval of the pore-waters is by suction, usually syringes, allowing for multiple temporal samples as the device does not need to be removed. The initial equilibration time allows for mitigation of sediment disturbance. Vertical resolution is often low, in some cases between 5 and 10 cm, which may miss key gradients due to redox processes (Montgomery et al., 1979; Berg and McGlathery, 2001).

Summary: This method is useful for long-term pore-water monitoring or studies where replicates are needed in sandy sediments, however the vertical resolution is relatively low compared to other methods. As the samplers can be left in place, sediment disturbance is diminished.

2.1.2.2 Piezometers/ depth samplers

Piezometers are pipes which are placed into the ground. They essentially are small scale wells and are predominantly used to determine the hydraulic head in shallow unconsolidated aquifers using dip meters. Water can also be sampled directly following flushing. Modifying the piezometers by the addition of chambers allows measurements of temperature, pH, trace metals, anions, cations and isotopic data, but prevents use for head measurements (Wassenaar and Hendry, 1999; Hendry and Wassenaar, 2000). The time of equilibration varies depending on the substrate being

sampled, for example, if they are placed into fine-grained clays, which have low *K* values, then the chambers could take months to years to fill (Wassenaar and Hendry, 1999).

Contamination of the piezometers is a concern. In coarse-grained substrates it is possible that leaks from the higher elevated waters down into the boreholes could induce chemical and microbial community contamination (Wassenaar and Hendry, 1999). Wassenaar and Hendry (1999) noted that the piezometers had a faint smell of H_2S a year and a half after construction which most likely came from formation of a microbial community within the piezometers themselves. As standard piezometers are open wells oxygen can diffuse down into the pore-waters. Using a piezometer with a seal does prevent oxygen diffusion but can cause additional contamination issues from the sealing materials, e.g. Na^+ and SO_4^{2-} contamination from bentonitic seals (Keller et al., 1991; Remenda and van der Kamp, 1997). However, if an air pocket is maintained between the sealing material and the top of the well screen then this can delay sealing material contamination for longer time periods (Remenda and van der Kamp, 1997); up to three years (Wassenaar and Hendry, 1999). Similar to sediment sippers, the main advantage of using piezometers is for long-term sampling.

Summary: Piezometers have the potential to collect an array of data. If results are needed over years or months, the use of piezometers ensures that data are collected from the same locality. Depending on the substrate, fluxes can take a long time to sample, and there is also potential for contamination. This method is more appropriate for aquifers and long-term sampling and is not very suitable for short-term salt marsh or peat bog studies.

2.1.3 Microelectrodes

Microelectrodes (Figure 2.1) were introduced in biology to understand ion transport over biological membranes (Revsbech and Jorgensen, 1986). Revsbech and Jorgensen (1986) first introduced the use of oxygen microelectrodes in sediments, after which they developed the method to measure pH and sulfide. The method has been continually developed to measure other species including nitrate, nitrite, carbon dioxide and ammonium (Fones et al., 1998; Luther III et al., 1998). Voltametric type microelectrodes can measure more than one species at a time including metals (Luther III et al., 1998; Luther III et al., 2008; Brendel and Luther III, 1995). This method is excellent for measuring pore-profiles at a very high resolution (sub-millimetre) within the upper centimetres of sediments (Berg and McGlathery, 2001). Additionally, results are obtained immediately in the field. The probes, however, are often delicate and can break if the sediment if compact or hard, or if the probe encounters a shell or gravel.

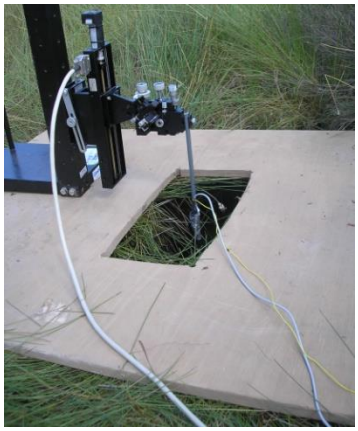

Figure 2.1 Unisense redox microelectrode in the field measuring O_2.
The main advantage of this method is that results are obtained within the field.

Summary: The major disadvantages are that the electrodes can break in hard and very compacted sediments, and that not all analytes can be measured from this

method yet. This method can be used for long-term sampling but the device is not left in-situ thus another method may be more useful if the samplers are needed to be left in place. A major advantage of this method is that results are collected in the field without further analysis.

2.1.4 Diffusion and equilibration methods

2.1.4.1 Diffusion dialysis samplers (peepers)

Peepers contain vertical fixed cells for pore-water sampling which are deployed straight in to the substrate. This type of sampling was developed by Hesslein (1976) and is a well-established method for sediment/soil sampling (e.g. Teasdale et al., 1995; Jezequel et al., 2007; Jacobs, 2002; Bufflap and Allen, 1995; van Oploo et al., 2008). Peepers work by having discrete cells (typically 6mm vertical thickness) which are filled with Milli-Q-water and are separated from each other by a polycarbonate layer (typically 4 mm vertical thickness) (Hesslein, 1976; Teasdale et al., 1995). A membrane filter (HT-450 0.45 μm) separates the direct contact between the cells and the sediment and allows ions to diffuse through (Hesslein, 1976). The clear advantage of this method is that it is in-situ sampling. Equilibration varies between analytes but is typically days to weeks (e.g. Brandl and Hasselmann, 1991; Teasdale et al., 1995; Bufflap and Allen, 1995; Jezequel et al., 2007; van Oploo et al., 2008). Sub-sampling from a peeper needs to be quick (approximately in 20 minutes) as the rate of oxygen diffusion into the chambers is high, which will alter the redox state of the pore-waters (Carignan, 1984). Using N_2 or Ar will allow for slower sampling (Teasdale et al., 1995).

Summary: Peepers can be carried out in-situ which greatly reduces the risk of oxidation. Equilibration time is typically days to weeks. The chambers/cells are at a

fixed size and are separated by a polycarbonate layer, which could miss out on important geochemistry; however, each cell can measure more than one analyte. Sub-sampling has to be quick or under N_2/Ar so that there is no oxidation of species after removal from the sediment.

2.1.4.2 DET and the DGT methods

Diffusive equilibration in thin film (DET) gels measure dissolved species in waters, sediment pore-waters and soil pore-waters, whilst diffusive gradient in thin film (DGT) gels measure fluxes of solutes to the pore-water (e.g. Davison et al., 1994; Davison and Zhang, 1994; Krom et al., 1994; Denney et al., 1999; Zhang and Davison, 1995; Zhang and Davison, 1999). Thin polyacrylamide gels have been used in biology for DNA sequencing since the late 1970s, although the practice has been used since 1959 (Sanger and Coulson, 1978). DET gel probes were first used in geochemistry by Davison et al. (1991) with the technique being modified and refined by others (e.g. Krom et al., 1994; Mortimer et al., 1998; Morford et al., 2003; Robertson et al., 2008; Jezequel et al., 2007; Fones et al., 2001). Polyacrylamide gels work by diffusive equilibration of dissolved species from pore-waters into the gel through a cellulose nitrate filter membrane (e.g. Davison et al., 1994; Davison and Zhang, 1994; Harper et al., 1997; Mortimer et al., 1998). The gels are then sliced into measured sections which can be cm to mm scale, and then a known volume of liquid is added (this is usually Milli-Q-water or acid) which extracts the analytes (e.g. Davison et al., 1994; Harper et al., 1997). The use of DET gels for many procedures often only requires a small amount of volume for analysis (e.g. Harris and Mortimer, 2002)

The DGT method is very similar except there is a 'backing' or 'trapping' gel which the species of interest either stick to, or undergo an irreversible chemical reaction with. For the most part the gels are also sliced and processed using the same procedure as the DET gels, but in some cases analysis may not involve slicing the gels, e.g. sulfide gels which are scanned and sulfide is measured by densitometry (Teasdale et al., 1999; Devries and Wang, 2003) and iron (II) as well (Robertson et al., 2008; Jezequel et al., 2007). Theoretically the DET method can be used to measure any major ions within pore-waters (Fones et al., 1998). The limiting factor on what DGT can measure is the availability of a suitable binding agent. Both the DET and DGT methods however, are predominantly limited to aquatic sediments as they are 96-98% water (e.g. Krom et al., 1994; Jezequel et al., 2007; Fones et al., 2001) and need to be kept hydrated when sampling.

The DET/ DGT gels sit within a Perspex/plastic probe with a protective cellulose nitrate filter membrane on top, which are sparged in nitrogen prior to deployment if sampling in reduced environments. These methods are carried out in-situ, with sediment disturbance usually minimal and mitigated by leaving the probe in for twenty-four hours. The gels only take around 10 minutes to equilibrate (e.g. Shuttleworth et al., 1999; Morford et al., 2003). After the gels are sliced and collected in the field they need to be back-equilibrated in liquid as it is the gel eluent(s) which are analysed. If measuring pore-waters with low ionic strength that are close to the lower limits of detection, then the process of eluting the gel could push the samples below detection.

Summary: The DET /DGT methods can measure an array of major ions (with more than one analyte being measured from one probe) and have quick equilibration times in saturated sediments. There is limited disturbance of the sediments during

sampling, and as the methods are in-situ with gels that are already conditioned to reduced environments, then oxidation reactions are unlikely after site sampling. The gels are sliced after deployment which can be defined per probe, thus resolution can often be high enough to distinguish the products of redox reactions. Depending on the type of analysis, often only a small volume is needed; however, if the pore-waters have a low ionic strength, this could push the samples below detection, due to the dilution steps used.

2.2 Methods used for this study

This study uses three field sites, two of which are modern day depositional environments: a saltmarsh and a raised peat bog. These have been discussed in detail in Chapter 1 (sections 1.7.1 and 1.7.2 respectively). The third site is a coastal Jurassic cliff. Rock sampling that was undertaken here was carried out by Nick Rukin, David Hatfield and Simon Bottrell in 1989 and 1990. As the sampling and analysis was not carried out by the author, evaluation of the methods is not included in this chapter. However, an overview of the pore-water sampling was an integral part of this study as it was necessary to evaluate an appropriate combination of pore-water sampling methods. A priority order was made to determine which methods would be the most useful for the field sites and research questions posed. Requirements were: 1) being able to have a vertical resolution of 1 cm or less; 2) be able to measure a suite of anions, cations (i.e. $\sum$Fe) and trace metals; 3) have minimum sediment disturbance to limit introduction of oxygen.

Sediment sippers have a low resolution and are more suitable for long-term monitoring, as are piezometers which are designed to be used in aquifers and are prone to contamination. Peepers have fixed cells and take a long-time to equilibrate.

Thus these three methods have not been used. Coring, which usually only obtains a low vertical resolution, is useful as both pore-waters and solid-phase chemistry are obtained from the same sample. DET and DGT gel probes acquire concentrations and fluxes respectively, equilibrate quickly and have a high vertical resolution, whilst having limited disturbance of the sediment. Detailed vertical measurements of oxygen are important as the amount of O_2 in the pore-waters will, in part, drive key redox zones and microelectrodes are the best tool for this. Combining the results from these three methods will help identify where steep gradients occur, thus identifying processes occurring in the substrate.

2.3 Data collection

Data have been collected at various field sites at various times. This section details the timings and the procedures undertaken.

2.3.1 Data collection from Thorne Moors

There were three visits to Thorne Moors, in spring of 2010, 2011 and 2012 (see Chapter 1 section 1.7.1 for a site overview) Six sites were chosen for sampling in three separate bays spread over a total distance of 200 m. Site 1 was an area of flat *Sphagnum* "lawn" close to the water table with small, shallow open pools and minor *Eriophorum*; site 2 was a hummocky area (hummocks up to 150 mm high above the water table) comprised of a more equal mix of *Sphagnum* and *Eriophorum*. Site 3 was an open pool and sites 4, 5 and 6 were also *Sphagnum* "lawns". Cores were collected and DET gels were deployed in sites 1 and 2 in 2010. Sites 1 and 2 are located approximately 5 metres apart and approximately 8 m away from the site sampled by Novak et al., (2008). The cores were taken very close to where the gel probes were deployed, but far enough away that any sediment disturbance due to the

gel deployment was avoided. DET gels were deployed at sites 2-6 in 2011. Oxygen profiles were measured *in situ* at site 1 in 2010 only using Unisense microsensors. Oxygen profile A was taken in a small open pool and profile B was taken from within a *Sphagnum*-filled area. Shear Vane tests were undertaken in 2012.

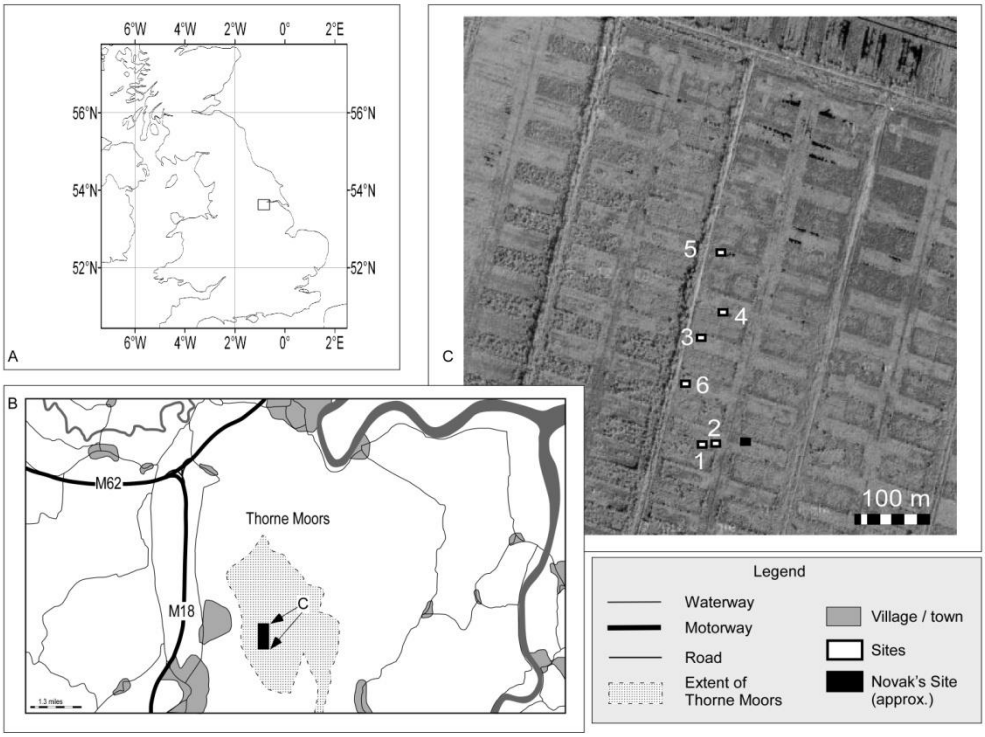

Figure 2.2 Thorne Moors study site.
Six sites were used, but data for site 6 was contaminated and thus ignored; however, the site is marked on the image for completion. Images modified from Google Map (2010). Site locations were obtained by GPS data (Garmin Forerunner 410).

Additional data were used; (sulfate and chloride analysed) rainwater was collected by Rebecca Bartlett between January to March and March to June 2009 immediately prior to the DET gel probe sampling from two stations on Thorne Moors following the methods described in Bottrell and Novak (1997).

Thorne Moors (Trace metals study and redox reactions)									
Site	Cores	Metals (DET)	Metals (DGT)	Iron (DET)	Iron (DGT)	Anions (DET)	Sulfide (DGT)	O2 (Probes)	Vane Shear Tests
1	1	1	1	1	1	1;2	1	1	3
2	1	1	1	1	1	1;2	1	1	3
3	-	-	-	-	-	2	-	-	3
4	-	-	-	-	-	2	-	-	3
5	-	-	-	-	-	2	-	-	3
6	-	-	-	-	-	2	-	-	3

Table 2.1 Collection of data for Thorne Moor.
Data collection information for Chapters 3 and 4. The key for the dates of data collection are: 1 is May 2009; 2 is April 2011; 3 is September 2012.

2.3.2 Data collection from Warham

Field trips to Warham were conducted in February and March 2008, February 2009, October 2011 and February 2012. Ants Pan (AP) is a large salt pan which is influenced heavily by the tides and is close to Concretion Creek, with a grassy area in between. The samples were taken from the grassy area (CC). Close to this there were two grassy areas; one was dominated by Halimone vegetation (HV), whilst the other was dominated by bush vegetation (BV); both of these areas were sampled, as well as a flat grassy area in between two pans (LWS). Figures 2.3 to 2.5 show the type of vegetation and sampling areas and Figure 2.3 shows where all the sites are in relation to one another.

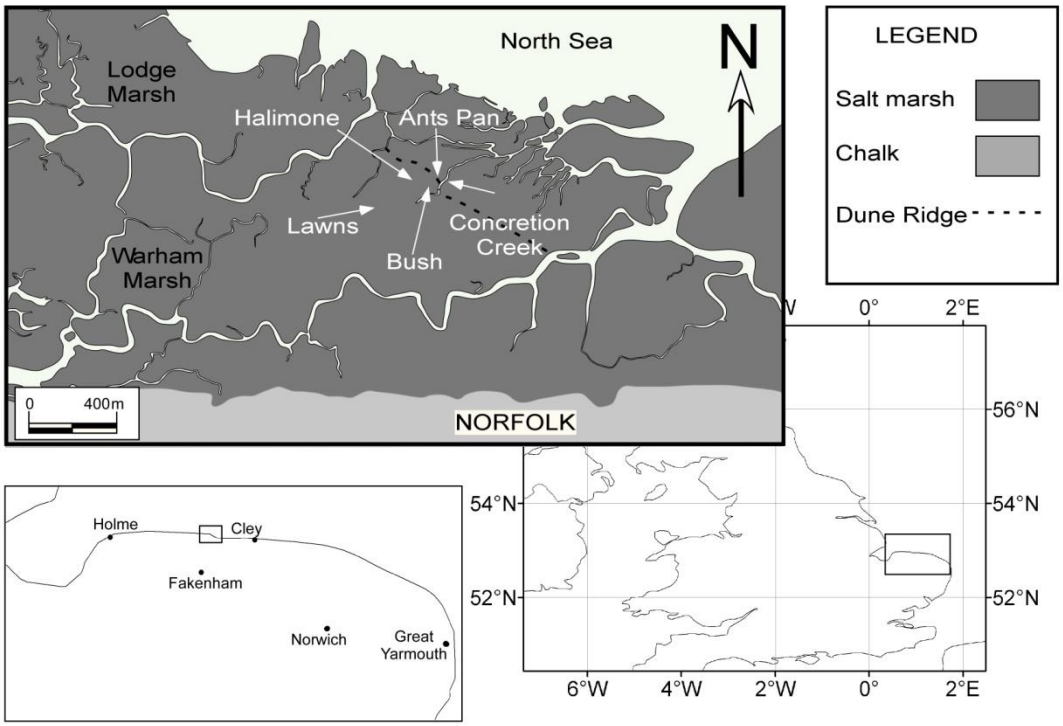

Figure 2.3 Warham study site.
Cores were collected from this site both for solid-phase (elemental sulfur profiles) and pore-water profiles (nitrate, sulfate and chloride). DET and DGT gel probes were also deployed here, however, only Fe DET probes were recovered. Image modified from Google Maps (2010).

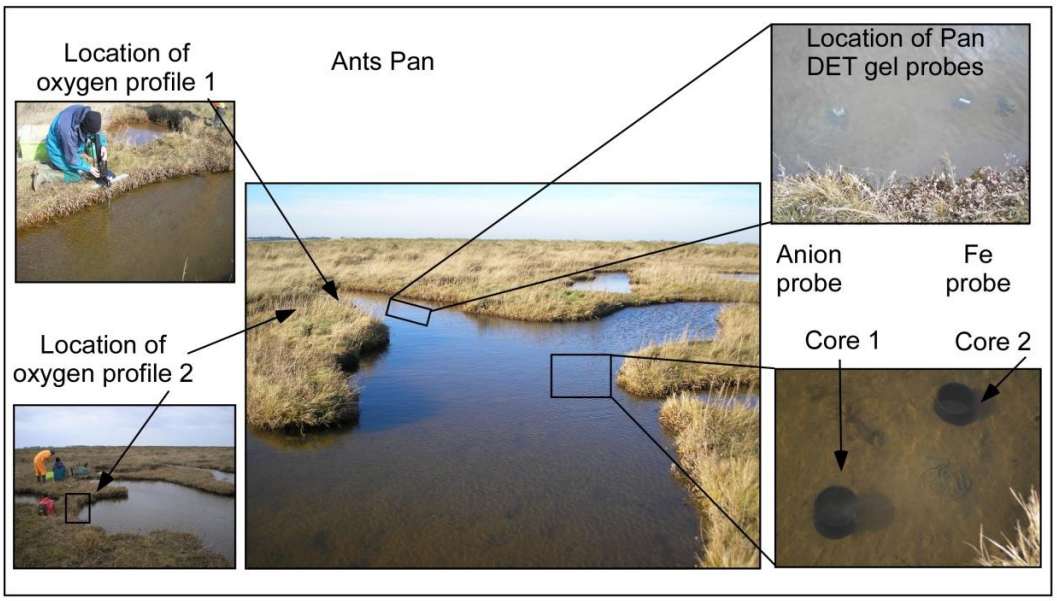

Figure 2.4 Ants Pan site.

This image shows the site sampling areas in relation to one another at Ants Pan. The samples were taken from the same place throughout all field trips at this site. Figure 2.3 shows this site in relation to the other sites at Warham.

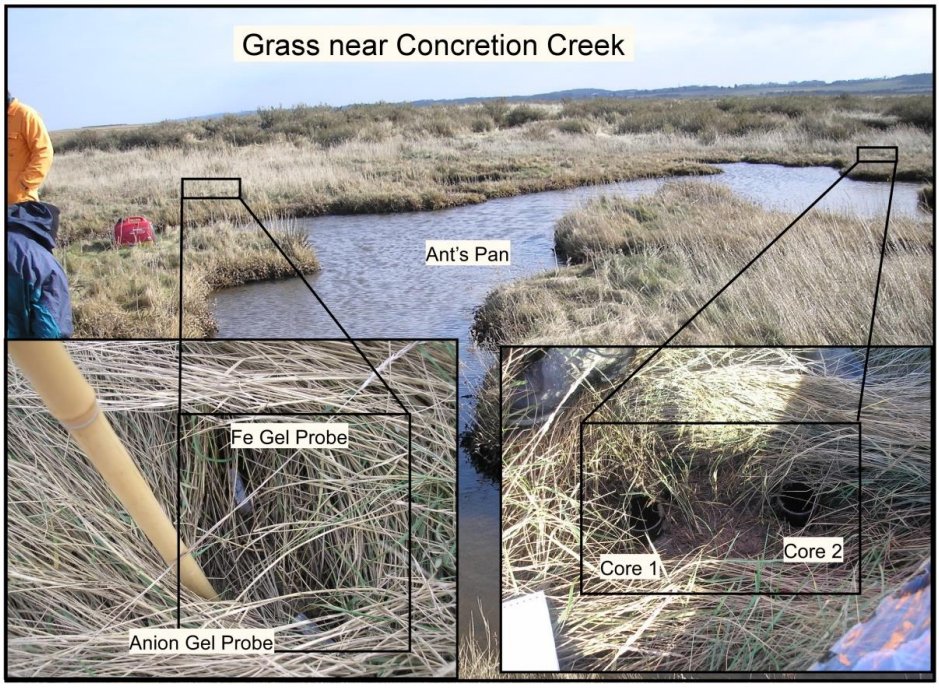

Figure 2.5 Concretion Creek.
This image shows the site sampling areas in relation to one another at the site near Concretion Creek. Figure 2.3 shows this site in relation to the other sites at Warham. This site was only used during the field trip undertaken in March 2008.

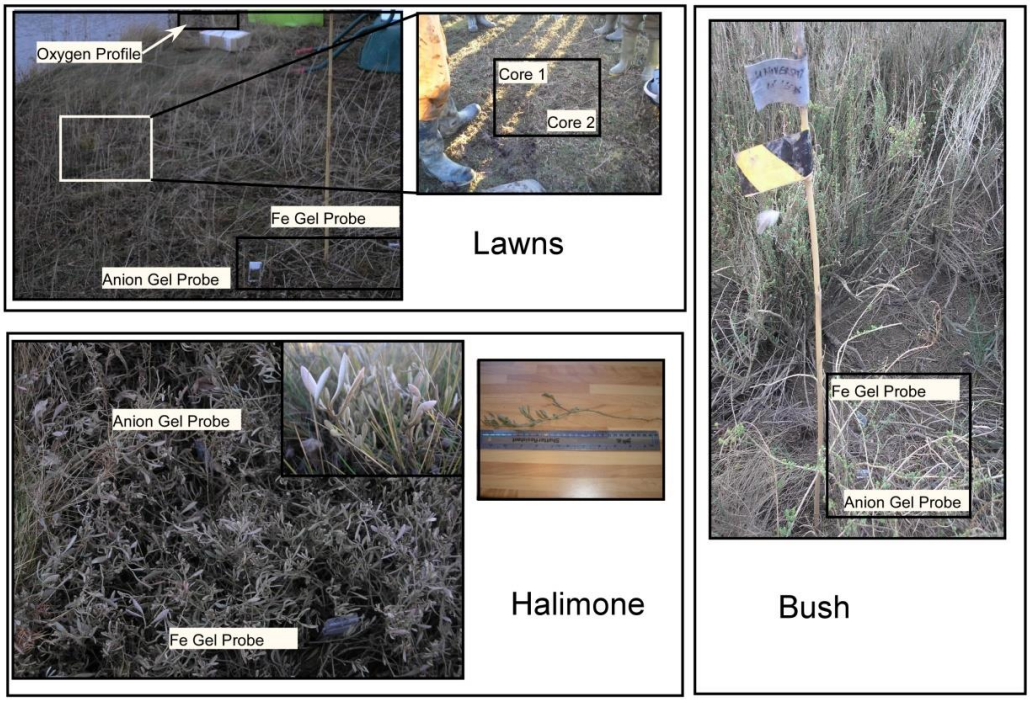

Figure 2.6 **Lawns site, Halimone and Bush.**
This image shows the site sampling areas in relation to one another at Lawns, Halimone and Bush. Lawns samples were taken in the same place for all field trips; Halimone and Bush were only used for the field trip which was undertaken in March 2008. Figure 2.3 shows this site in relation to the other sites at Warham.

Table 2.2 summarises the data that were collected during the various field trips.

Warham							
Site	Cores	Anions (DET)	Cations (DET)	Sulfide (DGT)	Iron (DET)	Iron (DGT)	O2 (Probes)
AP	1,2	2, 3, 4, 5	2	2, 3, 4, 5	2, 3, 4, 5	2, 3, 4, 5	2, 3
LWS	1,2	2, 3, 4, 5	2	2, 3, 4, 5	2, 3, 4, 5	2, 3, 4, 5	2, 3
CC	2	2	-	-	-	-	-
HV	-	2	-	-	-	-	-
BV	-	2	-	-	-	-	-

Table 2.2 **Collection of data for Warham.**

Data collection information for Chapter 5. The dates of the data collection are; 1 in February 2008: 2 in March 2008; 3 in February 2009; 4 in October 2001; and 5 in February 2012.

2.3.3 Data collection from Dorset

Nick Rukin collected the samples labelled Bv (number) in 1989, whilst the samples labelled Bv (letter) were collected by Simon Bottrell in 1991. David Hatfield carried out the analysis. Samples collected were from the Lower Lias "Shales-with-Beef" Member, from Black Ven, Dorset Coast, near Charmouth, U.K. Samples taken were from: I) the paper shales (BV8, bed 74b of Lang et al., 1923), located directly above the Birchi nodular horizon; II) from the Birchi nodular horizon (BV9, bed 75a of Lang et al., 1923); III) the paper shales located directly below the Birchi nodular horizon (BV10, 11 and 12, the upper part of bed 74 of Lang et al. (1923)). These horizons are illustrated in Figure 6.2.

2.4 Sampling

2.4.1 Cores

Cores used were modified drain pipes (8*50cm) that had been sharpened at the bottom to aid penetration of the core into the ground. At Warham only, a knife was used to cut the roots on the outside of the core, again aiding penetration of the core tube. However, this procedure wasn't necessary at Thorne moors as the cores went into the sediment easily. Additionally, trace metal concentrations were being measured at Thorne Moors and a knife would pose a contamination risk. The cores were removed as soon as compaction was measured, capped, placed into heavy duty plastic bags, labelled and taped up, and immediately placed into dry ice. The cores were always kept upright. On return to the laboratory the cores were transferred into

freezers. Prior to slicing the cores, they were used as a visual guide to assist with establishing the locations of zones, e.g. root zones and obvious changes in sediment density and hydraulic conductivity. Cores were then sliced in a nitrogen glove bag. The cores were sliced and divided into two portions at a resolution of 4 cm for both sites. One half of the sample was placed into a sample bag and returned to the freezer ready for solid-phase analysis. The other half of the sample (Warham only) underwent a pore-water extraction where the samples were placed into centrifuged tubes.

2.4.1.1 Pore-water chemistry obtained from cores

Warham samples were centrifuged at 10,000 rpm for 5 minutes and returned to the nitrogen glove bag, filtered and syringed into new tubes. The separated pore-waters were then kept in a fridge until analysis.

2.4.1.2 Solid-phase chemistry obtained from cores (elemental sulfur)

Elemental sulfur was extracted from half of the core for Warham only. Whilst still frozen, the solid sediment was placed in a reducing environment (nitrogen-flushed bottles), which contained 100 ml of acetone. These were mixed well so that the acetone could dissolve the sulfur. The acetone was then separated from the sediment using glass microfiber filtration, leaving the sulfur and residual salts. Flushing the washings with dichloromethyl (DCM) and filtering it with glass microfiber isolated the elemental sulfur. Results have been reported in Mortimer et al. (2011).

2.4.1.3 Solid-phase chemistry obtained from cores (trace metals)

Metals analysis of peats followed the protocol developed by Rowe et al. (1997). The peat cores were sliced at a resolution of 4 cm, dried, weighed and ground into a fine powder using a blender. Aliquots were weighed into crucibles (average weight of dry

sample was 2.76 g) and ashed in a furnace to 410°C. Crucibles were reweighed to determine ash content; then the ash was transferred to pre-cleaned beakers, 40 mL 7M ultrapure HNO_3 added and then heated (covered) to ~70°C. After 1 hour 5 mL ultrapure HCl was added and the reaction continued overnight. Samples were then quantitatively transferred to filtration on a pre-weighed 0.45 µm cellulose nitrate filter. Before each sample was filtered, the filter and apparatus were flushed with 2M ultrapure HCl. Filtrate was made up to 100 mL and transferred to pre-cleaned sample vials for analysis by ICP-MS (Perkin Elmer Optima 5300DV emission ICP) at the University of Hull. The filters were dried and reweighed to determine insoluble residue mass.

2.4.2 Gels: making the gels and constructing the probes

The DET gels and the backing gels are often stored in 0.01M $NaNO_3$ or 0.01M NaCl solution prior to construction. However, as this study measures both nitrate and chloride the gels are predominantly stored in Milli-Q-water (Krom et al., 1994).

2.4.2.1 DET gels

To prepare the polyacrylamide gels (following the method of Krom et al., 1994), 9.5 ml of Milli-Q water, 7.5 ml of Acrylamide (15%), 3 ml of Cross-linker (AcrylAide), 20 µl of TEMED (Tetramethylethylenediamine) and 200 µl of initiator (0.3 g di-potassium peroxdisulfate + Milli-Q water in a 10 ml volumetric flask) are mixed together in a beaker. These are then carefully pipetted into the mould, which are two clean dry glass plates (15.5*6 cm) that are separated by three plastic inserts in a U-shape (0.8 mm). The moulds are then placed in a pre-heated oven at 35°C for one hour for the mix to polymerise, after which, the polyacrylamide gels are left to hydrate in Milli-Q-water for at least twenty-four hours.

Once the gels are hydrated, they can be placed into the Perspex frame (Figure 2.7). A strip of wet (for ease of handling) 0.45 µM cellulose nitrate filter membrane is placed over the gel. The top frame can then be screwed into place (e.g. Krom et al., 1994; Mortimer et al., 1998). Once the gel probes were assembled, they were placed in 50 cm long Perspex canister filled with 18 MΩ deionised water and de-oxygenated by sparging with N_2 for 24 hours prior to deployment.

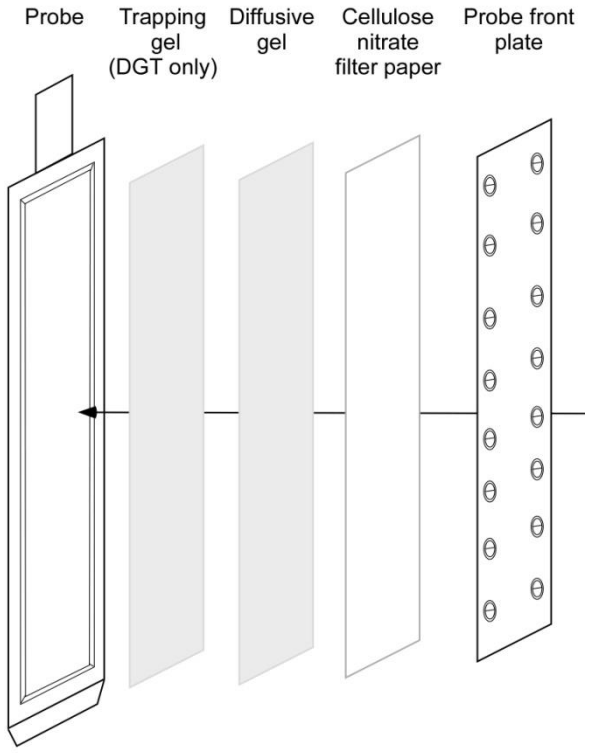

Figure 2.7 Construction of the gel probe.
The trapping gel (DGT only) sits in front of the frame, with the polyacrylamide gel next to it and finally the cellulose nitrate filter membrane over the top of these. Once the gel probes are constructed they are placed in water and sparged with nitrogen in preparation for deployment in anoxic sediments.

2.4.2.2 DGT gels

Davison and Zhang (1994) developed this method for measuring trace metals within waters and sediments. The backing gels are thinner (0.24mm thick) than the DET

gels and have chelex (100-µm bead size) resin impregnated in them (Zhang et al., 2002; Zhang et al., 1995). For this work the gels were ordered in from DGT Research, Lancaster, as they have facilities to reduce metal contamination (e.g. Pb within the atmosphere) when the gels were being made. However, the probes were assembled in a clean room to reduce Pb contamination from the atmosphere at the University of Leeds.

Sulfide gels were made for this study, however due to deployment problems, results were unobtainable, but the methodology has been included for completeness. AgI is impregnated onto a backing gel so that an irreversible reaction occurs when deployed in sediment where there is available hydrogen sulfide (Teasdale et al., 1999):

$$2AgI + HS^- \rightarrow Ag_2S + H^+ + 2I^- \quad (2.1),$$

In a dark room, 0.6 g of AgI and plastic beads are added to a small container and shaken vigorously to grind the AgI into a fine powder. After which 9.5 ml of Milli-Q water, 7.5 ml of Acrylamide (15%), 1.5 ml of Cross-linker (AcrylAide) 6 µl of TEMED (Tetramethylethylenediamine) and 60 µl of initiator (0.3 g di-potassium peroxdisulfate + Milli-Q water in a 10 ml volumetric flask) are added and mixed vigorously. As with the normal polyacrylamide gels, the mix is placed into a mould, however the U-shaped inserts are thinner and once the mix is in the moulds they need to be placed into black plastic so that no light penetrates though onto the gel. These are then placed into a pre-heated oven at 35˚C until the gel polymerises. The AgI impregnated backing gels are also left to hydrate in Milli-Q-water, however they must be stored in containers which are suitable for light-sensitive materials (Teasdale et al., 1999).

The DGT gel probes are assembled in a similar way to the DET gel probes. The backing gels are placed onto the Perspex frame first. Both the chelex and AgI impregnated gels undergo gravitational settling and concentrate on one side of the gel; this side needs to be facing upwards with the polyacrylamide gel on top. A wet 0.45 µM cellulose nitrate filter membrane sits on top of the polyacrylamide gel and then the top frame can be screwed in (Zhang et al., 1995). These are also placed in 50 cm long Perspex canisters (filled with 18 MΩ deionised water) and de-oxygenated by sparging with N_2 for 24 hours prior to deployment.

2.4.2.3 DGT and DET gel deployment and retrieval

Once the probes have been sparged for twenty-four hours, the gels can be placed into the sediments. All gel probes were inserted directly into the sediment by hand. At densely vegetated sites a dummy probe was inserted first to protect the gel from rupturing. In the earlier stages of this work, longer gel probes were used (50 cm), however, these often bent which allowed sediment to contaminate the gel. This problem was resolved by using two smaller probes (18 cm in length) placed on an aluminium rod (Figure 2.8).

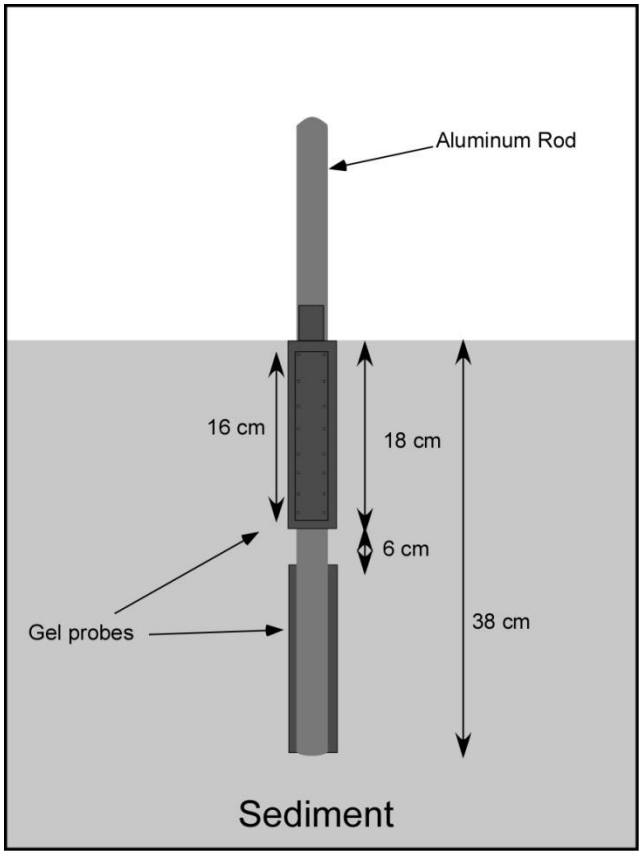

Figure 2.8 Method for gel deployment.
The long gel probes which can measure 40 cm of sediment tend to bend during deployment rendering the gel useless, thus a new method was used comprising two gel probes placed on an aluminium rod. Aluminium was used so that there wasn't any chemical contamination during sampling.

All probes at all sites were left in the sediment for twenty-four hours. The probes that were being analysed for anions, trace metals and (DET) total iron were sliced immediately in the field into 1 cm sections before being further subdivided in half, all within five minutes and placed into small (pre-weighed) centrifuge tubes. The rapid processing of the gel reduces any diffusional relaxation of gradients within the profile. The DGT total iron gels were placed in sodium hydroxide which chemically fixes the gels. These were also cut into 5 mm sections on the same day.

2.4.3 Vane shear

Vane shear testing is an in-situ procedure which tests the strength of soils by dropping a vane into the soil to measured depths, and obtaining a quantitative value for the amount of force that is needed to pivot the blades at the bottom of the vane (Geotechdata, 2010). This test has been used to determine changes in peat properties, which in conjunction with the visual overview of the peat cores, indicates where lateral water flows are likely to occur, which would drive redox zones in peats. The only complication in this test is when the blades became clogged with roots: however, it was clear when this happened as with every rotation of the blades, the pressure needed increased exponentially. At least two tests were performed at each site, with measurements made every 5 cm for the upper 30 cm and then every 10 cm down to a depth of one meter.

2.4.4 Microelectrodes

Oxygen profiles were measured using Unisense Microsensors that were calibrated in aerated DDW (100% oxygen saturation) and an anoxic solution (DDW sparged with N_2: 0% oxygen saturation) in the laboratory, immediately prior to field work. In the field, the microelectrodes were placed on a micromanipulator mounted on a stand and measured (using SensorTrace Pro) O_2 in the sediments at 0.5 mm (Thorne Moors) and 0.25 mm (Warham) vertical depth intervals.

2.4.5 Methods undertaken for Shales-with-Beef Member

The following work was carried out in 1990 and 1992 by David Hatfield; outlined below are the methods which were written up at the time.

Samples were crushed and dried; no acid-volatile sulfur was detected in the samples studied. Pyrite sulfur was extracted using the chromous chloride digestion of Canfield et al. (1986) and the H_2S evolved was precipitated as CuS from a standardised Cu solution and then back titrated with EDTA to determine pyrite sulfur. CuS precipitates were retained for isotopic analysis of pyrite-S. Reactive Fe was determined by both extractions with boiling HCl (Berner, 1970; Raiswell et al., 1988) and with dithionite (Canfield, 1989). Bitumen and zerovalent sulfur were extracted from the rock using dichloromethane in a soxhlet apparatus, and zerovalent sulfur was precipitated as CuS on Cu-wool and bitumen recovered by evaporation of the solvent. Extracted residues were treated with HF to removed mineral matter and hence beneficiate kerogen. Elemental analysis of total organic carbon (TOC), bitumen and kerogen were carried out on a Carlo-Erba 1106 Elemental Analyzer. Bitumen and kerogen sulfur were oxidised to sulfate by combustion at 30 bar O_2 in a Parr Bomb and recovered as $BaSO_4$, which was converted to SO_2 for isotopic analysis using the method of Halas et al. (1982). CuS precipitates were combusted with cuprous oxide to produce SO_2 for isotopic analysis (Robinson and Kusakabe, 1975) and bitumens combusted with CuO to produce CO_2 for carbon isotope analysis. All isotopic analyses were performed on a VG SIRA 10 gas source mass spectrometer and the data were corrected using standard procedures (e.g. Craig, 1957; Coleman, 1980). Molecular analysis of the bitumen fraction of BV8 was performed on a Hewlett Packard 1890 gas chromatograph with 25 m Scientific Glass Engineering DB5 fused silica column (id. 0.33mm, film thickness 0.5μm) using helium as carrier gas. The oven was held at 100°C for one minute, ramped at 6° C min^{-1} to 300C and held at 300° C for 20 minutes. Detection was by a VG Trio-1

quadruple mass spectrometer, scan range 40-500amu, 0.90s scan time, 0.10s interscan time.

2.5 Analysis procedures

2.5.1 Anions

2.5.1.1 Preparing the anions from DET gels

Gel samples were immediately weighed to determine weight by weight difference. They were then eluted in Milli-Q-water overnight to ensure back-equilibration and transferred into suitable Dionex sample tubes. Warham samples were eluted in 1500µl of Milli-Q-water, whilst Thorne Moors samples were eluted in 1000µl Milli-Q-water, reflecting the higher ionic strength of the salt marshes pore-waters compared with the peat pore-waters. Samples were gently agitated overnight on an orbital shaker prior to Cl^-, NO_3^-, SO_4^{2-} measurements being taken by a Dionex ICS 90 ion chromatograph with AS14 analytical column. This system separated the ions by measuring their charge which took a set amount of time per anion. Each sample took 20 minutes to analyse for Cl^-, NO_3^- and SO_4^{2-}. Every Dionex run had two blanks followed by a series of standards and then two reference materials before samples were run. The standards were different for both Thorne Moors and Warham due to the high concentrations at Warham and the low concentrations at Thorne Moors (see section 2.7 for both tables). Certified and quality assured reference materials used were Hamilton-20 and Thames River Water. Hamilton-20 is water taken from the Hamilton Harbour (Lake Ontario, Canada) and had 56 laboratories participating in analysis (National water Research Institute, 2006). The Thames River water reference material was taken downstream from Henley-on-Thames, UK by LGC Standards. Two standards were run after every 10 samples, as was Hamilton-20 and

a full set of standards were analysed at the beginning and the end of each Dionex run to ensure analytical accuracy (see appendix A.1). The repeated measuring of the reference material aided in determining how much, if any, analytical drift had occurred as well as the accuracy of the data. Precision of the data was determined by the repeated measuring of the standards. A few of the full sample runs were analysed twice as part of a quality control check (with runs being nearly identical). Although the samples and standards prepared had Milli-Q-water water used throughout (18.2 MΩ), the mean was taken from all blanks and removed from the final value which the Dionex calculated (all in mg/L).

The samples collected at Thorne Moors had very low concentrations of nitrate and sulfate and, due to the dilution step inherent in the DET method, were close to detection limits on the Ion Chromatography system used. Therefore the data were carefully checked, and detection limits were calculated individually for each analytical run (see appendix A.2). The detection limit for the blank corrected data was set at 3 times the standard deviation of the blank analyses (Miller and Miller, 1993). In all sites, chloride was well above the detection limit, unlike nitrate or sulfate, which were close to (and occasionally below) detection. The same procedure was carried out for the nitrate analysis at Warham due to the concentrations being low.

2.5.1.2 Preparing the anions from cores

Once the pore-waters were extracted from the sediment (this Chapter: 2.4.1.2), the samples were analysed on the Dionex and treated in the same way as the gels.

2.5.2 Total iron

Concentrations and fluxes of total iron (Fe (II) and Fe (III)) were measured from samples collected from Thorne Moors using the DET and DGT gel probes respectively. The method (based on Viollier et al., 2000) uses spectrophotometry to determine the amount of total iron in the eluted gel sample. As with the anions, the iron DET and DGT gel samples were weighed so that the weight can be determined from the difference. Samples were eluted (and gently agitated in an orbital shaker) overnight in 300µl nitric acid for a back-equilibration (oxidising Fe (II) to Fe (III)). 100 µL of gel eluent was added to a sample tube, followed by 50µL of sodium hydroxide, 100µL of ferrozine solution (0.492 g of ferrozine and 0.76g of ammonium acetate added to 100 ml Milli-Q-water), 200 µL of hydroxylammonium hydrochloride (9.7g of $H_2NOH.HCl$ made up to 100ml with 2M Analar HCl), and 100µL of buffer solution (ammonium acetate: adjusting to pH 9.5 with concentrated ammonium hydroxide solution, and then made up to 100ml with Milli-Q-water). Full colour development takes ten minutes after which the samples were measured on the UV spectrometer. For each sample run, full standards were measured (Table 2.9), then standard 6 and 8 followed by a repetition of ten samples and standard 6 and 8, until all samples were measured in that run. To finish the run three reference materials (from another stock solution) were measured followed by the full set of standards. The repetition of standard 6 was used to calculate the RSD (see appendix A.1) and drift calculations were applied by using standard 7.

2.5.3 Metals

The gels were ordered in to the University of Leeds from DGT Research, who also conducted the metal analysis on their own ICP-MS. Prior to the samples being sent

to Lancaster, both metal DET and DGT gels were sliced at 0.5 cm resolution and eluted into 300µl 0.1M HNO_3 and 1M HNO_3 respectively. Samples were also left to be gently agitated overnight on an orbital shaker.

2.6 Standards used for analysis

The following tables show the concentrations of the standards that were used for analysis of both anions and iron. Full standards were run at the beginning and at the end of analyses; two standards were run after every ten samples and a blank.

2.6.1 Anions

Standards (Thorne Moors) mg/L									
	1a	1b	2	3	4	5	6	7	8
Cl^-	0	2	20	40	80	120	160	200	200
NO_3^-	0	0.5	5	10	20	30	40	50	100
SO_4^{2-}	0	0.5	5	10	20	30	40	50	200

Table 2.3 Standards used for the analysis of Thorne Moors.
The concentrations of the standards used prior, during, and at the end of each run for Throne Moors IC analysis. As the concentrations are lower in the peat bog than in the salt marsh, the concentrations of the standards were lower for 1B than for Warham's standards.

Standards (Warham) mg/L									
	1a	1b	2	3	4	5	6	7	8
Cl^-	0	5	20	40	80	120	160	200	200
NO_3^-	0	2	5	10	20	30	40	50	100
SO_4^{2-}	0	2	5	10	20	30	40	50	200

Table 2.4 Standards used for the analysis of Warham.
The concentrations of the standards used prior, during, and at the end of each run for Warham Salt Marsh IC analysis. As the concentrations are higher in the salt marsh than in the peat bog, the

concentrations of the standards were higher for 1B than for Thorne Moors' standards.

2.6.2 Ferrozine

Standards										
Standard number	1	2	3	4	5	6	7	8	9	10
Mg/L Fe (from 1000 mg/L Fe stock solution)	0	0.025	0.05	0.1	0.25	0.5	1	2	3	4
	Into 0.01 M acid									

Table 2.5 Standards used during iron analysis.
The concentrations of the standards used prior, during, and at the end of each run for both Warham Salt Marsh and Thorne Moors peat bog.

2.7 Data retrieval

Numerous field trips have been carried out at these two sites, with not all data collection being successful. This section briefly describes the problems encountered.

2.7.1 Thorne Moors

The sediment here is very water-logged with gel probes easily penetrating the sediment, as did the oxygen microelectrodes, thus data collection was successful. However, one data set (from one probe) had to be discounted as it became contaminated.

2.7.2 Warham

Many of the trips to Warham were not successful for the DET and DGT methods. This is because the gel probes bent when penetrating the sediment and allowed sediment onto the gel. After reviewing the methodology and placing two probes onto

an aluminium rod, sediment still got on to the gels thus rendering them useless. Other problems included fauna (e.g. crabs) “attacking” the gel probes, sediment being too hard, or too much vegetation which damaged the gels on deployment. Probes that appeared to have successful deployment, did not give sensible results, that is, concentrations were an order of magnitude out of the expected range (relative to seawater concentrations and previous studies). The gels not working properly may be due to a marked difference between ionic strength between the Milli-Q water which the probes were stored in prior to deployment and the hyper-saline pore-waters. Conversely, cores were very successful at this site, with results that were in the expected concentration ranges; as was the oxygen data collected using the microelectrodes.

Chapter 3 Thorne Moors Redox Zones

3.1 Introduction

Ombrotrophic peatbogs, which receive all their nutrients from the atmosphere, are a carbon sink (e.g. Turunen et al., 2002; Holden, 2005; Belyea and Baird, 2006) and are estimated to have stored enough carbon to reduce global temperatures by 1.5° to 2°C over the last 10,000 years (Holden, 2005). However, due to anthropogenic activity the ability of a peatbog to sequester carbon may be compromised and in fact they may become a source of carbon rather than a sink (Holden, 2005; Novak et al., 2008; Clark et al., 2010; Silvola et al., 1996). Different disciplines tend to focus on their specialized key aspects of peatland processes and an integrated approach is needed to define the interactions between small-scale processes (e.g. Damman, 1978; Morris et al., 2011). For instance, hydrologists have often used a two-layered acrotelm-catotelm model to explain processes occurring in peat. This model is also used in ecohydrology as well as peat development modelling and budgeting (Holden, 2005). This two–layered model consists of an upper layer (acrotelm), which is considered to have a fluctuating water table and high hydraulic conductivity, in contrast to the lower layer (catotelm), the main body of the peatland, which has much lower hydraulic conductivity, is permanently saturated and relatively passive (Ingram, 1978; Holden, 2005; Morris et al., 2011). In contrast, geochemists often define processes taking place in peat layers by a series of characteristic changes in pore-water chemistry that are related to redox zonation. This redox zonation arises from a series of microbial respiration reactions that yield successively less energy: oxygen reduction; nitrate reduction; iron reduction (which converts Fe(III) in mineral form to dissolved Fe^{2+}); and sulfate reduction. For instance, sulfate is unstable in the

presence of organic matter in reduced environments leading to microbial sulfate reduction (MSR), reaction 3.1:

$$2H^+ + SO_4^{2-} + 2CH_2O \rightarrow H_2S + 2CO_2 + 2H_2O \quad (3.1).$$

The products of MSR are stable, including the neutralisation of acidity, as long as the conditions remain anoxic and the reduced sulfur species produced are not re-oxidized (e.g. Giblin et al., 1990; Morgan, 1995; Chapman, 2001).

Free oxygen is typically consumed close to the surface of peats by microbial and plant respiration typically within the "acrotelm" layer, and oxygen is not readily supplied to the deeper parts of the peatland (e.g. Shotyk, 1988; Shotyk et al., 1992). Unless there are mechanisms to add oxygen into the catotelm part of the system then the reduced products will be stable. Mechanisms to introduce oxygen deeper in the peat could be related to: a change in the water-table (Bottrell et al., 2004); plants releasing oxygen from their roots (e.g. Armstrong et al., 1991); lateral water flows (Holden, 2005); or peat disturbance e.g. through removal or drainage. Degradation of plant matter can also release relatively oxidized species (e.g. sulfate, nitrate) (Shotyk, 1988; Blodau et al., 2007). Introduction of oxygenated waters into the previously anoxic depths will result in sulfate and nitrate being released into the pore-waters, by reactions such as:

$$2FeS_2 + 7O_2 + 2H_2O \rightarrow 2Fe^{2+} + 4SO_4^{2-} + 4H^+ \quad (3.2)$$

$$R\text{-}S\text{-}H + 2O_2 + H_2O \rightarrow R\text{-}O\text{-}H + SO_4^{2-} + 2H^+ \quad (3.3)$$

(R- is an organic molecule)

$$2NH_4^+ + 3O_2 \rightarrow 2NO_2^- + 2H_2O + 4H^+ \quad (3.4)$$

$$2\ NO_2^- + 1\ O_2 \rightarrow 2\ NO_3^- \quad (3.5)$$

Conditions for nitrification (reactions 3.4 and 3.5) in a peat bog, however, are not ideal. *Nitrosomonas,* which mediate nitrification, are inhibited at acidic pH (e.g. Jones and Hood, 1980; Bowden, 1987), although laboratory experiments have shown that the inhibition of nitrification at low pH has been underestimated (Tarre et al., 2004). Additionally, nitrification needs a good supply of O_2 (see reaction 3.4). However, it is not impossible for nitrification to happen in reduced environments; indeed, Mortimer et al. (2004) demonstrated that anoxic nitrification occurred in marine sediments by reducing Mn Oxide (equations 3.6 and 3.7),

$$8MnOOH + NH_4^+ + 14H^+ \rightarrow 8Mn^{2+} + NO_3^- + 13H_2O \quad (3.6),$$

$$4MnO_2 + NH_4^+ + 6H+ \rightarrow 4Mn^{2+} + NO_3^- + 5H_2O \quad (3.7).$$

Peatlands are often dominated by one or two types of plant species, which in part, during the decomposition process, dictates the internal structure of the peat which can range from fibrous to amorphous (Shotyk, 1988). The plant types also have some control on the peat shear strength which can be reinforced within the root zone (Waldron et al., 1981), for instance *Sphagnum* does not have roots whilst *Eriophorum* does and furthermore has a high root turnover (Gebauer et al., 1995; Tolvanen et al., 2004; Currey et al., 2011), leading to a well-developed "root mat" layer. Thus *Eriophorum* contributes to higher peat strength where the roots are present. Additionally, plants exert some control over the micro-topology, which in turn controls the small-scale runoff and drainage channels. The dominant species of plant and the amount of organic matter present in peatbogs are some of the most important factors determining the overall porosity and permeability (Brown et al., 2000; Aldrich and Feng, 2000; Ma and Tobin, 2004). However, the porosity will not be homogenous throughout the peat due to seasonal and longer-term variation in

plant growth and therefore decay, which will cause vertical variability in the porosity and structure. Porosity and permeability are also affected by the amount of root layers and compaction that the peat has undergone. If lower density/higher porosity and permeability layers exist within the peat profile they may permit lateral water flows which could ultimately introduce oxygen (and/or other chemical contrasts) into the peat and thus change the redox chemistry in that layer, ultimately affecting the peatlands potential to store carbon, sulfur and other elements.

Over longer time-scales the decomposition of peatlands is usually viewed as essentially a homogeneous process (Clymo, 1984; Hatcher et al., 1986; Stevenson, 1994), although over shorter time-scales it is more heterogeneous as different components can undergo selective decomposition (Hatcher et al., 1983; Hatcher and Spiker, 1988). This selective decomposition would increase pore-water concentration of certain compounds in localised areas, for instance, the breakdown of organic S from OM may contribute significant amounts of sulfate to peatland pore-waters (Shotyk, 1988; Blodau et al., 2007). Peatland pore-waters contain a much smaller reservoir of reactive species, such as S and N, than the solid peat matrix. The pore-water reservoir is thus sensitive to short-term changes in inputs and outputs of these species and reflects active processes, whereas the peat matrix records the sum of all processes that have taken place during plant growth, decay and burial. Study of pore-water profiles is thus best suited to establishing the structure of active processes within the peat and their relation to peat structure.

It is clear that peat structure, decomposition, fauna and hydrology are inter-related in complex ways (e.g. Belyea and Baird, 2006; Holden, 2005; Morris et al., 2011), which influence the development of redox zones within a peat matrix and the rate of bog growth (e.g. Belyea and Baird, 2006; Holden, 2005), which ultimately control

the ability of a peat bog to sequester carbon from the atmosphere (Holden, 2005). This is especially important for northern peatlands as they are a significant global carbon reservoir (e.g. Gorham, 1991; Turunen et al., 2002). It is also clear the two-layered acrotelm-catotelm model is too simplified and therefore when rigidly applied, it rarely achieves proper explanation of small-scale processes occurring within the peat (e.g. Morris et al., 2011; Belyea and Baird, 2006). Instead, the hydraulic behaviour in these systems must be controlled by a combination of processes including flora, root layers, seasonality, rates of decomposition, macropores, topographical relief and other changes in peat matrix properties which define porosity and permeability (e.g. Holden, 2005; Morris et al., 2011). These processes allow heterogeneity in the geochemistry, sediment strength and hydrology, both horizontally and vertically, within peatlands.

3.2 Aims and approach of this work

Chemical evolution of peat and the processes involved are usually investigated via study of the peat matrix (which gives a time-integrated history of changes with depth) (e.g. Ukonmaanaho et al., 2006; Grover and Baldock, 2013) or by study of pore-water chemistry (e.g. Rausch et al., 2005). However, the spatial resolution of pore-water sampling by most techniques will fail to identify chemical changes associated with processes and interactions that operate at the small scales of heterogeneity associated with features such as macropores (Harper et al., 1997) and individual roots within the peat, or even possibly contrasts in peat matrix properties. Small scale features that affect the hydrology of the peat are likely to introduce geochemical gradients that may be important loci of biogeochemical activity. DET gel probes provide the opportunity to sample pore-water chemistry at mm-scale resolution and address the importance of these features. This coupled with vane

shear tests to measure the strength of peat (as a proxy for hydraulic conductivity) and a visual examination of peat cores allows us to investigate the processes occurring in a section of peatbog. Morris et al., (2011) noted that the well accepted theory of decomposition hot spots seen in many terrestrial sedimentary environments is relevant to peatlands, thus linking the hydrology, ecology, and biogeochemistry, and furthermore is not inconsistent with the use of the diplotelmic model to describe small-scale processes. Here, the combination of DET gels, vane shear tests and an assessment of peat cores are used to elucidate the biogeochemical processes which occur in the top 40 cm of peatland.

3.3 Results

The two cores show similar features with discrete layers of variable density. As these cores were frozen, it was visually very clear where there were large amounts of pore-water present in lower density layers. The top 5 cm in core A, and top 8 cm in core B, were comprised mainly of live and recently dead organic matter, and both of these layers also contained large amounts of frozen pore-water (Figure 3.1). Below this, both cores had low density and high pore-water content (5-12 cm in core A; 8-13 cm: core B). In core A there is dense root material from 12-37 cm, whilst a similar zone can be seen from 13-34 cm in core B. Fewer roots are present from 37-31cm (core A) and 34-37 cm (core B), with more humified peat. In core A from 31 cm to the end of the profile (approximately 44 cm) there is denser humified peat with a lower water content, although there is an exception at 33 cm, at the base of the root mat, where there is a thin low density zone with a large amount of pore-water. In core B from 37-41 cm, the core is similar to core A with well humified peat and low water content, with the exception between 33-34 cm where a zone of lower density and high pore-water content again coincides with the base of the root zone.

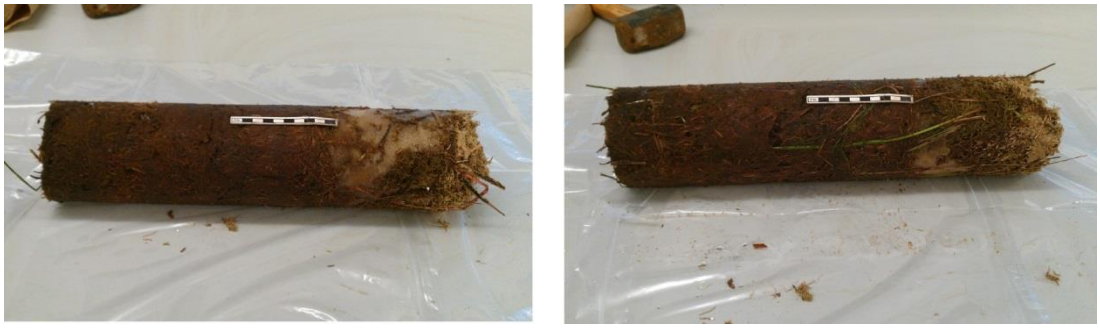

Figure 3.1 Frozen cores.
Core A to the left and core B to the right. The visual overviews of the cores reveal that there are areas of high and low density peat; this could allow for water pipes within the peat. These cores also show that roots are present throughout much of the depth sampled.

The vane shear profiles can be seen in Figure 3.2. In general, peat strength increases with depth, though there is a wide range of strength at depth in some sites, particularly sites 1 and 3. The exception is site 4 which has highest strength at around 25 cm depth, probably due to very strong root mat development. However, at sites 3, 4 and 5 there is a consistent local minimum in strength at 30 to 40 cm depth. This corresponds closely to the depth where a low density zone was observed below the root mat in the cores. Thus the vane shear strength data support the hypothesis that there may be a widely developed low density (= high permeability) feature below the root mat at many sites.

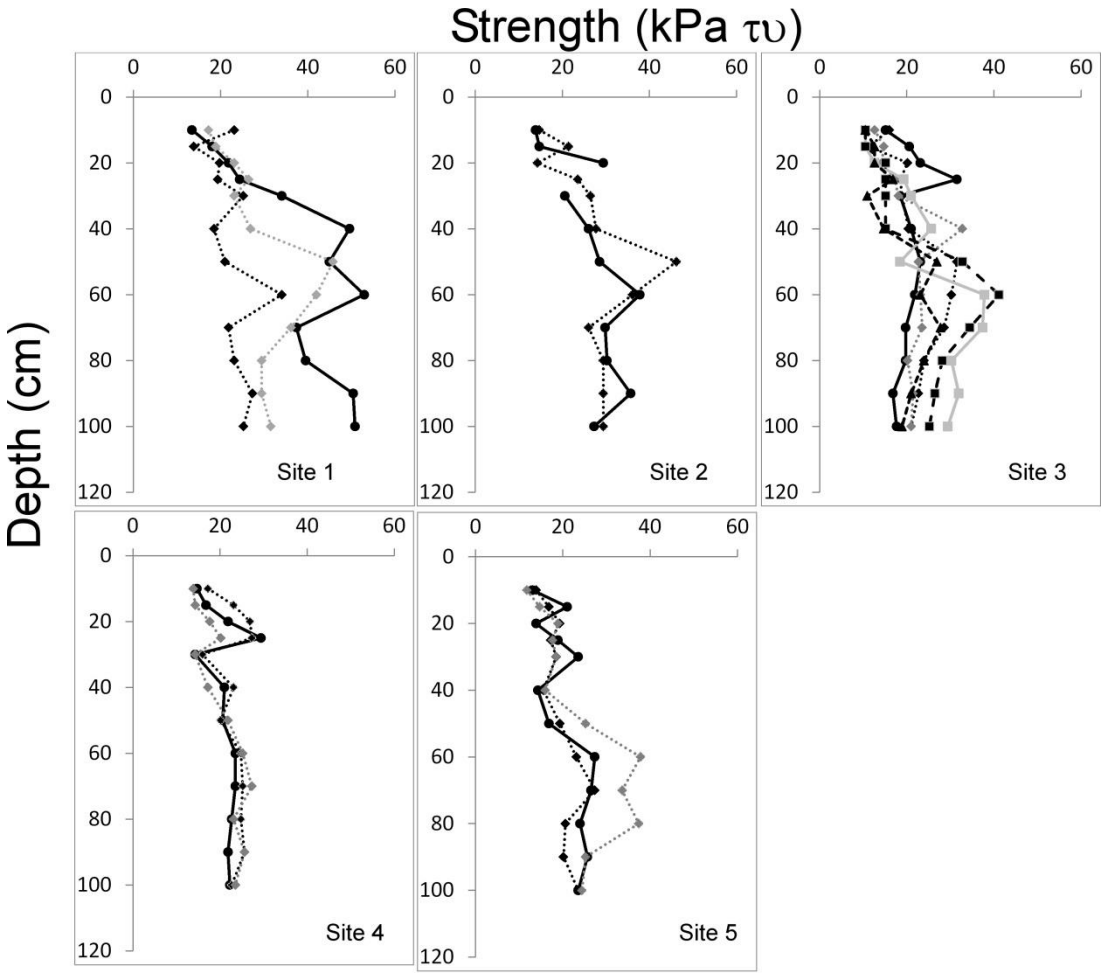

Figure 3.2 Vane shear depth profiles.
Vane shear profiles taken for all sites. There are three sets of data for all sites apart from site 2 (2) and 3 (6). The vane shear results show that strength of the peat is variable throughout all sites, however, the strength generally increases as depth does with localised zones of weaker peat.

In both oxygen profiles, oxygen concentrations are around 110% atmospheric saturation at the surface and quickly decrease to 0% by about 5 mm depth (Figure 3.3). Below this, both profiles exhibit fluctuating O_2 concentration, between 0% to 50% in profile A and 0% to 40% in profile B. The fluctuations decrease in amplitude with depth, and between 35 and 50 mm depth in site A the fluctuations are between 0% and 20%. In site B, there is a large increase in O_2 concentration between 26 mm

and 32 mm depth (up to 96% saturation) below which O_2 concentration fluctuates around 0%.

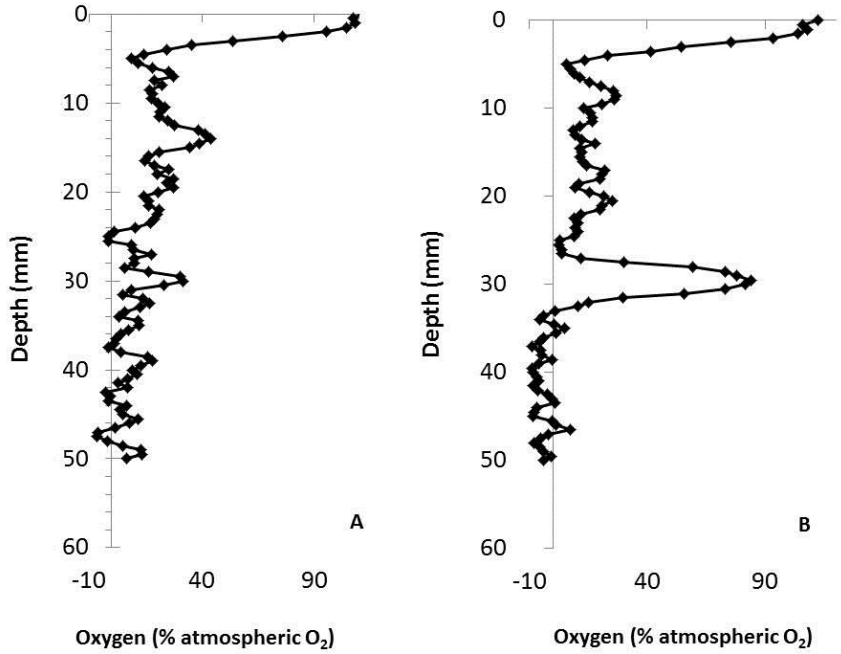

Figure 3.3 Oxygen depth profiles.
A) open pool and B) Sphagnum lawn which were taken from site 1 only. The shallowest two points are individual measurements, other points are a 5-point binomially weighted running mean which was applied to remove high frequency noise that was prevalent in the deeper parts of both profiles. Although there is noise in the profiles, they do show that by 5 mm, and in both sites, O_2 is depleted or at very low atmospheric O_2 saturation.

The chloride profiles are plotted in Figure 3.4. All chloride profiles exhibit fairly uniform concentrations with depth, with some superimposed peaks. At site 1, chloride concentrations are higher and more variable (20 to 45 mgL^{-1}) in the upper 10 cm, and fall to a range of 10 to 15 mgL^{-1} lower in the profile. At site 2(A) chloride concentrations are fairly uniform with depth (10 to 15 mgL^{-1}) but with an increase to around 35 mgL^{-1} between 20 and 23 cm depth. Site 2(B) has concentrations ranging from 15 to 35 mgL^{-1} throughout the profile. Two main

features are seen at site 3. In the top 20 cm values average out at 12 mgL^{-1} but range between 10 to 25 mgL^{-1}. Below 20 cm there is a general increase in concentrations from 12.5 to 25 mgL^{-1}. At site 4, pore-waters in the upper 7 cm have concentrations around 20 mgL^{-1} and there is a large peak at 7-10 cm which reaches 55 mgL^{-1}. Below 14 cm, chloride concentrations are generally higher at around 30 mgL^{-1} (range 21 to 40 mgL^{-1}). At site 5 chloride concentrations generally show a similar range at all depths (18 to 32 mgL^{-1}), superimposed in this are two peaks at 13.5cm and 28 cm of about 70 and 55 mgL^{-1}, respectively. Local rainwater data have been included for the chloride profiles, plotted as data points at 5 cm above water level in sites 1 and 2(A). In both sites the rainwater concentrations are significantly lower than the shallowest pore-water concentrations obtained from the gels.

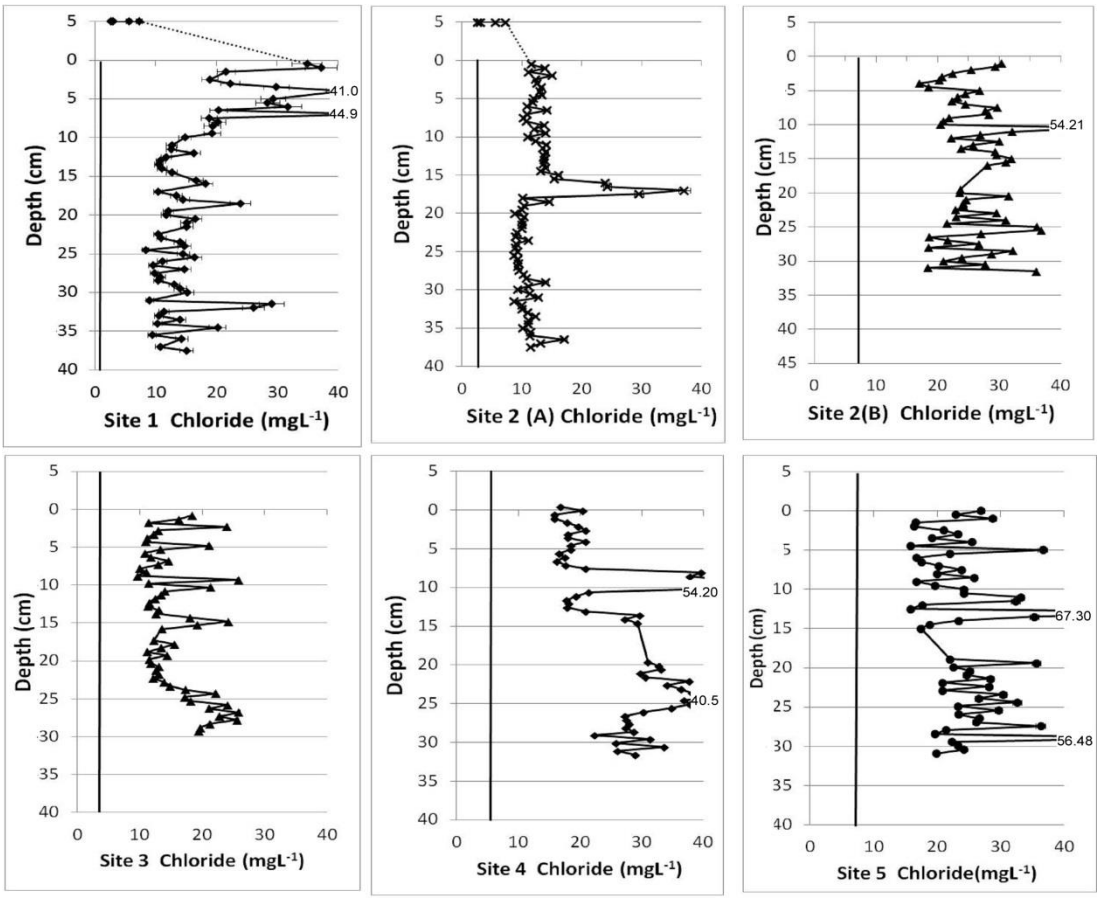

Figure 3.4 Chloride DET depth profiles.
Zero on the depth scale refers to the water level on deployment of the probes (i.e. it is the same zero as the oxygen profiles in Figure 3.3). Rainwater data for chloride is plotted at 5 cm above water surface on the depth axis at sites 1 and 2(A) only. Detection limits vary for each species in each gel deployment and are plotted as a vertical line in each profile. N.B. that these detection limits apply to gel data only and detection limits for rainwater data are far lower. Chloride profiles show variability through all sites. Excluding sites 1 and 2(A), depth profiles were obtained by placing two probes on an aluminium rod, which created a gap in the depth profiles. These are at; site 2(B) ~ 15.5 and ~ 20 cm depth; site 3 ~ 15 and ~17.5 cm depth; site 4 ~ 15 and ~20 cm depth; site 5 ~ 15 and ~19.5 cm depth.

The nitrate profile obtained from site 1 (Figure 3.5) shows that although there is an immediate drop in concentration at the top of the profile, concentrations then rise again (to about 15 mgL^{-1}) between 2 and 8 cm depth. Below this depth, concentrations are generally very low throughout the profile (1 to 4 mgL^{-1} but generally above detection limit), with some superimposed narrow peaks of nitrate at

18 to 21 cm, 31 and 33 cm. In site 2 (A), nitrate concentrations are generally lower (<2 mgL^{-1}, many points below detection limit in lower part of profile below 25 cm) but again there are large superimposed peaks at 3, 11, 18, 30 to 31 cm and 34.5cm (Figure 3.5). In the upper 20cm of site 2 (B) the concentrations are low and fairly uniform (mostly between detection limit and 1 mgL^{-1}, ranging to 2.5 mgL^{-1}), below 20 cm there is a trend of generally increasing concentrations with depth up to 2 mgL^{-1} at the base of the profile. At site 3 there are two distinct peaks at 15 and 20 cm (7 and 5 mgL^{-1} respectively). The profile is otherwise below detection limit which is relatively high at 2 mgL^{-1} in this case. Site 4 has elevated concentrations in the upper 3 cm of the profile reaching 13 mgL^{-1}. Below this, concentrations are lower around 2.5 mgL^{-1} until 14cm where there is an increase to 7.5 mgL^{-1}, below which there is a general, steady decrease for the rest of the profile. At site 5 the detection limit is higher than at other sites (5.1 mgL^{-1}) and all data lie below this.

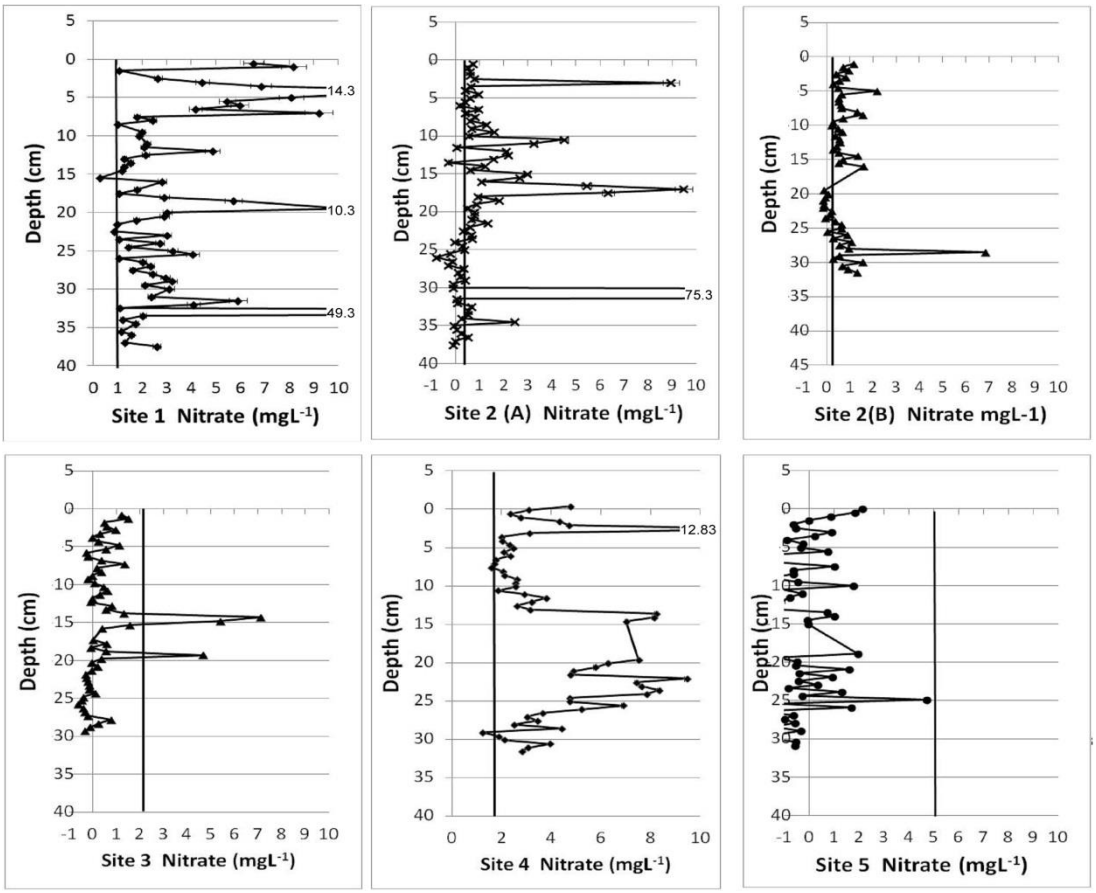

Figure 3.5 Nitrate DET depth profiles

Zero on the depth scale refers to the water level on deployment of the probes (i.e. it is the same zero as the oxygen profiles in Figure 3.3). Detection limits vary for each species in each gel deployment and are plotted as a vertical line in each profile. Nitrate is often close to detection or below detection in all sites; although all sites (excluding 5) show that there are small, sharp positive excursions of nitrate concentrations. Excluding sites 1 and 2(A), depth profiles were obtained by placing two probes on an aluminium rod, which created a gap in the depth profiles. These are at; site 2(B) ~ 15.5 and ~ 20 cm depth; site 3 ~ 15 and ~17.5 cm depth; site 4 ~ 15 and ~20 cm depth; site 5 ~ 15 and ~19.5 cm depth.

At site 1 there is a marked increase between rainwater sulfate concentrations (around 3 mgL^{-1}) and the shallowest pore-waters (5.5 mgL^{-1}, Figure 3.6). Below this, sulfate concentrations are generally lower (1 to 4 mgL^{-1}) but with several superimposed peaks at 7.5, 11.5, 16 and 19 cm depth. Between 22 and 28 cm depth, sulfate concentrations are below detection limit (<1.2 mgL^{-1}) or slightly above (up to 2 mgL^{-1}). Below 28 cm there are three large peaks in sulfate concentration and a rise to

~3.5 mgL^{-1} at the base of the profile. At site 2(A), sulfate concentrations in the upper 30 cm of the profile mostly fluctuate around the detection limit of 3.3 mgL^{-1} and are thus similar to rainfall inputs. Indeed, surficial sulfate concentrations are below detection limit and therefore lower than the rainwater values. Once again superimposed on these low values are large increases in sulfate concentration at various points through the profile. Below 30 cm depth there is one very large sulfate peak, below which sulfate concentrations are above detection limit, rising to 5.5 mgL^{-1}. In the top 15cm of site 2(B), concentrations are fairly uniform around 5 mgL^{-1}, below this there is a general increase in concentrations from 4 mgL^{-1} to 9 mgL^{-1}. One large peak is found on this profile at 15 cm with maximum sulfate concentration at 17.5 mgL^{-1}. At site 3 the upper 23 cm has sulfate concentrations around 4 mgL^{-1} (values range from below detection limit to 6 mgL^{-1}) but with one large sharp peak (maximum 16 mgL^{-1}) superimposed at 19.5 cm. Below this, sulfate concentration increases to around 14 mgL^{-1} at the base of the profile. Site 4 has higher sulfate concentrations than other sites; in the top 7 cm concentrations are around 10 mgL^{-1}; there is a general increase in concentration between 10 and 25 cm, from 10 to 35 mgL^{-1}, superimposed on which are two large excursions, both reaching around 400 mgL^{-1}, at 7-10 cm and 25-26 cm. Below the lower peak concentrations fall to around 10 mgL^{-1} and increase to ~20 mgL^{-1} at the base of the profile. In the uppermost 15 cm at site 5 sulfate concentrations are close to (mostly below) detection limit of 3.7 mgL^{-1}. Below this there is a slight increase in concentration above a sharp peak (30 mgL^{-1}) at 26 cm. Below the peak concentrations are around 4 mgL^{-1} at the base of the profile.

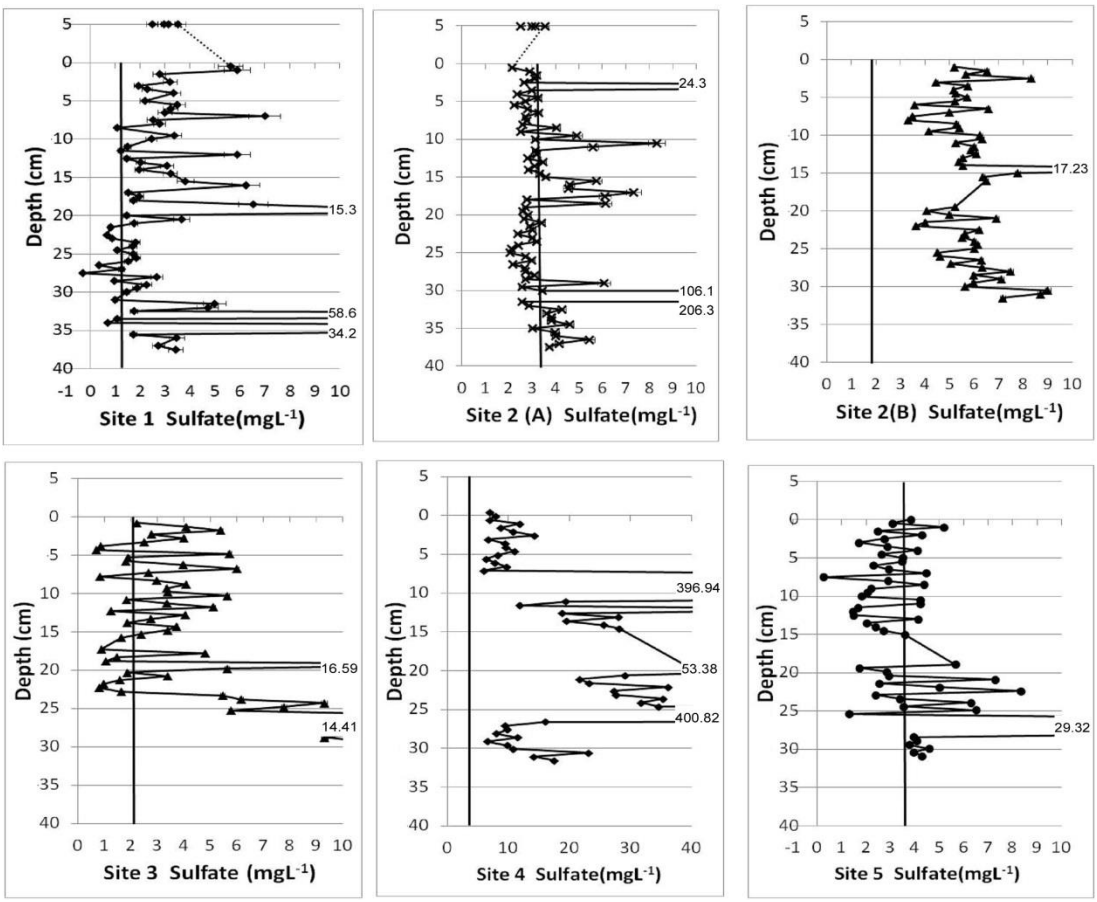

Figure 3.6 Sulfate DET depth profiles.
Zero on the depth scale refers to the water level on deployment of the probes (i.e. it is the same zero as the oxygen profiles in Figure 3.3). Rainwater data for sulfate is plotted at 5 cm above water surface on the depth axis at sites 1 and 2(A) only. Detection limits vary for each species in each gel deployment and are plotted as a vertical line in each profile. N.B. that these detection limits apply to gel data only and detection limits for rainwater data are far lower. Sulfate profiles show that in all sites the concentrations are variable; however as with nitrate there are clear sharp positive excursions throughout the profiles of So_4^{2-}. Excluding sites 1 and 2(A), depth profiles were obtained by placing two probes on an aluminium rod, which created a gap in the depth profiles. These are at; site 2(B) ~ 15.5 and ~ 20 cm depth; site 3 ~ 15 and ~17.5 cm depth; site 4 ~ 15 and ~20 cm depth; site 5 ~ 15 and ~19.5 cm depth.

3.4 Discussion

3.4.1 Core characteristics and vane shear strength

Two cores were taken from sites A and B, which underwent a visual examination (Figure 3.1). In both cores, there is a large root mass and clear evidence for low

density/high permeability zones that might promote lateral water flow. The widespread areal extent of some of these zones is revealed by the peat strength data. Roots are found throughout the cores and will have increased the strength of the peat in those areas. Figure 3.2 demonstrates that there is greater fluctuation in peat strength over the top half of the profile than the bottom half. The bottom half has strength changes which are over a greater distance than in the top half, which contains both peaks and troughs in strength. This reveals a combination of low density zones (decreasing the strength), roots (increasing the strength) and potentially the amount of decay that has occurred (the more humified and compacted the peat the more likely the strength will increase). Higher strength root mats and more compacted zones will both tend to have lower porosity and permeability than the weaker, less dense layers. Additionally, apart from site 5 there is some heterogeneity within the sites. This probably reflects roots reaching different depths, differing amounts of organic matter decomposition and differing states of decomposition and lower density zones of various thicknesses across the peat.

3.4.2 Chloride

The shallowest waters recorded in all the gel probe profiles have higher chloride concentrations than the rainwater inputs (Figure 3.4). This results from evapotranspiration, which removes water but not dissolved ions, resulting in increased chloride concentrations. Chloride is not expected to show major changes in concentration down through the profile, because it is chemically conservative as it is not released or taken up by plants and it doesn't undergo any speciation changes by redox reactions (Bottrell et al., 2007). Sites 1, 2(B) and 5 illustrate this, with the near-surface chloride concentrations representing recent evapotranspiration while the deeper values represent the averaged effect of evapotranspiration on the input

concentrations. However, in site 2(A) whilst the majority of chloride concentrations indicate the same averaged evapotranspiration as site 1, there is a major peak in chloride concentration around 17 cm depth. At site 3 there is a trend to higher chloride toward the base of the profile (25 vs. 12 mgL^{-1}) and site 4 has chloride concentrations around 30 mgL^{-1} below 13.5 cm compared with 15 to 20 mgL^{-1} above (albeit with a peak superimposed at 8 to 10 cm). Bottrell et al. (2007) showed that evapotranspiration caused seasonal increases in chloride at similar sites at Thorne Moors, thus increases in chloride at the base of some profiles could represent mixing with deeper (and older) more evapo-concentrated waters. The presence of distinct peaks in chloride concentration at sites 2(A) and 4 cannot be explained in this way; these peaks could be due to lateral water flows (which could have slightly differing chloride concentrations, thus they would appear to peak at these horizons) at these depths and there is evidence for low density (and thus higher porosity and permeability) layers in both the vane shear tests and the cores. High chloride concentrations could result from summer evapo-concentration or winter additions of chloride from road gritting via aerosol/dust transport (e.g. Nicholson and Branson, 1990; Blomqvist, 2001). Thorne Moors lies close to two motorways (Figure 2.2; Chapter 2) and there was significant road salt application during the winters of the study period. Whichever the source of elevated surface-water chloride, high chloride waters could then migrate from surface to depth via lateral flow along higher permeability pathways.

3.4.3 Oxygen

In both profiles there is a high oxygen concentration very close to the surface (up to 110% saturation) that quickly decreases to a lower but variable concentration (10 to 40% saturation) by 5 mm depth (Figure 3.3). This is the result of photosynthetic

production of O_2 close to the surface and diffusion of O_2 from the atmosphere which is then rapidly consumed by respiration below this. The subsurface peak in profile B is probably due to plant roots (e.g. *Eriophorum*) releasing oxygen; the core data back this up as both cores have large amounts of live plant material in the top 5cm. The variable low concentrations below 5 mm depth in both profiles thus represent competition between minor oxygen input from roots and consumption by respiration. Negative oxygen concentrations recorded at depth are probably due to a small offset between the laboratory calibration and field response in the more complex peatland groundwater solution.

3.4.4 Sulfate and nitrate

At all sites concentrations of sulfate in the shallowest waters are similar to, or higher than rainwater inputs indicating variable degrees of evapoconcentration (Figures 3.5 and 3.6). The ratio of sulfate: chloride can be used to remove the effects of variable evapoconcentration and vertical profiles of SO_4/Cl are plotted in Figure 3.7. Rainwater inputs have SO_4/Cl around 0.7 whereas SO_4/Cl throughout all the pore-water profiles are generally between 0.2 and 0.4 (albeit with superimposed peaks), thus in all cases sulfate is rapidly consumed in the uppermost part of the profile, as evidenced by a marked decrease in SO_4/Cl below that of the rainfall (Figure 3.7). Consumption of sulfate at such shallow depths is most likely by plant uptake as dissolved oxygen is still present and sulfate reducing bacteria are obligate anaerobes (cf. Bartlett et al., 2009).

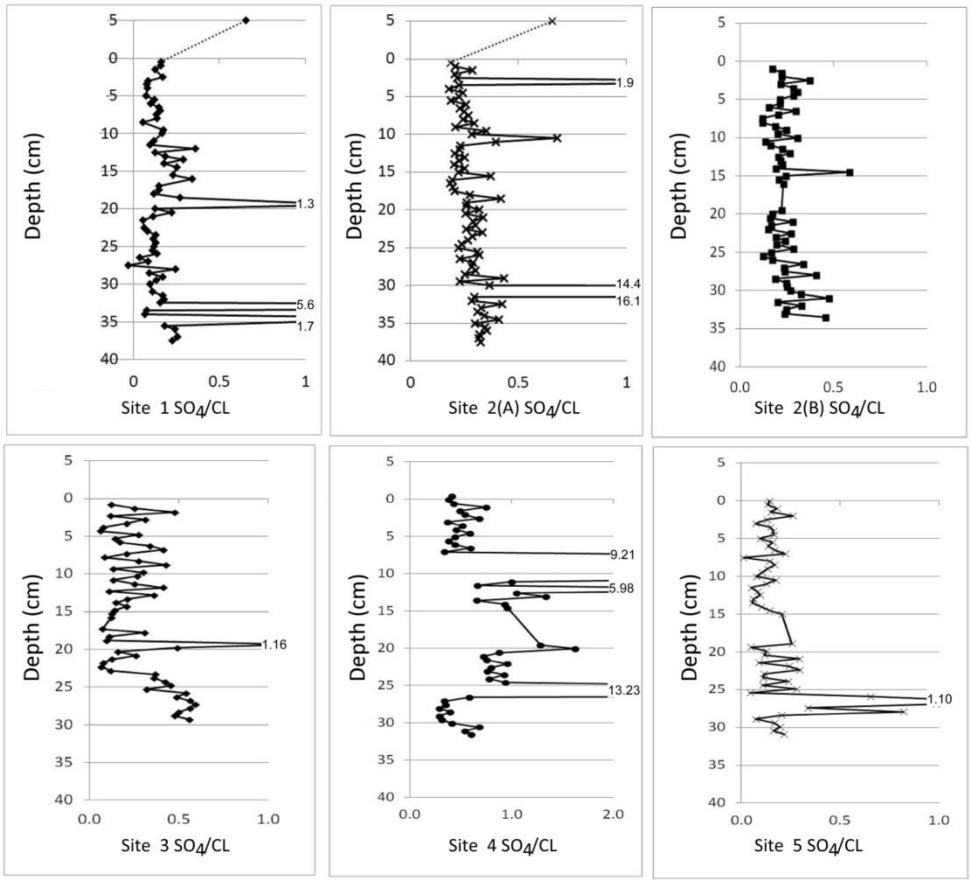

Figure 3.7 Depth profiles of sulfate to chloride ratio.
As chloride is a conservative species and is not expected to undergo changes deeper in the peat matric, any changes in sulfate/chloride ratios are expected to be dominated by removal of sulfate by bacterial processes. These profiles, however, show that there are large peaks of sulfate relative to chloride in the peat matrix which can be seen in all sites scattered throughout the depths measured; showing that there are processes occurring deeper in the peat which must be either oxidising the H_2S species or there are oxidised zones. Average SO_4/Cl (ppm) for rainwater inputs is plotted at 5 cm above water surface on the depth axis. Excluding sites 1 and 2(A), depth profiles were obtained by placing two probes on an aluminium rod, which created a gap in the depth profiles. These are at; site 2(B) ~ 15.5 and ~ 20 cm depth; site 3 ~ 15 and ~17.5 cm depth; site 4 ~ 15 and ~20 cm depth; site 5 ~ 15 and ~19.5 cm depth.

Deeper in most profiles, sulfate concentrations are close to or below detection, so concentrations are very low (typically < 6 mgL^{-1}). In the lower part of the profiles there is a steady increase in sulfate concentrations (Figure 3.6; and SO_4/Cl, Figure 3.7), to values above detection limit, toward the base. Superimposed on this

increasing trend are peaks in sulfate concentration down through the peat profiles that are at much higher concentrations than the background levels. The SO_4/Cl ratios increase at the same depths, confirming that this is the result of releasing sulfate to the pore-water as the ratio of SO_4 to Cl increases at the same intervals as the peaks (Figures 3.6 and 3.7). The nitrate depth profiles are similar to those of sulfate, in the sense that there are sometimes higher concentrations in the surface layers before decreasing to low concentrations or the nitrate is below detection limit. The nitrate profiles also show narrow (one or two data points) sharp peaks of increased nitrate down through the profile (Figure 3.5). Indeed, the loci of the sulfate and nitrate peaks in each profile coincide, suggesting that both species are produced by the same process. As these peaks are often defined by more than one data point, and can be seen in all profiles, it suggests that they are genuine peaks and not an artefact due to gel contamination or analytical procedures. Additionally, as these probes have been placed up to 200m apart and over a year between them, there is clear evidence that there is a continual and widespread process creating these excursions. Gel probe techniques have the capability to record very high spatial variability in pore-water chemistry (e.g. Stockdale et al., 2009) and have recently been used to identify localized production of sulfide in reducing microniches in sediment (Stockdale et al., 2010). Additionally, Widerlund and Davison (2007) were able to identify sulfide-producing microniches <1 mm^2 in size. Thus the peaks observed in this study are interpreted to record some localized process operating within the peat profile. Two processes could cause such peaks: i) oxidation reactions (e.g. reactions 3.2 and 3.3 releasing sulfate or 3.4 and 3.5 releasing nitrate): or ii) localized zones of degradation of plant matter. Oxidation processes will not be caused by water table fluctuations as the management at this site has ensured they are stable, unless there is

a major drought. No droughts were recorded at this site during the period of data collection and historic draughts will not cause the geochemistry seen at this site due to diffusion of these species. Any oxygen at depth, which is needed to fuel oxidation processes, must be released from within the peat itself rather than diffusing in from the surface, shown by the oxygen profiles in Figure 3.3. There are a few mechanisms which could do this. Radial oxygen loss is where oxygen is released into the rhizosphere by plant roots (Gaynard and Armstrong, 1987), oxidising the surrounding sulfide and organically bound nitrogen. This will only happen in the root zone; although roots are present throughout most of the profiles analysed. Decaying plant material can release oxidised species. As plant material becomes humified, S, N and O are lost (Novak et al., 2009; Zaccone et al., 2007; 2011). The original photosynthetic carbohydrate is very oxygen-rich, close to CH_2O, 53% O by weight, and during humification large amounts of O are released and O:C and H:C in the humus residue fall (Stevenson and Goh, 1971; Bohlin et al., 1989; Stevenson, 1994; Bottrell, 1996; Olk et al., 2000). Thus S and N can be released as oxidised forms, as previously reported by Bartlett et al. (2005) and Blodau et al. (2007). Although the water table has been stabilised, this does not have much, if any, control over lateral flows within peatlands. Lateral flows within peatbogs are permitted by the high porosity and permeability zones discussed above. These flows may introduce oxygen-containing surficial waters into deeper anaerobic layers, locally oxidising the surrounding sulfide and organically bound nitrogen. These are then used up quickly by both the nitrate and sulfate reducing bacteria, returning them into a reduced state. These reactions will be continuous unless the water flow is shut off, leaving the reduced ions in a stable state. As discussed above these lateral water

flows additionally add chloride to the system from the surface. However, as it is a conservative ion, it will simply diffuse up and down into the surrounding peat layers.

Regardless of the mechanism for introducing oxygen within the peat, once it is used up (with no more oxygen being introduced), the peaks observed will then only be transient. As the sharp peaks in concentrations contain only a very small mass of sulfate or nitrate, they will diffuse very quickly both to upper and lower depths. For example, the large sulfate peak seen at 31 cm depth in site 2(A) will last only around 22 hours, according to the following calculation (Fick's Law for diffusion);

$R = D(dc/dz)$,

where R = diffusional flux, D = diffusion coefficient and (dc/dz) is the vertical concentration gradient. The diffusion coefficient for sulfate was calculated from Li and Gregory (1974) for a temperature of 10˚C and a porosity of 80%. The peak contains ~300 μg SO_4^{2-} per cm^2 of plan area but SO_4^{2-} is diffusing away at ~1.9 pg s^{-1} (both upward and downward) per cm^2 of plan area. The gels equilibrate with the pore-waters very quickly and the peaks likely record loci of sulfate and nitrate release during the latter part of the gel deployment period. The high vertical spatial resolution of the gels, less than 0.5 cm, also allows these "flashes" to be resolved.

Furthermore, by integrating the flux of sulfate and nitrate away from all peaks in each profile, it is possible to calculate the equivalent oxidation (expressed as O_2 required) taking place (Table 3.1), using the following equation:

$z*A*(C-C_{backgr})*ø$

where; z = vertical thickness; A = area; C = concentration; C_{backgr} = background concentration; and ø = porosity; this calculation has been done for peaks within the

anoxic zone only. The equivalent oxidation varies from 0.6 to 9.5 pg s^{-1} cm^{-2} O_2, and represents the combination of oxidation capacity of humics, root oxygen release and oxygen introduced by lateral flow. This shows that most of the processes occurring in the deeper peat must be dominated the addition of O_2 as more sulfate is produced than nitrate, whereas if OM decay were the dominant source of the spikes, than more nitrate should be released than sulfate due to the N:S ratio being an average of 5:1 in the peat matrix (Moore et al., 2004). This is confirmed in the N:S ratios calculated for individual peaks in the pore-waters (Table 3.2). The molar ratios indicate that the addition of O_2 must be the main source of the nitrate and sulfate peaks; however, there are other peaks that suggest that OM release (i.e. hotspots of decomposition) occur as the ratios are nitrate-dominated, closer to the N:S of the peat (site 1, 4 cm depth 4:1; site 3, 14.5 cm depth; 3:1). Whilst not conclusive evidence for anoxic hotspot decomposition, these data imply that there may be zones of OM degradation that supply nitrate and sulfate to the peat pore-waters.

	Site number					
Species	1	2(A)	2(B)	3	4	5
SO_4^{2-}	5.0	4.4	0.7	1.2	13.4	0.9
NO_3^-	3.1	2.0	0.6	0.4	0.7	b.d.
Total, recalculated as O_2	5.7	4.5	0.9	1.1	9.5	0.6

Table 3.1 Calculated fluxes of oxidized species produced in a vertical section.
This table demonstrates how much O_2 is needed to produce the 'outliers', that is, the positive concentration excursions of sulfate and nitrate deviating away from the background concentrations. Fluxes are in pg s^{-1} per cm^2. b.d: all concentrations in profile lie below detection limit.

Site 1		
Depth	**Molar ratio**	
cm	**N/S**	**N:S**
4.0	*4.1*	*4:1*
7.0	1.0	1:1
19.5	0.3	1:2
33.5	0.6	1:2
Site 2(A)		
Depth	**Molar ratio**	
cm	**N/S**	**N:S**
10.5	0.4	1:2
17.5	1.2	1:1
18.5	0.2	1:3
30.75	0.3	1:3
Site 2(B)		
Depth	**Molar ratio**	
cm	**N/S**	**N:S**
5	2.3	1:1
14.5	0.1	1:12
Site 3		
Depth	**Molar ratio**	
cm	**N/S**	**N:S**
4.8	0.1	1:5
14.5	*2.5*	*3:1*
17.8	0.1	1:6
19.3	0.2	1:5
Site 4		
Depth	**Molar ratio**	
cm	**N/S**	**N:S**
9.1	0.000	1:1843
25.6	0.001	1:480

Table 3.2 **Calculated nitrogen and sulfur ratios.**
The concentration background levels close to the peaks and the peaks themselves were determined for both sulfate and nitrate. This was then used to calculate the molar ratios of N:S in the pore-water concentration within the deeper peat matrix (no spikes shallower 4 cm depth were calculated). As the N:S ratio of peats average at 5:1(Moore et al., 2004), then this table would suggest that most of the spikes are an introduction of pore-waters into the peat matrix rather than purely coming from the decomposition of peats. However, there are some concentration excursions (site 1 and site 3) which would suggest that there is more of an influence of peat decomposition. NB: site 5 nitrate was below detection and thus not collected. Site 4 shows

very high sulfate throughout the profile and is therefore reflected in the N:S ratios.

3.4.5 Thorne Moors peatland recovery

Peatlands exhibit complex responses to acid sulfate pollution (e.g. Lamers et al., 2001, 2002) and there is considerable debate over their ability to recover and timescale over which this could occur. The recent concentration profiles of sulfate reported here in surface waters at Thorne Moors are similar to profiles seen in non-polluted, non-maritime peatlands (Steinman and Shotyk, 1997). This would suggest that Thorne Moors has recovered from acid deposition and the dominant sink for sulfur is no longer BSR at depth but near-surface plant uptake, as happens in unpolluted wetlands (Lamers et al., 2002). Thus, from the perspective of the biogeochemical cycling of sulfur, the peatland ecosystem at Thorne Moors appears to largely have recovered in the 40 years since the peak sulfur loadings of the early 1970s. This is in line with model predictions for recovery of headwater lakes in peatland catchments in Finland, where declining sulfate and increasing acid neutralising capacity (ANC) should lead to recovery during the period 2010 to 2030 (Posch et al., 2003).

3.5 Conclusions

Figure 3.8 (below) is a schematic representation of the processes occurring in the top 40 cm of a peat bog at Thorne Moors. In the surface of the peat, *Sphagnum* and *Eriophorum* take up the sulfate and nitrate from the surface pore-waters (A), below which the background values are close to detection limits (B). The chloride is not reactive, although there are some subsurface peaks, which may be related to transport of higher chloride water from the surface via preferential flow paths. There are three major processes which increase the sulfate and nitrate at depth and one of

these will affect the chloride concentrations as well. Process C (Figure 3.8) is where there is a “hotspot of decomposition” and can occur at any depth; this can produce elevated sulfate and nitrate but not chloride.

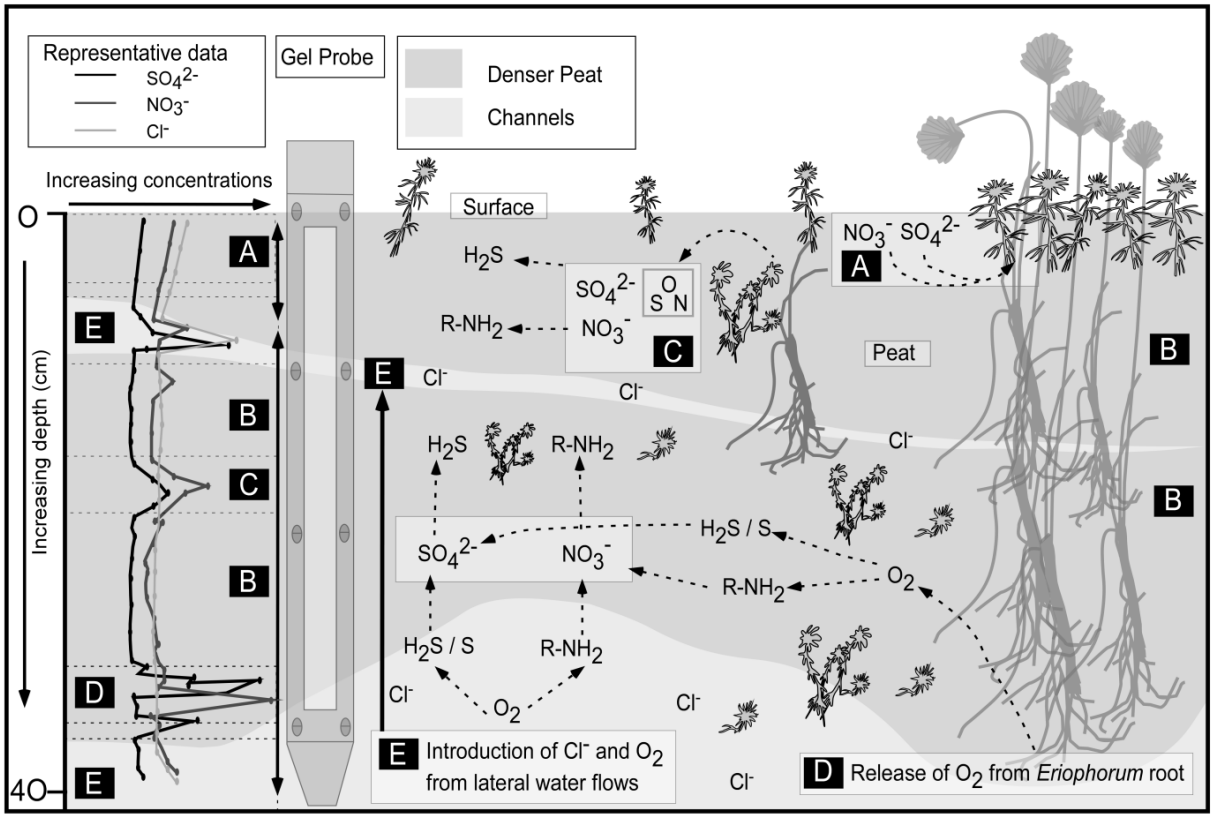

Figure 3.8 Processes at Thorne Moors.

An overview diagram of the processes affecting the DET profiles at Thorne Moors. The far left are real profiles from site 1; the X-axis does not show absolute values due to values being different for each species. Oxidised species of S and N are added to the peatbogs in the surface by atmospheric deposition which bacteria then use up as a source of energy (A) leaving low values throughout the peat (B). Over time the peat can be seen to decompose at the same rates but over very short-periods the peat decomposes differentially which adds short-lived spikes of SO_4^{2-} and $N0_3^-$ (but not Cl^-) which diffuse quickly both up and down the

peat (C). Eriophorum have roots and these exude O_2 which could release O_2 and thus create a microenvironment whereby oxidation of both N and S occur (D). The visual examination of the peat and the shear-vane show evidence for lateral water flows (pipes) which could bring in O_2 from the surface, or at least differing amounts of Cl^-, SO_4^{2-} and NO_3^- from other parts of the peat (E).

When plant material decays and gradually becomes humified to form peat, it releases oxygen, sulfur and nitrogen (Novak et al., 2009; Zaccone et al., 2007, 2011). The decaying plant material releases oxidised forms of sulfur (sulfate) and nitrogen (nitrate). Release of oxidised forms of sulfur at depth has previously been reported by Bartlett et al. (2005) and Blodau et al. (2007) and Knorr and Blodau (2009) suggested that S could be recycled to sulfate by the electron accepting capacity of humics. This process can be seen as discrete peaks in the DET gels that must be only transitory as a steep diffusion gradient is set up, moving nitrate and sulfate upwards and downwards away from the locus of production. Although the decomposition of peat is essentially homogenous, the use of DET gels reveals the heterogeneity of decaying plants when the gel is placed in close proximity to the site of a decay hotspot allowing the observation of transient species on very small spatial and time-scales. At Thorne Moors, there are two main species present within the peatbog, *Sphagnum* and *Eriophorum*, with only the latter having roots. These roots are long which is evident from both the vane shear tests and the cores which were examined before being sliced. The end of the roots release oxygen (Gaynard and Armstrong, 1987) which then reacts with the reduced forms of nitrogen and sulfur, releasing both nitrate and sulfate in the surrounding pore-waters (Process D, Figure 3.8). The data from the DET results strongly suggest that this process occurs between the depths of 30 to 35 cm, additionally the vane shear tests and the visual examination of the peat-cores concur with this. Again, this process will not add

chloride to the pore-water. Where peaks in chloride, nitrate and sulfate coincide, then lateral flow (process E, Figure 3.8) is occurring, associated with a change in hydraulic conductivity that allows lateral water flows to introduce water containing oxygen and high chloride into previously reduced environments, promoting reactions such as 3.2, 3.3, 3.4, and 3.5. Depending on the type of flow, the oxygen may be continuously introduced or it may be a short-lived event. If it is the latter then the resultant sulfate and nitrate will be quickly reduced. The chloride, which is a conservative ion, will diffuse into the surrounding pore-waters.

This sub-study highlights the need for more data and better peat monitoring, if we are to move away from the more simplified acrotelm - catotelm concept, to understand the functionality of peatlands as carbon sinks or sources. The multiple fine scale processes are more complicated than previously thought, and although not directly demonstrating how these systems are likely to respond to changes in anthropogenic activity/inputs, it does suggest that the reduced sulfur loading which Thorne Moors was subjected to until the early 1970s, has now been mitigated giving a recovery of approximately 40 yrs.

3.6 Further work

This work was originally undertaken to compliment the trace metals data; however, the results show that processes occurring in the upper 40 cm are more complicated than previously thought. This dataset was never intended to be a whole sub-study, thus field samples have been collected at different times for different methods. Indeed, a more robust dataset is needed to understand the peat dynamics. Information should be obtained on: water table, peat soil moisture, conductivity porosity and density to understand the bulk properties quantitatively. O_2 data should be acquired

until at least 40 cm depth. The data presented above clearly shows trends both spatially and temporally. Nitrate and sulfate are released at depth whilst chloride isn't suggesting that the process(es) releasing these species are not related to evapotranspiration. It has been hypothesised that some of these peaks are related to 'hotspots' of decomposition, if so then there should be correlating ammonium peaks. Testing for ammonium can be done via the DET gels which can then be analysed by IC for example. Additionally, as the formation of nitrate via nitrification is typically slow, then the amounts of nitrate, ammonium and sulfate should give sensible N:S ratios, which are approximately 5:1. Further knowledge could be gained on the reactions under which sulfate and nitrate are subjected to by sulfur and nitrogen isotope data, which would determine bacterial fractionation of these species. Moreover, if sampled regularly over a set distance and time then a 3D model could be developed, thus so would a comprehensive understanding of how the peat dynamics change over time.

Chapter 4 Thorne Moors Metal Mobility

4.1 Introduction

Ombrotrophic peatbogs have often been used to reconstruct atmospheric deposition as they receive all their inputs, including trace metals, from the atmosphere (e.g. Xia et al., 1997; Shotyk, 1996; Shotyk et al., 2001). These atmospheric trace metals can be from natural sources, e.g. volcanic dust, meteoric and windblown dust (e.g. Nieminen et al., 2007), or anthropogenic, e.g. from heavy industries, hydrocarbon combustion, coal burning, transport, municipal waste, sewage sludge incineration (e.g. Hutton and Symon, 1986) and motor vehicles (Ndiokwere, 1984 and references therein). Consequently anthropogenic sources have significantly increased the amount of trace metals in the atmosphere since the industrial revolution (e.g. Settle and Patterson, 1980; Fengxiang et al., 2002). These trace metals are considered by many to be immobile once deposited because of the peat's high metal-binding capacity (Shotyk, 1996; Crist et al., 1996; Olid et al., 2010). At a broad scale, this appears to be confirmed; many studies using Pb^{210} dated ombrotrophic peatlands have shown that there is a strong correlation between increased atmospheric deposition of trace metals and the start of the industrial revolution, and a decrease in trace metal concentrations with more recent decline of heavy industry and use of leaded petrol (e.g. Mackenzie et al., 1998a; Mackenzie et al., 1998b; Martinez Cortizas et al., 2002; Novak et al., 2008). Similarly in older peat, Bronze Age copper mining can be linked to increased trace metal concentrations (Appleby and Oldfield, 1992; Mighall et al., 2009). Nevertheless, it is still contentious whether peat faithfully records trace metal atmospheric deposition because there are a number of earlier studies that clearly highlighted trace metal mobility within peat bogs (e.g.

Damman, 1978; Urban et al., 1990; MacKenzie et al., 1997). Remobilisation of trace metals within peat bogs could be attributed to any of the following factors: change in the chemical speciation of an element; whether the trace metals were strongly bound to organic matter (OM) or to dust particles when they entered the peat bog; dissolution or precipitation of sorbing phases, e.g. Fe-Mn (hydr)oxides; reactivity and redox sensitivity; changes in physico-chemical conditions within the peatbog (e.g. Shotyk, 1996a; Martinez Cortizas et al., 1997; Twardowska et al., 1999; Brown et al., 2001; Koretsy et al., 2006; Kumpiene et al., 2007 and references therein; Sipos et al., 2008).

Most studies that try to elucidate the mobility of trace metals in peatbogs use a derivative method based on the collection and analysis of cores (e.g. Schell et al., 1989; Urban et al., 1990; Jones and Hao, 1993; Vile et al., 1999; Shotyk et al., 2001; Novak et al., 2011), which generally only achieves a low vertical spatial resolution (typically cm-scale). Alternative methods that can achieve mm-scale resolution are diffusive equilibration in thin films (DET) and diffusive gradient in thin films (DGT), which quantitatively measure pore-water concentrations and fluxes respectively (Zhang et al., 1995; Odzak et al., 2002; Scally et al., 2004; Leermakers et al., 2005). The high spatial resolution allows identification of small individual peaks and steep geochemical gradients, reducing the risk of erroneous interpretations. These methods also make in-situ sampling easy in hydrologically complex peat bogs.

Lead mobility has been previously identified by Urban et al. (1990), who demonstrated (by mass balance equations among other methods) that Pb was mobilised in peatlands. In contrast, Novak et al. (2008), who studied various peatbogs in Europe, showed that there were good correlations with regional peaks in

Pb and increased atmospheric Pb emissions. This sub-study investigates the mobility of trace metal behaviour in a peat bog using DET, which identifies pore-water gradients in metal concentrations that might imply diffusional redistribution of metals, combined with DGT, which identifies rates of supply from the solid to the pore-water, to determine the behaviour of Pb and other metals in a peat bog. The use of DET and DGT alone will not elucidate the sources of the metals, which is crucial to understanding how the metals behave in the peatland, thus the solid-phase concentrations (of major and trace components) are measured in order to help identify their sources. For example, the ash content of the peat bog is a proxy for atmospheric dust input and hence if the trace metal concentrations are related to ash content, this suggests an atmospheric dust source (Kylander et al., 2005). Additionally, the concentrations taken from the solid-phase chemistry help understand longer term behaviour of the metals than is possible from DET or DGT.

4.2 Results

4.2.1 Core bulk properties

Whilst still frozen (Figure 4.1), cores were examined for any obvious changes in peat density and hydraulic conductivity; both cores had discrete layers of variable density which were comparable to each other in terms of depth and location. The upper parts of both cores, i.e. the top 5 cm (core A) and 8cm (core B), contained large amounts of frozen pore-water and live and dead organic matter. A dense root zone was seen down to 37 (core A) and 34 cm (core B) whilst the deepest part of the peat contained fewer roots. Throughout the profile there were discrete zones of lower peat density where larger amounts of frozen pore-water were present.

Figure 4.1 Frozen cores.
Core A to the left and core B to the right. The visual overviews of the cores reveal that there are areas of high and low density peat; this could allow for water pipes within the peat. These cores also show that roots are present throughout much of the core.

4.2.2 Ash

The uppermost peat has an ash content of around 2% in both cores, and it increases with depth (Figure 4.2). In site 1 the ash content initially increases to ~4%, then decreases to less than 2%, increasing to ~8% at approximately 33 cm. Below this there is a sharp decrease, although the last data point shows that the ash content has increased. Site 2 has lower values overall then site 1 and the peaks are less pronounced. Ash in site 2 shows a generally increasing trend with depth, with a local minimum at 26 cm.

4.2.3 Aluminium and scandium

Apart from a major difference in the magnitude of absolute concentrations (Figure 4.2), up to nearly 4000 ppm in Al and 1.5ppm in Sc, these profiles are very similar and follow the ash trend closely in each core.

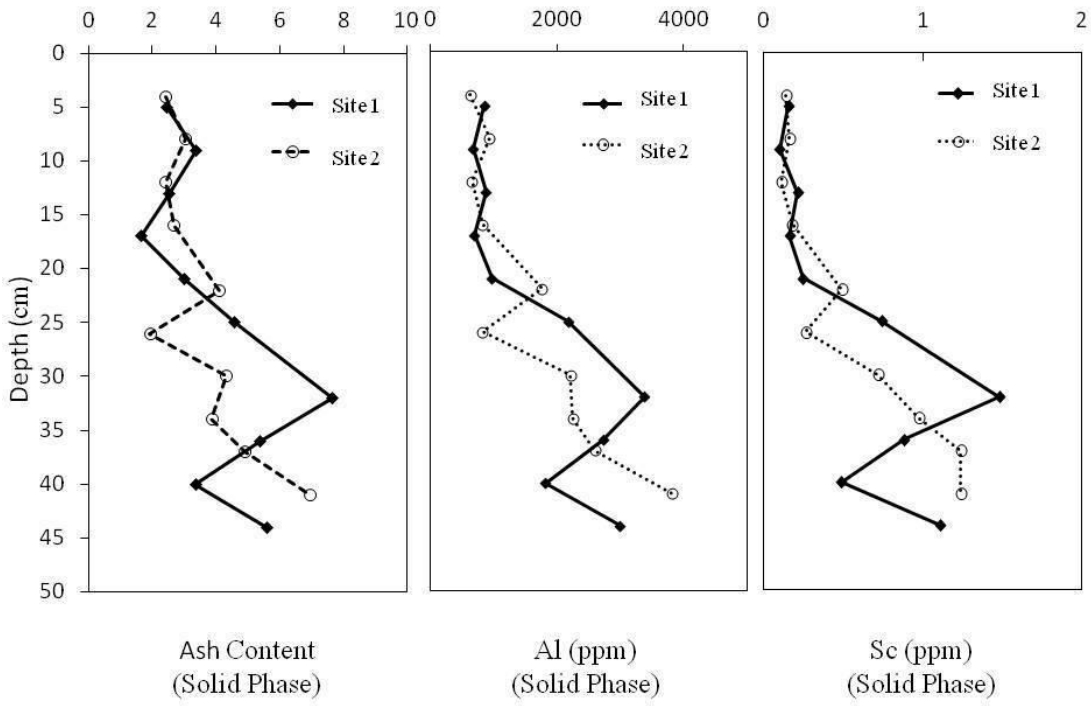

Figure 4.2 **Ash, Al and Sc solid-phase profiles.**
Ash, Al and Sc profiles for Thorne Moors peat bogs for sites 1 and 2. The concentrations of Al, Sc and ash increase towards the deeper measured section, although there is a maximum concentration at approximately 35 cm.

4.2.4 Iron

Solid Phase Iron (Fe_{S-P}): Concentrations in the solid-phase (Figure 4.3) range from ~ 2000 (site 1) and 1300 (site 2) to 4000 ppm, with a median of ~ 2900 in both sites (Table 4.1). At site 1, there is an increase in total Fe concentrations from 21 cm to 40 cm. At site 2, iron concentrations show a local minimum around 26 cm.

Iron Concentrations from Pore-waters (Fe_{DET}): At both sites the iron concentrations (Figure 4.3) are similar throughout the profile, with some scatter and short localized increases in concentrations.

Iron DGT Fluxes (Fe_{DGT}): The upper part of the DGT profiles (Figure 4.3) shows an increase in availability with depth (from 0 to approximately 0.03 $pgcm^{-2}s^{-1}$ in both sites) to a maximum at about 5 cm. Fluxes stay approximately constant to 10 cm

then decrease to lower values in the rest of the profile. At site 2, there are a number of localised peaks that are not evident in site 1.

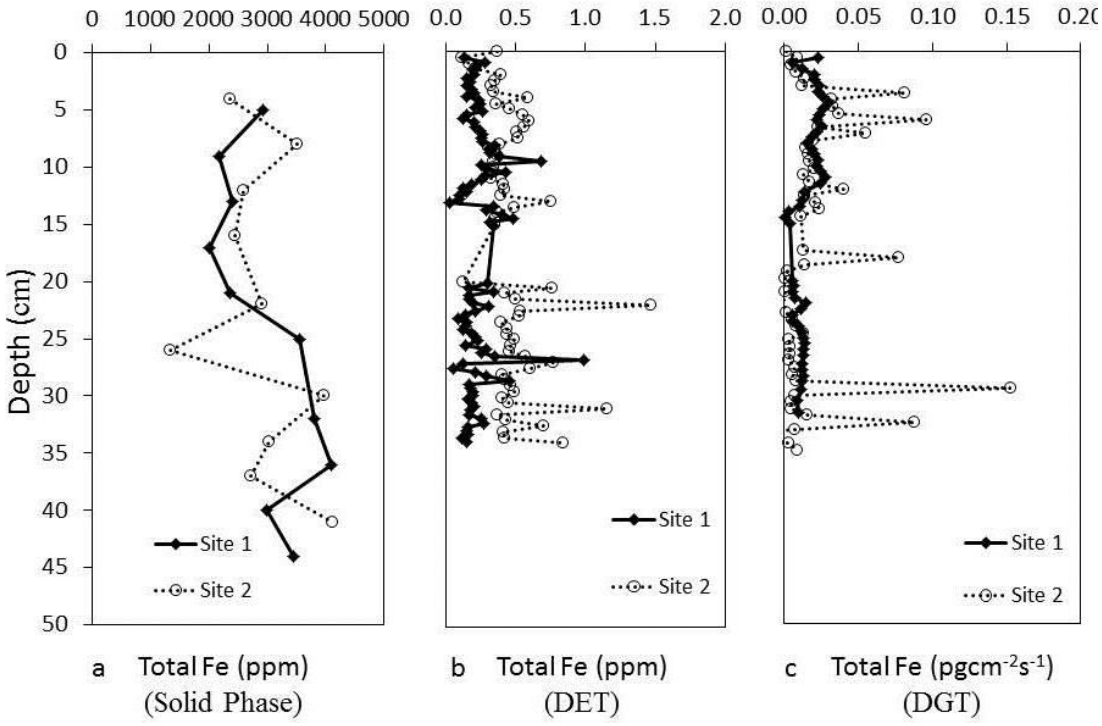

Figure 4.3 Solid-phase and pore-water profiles for iron.
The general trends for the solid-phase Fe concentrations are that it increases with depth. Iron concentrations from DET, although noisy, have a baseline between 0.2 and 0.3 ppm but have sharp 'spikes' in concentrations. Fluxes of available Fe are higher in the near surface than in the deeper part of the peat; again these profiles have flux 'spikes'. So that a longer depth profile is obtained, two probes are placed on an aluminium rod; this creates a gap between the two probes and is between Site 1: 15 and 20 cm (DET) and 15 and 20 cm (DGT). For Site 2 these gaps are at 15 and 20 cm (DET) and 14.5 and 17.5 cm (DGT).

4.2.5 Zinc

Solid Phase Zinc ($Zn_{S\text{-}P}$): Zinc concentrations within the solid phase (Figure 4.4) show a narrow range in concentration between 40 and 50 ppm over the upper 22 cm, below this, concentrations are generally higher with the exception of a local minimum at 26 cm in site 2.

Zinc DET Concentrations (Zn_{DET}): Both sites (Figure 4.4) are generally characterized by a narrow range of Zn concentrations (200 to 400 ppb) throughout the profile, however, there are numerous localized increases in concentration at site 2 (compared with only one in site 1).

Zinc DGT Fluxes (Zn_{DGT}): Below 10 cm depth (Figure 4.4) both profiles generally exhibit a narrow range in Zn flux (around 3 $pgcm^{-2}s^{-1}$). However, in the uppermost 10 cm the two profiles are more different; site 1 shows a minimum of approximately 1 $pgcm^{-2}s^{-1}$ between 2 and 4 cm depth whilst site 2 shows a maximum of 7 $pgcm^{-2}s^{-1}$ over the same interval.

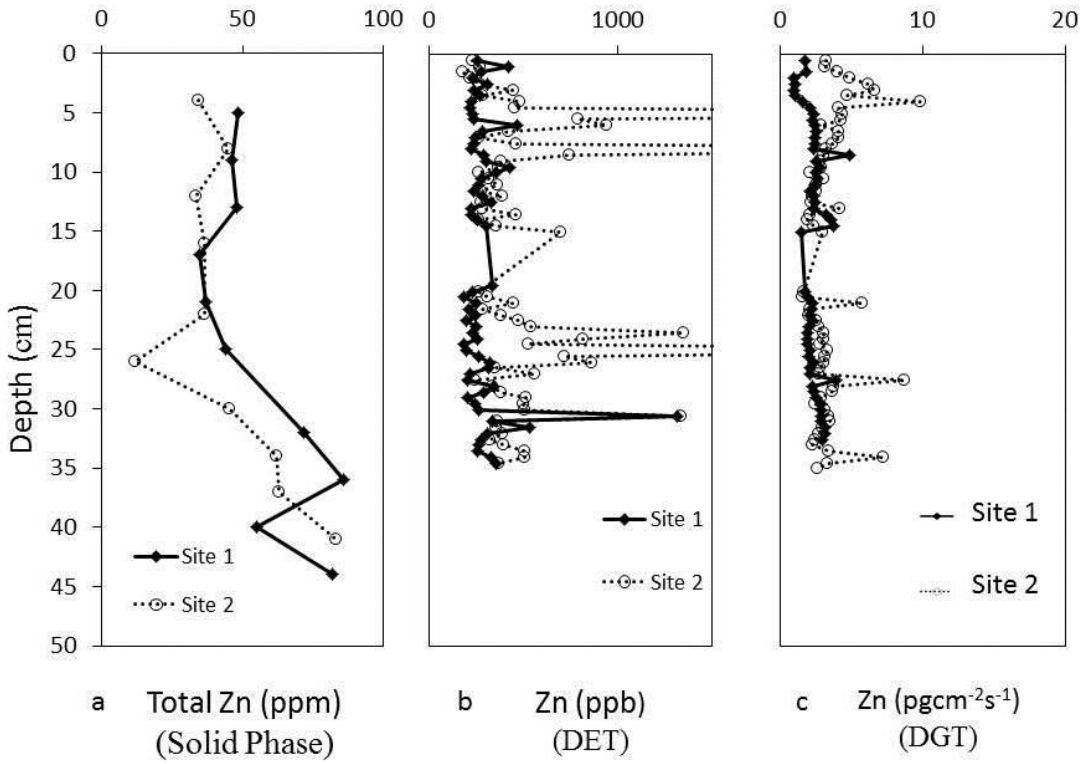

Figure 4.4 Solid-phase and pore-water profiles for zinc.
The general trend for the solid-phase Zn concentrations is that it increases with depth in both sites 1 and 2. Zn concentrations, similar to the other trace metals data are noisy, but have a baseline between 300 and 350 ppb and also have sharp 'spikes' in concentrations. Fluxes of available Zn are higher in the near surface for site 2 than in the deeper part of the peat, whilst there are no major changes in fluxes for site 1; again these profiles have flux 'spikes'. So that a

longer depth profile is obtained, two probes are placed on an aluminium rod; this creates a gap between the two probes and is between Site 1: 15 and 20 cm (DET) and 15 and 20 cm (DGT). For Site 2 these gaps are at 15 and 20 cm (DET) and 14.5 and 17.5 cm (DGT).

4.2.6 Nickel

Solid Phase Nickel ($Ni_{S\text{-}P}$): Nickel concentrations within the solid phase for both sites (Figure 4.5) generally show a gradual increase with depth. However, site 2 shows a pronounced maximum (11 ppm) at 8 cm.

Nickel Concentrations from Pore-waters (Ni_{DET}): For both sites the Ni concentrations generally lie in a range of 15 to 40 ppb throughout the depth profile (Figure 4.5), however, there are a number of localized increases in concentration in the site 2 profile.

Nickel DGT Fluxes (Ni_{DGT}): Both sites (Figure 4.5) show a similar range of variation (0.2 to 0.8$pgcm^{-2}s^{-1}$) but the locations of maxima and minima differ between the two profiles.

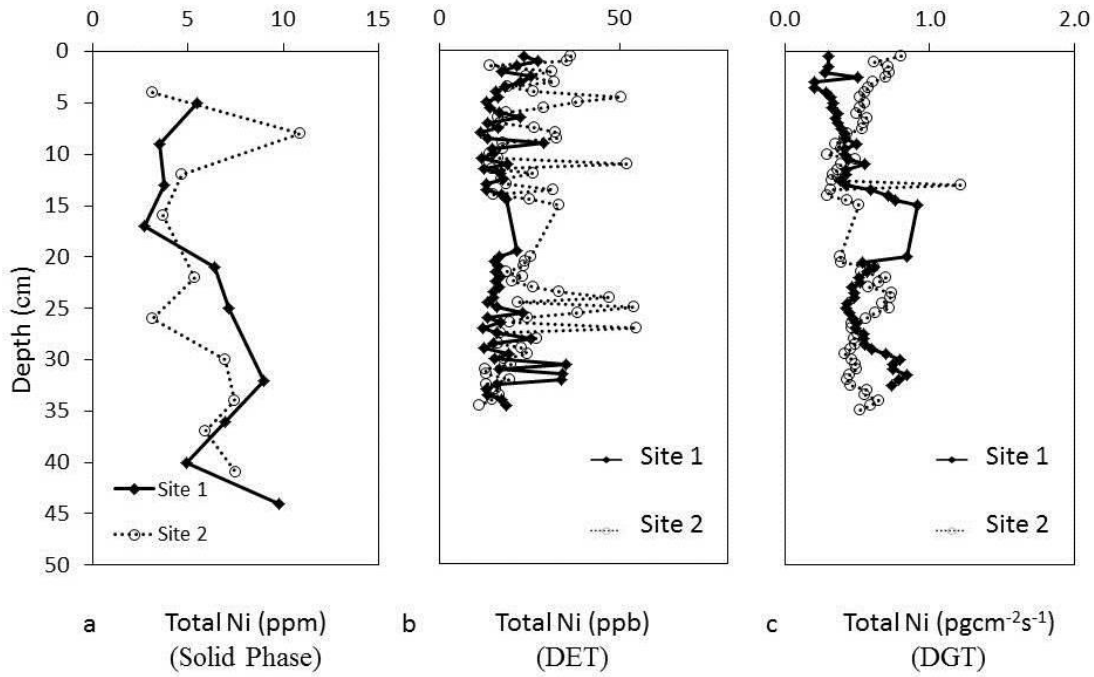

Figure 4.5 Solid-phase and pore-water profiles for nickel.
The general trend for the solid-phase Ni concentrations is that it increases with depth in both sites 1 and 2. The DET pore-water concentration profiles show lots of sharp increases in Ni concentrations throughout the measured section superimposed on background levels which are between ~12 and ~17 ppb (site 1) ~18 and ~30ppb (site 2). Fluxes of available Ni are higher in the near surface for site 2 than in the deeper part of the peat, whilst in site 1 the near surface shows a lower amount of available Ni in the near-surface; however, available Ni is between 0.2 and 0.8 pgcm^{-2}s^{-1} throughout the measured section. So that a longer depth profile is obtained, two probes are placed on an aluminium rod; this creates a gap between the two probes and is between Site 1: 15 and 20 cm (DET) and 15 and 20 cm (DGT). For Site 2 these gaps are at 15 and 20 cm (DET) and 14.5 and 17.5 cm (DGT).

4.2.7 Cadmium

Solid Phase Cadmium ($Cd_{S\text{-}P}$): In both profiles (Figure 4.6), Cd concentrations increase with depth from 0.3 ppm to 1.6 ppm, however, there are superimposed local minima at 40 cm (site 1) and 26 cm (site 2).

Cadmium Concentrations from Pore-waters (Cd_{DET}): Both profiles (Figure 4.6) are characterized by a similar range of variation (1 to 5 ppb) over the depth investigated.

However, superimposed upon this there are a number of local maxima in both profiles.

Cadmium DGT Fluxes (Cd_{DGT}): Measured Cd fluxes are low compared to the other metal fluxes described above (Table 4.1). In site 1, there is very little variation in flux values (0.005 to 0.01 $pgcm^{-2}s^{-1}$) over the whole profile, apart from a sharp peak at 22.5 cm where fluxes reach 0.05$pgcm^{-2}s^{-1}$(Figure 4.6). Site 2 however, has higher fluxes (0.02 to 0.05, single point at 0.3 $pgcm^{-2}sec^{-1}$) in the upper 15 cm. Below 15 cm, the profile at site 2 is similar to site 1.

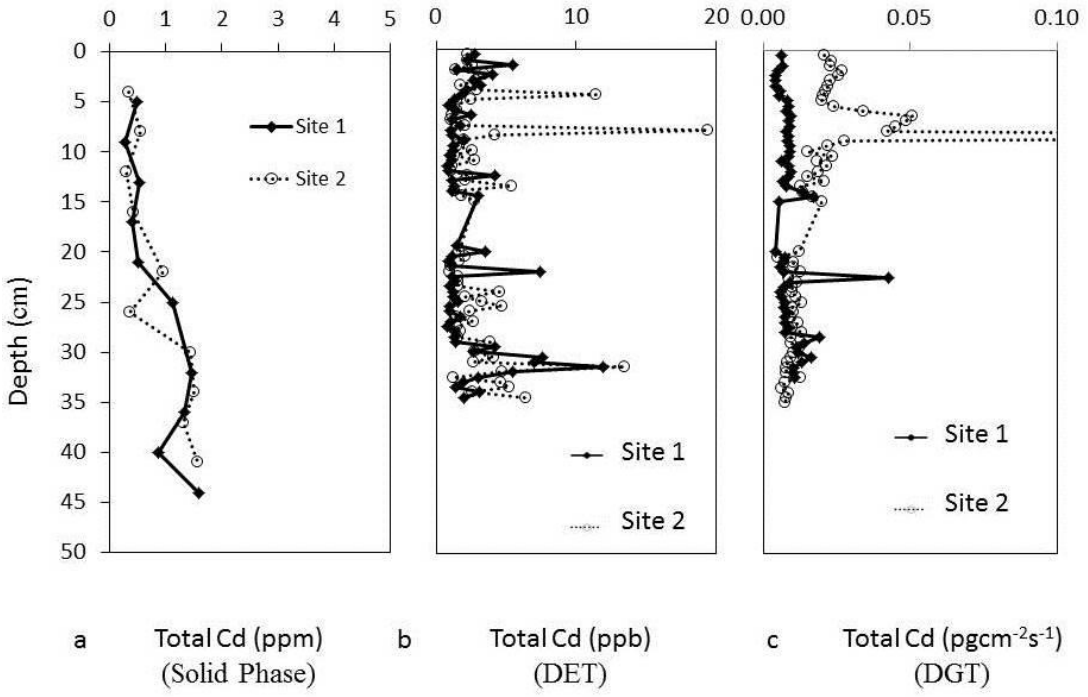

Figure 4.6 Solid-phase and pore-water profiles for cadmium.
The general trend for the solid-phase Cd concentrations is that it increases with depth in both sites 1 and 2. The DET pore-water concentration profiles for Cd show that the concentrations are low throughout (around 1 to 2 ppb site 1; 1 to 5 ppb site 2); again there are sharp increases in concentrations of Cd, particularly so for site 2. Fluxes of available Cd are higher in the near surface for site 2 than in the deeper part of the peat, whilst in site 1 the fluxes are close to 0.009 $pgcm^{-2}s^{-1}$ throughout the measured section. Below ~20 cm, flux values are close to 0.009 $pgcm^{-2}s^{-1}$ throughout the rest of the profile. So that a longer depth profile is obtained, two probes are placed on an aluminium rod; this creates a gap between the two probes and is

between Site 1: 15 and 20 cm (DET) and 15 and 20 cm (DGT). For Site 2 these gaps are at 15 and 20 cm (DET) and 14.5 and 17.5 cm (DGT).

4.2.8 Cobalt

Solid Phase Cobalt (Co_{S-P}): In both profiles (Figure 4.7), Co concentrations increase with depth from 0.4 ppm to 1.8 ppm, however, there are superimposed local minima at 40 cm (site 1) and 26 cm (site 2).

Cobalt Concentrations from Pore-waters (Co_{DET}): At both sites (Figure 4.7) Co concentrations in the upper 1.5 cm (0.3 to 0.7 ppb) are lower than the rest of the profile (0.8 to 1.5 ppb).

Cobalt DGT Fluxes (Co_{DGT}): Measured Co fluxes (Figure 4.7) are very low compared to the other metal fluxes described above (Table 4.1). In site 1, there is little variation in flux values (0.001 to 0.004 $pgcm^{-2}s^{-1}$) over the whole profile. Site 2 however, has far higher fluxes (0.003 to 0.006 $pgcm^{-2}s^{-1}$) in the upper 8 cm. Below this the profile at site 2 is similar to site 1.

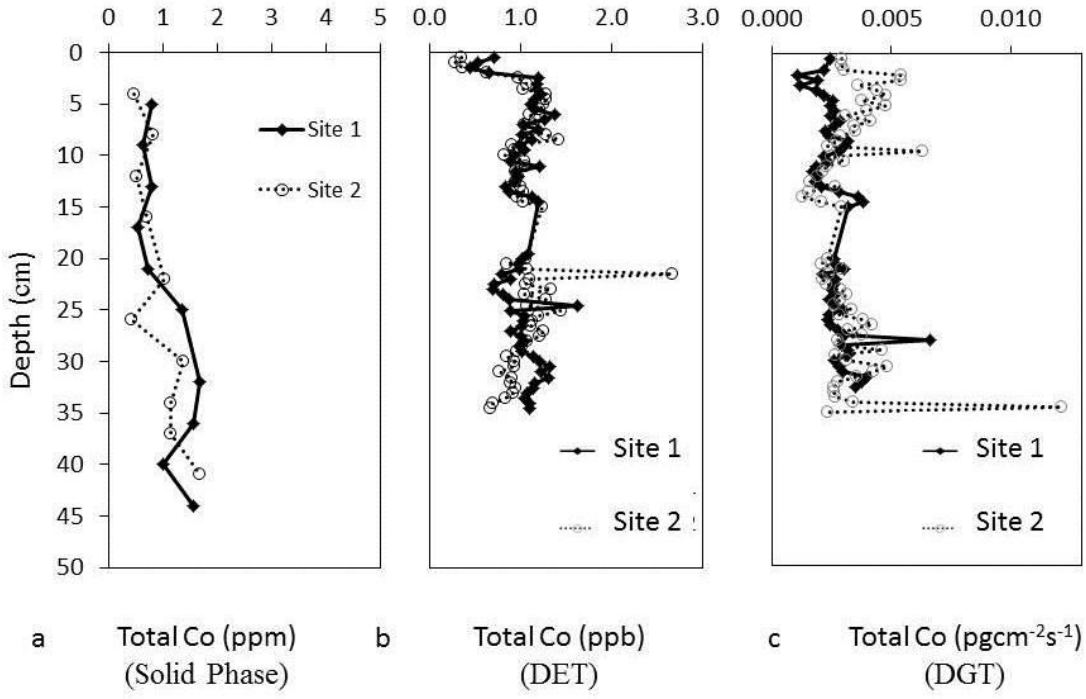

Figure 4.7 Solid-phase and pore-water profiles for cobalt.
The general trend for the solid-phase Co concentrations is that it increases with depth in both sites 1 and 2. There is a sharp decrease, followed by a sharp increase in concentrations for both sites 1 and 2 in the very near-surface; after this and in both sites the Co concentrations are close to 1 ppb. Fluxes of available Co are higher in the near surface for site 2 than in the deeper part of the peat, whilst in site 1 the fluxes are lower in the near surface. Deeper than this, fluxes are close to 0.002 and 0.003 pgcm^{-2}s^{-1} throughout the rest of the profiles. So that a longer depth profile is obtained, two probes are placed on an aluminium rod; this creates a gap between the two probes and is between Site 1: 15 and 20 cm (DET) and 15 and 20 cm (DGT). For Site 2 these gaps are at 15 and 20 cm (DET) and 14.5 and 17.5 cm (DGT).

4.2.9 Lead

Solid Phase Lead (Pb_{S-P}): Both profiles are characterized by low concentrations in the upper 20 cm (15 to 35 ppm) (Figure 4.8). Below this there are maxima at 32 cm (102 ppm) site 1 and 34 cm (135 ppm) site 2, with superimposed local minima at 40 cm site 1 and 26 cm site 2.

Lead Concentrations from Pore-waters (Pb_{DET}): In both profiles Pb concentrations in the uppermost 1.5 cm are low (5 to 20 ppb) below which there is a well-defined maximum (93 ppb at 3 cm). Below 5 cm depth both profiles exhibit a similar range of variability, between 20 and 40 ppb (Figure 4.8).

Lead DGT Fluxes (Pb_{DGT}): Both profiles (Figure 4.8) are similar with fluxes between 0.05 and 0.11 pgcm^{-2}s^{-1} over the depth range measured, with the exception of site 1 which has lower fluxes (0.03 to 0.06 pgcm^{-2}s^{-1}) in the upper 5 cm.

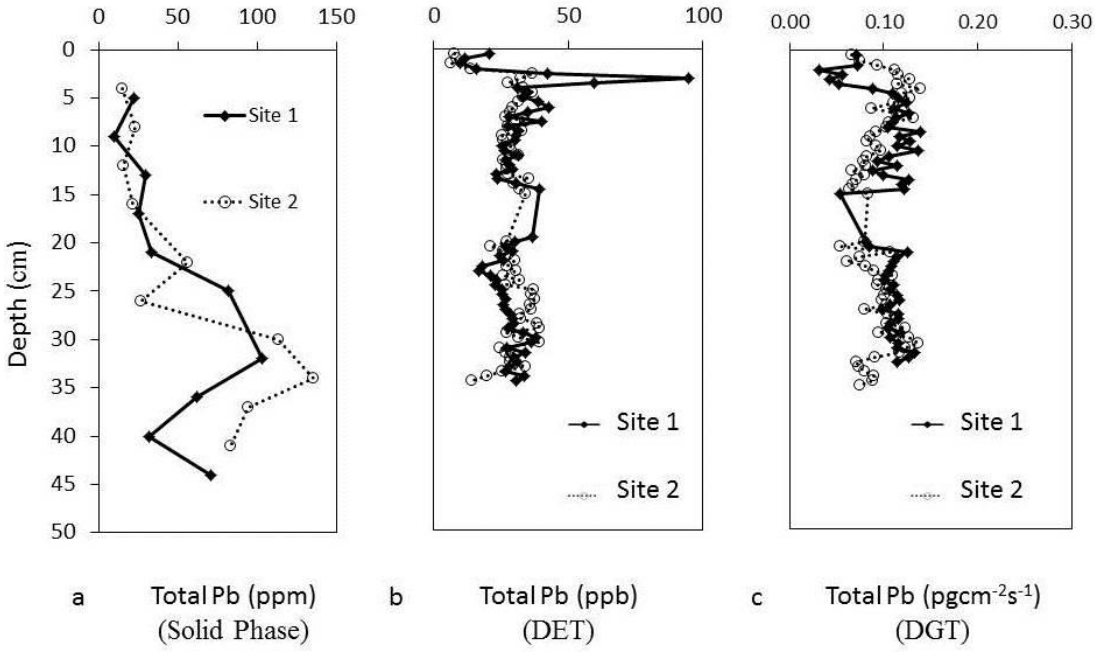

Figure 4.8 Solid-phase and pore-water profiles for lead.
The general trend for the solid-phase Pb concentrations is that it increases with depth in both sites 1 and 2. Similar to the profiles for Co, there is a sharp decrease, followed by a sharp increase in concentrations for both sites 1 and 2 in the very near-surface; however the increase in much larger in Pb for site 1. Concentration values lie between 25 and 35 ppb. Fluxes of available Pb are lower in the near surface for sites 1 and 2 than in the deeper part of the peat. Deeper than this, fluxes remain between 0.055 and 0.13 pgcm^{-2}s^{-1}. So that a longer depth profile is obtained, two probes are placed on an aluminium rod; this creates a gap between the two probes and is between Site 1: 15 and 20 cm (DET) and 15 and 20 cm (DGT). For Site 2 these gaps are at 15 and 20 cm (DET) and 14.5 and 17.5 cm (DGT).

4.2.10 Copper

Solid Phase Copper ($Cu_{S\text{-}P}$): Both profiles (Figure 4.9) are characterized by low concentrations in the upper 20 cm (3 to 13 ppm). Below this there are maxima at 32 cm (36 ppm) site 1; 37 cm (31 ppm) site 2, with a superimposed local minima at 40 cm site 1 and 26 cm site 2.

Copper Concentrations from Pore-waters (Cu_{DET}): The profiles for sites 1 and 2 are very similar to each other (Figure 4.9). Most data lie in the range 24 to 60 ppb but there are numerous localized increases in both profiles (up to 250 ppb).

Copper DGT Fluxes (Cu_{DGT}): Over the depth interval 6 to 15 cm (Figure 4.9), profiles for sites 1 and 2 are similar, with fluxes of 0.25 to 0.35pgcm^{-2}s^{-1} between 6 and 12 cm depth increasing to approximately 0.7 pgcm^{-2}s^{-1}at 15 cm. In the uppermost 6 cm, fluxes at site 1 (0.2 to 0.4 pgcm^{-2}s^{-1}) are lower than those at site 2 (0.4 to 0.65 pgcm^{-2}s^{-1}). Below 20 cm, fluxes are also generally higher at site 2 than site 1.

NB: in the DGT data where the probe joins (between 15 and 20 cm) and in both sites, there is potentially one large peak in the Cu flux or two sharp peaks. As this is where the two probes join it is hard to interpret if this is an artefact of the probe construction or is a real flux increase, thus interpretation has been approached with caution.

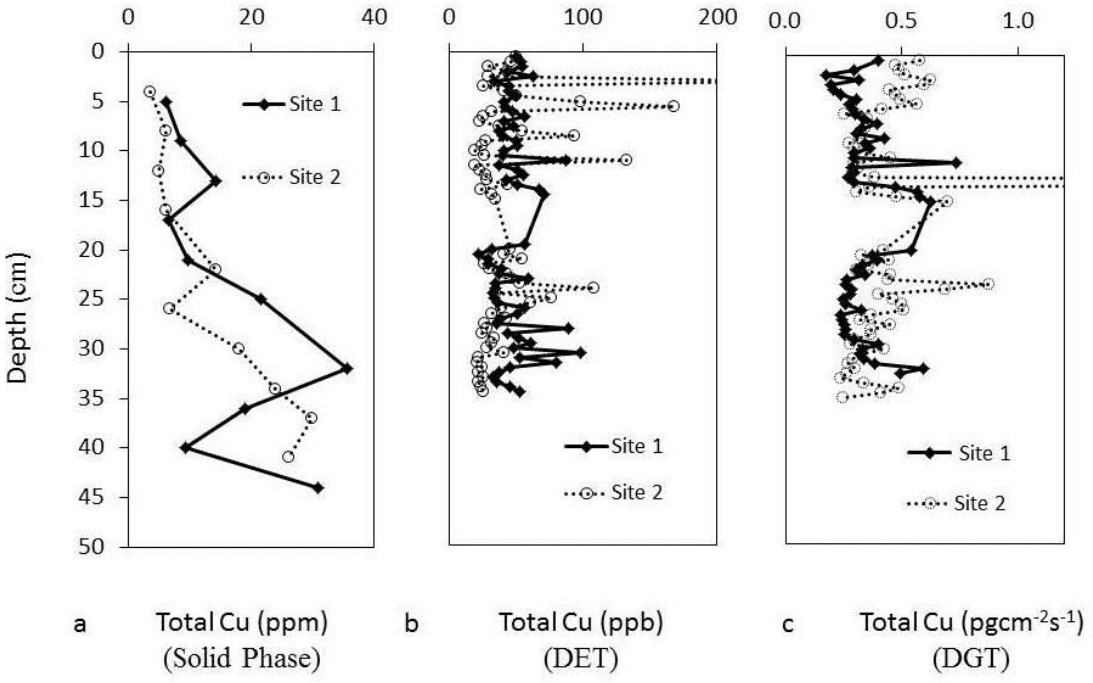

Figure 4.9 Solid-phase and pore-water profiles for copper.
The general trend for the solid-phase Cu concentrations is that it increases with depth in both sites 1 and 2. The DET pore-water profiles for site 2 shows that there are many spikes of Cu throughout the measured section; however, the background concentrations of Cu lie between 20 and 50 ppb for both sites 1 and 2. Fluxes of available Cu are higher in the near-surface for site 2 and are then between 0.3 and 0.5 pgcm^{-2}s^{-1}, however there are 'spikes' of flux increases throughout the measured section. So that a longer depth profile is obtained, two probes are placed on an aluminium rod; this creates a gap between the two probes and is between Site 1: 15 and 20 cm (DET) and 15 and 20 cm (DGT). For Site 2 these gaps are at 15 and 20 cm (DET) and 14.5 and 17.5 cm (DGT).

4.3. Discussion

4.3.1 Solid-phase

4.3.1.1 Correlation with ash (mineral matter)

Atmospheric particles can be classified into three types; the "transient nuclei mode" (~0.01μm); "accumulation" (~0.1 to 1.0 μm) and 'mechanical aerosol' (~10 μm) (e.g. Williams and Harrison, 1984; Allen et al., 2001). For any element, the size of the particle, particle surface roughness and wind velocities determine the distance a particle will travel before being washed out of the atmosphere (Williams and Harrison, 1984), whilst the type of deposition process (i.e. dry or wet deposition) the metal compounds undertake depends on particle size, vapour pressure, heat of solution and solubility (e.g. Galloway et al., 1982). In the UK, the principal anthropogenic source for Co and Ni is fossil fuel combustion and a large contributor for Cu and Zn; Cd, Cu, Ni, Pb and Zn are produced from industrial metallurgical processes (Pacyna, 1986; Allen et al., 2001; Lee et al., 1994). Exhaust emissions (petrol and diesel) increase Pb, Fe, Cu, Zn, Ni and Cd into the atmosphere and tyre rubber abrasion is a source of Zn and Cd (Pacyna, 1986; Allen et al., 2001). Allen et

al. (2001) determined that Cu and Pb were mainly found in the accumulation mode in sites across the UK, whilst Fe was mainly found in the coarse mode, and Ni, Zn, Cu and Co were in varying modes in-between. Thus it is hard to determine which type of deposition will be dominant at Thorne Moors. However, prevailing winds for Thorne Moors are from the SW, therefore pollution will principally be from the industrialised Midlands (Thorne Moors is downwind of power stations within the Trent Valley), as well as pollution from the nearby motorway networks (Figure 1.5; Chapter 1) and therefore most pollutants at this site are likely to be deposited via dry deposition (e.g. dust). For example, some pollutants from the motorways will only travel short distances as they are large particles, (Cd, derived principally from impurities within zinc compounds (engine oil and tyre debris) could be as large as 30μm; e.g. Ward et al., 1977; Mankovska, 1977; David and Williams, 1975). Therefore most of the trace metal input to Thorne Moors is from vehicle and coal burning activities.

By definition ombrotrophic peatbogs only receive metal inputs from the atmosphere (e.g. Xia et al., 1997; Shotyk, 1996). Ash is a proxy for dust, which controls the supply flux of metals into the peatbog and it is therefore assumed that the dust input will correspond with the ash content profiles of the peat. Given that the profiles follow similar trends to the ash, then it can be assumed that dust is the main source (Figure 4.10).

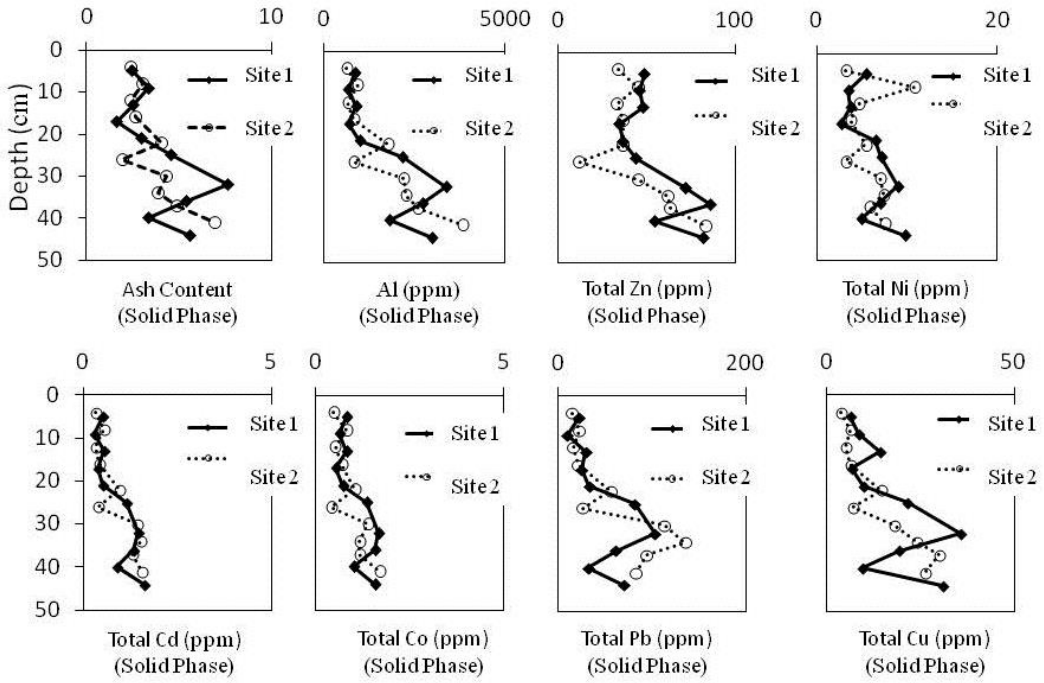

Figure 4.10 Solid-phase profiles for all sites and all elements.
The solid-phase data shows that all profiles (apart from Ni in site 2; discussed later) show similar trends with maximum ash content and concentrations for all trace metals are within the deeper part of the peat whilst the minimum is within the shallower section.

The trends in the profiles show that for both sites the maximum ash content and concentrations for all trace metals are within the deeper part of the peat whilst the minimum is within the shallower section; the exception to this is Ni in site 2 (discussed later). This would suggest that all metals are relatively immobile as the peaks in concentrations within the solid-phase broadly correlate with one another. However, iron mimicking the pattern of the ash content is unexpected as it is a redox-sensitive species and peatbogs show more reducing conditions with depth. Additionally, Fe is likely to have been used in the uptake and recycling by vegetation (e.g. MacKenzie et al., 1998). This therefore implies that, even though all metals analysed largely follow the ash pattern, there must be detail missing. There are two mechanisms which affect the ash content relative to the organic matter content: i)

initial dust input relative to peat formation: ii) extent of organic matter decomposition throughout the peat bog profile (Kylander et al., 2005). The latter would cause an increase in ash content relative to organic matter with depth as decomposition of organic matter proceeds. Comparing the ash content to Sc and Al is useful as these are relatively geochemically conservative metals that have no significant anthropogenic source and dust input is their only significant source (e.g. Shotyk, 2000; Shotyk, 1996; Steinmann and Shotyk, 1997; Shotyk et al., 2001; Voldrichova et al., 2014). Indeed, Al in surface waters in pH < 4.9 shows conservative behaviour (Nordstrom and Ball, 1986) and is likely to be in the relatively insoluble aluminosilicate fraction (Shotyk, 1996; Steinmann and Shotyk, 1997; MacKenzie et al., 1998; Shotyk et al., 2001). Additionally, Sc is widely dispersed due to its association with light Fe- Mn-rich minerals (Curtis, 1972). Thus any changes to inputs of atmospheric dust can be identified easily as coincident changes in the profiles of ash content, Al, and Sc, which are very similar (Figure 4.2). As Al and Sc correlate so closely with ash, plots of metal ratios to Al and Sc in the solid-phase can be used to remove the effects of variability of dust content (Figures 4.11 and 4.12 respectively).

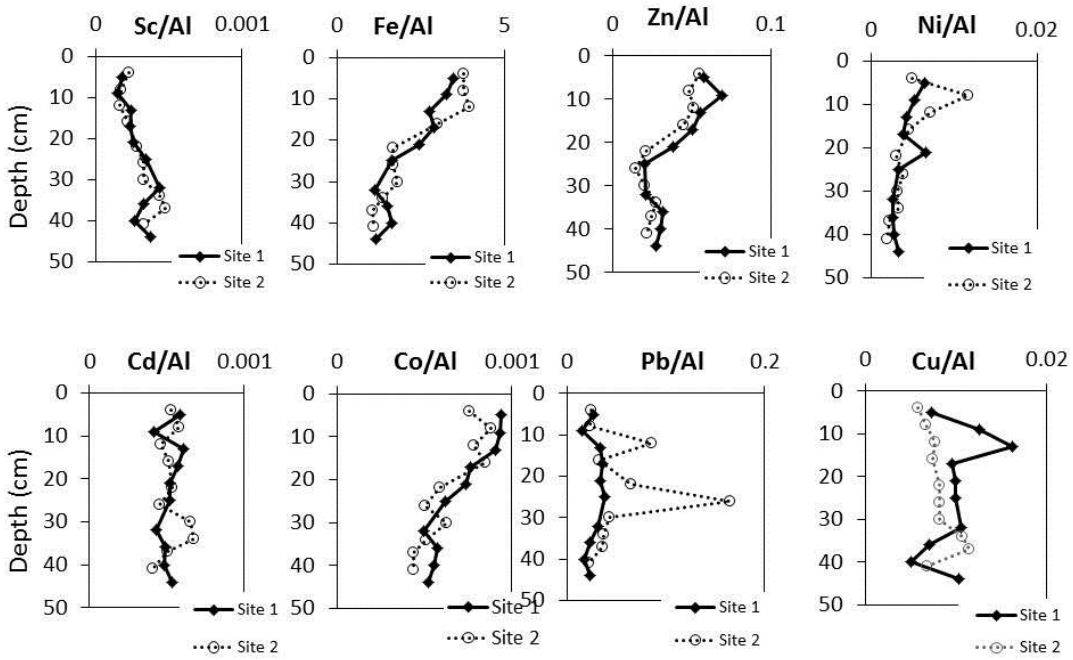

Figure 4.11 Metal ratios to Al.

Al is added to the peatbog via dust and is likely to be in the relatively insoluble aluminosilicate fraction. As Al correlates so closely with ash, plots of metal ratios to Al in the solid-phase can be used to remove the effects of variability of dust content. Any increases in the trace metal will then identify either: i) increase or decrease in trace metal deposition from the atmosphere or: ii) trace metal mobility.

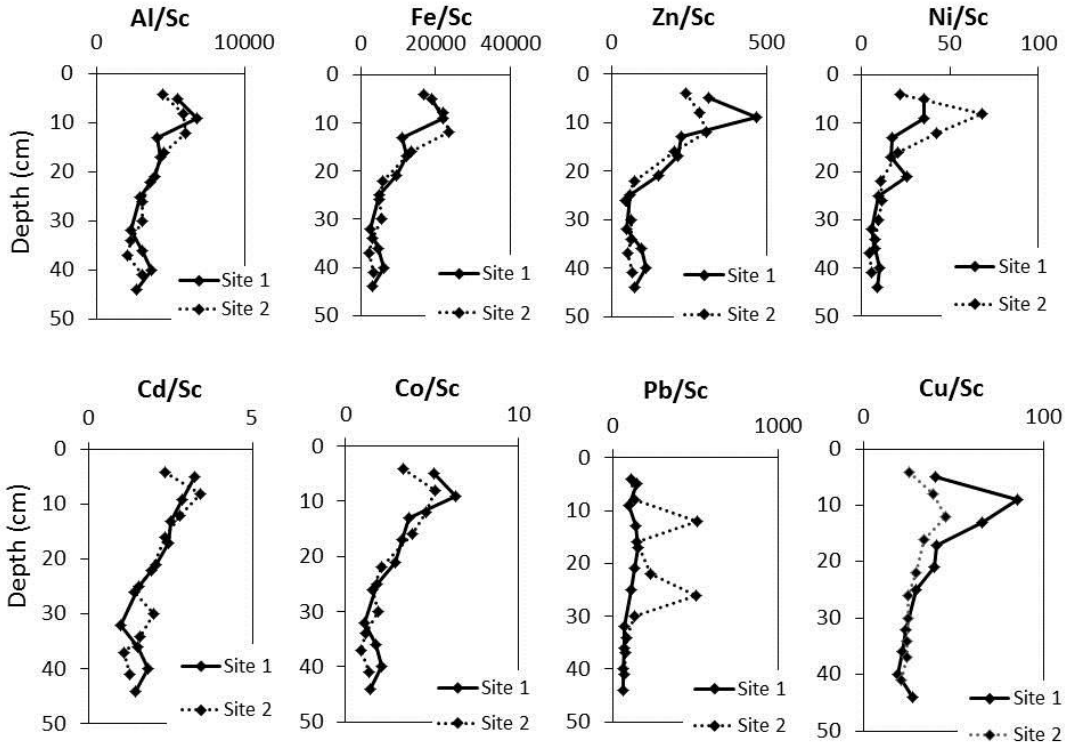

Figure 4.12 Metal ratios to Sc.
Similar to Al, Sc is added to the peatbog via dust and is unlikely to be mobile. This data is useful to check against the Al data and see if the Sc correlation matches with the Al:trace metals. As with Al, Sc in the solid-phase can be used to remove the effects of variability of dust content. Any increases in the trace metal will then identify either: i) increase or decrease in trace metal deposition from the atmosphere or: ii) trace metal mobility.

Al and Sc show that they are marginally variable compared to one another (Figures 4.11 and 4.12), with a minor amount of Sc increase with depth compared to Al; suggesting either that one of the elements is mobile or that there has been a marginal reduction in atmospheric Sc recently compared to Al. MacKenzie et al. (1998) observed that in an ombrotrophic peatbog in Scotland, although for the most part the trends matched between the Al and ash profiles, the maximum concentration peaks did not; suggesting that ash had a significant source of another mineral that wasn't aluminosilicate minerals. Al:Sc profiles from this study suggest that there is an

increase in the aluminosilicate minerals compared to Sc minerals in the recent past. This could potentially be related to minor changes in the composition of fly ash to the atmosphere.

Fe/Al and Fe/Sc show similar trends with a zonation pattern of high values in the upper part of the peat, lower values in the middle section and lowest values in the deepest section measured. Clearly Fe has been mobilised relative to Al and Sc, and the high near surface Fe/Al, Fe/Sc, ratios in the solid-phase records a history of Fe accumulation in the upper parts of the peat. Similar to Fe, both Zn and Co also show zonation patterns when normalised to Al or Sc, again with the same three zonation patterns; highest values within the upper layers of the peat, lower values in the middle section, and the lowest values within the deeper section (Figure 4.11 and 4.12). This suggests mobility with the ratios recording a history of accumulation of Zn and Co within the upper parts of the peat. Ni/Al and Ni/Sc profiles (Figure 4.11 and Figure 4.12) in both sites show a decrease of Ni relative to Al and Sc throughout the profiles from the top of the peat to the deeper section. In both datasets this shows a near-surface accumulation of Ni within the peat. This suggests that Fe, Zn, Co and Ni are mobile within Thorne Moor peatbogs.

Pb (site 2 only) shows two large peaks of Pb enrichment compared to Al at approximately 12 and 25 cm depth, which is shallower than the large peak of Pb seen within the Pb solid-phase profiles. This suggests that there is another source of Pb. The most documented pollution from vehicles is lead tetraethyl which was added to fuel from c. 1930's to 2000 (dates are for the UK), where it was readily released into the atmosphere when combusted (Lee & Tallis, 1973; Ndiokwere, 1984). Both peaks are postulated to be related to anthropogenic activity and potentially both are related

to the use of leaded petrol, which releases more Pb than Al into the atmosphere. It is unclear why the lead peaks have been retained in site 2 and not site 1.

The ratios for Cd compared to Al and Sc do not show similar patterns. When comparing Cd against Al, there doesn't appear to be much change and therefore it is suggested that Cd does correlate well with Al and therefore ash, suggesting that Cd is immobile. Using Sc, however, there appears to be an enrichment of Cd from depth to the near surface compared to Sc; suggesting mobility of Cd. Similarly, the profiles for Cu compared to Al and Sc do not show similar trends, however the ratio profiles do however suggest a near-surface sink (Figures 4.11 and 4.12). Cu/Sc profiles show a slight enrichment of Cu compared to Sc from depth to the near surface. Cu/Al, however, show no change in the profiles apart from a major enrichment of Cu in the near-surface and a major decrease in the deeper part of the peat. It is unclear why the comparisons of both Al and Sc to Cu and Cd are returning different results. As there is not much variation between the other profiles and Al or Sc however, it suggests that there must be some interaction between Al or Sc and Cd and Cu. As noted earlier, the Al:Sc profiles from this study suggest an increase in the aluminosilicate minerals compared to Sc minerals in the recent past, which has been postulated to be related to variations in composition with fly ash received by the peatbog. If Cu has also increased because of the fly ash than this would cause the profile of Cu/Al to not vary much (ignoring the large enrichments of Cu relative to Al), which would also cause an apparent increase of Cu relative to Sc from depth to the surface. This is the same with Cd. Therefore it is postulated that some fraction of both Cd and Cu are associated with the aluminosilicate minerals compared to Sc minerals in the recent past.

Comparing the trace metals to Al and Sc has helped to identify which metals are potentially mobile; however, plotting each metal against ash content determines how strong the correlations are, as shown by r^2, which helps identify which trace metals are predominantly related to dust deposition (Figure 4.13 and Table 4.1). Al, Sc and Co all correlate very strongly with ash (r^2>0.8), Cu and Cd have r^2>0.7. Fe and Zn correlate considerably less well with ash (r^2>0.6) and Pb and Ni exhibit much weaker correlations (r^2>0.4); Table 4.1. Even though all trace metals appear to closely follow the ash profiles, those with weaker correlations are likely to be more strongly affected by post-depositional processes occurring within this peat or have another atmospheric source.

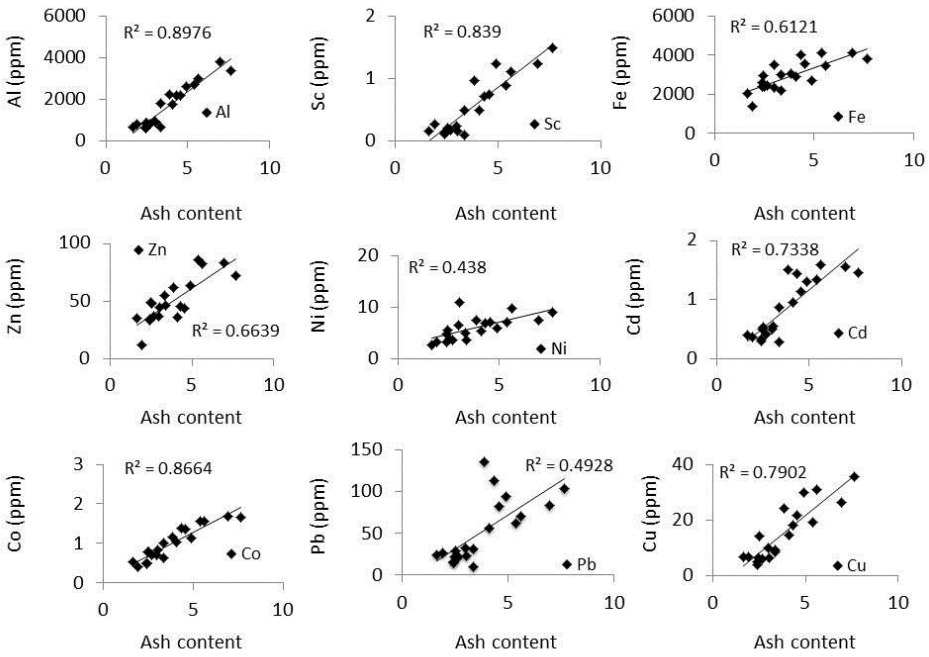

Figure 4.13 Metals against ash content.
Ash is a proxy for dust, which controls the supply flux of metals into the peatbog. Given that the profiles follow similar trends to the ash, then it can be assumed that dust is the main source. Numbers with a higher r^2 show that there is a good correlation with ash, whilst numbers with a lower r^2 do not correlate well with ash suggesting more than one source (e.g. additional Pb from motor vehicle emissions) or mobility within the peat matrix.

		R^2 Values			Confidence Interval		
Element	Correlation with ash?	Core A	Core B	Combined Cores A & B	Core A	Core B	Combined Cores A & B
Al	Yes	0.882	0.9458	0.8976	>99.9%	>99.9%	>99.9%
Sc	Yes	0.9196	0.7662	0.839	>99.9%	>99.9%	>99.9%
Fe	Not at the top	0.694	0.4817	0.6121	>99.9%	>99.9%	>99.9%
Zn	Not at the top	0.604	0.7972	0.6639	>99.9%	>99.9%	>99.9%
Ni	Not at the top	0.7224	0.2051	0.438	>99.9%	99.9%	>99.9%
Cd	Yes	0.7764	0.7386	0.7338	>99.9%	>99.9%	>99.9%
Co	Yes	0.8544	0.8986	0.8664	>99.9%	>99.9%	>99.9%
Pb	Sometimes	0.7924	0.4254	0.4928	>99.9%	>99.9%	>99.9%
Cu	Yes	0.8546	0.7164	0.7902	>99.9%	>99.9%	>99.9%

Table 4.1 **Information retrieved from solid-phase chemistry.**
This data establishes if there is a correlation with ash and the overall trends. Numbers with a higher r2 show that there is a good correlation with ash whilst numbers with a lower r^2 do not correlate well with ash suggesting more than one source (e.g. additional Pb from motor vehicle emissions) or mobility within the peat matrix. The confidence interval shows that the numbers were not determined by chance.

Al and Sc correlating well with dust is unsurprising as both these elements are conservative and the main source for the elements are dust (e.g. Nordstrom and Ball, 1986; Shotyk, 1996; 2000; Steinmann and Shotyk, 1997; MacKenzie et al., 1998; Shotyk et al., 2001; Voldrichova et al., 2014). Co correlating well with ash suggests that it is immobile; this is in agreement with other studies and is due to Co not being influenced by redox driven processes, and any uptake and recycling of Co in plants is negligible (e.g. MacKenzie et al. 1998).

Major sources of Cu to the peatbog are expected to be trace Cu in natural dust inputs or anthropogenic sources such as coal burning or smelter emissions. Within these sources Cu is likely to be present as copper oxides or copper sulfides. The main atmospheric source of Cu to a peatbog exerts influence over Cu diagenesis once deposited in the peat matrix. For example, if the main source of Cu to the peatbog is copper sulfide, and the peat accumulation rates are fast relative to the dissolution rates, then the Cu sulfides which are thermodynamically stable under reducing conditions, will be preserved and rendered immobile as long as the conditions remain (Rausch et al., 2005). As coal burning is the main pollutant for this site then Cu oxides are the main pollutant of Cu to Thorne Moors and these minerals are expected to undergo dissolution within the peat (Rausch et al., 2005). Cu has a high affinity with OM though and binds strongly in ombrotrophic peatbogs (e.g. Rothwell et al., 2010) resulting in Cu being either mobile or immobile. The Cu data correlates well with ash suggesting immobility, thus we postulate that the high affinity Cu has with OM renders it immobile. It has been suggested that Cd also has a high affinity with OM and forms stable organic compounds in peatbogs similar to Cu (Stewart and Fergusson, 1994). Motor vehicles emit Cd predominantly as impurities within zinc compounds, e.g. zinc dithiophosphate in engine oil and tyre debris when zinc-

diethyl is used during tyre vulcanisation. These dust particles are typically large (30μm; e.g. Ward et al., 1977; Mankovska, 1977; David and Williams, 1975) and therefore remain in the atmosphere for shorter periods of time. Therefore concentrations of Cd at Thorne Moors are probably influenced by the network of motorways close by and most likely entered the peatbog as dust. As ash is a proxy for dust and ash correlates well with cadmium then Cd shows negligible mobility.

Fe and Zn are not expected to correlate well with ash as Fe is influenced by pH and redox conditions within the peat and there is evidence that Zn is mobile within peatbogs (e.g. Sugden, 1993; MacKenzie et al., 1998; Weiss et al., 2007). For example, Weiss et al. (2007) showed that peaks in Zn concentrations and changes in isotopic signatures pre-dated the anthropogenic input in three Finish peatbogs. MacKenzie et al. (1998) also show that Zn is mobile as peatbog cores did not faithfully record the heavy industry in Scotland. Post-depositional processes included biological cycling by vegetation, and ion exchange and adsorption (MacKenzie et al., 1998: Weiss et al., 2007). Iron is also strongly affected by biological cycling by vegetation and is a well-known redox sensitive species (e.g. Chesworth et al., 2006). In addition, the majority of iron entering the peatbog is likely to be in the oxidised form which will undergo dissolution as it is buried in the peat matrix. The redox - pH diagram (Figure 4.14) demonstrates that the most dominate form of iron is Fe^{2+}, although a minor amount of iron sulfides are expected to form in the deeper anoxic part of the peat, and iron oxides in the very oxygen-rich near-surface. Iron is also expected to form complexes with OM (e.g. Chesworth et al., 2006).

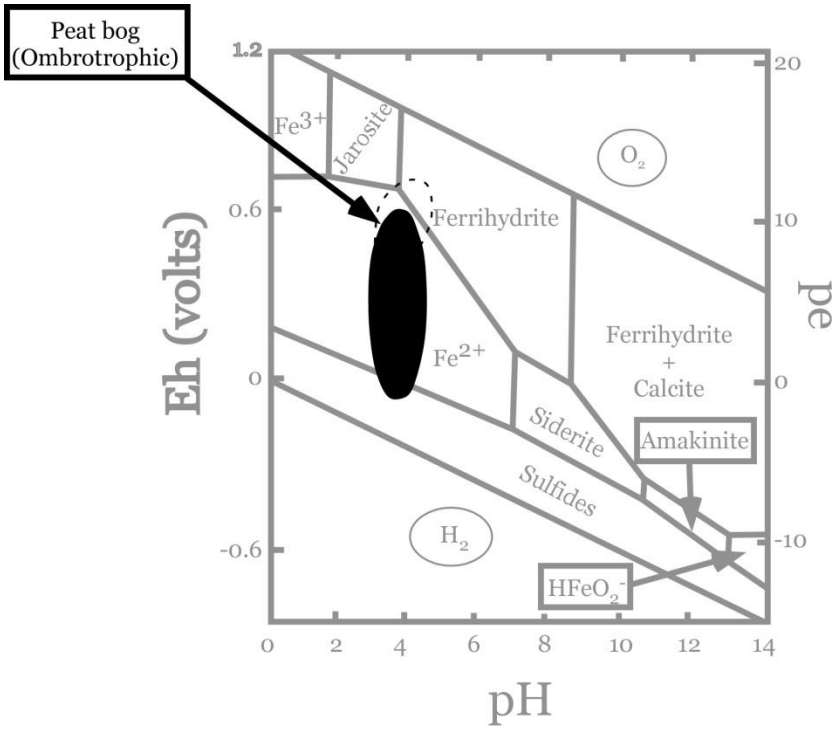

Figure 4.14 Phase diagram for iron in ombrotrophic peatbogs.
The redox - pH diagram shows which Fe-species are stable in an ombrotrophic peatbog; it is clear that most of the iron will be stable in the divalent form (Fe^{2+}). The dashed black line represents the very near-surface, or if the water table has substantially dropped (e.g. due to a drought), as iron oxides can form in the oxic part of the peatbog. Modified from Chesworth et al., 2006.

Nickel and lead showed no correlation with ash. Pb is well-known to strongly bind with OM in ombrotrophic peatbogs (e.g. Rothwell et al., 2010), and if the only input of Pb to the peatbog were dust than it would be expected to correlate well. Lead tetraethyl, however, was added to fuel between c. 1930's to 2000 (dates for the UK), where it was readily released into the atmosphere when combusted (Lee & Tallis, 1973; Ndiokwere, 1984). This major additional vehicle pollutant which is not related to ash or dust will weaken the ash correlation and no information can be gained on the mobility of Pb in peatbogs in this manner. Although Ni also has a source of pollution from vehicles (diesel oil e.g. Baralkiewicz and Siepak, 1999 and references therein), this is not a major source of atmospheric Ni and the weak

correlation suggests mobility. Ni mobility has been reported previously (e.g. Rausch, 2005; Nieminen et al., 2007) and has been related to the mineral forms in which Ni entered the peatbog, peat accumulation rates, the phyio-chemical conditions of the peatbog, and if there has been oxidation of Ni sulfides in the surface layers (Rausch, 2005; Nieminen et al., 2007). Only when Ni is related to dust silicate minerals has Ni shown to be immobile (Nieminen et al., 2007).

4.3.1.2 Lead dating correlation

Novak et al. (2008) dated peat close to these sites using Pb^{210} (see Figure 1.5 Chapter 1 for location relative to this study) from samples collected in 1994. Novak's peak in Pb concentrations was at 12 cm and was dated to 1945. In our study, the maximum peak in $Pb_{S\text{-}P}$ concentrations (Figure 4.8) is at 32 cm depth (site 1) and 34 cm depth (site 2). Assuming the two peaks coincide (i.e. the age of the peak in Pb from this data is at 1945), then this would equate to approximately 32 cm of peat accumulation in 64 years; averaged out this gives approximately 0.5 cm of peat accumulation per year. Average accumulation rates of peat are approximately 1 mm per year. Although the value estimated from this dataset seems high, rapid rates of accumulation have previously been recorded (e.g. up to 0.6-1.3 cm per year; Neuzil, 1997). This suggests that Pb is not mobile or negligibly mobile as the large peak seen in Novak et al. (2008) data appears to largely correspond to the large peak seen within these solid-phase datasets. Many authors demonstrate that Pb is immobile in peatbogs (e.g. Shotyk et al., 1996; 2002; MacKenzie et al., 1998; Weiss et al., 1999). Assuming that both peat growth and degradation rates are constant over time, then a comparison could be made between relevant dates that have affected Pb concentrations in the atmosphere, and relate them to Pb concentrations in the peat matrix (Figure 4.13). This must be treated with caution however, as peat growth can

be variable over the short-term (Belyea and Clymo, 2001). Only if the other trace metals are immobile then can the inference can be made that these are also the same age as the Pb depth (discussed later).

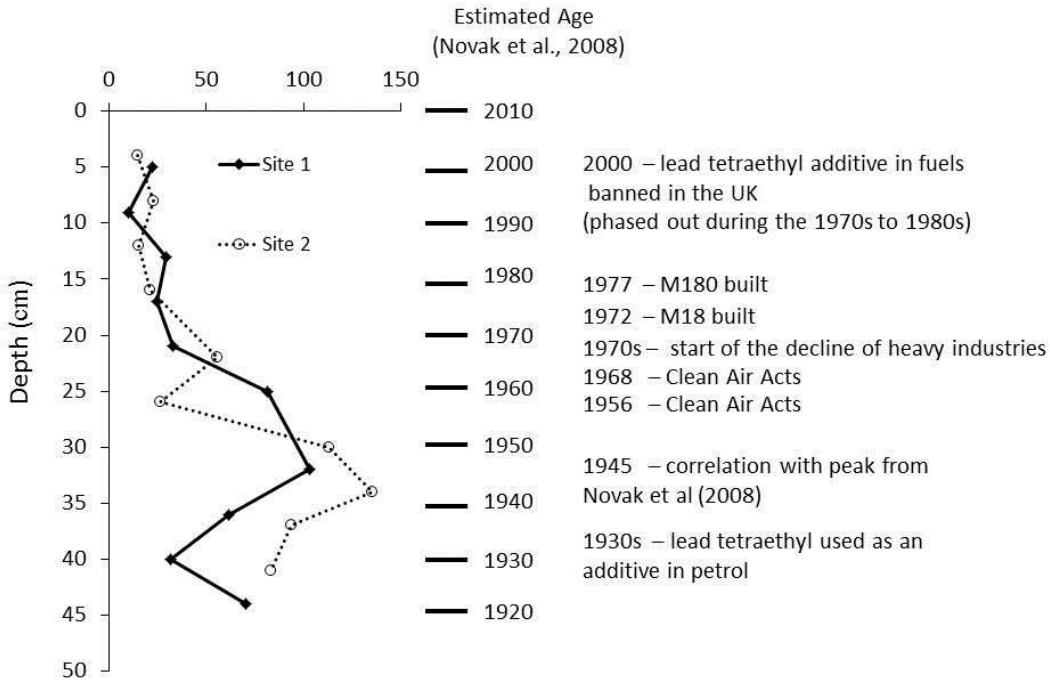

Figure 4.14 Tentative correlation peat dating.
Using Pb^{210} Novak et al. (2008) dated peat close to the sites used in this study from samples collected in 1994. Novak's peak in Pb concentrations was at 12 cm (1945). In our study, the peak in $Pb_{S\text{-}P}$ *concentrations is at 32 cm depth (site 1) and 34 cm depth (site 2). Assuming the two peaks coincide then this would equate to approximately 32 cm of peat accumulation in 64 years (0.5 cm of peat accumulation per year). This suggests that Pb is not mobile as the large peak seen in Novak et al. (2008) data appears to largely correspond to the large peak seen within these solid-phase datasets. Local and regional important dates that have implications for trace metals in the atmosphere have also been included.*

4.3.1.3 Enrichment factors

Enrichment factors can be used to determine the anthropogenic input of trace metals into the peatbog overtime using reference materials for geogenic dust sources. This assumes that the trace metals remain immobile after deposition (e.g. Shotyk et al., 2000; 2002). In this study, Al and Sc are used due to their conservative chemical

behaviour which is supported by their strong correlation with ash at Thorne Moors. Using a series of calculations (below) the anthropogenic input can be calculated which can help identify the mobility of trace metals. If maximum and minimum concentrations correlate well with maximum and minimum anthropogenic pollution at expected times (using Pb as a proxy for timing of the peat) then this suggests immobility.

Enrichment factors were calculated following the method outlined in Shotyk et al. (2000). In all calculations the trace metals have been normalised to Al and Sc to allow for variations in mineral matter (Shotyk et al., 2000).

$$EF = (TM/RM\ [peat]) / (TM/\ RM\ [crustal]) \quad (4.1),$$

where EF is enrichment factor, TM is trace metal, RM is reference material and is Al or Sc.

Enrichment Factor Core A							
Depth	**Zn/Al**	**Ni/Al**	**Co/Al**	**Cu/Al**	**Pb/Al**	**Cd/Al**	**Fe/Al**
5	59	6	3	9	213	322	4
9	71	5	3	15	118	229	4
13	57	4	2	20	273	335	4
17	52	4	2	12	291	311	4
21	39	6	2	12	278	284	3
25	21	3	2	12	308	285	2
32	22	2	1	13	250	236	1
36	33	2	2	8	185	267	2
40	31	2	2	6	143	264	2
44	28	3	1	12	192	292	2

Table 4.2 Enrichment factors for Core A using Al as a reference material. *These show the enrichment of trace metals relative to the amount of trace metals found in the Earth's Crust for Core A using Al as a reference material. Equation 4.1 was used to calculate these numbers.*

Enrichment Factor Core B							
Depth	**Zn/Al**	**Ni/Al**	**Co/Al**	**Cu/Al**	**Pb/Al**	**Cd/Al**	**Fe/Al**
4	57	5	2	7	194	288	5
8	50	11	2	8	199	318	5
12	53	7	2	9	194	254	5
16	46	4	2	9	213	280	4
22	21	3	2	10	259	294	2
26	15	4	1	10	263	249	2
30	21	3	2	10	421	355	2
34	29	3	1	13	494	368	2
37	25	2	1	14	296	275	1
41	23	2	1	8	179	223	1

Table 4.3 **Enrichment factors for Core B using Al as a reference material.** *These show the enrichment of trace metals relative to the amount of trace metals found in the Earth's Crust for Core B using Al as a reference material. Equation 4.1 was used to calculate these numbers.*

Enrichment Factor							
Depth	**Zn/Sc**	**Ni/Sc**	**Co/Sc**	**Cu/Sc**	**Pb/Sc**	**Cd/Sc**	**Fe/Sc**
5	103	10	4	15	370	560	8
9	154	10	6	33	254	494	9
13	74	5	3	25	353	432	5
17	71	5	3	16	395	422	5
21	49	8	3	15	346	354	4
25	20	3	2	11	287	266	2
32	16	2	1	9	180	170	1
36	32	2	2	8	181	261	2
40	37	3	2	7	168	311	3
44	24	3	1	11	164	249	1

Table 4.4 **Enrichment factors for Core A using Sc as a reference material.** *These show the enrichment of trace metals relative to the amount of trace metals found in the Earth's Crust for Core A using Sc as a reference material. Equation 4.1 was used to calculate these numbers.*

Enrichment Factor							
Depth	**Zn/Sc**	**Ni/Sc**	**Co/Sc**	**Cu/Sc**	**Pb/Sc**	**Cd/Sc**	**Fe/Sc**
4	79	6	3	10	271	404	7
8	93	20	4	15	370	591	9
12	101	12	4	18	366	482	10
16	67	6	3	13	306	403	6
22	24	3	2	11	294	333	2
26	15	3	1	10	256	242	2
30	21	3	2	10	409	345	2
34	21	2	1	9	361	269	1
37	17	1	1	9	197	183	1
41	22	2	1	8	174	218	1

Table 4.5 Enrichment factors for Core B using Sc as a reference material. *These show the enrichment of trace metals relative to the amount of trace metals found in the Earth's Crust for Core B using Sc as a reference material. Equation 4.1 was used to calculate these numbers.*

There has been more enrichment (from lowest to highest) Co>Fe>Ni>Cu>Zn>Pb>Cd compared to either Al or Sc (Table 4.2). Pb and Cd have clearly been enriched the most though.

The lithogenic component of trace metals within the peat is calculated using the following:

TM [lithogenic] = RM [peat] * (TM/RM [crustal]) (4.2),

which in turn can then be used to calculate the anthropogenic input of metals using:

TM [anthropogenic] = TM [peat] - (TM [lithogenic]) (4.3).

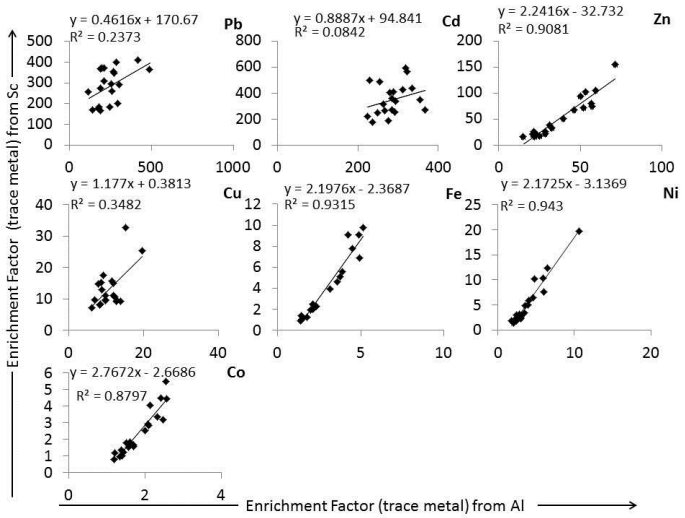

Figure 4.15 Trace metal enrichment factors comparison between Al and Sc. *This plot shows the differences in calculating enrichments factors with Al or Sc as a geogenic reference (equation 4.1). Good correlations are between Co, Ni, Fe and Zn to Sc and Al. Correlations are weak with Pb, Cu and Cd to Sc and Al.*

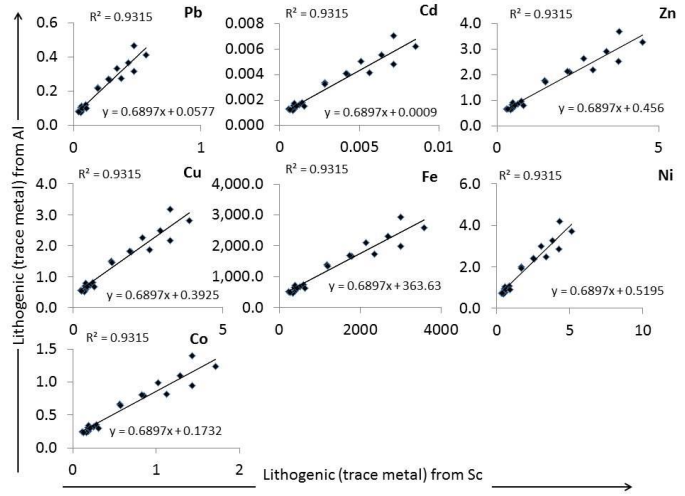

Figure 4.16 Trace metal lithogenic component comparison between Al and Sc. *This plot shows the differences in calculating the lithogenic component between Al and Sc as a geogenic reference (equation 4.2). All trace metals show good correlations, suggesting that the lithogenic ratios references are accurate and probably close to dust.*

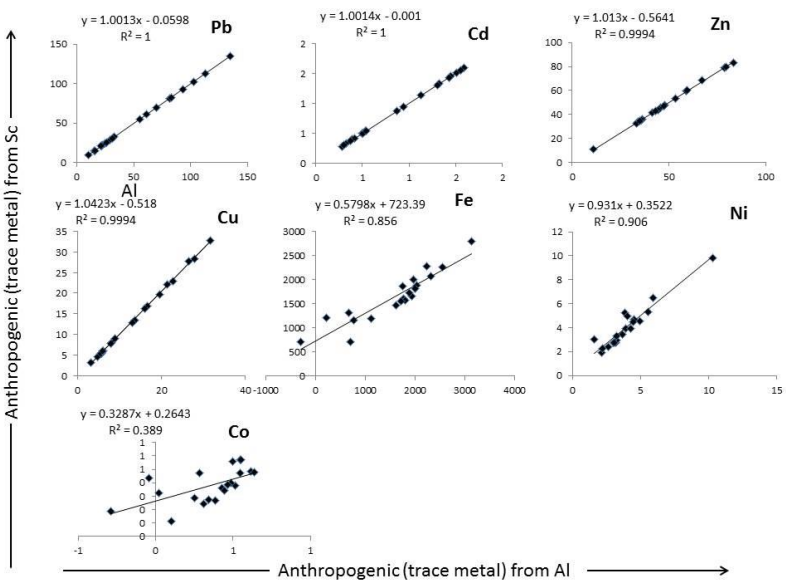

Figure 4.17 Trace metals anthropogenic comparison between Al and Sc.
This plot shows the differences in calculating the anthropogenic input using Al and Sc as a geogenic reference (equation 4.3). For all trace metals with the exception of Co and Fe, the slope values are close to one. This suggests that both Sc and Al can be used as a geogenic reference material for all metals except Fe and Co.

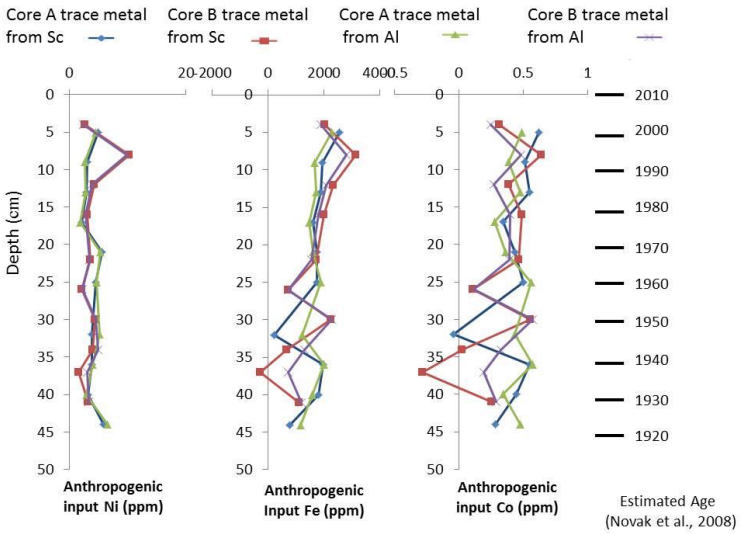

Figure 4.18 Calculated anthropogenic trace metal concentrations.
Using the calculations (see text) anthropogenic input was calculated. Profiles for Ni, Fe and Co suggest mobility as they do not follow closely with maximum loadings of atmospheric pollution.

Figure 4.18 shows the anthropogenic trace metals concentrations for Ni, Fe and Co; on the right-hand side of the figure, key dates of UK atmospheric pollution have been included. Ni does not follow the patterns of atmospheric input into the atmosphere, strongly suggesting that Ni is mobile at Thorne Moors; as discussed above Ni has already been found to be mobile in peatbogs. The profiles for Fe and Sc and Al are decoupled suggesting that either Al or Sc cannot be used to determine the atmospheric pollution, or Fe is mobile. This is the same for Co. Notably Fe and Co profiles follow each other in trends suggesting that either the anthropogenic input of Co is associated with Fe, or that the once deposited Co undergoes diagenesis which is related to Fe. Co correlated well with ash and the Co solid-phase profiles followed similar patterns of the other assumed immobile trace metals (e.g. Pb, Cu). This suggests that the anthropogenic input to the peatbog is mobile and the natural input is immobile. Moreover the anthropogenic fraction of Co to the peatbog is small; this is supported by the enrichment factor calculations (Tables 4.2 to 4.5). This suggests that Co shows mobility depending on the form in which Co entered the peatbog, and that Co associated with anthropogenic activity is mobile and associated with Fe. Therefore there must be more of a higher fraction of geogenic input of Co at Thorne Moors, giving the overall impression that it is immobile within peatbogs. Iron not correlating with anthropogenic input is unsurprising as it is a redox-sensitive species and mobility is expected which Figure 4.18 supports.

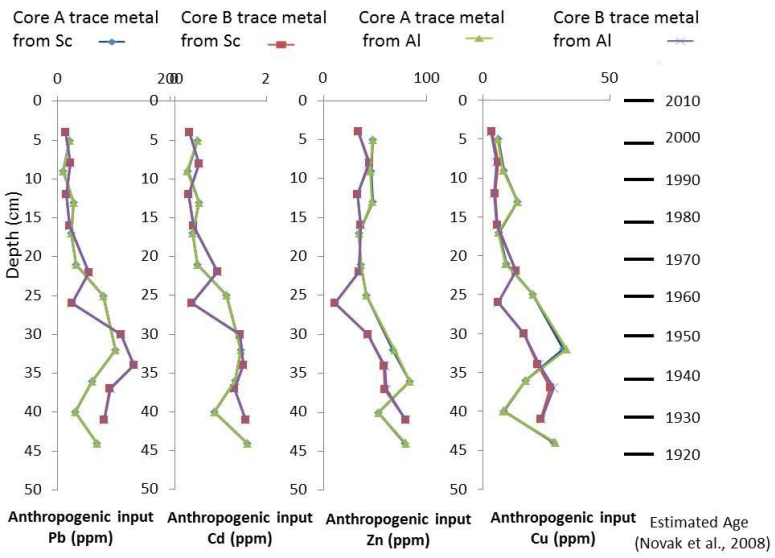

Figure 4.19 Calculated anthropogenic trace metal concentrations.
Using the calculations (see text) anthropogenic input was calculated for the metals Pb, Cd, Zn and Cu. The profiles suggest immobility as the higher concentrations of these elements are within the deeper peat. This is because anthropogenic inputs have decreased in more recent times due to cleaner air (Clean Air Acts) decline of heavy industry, and removal of Pb from fuel. The anthropogenic calculations suggests that using Pb, Cd, Zn and Cu can be used to determine the historical atmospheric input at Thorne Moors as these metals show negligible mobility.

Figure 4.19 shows the calculated anthropogenic input of Pb, Cd, Zn and Cu have very similar trends at Thorne Moors. The dates on Figure 4.18 and 4.19 have to be used with caution; however, the peaks in concentrations of these metals loosely correspond with the peaks in anthropogenic atmospheric pollution in the UK (e.g. Clarke et al., 1992; Novak et al., 2008). Figure 4.14 has the key dates which will have exerted major influences of trace metals in the atmosphere and include, when lead was used as an additive in petrol (1930s), the Clean Air Acts (1956; 1968), the start of the decline of the heavy industries in the UK (1970s), when the motorways local to Thorn Moors were built (1970s), and when Pb was removed as an additive to fuel. Broadly speaking the peaks and declines in concentrations correspond to the anthropogenic pollution, suggesting that Pb, Cd, Zn and Cu are immobile at Thorne

Moors. Thus the nearby motorway network could have acted as a significant source of metals, particularly lead, that occurred later than the regional pollutant inputs (that is coal burning). This therefore adds further uncertainty to the correlation of peat metal burden versus timing of emissions. Using the DET and DGT method allows mobility to be investigated independently of the need to know peat age or time of maximum pollutant emissions.

4.3.2 DET and DGT profiles

DET gel probes measure concentration of trace metals by equilibrating with the surrounding peatbog pore-waters and, although there is minor sediment disturbance when first deployed, it is essentially a non-intrusive method (in that it minimally perturbs the in-situ pore-waters). The DGT method does (intentionally) perturb the system because it introduces an additional sink for trace metals from the pore-waters but it then provides information on metal availability. The magnitude of the DGT fluxes is indicative of the potential for trace metal mobility. Trace metal mobility within the DET data will be identified as gradients throughout the profile, or sharp concentration excursions away from the main trend. The former is indicative of long-term trends and shows that there is diffusion away from a high-concentration source, which may be from the surface or deep within the profile. Sharp peaks in concentrations however, represent very local perturbations and contain only a very small mass of trace metals and will diffuse away very quickly in all directions. For example, the large positive excursion away from the baseline for Co in site 2 at 21.5 cm, will only last for 7.8 hours (as it will diffuse out of the profile unless resupplied), following the calculation determined by Fick's Law for diffusion.

$R = D(dc/dz)$,

where R is diffusional flux, D is diffusion coefficient and (dc/dz) is the vertical concentration gradient.

There are several similar sharp peaks that occur throughout the DET metal profiles (figures 4.3 to 4.9). It is unlikely that any of these spikes are being re-supplied continuously because if they were, then gradients over longer depth ranges would be seen within the profiles. Instead these sharp excursions are probably due to very localised changes in physico-chemical conditions within the peatbog. Morris et al. (2011) hypothesise that there should be hot-spots of decomposition in aquatic systems which supply small amounts of organic matter (which is believed to occur at this site; see Chapter 3). Additionally, these short-lived hot-spots of decomposition allow organic matter to act as an electron acceptor. Thus in this region of decaying organic matter, there may be changes in the metal speciation that influence the mobility. Although these sharp peaks are evidence for trace metal mobility, the nature of the limited supply of short-lived decomposition means that this process is only transient and localised, with no resupply of trace metals. As these small outliers cause high frequency excursions in the data, they tend to make the baseline appear larger (or smaller) than it should be. Therefore the use of median (rather than mean) and median absolute deviation (MAD) statistics limits the effect of these outliers (as the data are not normally distributed) deriving a median value which more closely reflects the actual baseline trend of the majority of the data. This statistical information, as well as the derived median statistics for the DET, solid-phase and DGT metals are summarised in Table 4.6. It can be seen that the MAD-derived medians have a lower baseline value, showing that the localised perturbations increase the mean values considerably. Table 4.7 summarises the order of concentrations and fluxes from highest to lowest from both the median and the

MAD statistics. These are generally in agreement with each other for both sites and through all the data sets. For instance, it is usually Fe and Zn which have the highest concentrations and fluxes and Co and Cd the lowest, while Cu, Ni and Pb lie in between. Notably, in the solid-phase Pb has a high concentration, only surpassed by Fe for the metals that were analysed when using MAD statistics in both sites 1 and 2 and as the median for site 2. Pb has a relatively high median solid/dissolved concentration but a relatively low flux indicating that it must be less mobile than the other metals. Conversely, Ni has a relatively low median solid and dissolved concentration but relatively high median flux, showing that it must be more mobile than the other metals.

Site 1							
	Fe	**Zn**	**Pb**	**Cu**	**Ni**	**Co**	**Cd**
Solid-phase	2949.95	48.28	32.22	11.96	5.95	0.9	0.71
	(594.24)	(8.98)	(16.43)	(5.56)	(1.67)	(0.32)	(0.37)
	[0.20]	[0.19]	[0.51]	[0.46]	[0.28]	[0.36]	[0.52]
DET	202.83	260.52	28.85	45.15	16.25	1.03	1.39
	(54.14)	(34.62)	(3.39)	7.94)	(2.31)	(0.12)	(0.42)
	[0.27]	[0.13]	[0.12]	[0.18]	[0.14]	[0.12]	[0.30]
DGT	12.88	2.32	0.11	0.31	0.48	0.003	0.008
	(7.17)	(0.28)	(0.01)	(0.04)	(0.09)	(0.0004)	(0.001)
	[0.56]	[0.12]	[0.06]	[0.14]	[0.19]	[0.14]	[0.18]
Site 2							
Solid-phase	2810.19	40.72	40.92	10.52	5.62	0.93	0.75
	(403.11)	(6.88)	(25.82)	(6.19)	(1.85)	(0.32)	(0.43)
	[0.14]	[0.19]	[0.63]	[0.59]	[0.33]	[0.35]	[0.52]
DET	423.65	387.35	28.69	32.11	22.94	1.03	2.23
	(72.88)	(111.95)	(3.16)	(8.72)	(6.3)	(0.11)	(0.72)
	[0.17]	[0.29]	[0.11]	[0.27]	[0.27]	[0.11]	[0.33]
DGT	11.28	3.05	0.09	0.37	0.52	0.003	0.01
	(7.7)	(0.6)	(0.01)	(0.08)	(0.09)	(0.0006)	(0.005)
	[0.68]	[0.20]	[0.15]	[0.21]	[0.16]	[0.19]	[0.39]

Table 4.6 Site 1 and site 2 medians.
These are the medians and MAD values for each site and each method. MADs (brackets) MAD/median [square brackets] for solid-phase, DET and DGT, units are in ppb for concentrations (solid-phase and DET) and $pgcm^{-2}s^{-1}$ *for fluxes (DGT).*

Method and site	Statistic Type	Metal												
Site 1: Solid-phase.	Median	Fe	>	Zn	>	Pb	>	Cu	>	Ni	>	Co	>	Cd
Site 2:Solid-phase	Median	Fe	>	Pb	>	Zn	>	Cu	>	Ni	>	Co	>	Cd
Site 1: DET pore-water.	Median	Zn	>	Fe	>	Cu	>	Pb	>	Ni	>	Cd	>	Co
Site 2:DET pore-water	Median	Fe	>	Zn	>	Cu	>	Pb	>	Ni	>	Cd	>	Co
Site 1: DGT fluxes.	Median	Fe	>	Zn	>	Ni	>	Cu	>	Pb	>	Cd	>	Co
Site 2: DGT fluxes	Median	Fe	>	Zn	>	Ni	>	Cu	>	Pb	>	Cd	>	Co
Site 1: Solid-phase.	MAD	Fe	>	Pb	>	Zn	>	Cu	>	Ni	>	Cd	>	Co
Site 2:Solid-phase	MAD	Fe	>	Pb	>	Zn	>	Cu	>	Ni	>	Cd	>	Co
Site 1: DET pore-water.	MAD	Fe	>	Zn	>	Cu	>	Pb	>	Ni	>	Cd	>	Co
Site 2:DET pore-water	MAD	Zn	>	Fe	>	Cu	>	Ni	>	Pb	>	Cd	>	Co
Site 1: DGT fluxes.	MAD	Fe	>	Zn	>	Ni	>	Cu	>	Pb	>	Cd	>	Co
Site 2: DGT fluxes	MAD	Fe	>	Zn	>	Ni	>	Cu	>	Pb	>	Cd	>	Co

Table 4.7 Order of fluxes and medians for each site and metal.
Following on from Table 4.2, the trace metals are placed in order of highest concentrations or fluxes for each method (e.g. pore-water DET/DGT or solid-phase); highest flux or concentration to the left and lowest to the right.

4.3.3 Metal behaviour

4.3.3.1 Iron

All solid-phase data suggests mobility. Variability in ratios of Fe:Al and Fe:Sc show that Fe has been mobilised relative to Al and Sc (Figures 4.11 and 4.12 respectively). Both DET pore-water profiles show a gradient from 10 or 7 cm depth to the surface (Figure 4.3), and these gradients would drive diffusion of Fe upwards. At both sites DGT data (Figure 4.3) show higher availability between 4 and 12 cm depth and minimum availability in the shallowest part of the profile, which is consistent with upward migration of Fe from a source to a near surface sink. The steeper gradient in the DET pore-water Fe at site 2 corresponds with higher Fe availability within the DGT profile at this site. The high near surface Fe/Al ratio in the solid-phase records a history of Fe accumulation in the upper parts of the peat. There appears to be zonation in the mobility of Fe. In the upper 4 cm, the peat has a low density and oxygen is available from surface diffusion and/or photosynthetic production. Smieja-Krol et al. (2010) found that Fe(III) oxyhydroxides formed in the uppermost peat and on the plants growing on the peat surface. Thus it is likely that in this zone soluble Fe^{2+} will be oxidised to produce insoluble Fe(III)oxyhydroxides (e.g. reaction 4.4) and as a result DGT Fe availability is low.

$$Fe^{2+} + ¼\ O_2 + 2.5H_2O \rightarrow Fe(OH)_3 + 2H^+ \qquad (4.4)$$

The Fe(III)oxyhydroxides produced contribute to the high Fe/Al content in the solid-phase. In the zone between 4 and 12 cm depth, residual dissolved oxygen is rapidly removed. DGT Fe availability is significantly higher than in the oxidised zone above and DET pore-water Fe concentrations also increase, leading to concentration gradients that drive upward migration of dissolved Fe. Solid-phase Fe/Al remains

high throughout this zone. The increase in available Fe and high Fe/Al is most likely due to buried iron oxides undergoing dissolution reactions (e.g. Lovely and Phillips, 1986), releasing Fe^{2+} to the pore-waters; additionally any trace metals associated with the oxides are also added to the pore-waters. In the 12 to 25 cm zone, DET pore-water Fe concentrations remain relatively high, particularly at site 2, and over this interval, solid-phase Fe/Al decreases significantly. DGT Fe availability falls in the upper part of this zone, driven by the declining solid-phase Fe pool available shown by the decreasing Fe/Al ratio. The fact that the DET Fe remains high is evidence for Fe solubilisation. Below 25 cm solid-phase Fe/Al has low, more or less constant, values and DGT Fe availability is generally low. DET pore-water Fe concentrations remain relatively high as dissolved Fe^{2+} is stable in these reducing environments (Figure 4.14; Eh-pH phase diagram for Fe).

4.3.3.2 Correlation with Fe

Similar to Fe, the depth profiles of Zn/Al ratios show zonation with Zn mobility (Figure 4.12), with high near surface Zn/Al ratios recording a history of accumulation of Zn within the upper parts of the peat. The Zn_{DGT} profile for site 2 (Figure 4.4) shows more Zn availability towards the shallower part of the peat. In site 1, the Zn_{DGT} profiles show a decrease towards the shallower part of the peat. Clearly there is also zonation in Zn mobility, which is similar to Fe. In the upper part of the peat, atmospheric Fe(III)oxyhydroxides particles enter the peatbog and break down easily after burial into more reducing conditions. Smieja-Krol et al. (2010) found that that the Fe(III)oxyhydroxides often had Zn associated with it. This could explain the similarities (specifically site 1 rather than site 2) with the Zn and Fe data which may be due to Zn sorbing on to newly formed Fe oxyhydroxides in the top 5 cm. Conversely, when the iron oxides are solubilised, Zn is released into solution.

Thus, although Zn itself is not redox-sensitive, the pattern of Zn behaviour might be, in part, controlled by Fe in this zone.

The Co/Al profiles are also similar to Fe/Al (Figure 4.12) recording a history of accumulation of Co within the upper parts of the peat. Co, although showing some correlation with Fe for the solid-phase, does not show many similarities within the Fe DET/DGT datasets and also correlated well ash. In fact the Co_{DET} shows very similar trends to the Pb dataset. This may be related to the sources of Co into the peatbog. The anthropogenic input calculated above suggested that a small fraction of Co was related to Fe, whilst the strong correlation with ash and the maximum peak of Co was deeper in the peat (as expected for pollution within the UK if immobile). This overall control of Co behaviour in the peatbog is more likely to be related to the source of Co into the peatbog, and the subsequent differences in diagenetic behaviour. That is, the anthropogenic Co (apparently associated with Fe) appears to be more susceptible to dissolution and remobilisation than then geogenic related Co, explaining why there is a disjunction between the solid-phase and pore-water datasets.

4.3.3.3 Evidence of sinks within the shallower peat

The data show a sink for all metals within the shallower part of the peat. Pb and Co have similar profiles in the shallower part of the peat with clear evidence of a sink. In the upper 1 cm of the Pb_{DET} profiles and for both sites, lead decreases in concentration from the surface and from approximately 1 to 3 cm there is a very sharp increase in concentration. Between the surface and 1 cm depth, the Co_{DET} pore-water profiles also show that there is a decrease of concentrations from the surface to 1 cm, with a very sharp increase to higher values; over 1 cm depth in site 1

and over 3 cm depth in site 2. In the DGT data, both Pb and Co fluxes show divergent profiles from the surface to 7cm (Co) and from 1 to 5 cm (Pb). For both these trace metal fluxes, there is a decrease in site 1 and an increase in site 2 over the specified distances. This would suggest that the rapid sink highlighted by the DET data is more prominent in site 1 than site 2 as there is more of a rapid decrease of Co and Pb concentrations which coincide with the decreased availability of Co and Pb. The initial decrease in these metals could be related to plant uptake or they could be associated with sorbtion to/incorporation with newly formed Fe oxides (as discussed above), rendering them immobile. The rapid increase may be related to the decomposition of plants releasing trace metals into the pore-waters or metal oxides (including trace metals associated with Fe oxides) undergoing dissolution in the peat bog. Once released the trace metals may react /adsorb with organic matter, and as there are no vertical gradients seen in the DET data, it suggests that the trace metals are reacting /adsorbing (probably to OM), again rendering them immobile.

The Cu and Cd datasets also show evidence for a near surface sink. The $Cu_{S\text{-}P}$ profiles are similar to both $Al_{S\text{-}P}$ and $Sc_{S\text{-}P}$ (Figures 4.9 and 4.2, respectively) for both sites. Both Cu and Cd strongly correlate well with ash, having a high combined r^2 value (i.e. data from both cores); 0.80 and 0.73 respectively (Table 4.1; Figure 4.11), suggesting that the main source of both Cu and Cd is dust with no other major processes occurring. There is marginally more evidence for a near-surface sink of Cd than for Cu as the Cd_{DET} profiles do show a slight decrease in both sites from the surface to approximately 5cm. This decrease in concentrations coincides with decrease in the Cd_{DGT} data. Site 2 has a marked decrease in fluxes from the surface down to 13.5cm, whilst site 2 shows a small decrease in fluxes from the surface down to 2 cm. In the Cu_{DET} there are positive concentration excursions, but they are

over small depth ranges in both datasets suggesting that they are transient and not resupplied. Instead, evidence for a Cu near-surface sink comes from the Cu/Al ratios where there is enrichment of Cu from the surface down to 13cm (site 1) and a small enrichment from the surface to 6 cm (site 2). The Cu_{DGT} pore-water profiles also suggest a sink in the near-surface. There is a decrease in Cu fluxes from the surface down to 2 cm and in site 1 there is a decrease from the surface to 6 cm in site 2. Even though there isn't a corresponding decrease seen within the Cu_{DET} profiles, it is postulated that there is a sink in the near-surface of the peat, but the available Cu does not remain in the pore-waters for very long, as it is reacting / adsorbing very quickly with the organic matter (Gundogan et al., 2004).

The Ni/Al profiles (Figure 4.12) in both sites show a decrease of Ni relative to Al throughout the profile from the top of the peat to the deeper section. In both datasets this shows a near-surface accumulation of Ni within the peat. The Ni_{DET} data show that, although scattered, there aren't significant peaks and thus no significant concentration gradients (Figure 4.5). However, the Ni_{DGT} profiles (Figure 4.5) reveal that there is variable availability throughout these two sites. The Ni_{DGT} show a decrease in Ni availability from the surface down to 14 cm, showing that there is either a change in source or sink in site 2, but there is no corresponding change in Ni concentrations in the pore-water profiles. As Ni is well known to be one of the most mobile trace metals (e.g. Ukonmaanaho et al., 2004 and references therein) it is postulated that the available Ni does not remain in the pore-waters for long as it adsorbs / reacts quickly with the surrounding organic matter, or another biotic/abiotic process which removes Ni. However, perturbing the system does make it easily available. Roots exuding O_2 may be enough of a perturbation to allow Ni mobility (as seen in the solid-phase dataset).

4.3.3.4 The deeper peat

There is consistency throughout all solid-phase datasets with highest metal concentrations in the deeper part of the peat for both sites (with the exception of Ni). The solid phase profiles represent the cumulative history of ash (and therefore dust inputs) and post-depositional processes that act thereupon. Trace metal pollution to Thorne Moors site, with the exception of Pb, comes predominantly from coal burning, and anthropogenic pollution has been reduced in the last 40 years. Accumulation rates have been calculated at 0.5 cm per year (average for compacted peat is at 1mm per year); therefore the concentration maxima lie within the expected depth range.

The ratio of trace metals to Al in the deeper section of the peat, generally show that there is either a small enrichment relative to Al from depth upwards, or no change in ratios. Pb, however in site 2, shows there are two large peaks of Pb enrichment compared to Al at approximately 12 and 25 cm depth, which is shallower than the large peak of Pb seen in the solid-phase. Given that the accumulation rates averaged out is approximately 0.5 cm per year, then these peaks are dated around the mid-1980s (12 cm) and early 1960s (25cm). Both peaks are postulated to be related to anthropogenic activity, with the shallower peak possibly being related to the use of leaded petrol, which releases more Pb than Al into the atmosphere. This is plausible as, by this time the nearby M18 and M62 motorways had been constructed, there were more cars were on the road, and leaded petrol was still in use.

The DET pore-water concentrations for Ni, Pb, Co and Cu show limited variability in concentration in the deeper part of the peat. Cd and Zn, however, both exhibit a peak between 29 and 33cm in the DET pore-water profiles in both sites, although it

is more apparent in site 1. There isn't a corresponding peak in the DGT data, showing that whatever has caused this increase in concentrations has not increased the availability of both these species. Additionally, this peak is transient as it is sharp. Zn also shows an increase in concentrations between 21 and 27 cm, with a corresponding small increase in availability. This increase is not seen in any other dataset at this depth, thus it is not likely to be related to Fe behaviour. It is unclear why Zn is increasing in both concentrations and availability, however Zn is known to be used in the uptake and recycling by vegetation and roots are present in this zone.

The DGT profiles do not show much variation in the deeper parts of the profile for Fe, Zn and Cd; there are only minor variations for Co and Pb. Cu, however, does show variable availability, as does Ni. This doesn't necessarily mean that either species are becoming mobile, but they are becoming available, and as they are not collecting in the pore-waters (the DET data shows a lack of gradients), they are most likely becoming bound very quickly at the same depth. Possible mechanisms for this could be i) as soon as it is released it is binding/sticking onto the organic matter; ii) it is being incorporated into other minerals which are forming in the same location; iii) it is related to *Eriophorum* plant roots. As Cu is known to have a high affinity with organic matter, which is degrading at this depth, it could be related to its breakdown. Ni, is known to be a mobile element (e.g. Ukonmaanaho et al., 2004 and references therein) and although the processes of its mobility are not well known, it is expected to have variable availability; again it is postulated that the available Ni does not remain in the pore-waters for long as it adsorbs / reacts quickly with the surrounding organic matter, or other biotic and/or abiotic process remove Ni from the pore-waters to the solid-phase.

4.3.4 Key depths and site variability

There are clearly some differences with respect to the geochemistry between sites 1 and 2, which could be related to slight differences in morphology and ecology of the two sites. The main difference between site 1 and site 2 is the surface layer; site 1 is a "lawn" which has small open pools present, whilst site 2 is hummocky with no open pools. Both sites contain the dominant vegetation found at Thorne Moors; *Sphagnum* and *Eriophorum*, although site 2 contained more of the latter. The inspection of the frozen cores showed that both sites have similar profiles deeper in the peatbog with large amounts of frozen pore-water with live and dead organic matter just below the surface (down to 5 cm site 1 and 8 cm site 2). The large amount of frozen water indicates high permeability that might allow ingress of oxygenated surface water. The trace metal data show that there are sinks seen within the upper part of the peat, typically between 1 and 5 cm. This correlates well with the live organic matter seen within the cores and the sink is most likely processes related to plant uptake or Fe (hydr)oxide formation which can take-up trace metals. Deeper in the peatbog, a dense root zone (37 cm site 1 and 34 cm site 2) can be seen, after this and in both sites there were fewer roots; this correlates well with the data as there were limited concentration changes and availability changes with most metals.

4.3.5 Relative metal availability

Some conclusions can be drawn for relative metal mobility of the trace metals. For instance, when comparing the $Cd_{S\text{-}P}$ and $Co_{S\text{-}P}$ data (Figures 4.6 and 4.7 respectively) the profiles look very similar and the concentrations are also very similar. The concentrations for Co_{DET} and Cd_{DET} are also similar. However, the overall fluxes are 100 times higher for Cd than Co. This shows that Cd is potentially 100 times more

mobile than Co. As the flux shows how much of a species is available in twenty-four hours, and the solid-phase concentrations show how much of a species is being stored longer-term in the peat, then conclusions can be drawn about the relative mobility of each element. Dividing the DGT fluxes by the median and MAD solid-phase concentrations reveals relative metal mobility (Table 4.8).

Site 1 (Median)						
Ni	**Zn**	**Cu**	**Cd**	**Fe**	**Pb**	**Co**
0.081	0.048	0.026	0.011	0.004	0.003	0.003
Site 1 (MAD)						
Ni	**Zn**	**Fe**	**Cu**	**Cd**	**Pb**	**Co**
0.054	0.031	0.012	0.007	0.003	0.001	0.001
Site 2 (Median)						
Ni	**Zn**	**Cu**	**Cd**	**Fe**	**Co**	**Pb**
0.093	0.075	0.035	0.013	0.004	0.003	0.002
Site 2 (MAD)						
Zn	**Ni**	**Cu**	**Fe**	**Cd**	**Co**	**Pb**
0.087	0.049	0.013	0.019	0.012	0.002	0.0004

Table 4.8 Relative mobility

DGT data relative to the solid-phase concentrations (medians and MAD). These numbers were obtained by dividing the DGT fluxes by the median and MAD solid-phase concentrations in order to demonstrate the relative metal mobility, that is, how much is stored in the peat long term, versus how much is available in the pore-waters when a sink is added.

Table 4.8 reveals that although Fe is present in much higher quantities than the other trace metals it is not as mobile. The most likely reason for this is because it is redox-sensitive and when the roots release small amounts of O_2 it oxidises it to Fe oxyhydroxides which are extremely insoluble and thus collect in the solid-phase. Conversely both Cd and Ni are relatively mobile given the amount of species found within the pore-waters. All other metals presented in Table 4.8 are in the order of relative mobility that would be expected given the evidence from the solid-phase analysis and evidence or mobility or lack of. That is, Zn and Ni is expected to be

high, Cu in the middle and Co and Pb the least mobile. Nevertheless, regardless of how mobile each element is with respect to each other it must be noted that, apart from Fe, Ni and Zn, the other trace metals studied are present within the peatbog in very low quantities. Specifically, lead has very limited mobility which is in agreement that Pb^{210} is suitable for dating ombrotrophic peatbogs at sites similar to Thorne Moors.

This study shows that using the above combination of methods (DET, DGT and cores) can identify metal mobility within sediments. These methods are relatively cheap compared to Pb isotope studies. Indeed, these methods can be used as a cheap preliminary investigation to determine if sediments are suitable for Pb^{210} dating studies.

4.4 Conclusions

The similarity of the solid-phase trace metal profiles and their close correspondence to the ash profile suggest that their long-term accumulation is controlled by dust deposition, since ash is a proxy for dust. However, there must be some minor post-depositional processes as not all trace metals correlate well with ash. There is clear evidence for the mobility of Fe, Ni, Zn in the solid-phase datasets, whilst Cu and Pb immobile, and Co is, for the most, part immobile. There is evidence to support that a smaller fraction of Co, which is related to anthropogenic activity and coupled with iron, is mobile. Detail from the DET and DGT gels show that there are horizons in the sediment where availability increases yet it is not coupled with a corresponding increase in concentration, suggesting that some trace metals are available at depth but move into the solid-phase at the same horizon.

Most processes seem to occur in the shallowest part of the peat, which is expected as this is where there is live and partially decomposed organic matter, and oxygen can penetrate into the surface layers. As there is little or no O_2 in the deeper parts of the peat (see Chapter 3 conclusions) and not much live organic matter (apart from roots), only minor variations in both concentrations and fluxes are expected; the DET/DGT data confirms this. Both median and MAD statistics consistently show that Fe and Zn had the highest concentrations and fluxes whilst Co and Cd had the lowest. Cu, Ni and Pb tended to lie in between. However, this does not reflect the relative metal mobility as Ni is the most mobile metal of those studied, whilst Co and Pb where the lowest.

This study strongly suggests that Pb is not mobile and can be used in atmospheric Pb^{210} studies. Moreover, this study also demonstrated that using these combined methods is a cheap and quick effective evaluation of determining if trace metal are mobile within sediments. Indeed, these combined methods can be used to screen sediments for their appropriateness of using isotope studies.

4.5 Further work

The combined method limitations are that they do not reveal the reactions which occur in the sediment to move species from the pore-waters into the solid-phase. It would be useful to use tracers in a controlled, as natural as possible environment, to determine their reactive pathways from entering the peatbog to being stable and immobile within the solid-phase. Collecting mineral profiles from the peatbogs would be useful to determine the dominant solid-phases of the metals.

Chapter 5 Deposition and diagenetic model: Warham Salt Marsh

5.1 Introduction

Salt marshes are thought to sequester 210g CO_2 m^{-2} yr^{-1} (Chmura et al., 2003) thus they are an important reservoir for carbon. They typically have high rates of microbial respiration (Alongi, 1998), which also cycles Fe, S, and trace metals (Mortimer and Rae, 2000). These highly productive ecosystems become reduced within the top few millimetres as oxygen is utilised rapidly by microbial uptake (King, 1988). Due to the high abundance of sulfate in seawater and abundant OM, anoxic sulfidic conditions prevail in saltmarshes as microbial sulfate reduction is the dominant OM degradation process; reaction 5.1 (Howarth and Hobbie, 1982; Howarth, 1993; Alongi, 1998; Kostka, 2002):

$$2H^+ + SO_4^{2-} + 2CH_2O \rightarrow H_2S + 2CO_2 + 2H_2O \quad (5.1).$$

However, complex chemical interactions occur within salt marshes as they typically have a high content of iron oxide (Kostka and Luther, 1994), which is also available for bacterial degradation of OM (Chapter 1, Table 4.1) (e.g. Chapelle et al., 2009):

$$Fe(OH)_3 + 1/4\ CH_2O + 2H^+ + ¼H_2O \rightarrow\ ¼Fe^{2+} + ¼\ CO_2 + 3H_2O \quad (5.2).$$

Iron reduction is more energetically favourable than sulfate reduction. However, iron can be reduced by abiotic reactions as well, for instance by iron monosulfides (reaction 5.3) or sulfide (reaction 5.4; e.g. Thamdrup et al., 1994 and references therein):

$$FeS + 2FeO(OH) + 2H_2O \quad \rightarrow \quad 3Fe^{2+} + S^0 + 6OH^- \quad (5.3),$$

$$2FeOOH + H_2S \rightarrow 2Fe^{2+} + S^0 + 4OH^- \quad (5.4).$$

Indeed, having both high iron and sulfide concentrations often results in rapid abiotic reactions between sulfide and Fe(III) oxyhydroxide minerals (e.g. Poulton, 2003). Since this reaction is rapid it is favoured over the reduction of Fe(III) by bacteria, with heterotrophic Fe (III) reducers potentially being denied a source of Fe(III) for respiration (Koretsky et al., 2003).

The reduced iron and H_2S can react to form monosulfides (Berner, 1970), with potentially many cycles of oxidation and reduction before the final burial as pyrite by reactions such as 5.5 (Berner, 1970; Burdige, 2006):

$$Fe^{2+} + H_2S + S^0 \rightarrow FeS_2 + 2H^+ \quad (5.5).$$

If one pool is depleted then other compounds will form, for instance, if there is limited Fe but abundant sulfide then organosulfur compounds will form (Kohnen et al., 1989; Bruchert and Pratt, 1996), or in rare cases MnS can form in highly sulfidic conditions (Mort et al., 2010). In sediments where there is reactive Fe, but limited sulfide, siderite forms, often as concretions (Postma, 1981).

Early diagenetic reactions are not only affected by the concentration of species in the sediments but also by sedimentation rates (e.g. Raiswell, 1987). Slow sedimentation rates can cause precipitation due to increased residence times of species within the early diagenetic zones, and/or juxtaposing chemical species that are not normally within the same horizon into the same zones (Taylor et al., 1995; Bréhéret and Brumsack, 2000). Similarly, fast sedimentation rates also cause changes in early diagenesis. During fast sediment accumulation rates pore-water advection rates

increase, thus pore-water microbial communities enter sediment horizons that they are not normally associated with (Schmidt and Schaechter, 2012).

A change in sedimentation rates combined with the differing reactivity of species, for example, the highly reactive Fe(oxyhydro)oxide minerals such as ferrihydrite and goethite versus the relatively unreactive crystalline Fe-oxides and silicate-minerals (e.g. Poulton et al., 2004) can also make a difference to the diagenesis within the sediments. During times of rapid sedimentation a proportion of the reactive Fe-minerals and the majority of the less reactive Fe-minerals are buried before they undergo diagenetic reactions, providing a pool of electron acceptors deeper in the sediment (Aplin et al., 1993).

5.1.1 Rationale and aims

Warham salt marsh, (North Norfolk, UK; site details below) has siderite nodules forming locally whilst FeS is also present within the sediment (Pye, 1981; Pye et al., 1990; Coleman et al., 1993). This is unusual as ferrous iron normally reacts with the H_2S formed by SRB (e.g. Berner, 1981; Gautier, 1986) and siderite is unstable in the presence of H_2S (Coleman et al., 1993). Previous studies have shown that the siderite has carbonate isotope signatures that are too low (-5.9‰ PDB) for the siderite to have formed under methanogenic conditions (Coleman et al., 1993). It has been suggested that iron is being reduced by SRB, e.g. by *Desulfobacter* in the zones of concretions (Coleman et al., 1993).

The aim of this study is to understand the geochemistry of both sulfur and iron and relate this to the known fast sedimentation rates at this site.

5.1.2 Warham Salt Marsh

Warham Salt Marsh (Figure 5.1) can be separated into an upper and lower marsh, separated by sands on a low beach ridge (Pye et al., 1990). The lower salt marsh has developed quickly. Aerial photography taken in 1948 shows the area poorly vegetated with a limited creek system, but by 1960 there was a well-defined creek system on a vegetated salt marsh (Pye, 1984).

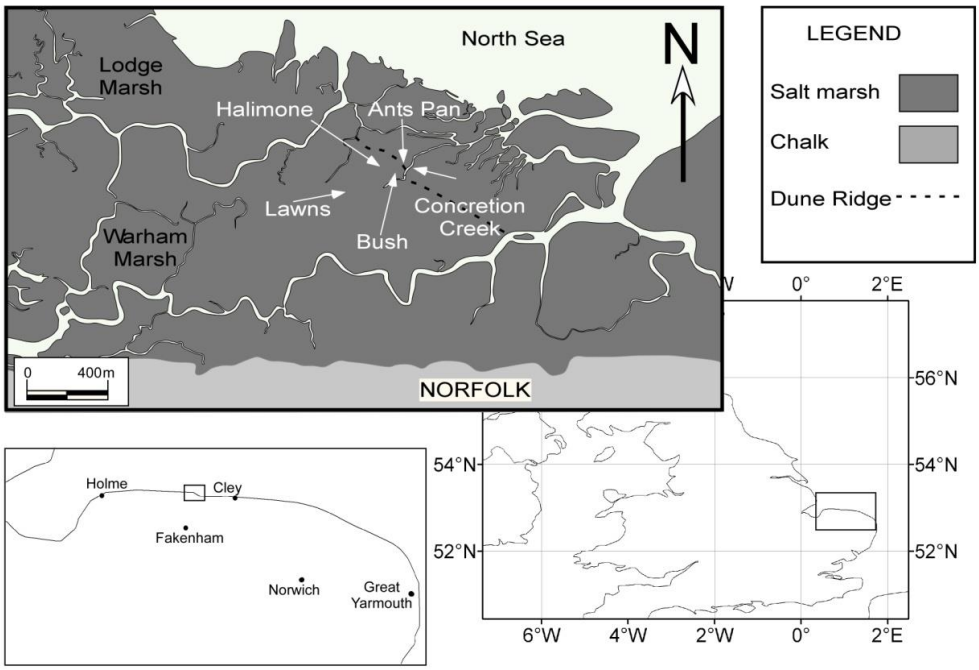

Figure 5.1 Warham Salt Marsh.
Warham site is an accreting salt marsh located in North Norfolk, U.K. The aim of using this site was to understand the iron and sulfur cycling within these sediments. Cores were collected from this site both for solid-phase (elemental sulfur profiles) and pore-water profiles (nitrate, sulfate and chloride). DET and DGT gel probes were also deployed here; however, only Fe DET probes were recovered. See Chapter 2 for full information on work carried out in the field and methods used. Image modified from Google Maps (2010).

The sediments consist of a basal, gravelly and sandy section overlain by predominantly brown, mottled silty sands that are 60 to 80 cm thick (e.g. Wilmot, 2006). Elemental sulfur can be seen on the surface of the water pans and creeks.

Deeper in the sediments, in-situ formed concretions, which are mainly cemented by siderite, Mg-calcite and iron monosulfides (e.g. Pye et al., 1990), which often have shrapnel or rootlets as their nuclei, are found throughout the lower marsh, although they are more abundant close to the major creeks (e.g. Pye et al., 1990; Mortimer et al., 2011). These concretions have been found in both the oxidised and reduced zones; however, they are more prevalent in the upper layers of the latter (Pye, 1984). Discontinuous zones of 10-30 cm thick iron monosulfide layers are also found and again are more prevalent near the creeks. In the permanent pans, which are commonly found on the lower marsh, sediments are rich in iron monosulfides and organic matter (Pye et al., 1990). The shrapnel is from RAF bombing practise at this site during the second world war, revealing that the concretions must form faster than what is usually suggested in the literature, for example 10^3 to 10^5 years (Berner, 1968; Coleman and Raiswell, 1993).

5.2 Results

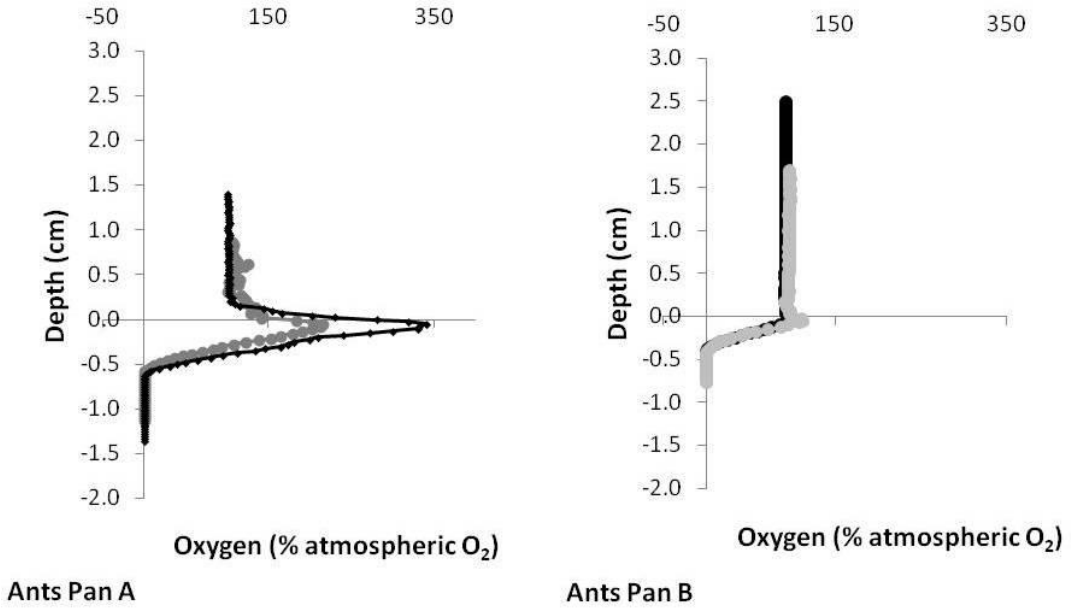

Figure 5.2 Oxygen depth profiles for Ants Pan (% of atmospheric saturation).

Four oxygen profiles were taken from Ants Pan from different sites. Sites A and B are from the same pan (Ants Pan) approximately 2 m apart. Sediment was sampled during March, 2008.

All oxygen profiles recovered were from Ants Pan. The two localities were within approximately 2 m of each other. The oxygen profiles from Lawns were not recovered as the probe broke when entering the firmer ground. The profiles on the left were taken earlier during the day during a sunny period (Ants Pan A), whilst the profiles on the right were taken in the early evening when it was cloudy (Ants Pan B). The two profiles from Ants Pan A exhibit similar trends. Initial values are close to 100% atmospheric saturation until the sediment water interface (SWI; represented by the 0 line), although the profile represented by the grey line exhibits more fluctuations. At the surface, both profiles increase in oxygen concentrations to a peak of 340% (black profile) and 230% (grey profile). Below this peak, oxygen concentrations in both profiles drop to zero, by 0.6 cm in the grey profile and 0.8 cm in the black profile. Ants Pan B also has two profiles that exhibit similar trends; they have consistent oxygen percentage of approximately 95% atmospheric saturation throughout water, and at the SWI there is a minor increase to 110% O_2 (grey profile) and 98% O_2 (black line). Both profiles then drop to zero oxygen by 0.4 cm.

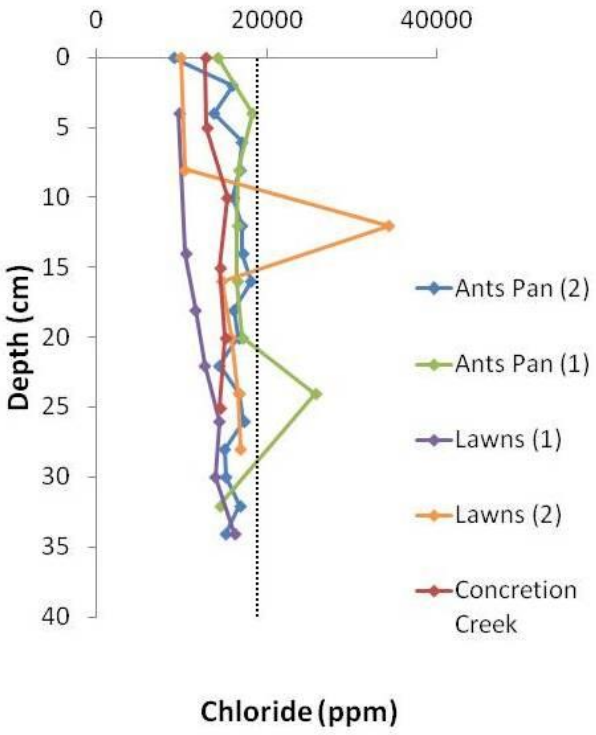

Figure 5.3 Pore-water chloride depth profiles from cores.
Concentrations of Cl are below seawater concentrations (black dotted line) in all sites, suggesting that at the time of sampling there was an influence of rainwater. In all sites the chloride concentrations increase with depth. This core was sampled during March, 2008.

Concentrations of Cl in Ants Pan (1) have initial surface values of 14,260 ppm which increases up to 18,300 ppm by 4 cm. Concentrations below this depth tend to be close to 16,500 ppm, apart from a peak at 24 cm (25,000 ppm). In Ants Pan (2) values are slightly lower at the surface (9000 ppm) than they are for the rest of the profile which tends to lie close to 16,500 ppm. The surface sample from Lawns (1) was contaminated during analysis, thus the profile begins at 4 cm (9,700 ppm); the profile then shows a general increase in concentrations throughout the rest of the profile with the maximum value (16,200 ppm) in the deepest measured sediment (34 cm). Lawns (2) has a profile that also increases down throughout the profile but not as markedly, additionally there is a large peak in concentration at 12 cm (34,400 ppm). Surface concentrations are close to 9,900 ppm and the deepest sample (28 cm)

is 16,900 ppm. The profile for concretion creek has surface concentrations at 12,700 ppm, and the deepest data sample (25 cm) has 14,500 ppm of Cl; maximum concentration is found at 10 cm depth and is 15,400 ppm.

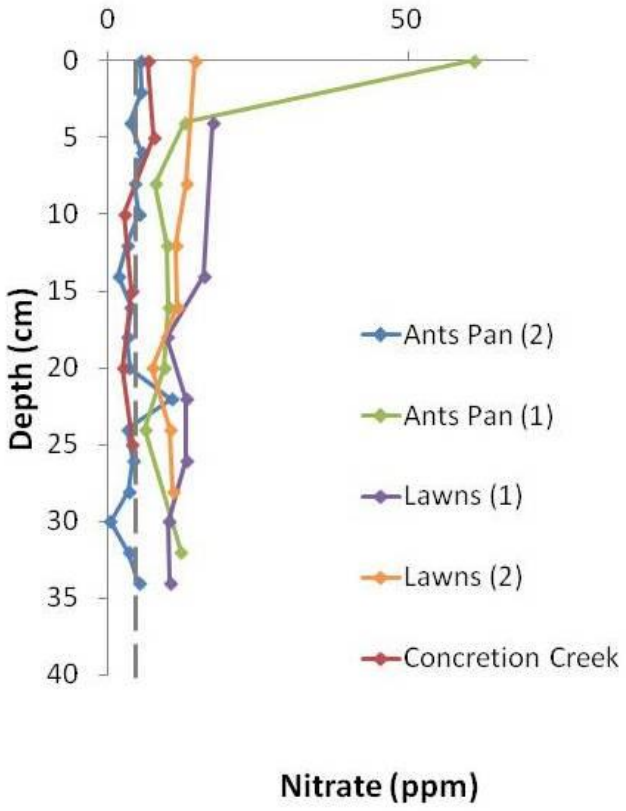

Figure 5.4 Pore-water nitrate depth profiles from cores.
Seawater nitrate average concentration is not added as it is highly variable and fertilisers will influence the amount of nitrate found at this site due to the agricultural land found inland of Warham. Detection limits were used for the nitrate runs, which is represented by the grey dashed line. Ants Pan (2) and Concretion Creek are close to and below detection, whilst the other sites are above detection. In all sites nitrate concentrations are higher in the near-surface than at depth. This core was sampled during March, 2008.

The grey dotted line indicates the detection limit of nitrate on the Dionex IC machine. This was determined by calculating the standard deviation of the blank and multiplying by 3. Surface concentration of nitrate at Ants Pan (1) is at 60 ppm, and drops to 13ppm by 4 cm depth. From 8 to 32 cm (last sample depth), NO_3^-

concentrations range between 7 and 12 ppm. Ants Pan (2) profile is always close to the detection limit. Initial values are approximately 5 ppm and stay close to this value until 10 cm, where values go below detection until a peak at 22 cm (10.5 ppm). Below this depth values are again below detection. The first data sample for Lawns (1) is at 17 ppm (4 cm), which drops to 9.8 ppm by 18 cm. Below this depth, concentrations range between 10 and 13 ppm. At Lawns (2), surface values are at 14.5 ppm dropping to 7.4 ppm by 20 cm; deeper than this nitrate concentrations began to increase and are up to 10.7 ppm by 28 cm. Concretion Creek has surface values at 6.7 ppm which by 10 cm are below detection and stay below for the rest of the measured profile.

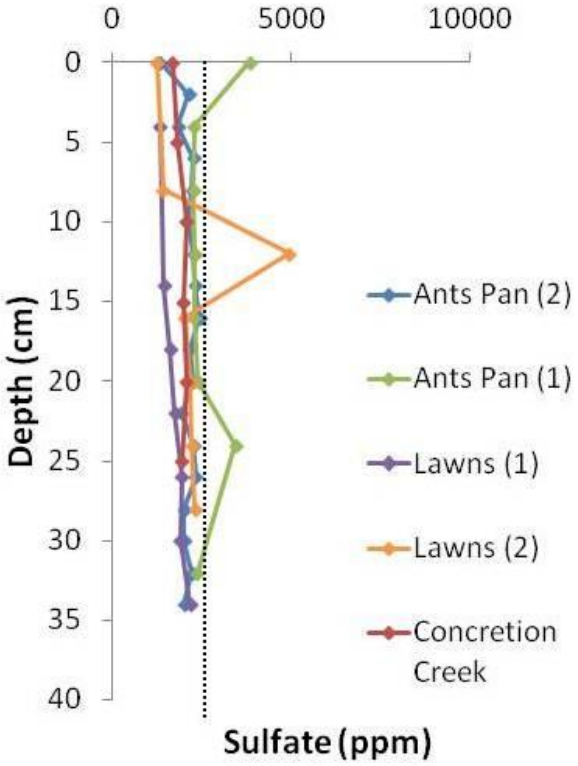

Figure 5.5 **Pore-water sulfate depth profiles from cores.**
Concentrations of SO_4^{2-} are below seawater concentrations (black dotted line) in all sites, suggesting that at the time of sampling there was an influence of rainwater. SO_4^{2-} concentrations in both Lawns sites, Concretion Creek and Ants Pan (2) show an increase with depth

whilst Ants Pan (1) has little overall variation of concentration throughout, however there is a peak at depth in this profiles (as there is with Lawns 2). This core was sampled during March, 2008.

Surface concentration at Ants Pan (1) is at 3,800 ppm and between 4 and 32 cm, sulfate concentrations lie close to 2,300, however a peak of 3,400 pm is found at 24 cm depth. Sulfate in Ants Pan (2) has surface concentrations of 1,300 ppm, which increase to 2,130 ppm by 2 cm. Deeper in the sediment and throughout the rest of the profile values range between 1,800 and 2,400 ppm. At 4 cm in Lawns (1) concentration of sulfate is at 1,300 ppm and values increase gradually up to the deepest part of the measured section (34 cm) to 2,200 ppm. Lawns (2) has surface concentrations of 1,200 ppm with the rest of the profile gradually increasing in concentration until the end of the measured section; 2,300 ppm at 28 cm. Superimposed on this trend is a large peak at 12 cm (4,900 ppm). Surface concentrations are close to 1,700 ppm of sulfate, reaching a peak by 10 cm (2,060 ppm) in Concretion Creek's profile. Concentrations than gradually decrease to 1,900 ppm by 25 cm.

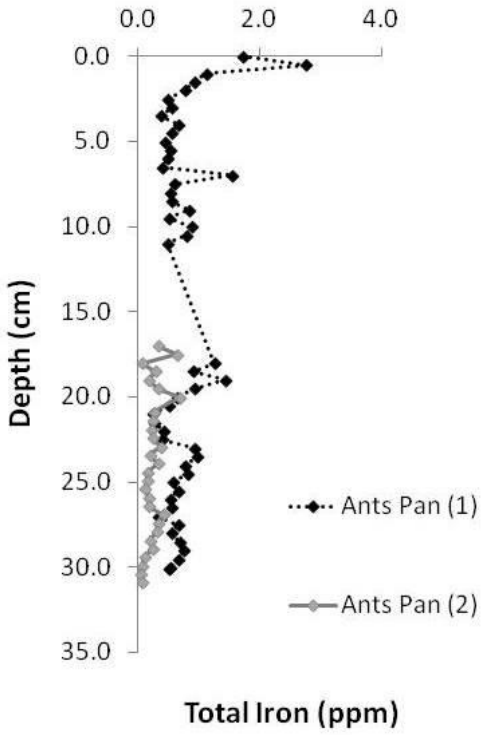

Figure 5.6 Iron DET gel probe pore-water depth profiles.
The gel data were obtained in March, 2010. NB in Ants Pan 2 the upper section of the gel was contaminated and therefore discarded. Depth profiles were obtained by placing two probes on an aluminium rod, which created a gap. This is between ~ 11 and ~17 cm depth. Ants Pan shows low concentrations of total Fe as does Ant Pan 1. At the top of Ants Pan 1 there is a large increase in total Fe concentrations followed by a decrease.

Iron DET depth profiles could only be retrieved for Ants Pan (1) and (2), and for the latter only the deeper probe worked. Initial concentrations in Ants Pan (1) are at 1.7 ppm, followed by an increase in concentrations to 2.7 ppm by 0.5 cm, this peak in concentration drops to a minimum by 3.5 cm (0.4 ppm). Deeper than this the profile, although scattered, Fe concentrations range between 0.4 ppm and 0.9 ppm until 11 cm. Coinciding with a change in probes (see methods chapter) is an increase in concentrations to 1.2 ppm at 18 cm that decreases to 0.2 ppm by 21 cm. Deeper than this is an another small peak up to 0.9 pm (by 23.5 cm) and a minimum at 27 cm (0.3). There is either another small peak between this depth and the end of the profile or the profile is scattered, but maximum concentration here is 0.8 ppm (29 cm) and

minimum is 0.5 ppm (at 30 cm). The only retrievable part of Ants Pan (2) was the lower probe. There is a trend of iron concentrations decreasing from 0.3 ppm (17 cm) down to 0.04 ppm by 30.4 cm depth, however this is scattered; additionally some peaks are superimposed on this trend (0.7 ppm at 20 cm; 0.4 ppm at 26.9 cm).

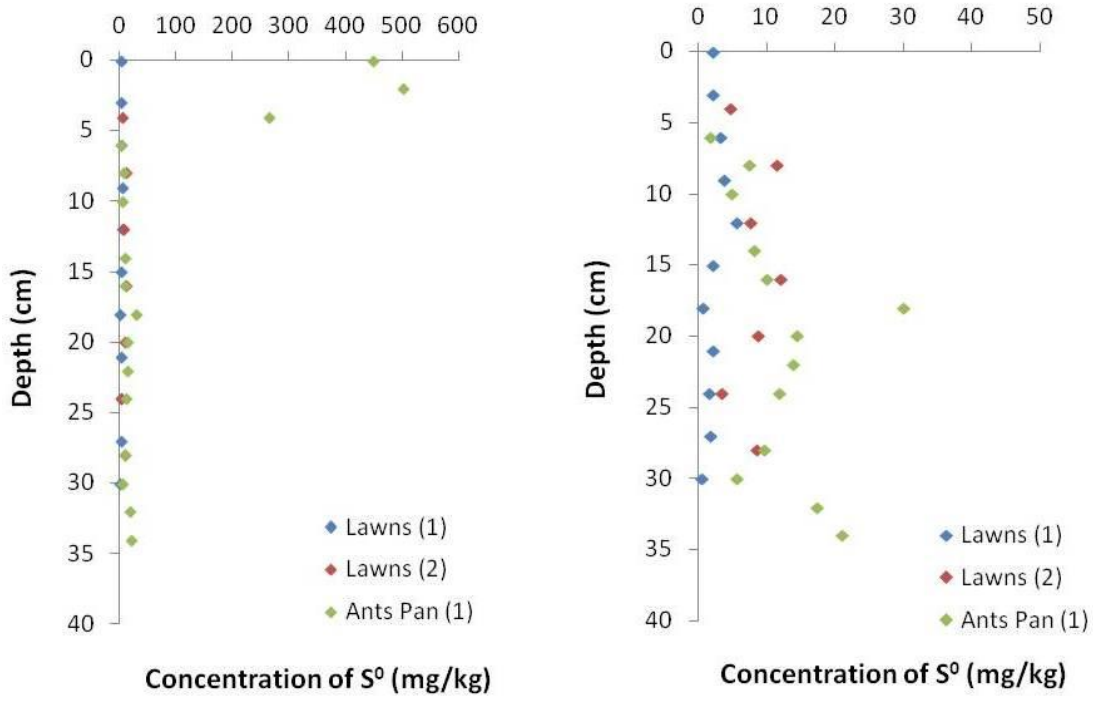

Figure 5.7 **Solid-phase elemental sulfur depth profiles.**
Both left and right images are from the same data set (sampled March, 2008), however, the left image shows the full-scale range to incorporate the high values at the surface for Ants Pan site 1 and the image to the right is scaled to show the detail for all sites. This figure clearly shows that elemental S is found at depth and in large amounts at the surface.

The S^0 sediment profile from Ants Pan (1) show high concentrations in the upper 5 cm (values up to 500 mg/kg), in contrast to the Lawns (1) profile, which in the upper 5 cm are lower than the peak between 6 cm and 12 cm (maximum concentration is 5.6 mg/kg). Apart from two minima at 18 and 30 cm, 0.7 and 0.5 mg/kg respectively, concentrations of S^0 are close to 1.7 mg/kg in Lawns (1). Lawns (2) has no surface values (due to extraction problems) in the upper 4 cm, however, the concentrations

are higher than Lawns (1) (throughout the entire profile) and peaks at 8 (11.5 mg/kg), 16 (12.2 mg/kg) and 28 cm (8.6 mg/kg). Ants Pan (1) has the most scattered profile and the highest concentration; highest concentration peaks are at 18 (30.1 mg/kg) and 34 cm (21.1 mg/kg) and minimum is at 6 cm (1.8 mg/kg). The rest of the profile, although scattered has concentrations ranging between 5 and 14.5 mg/kg.

5.3 Discussion

5.3.1 Oxygen profiles

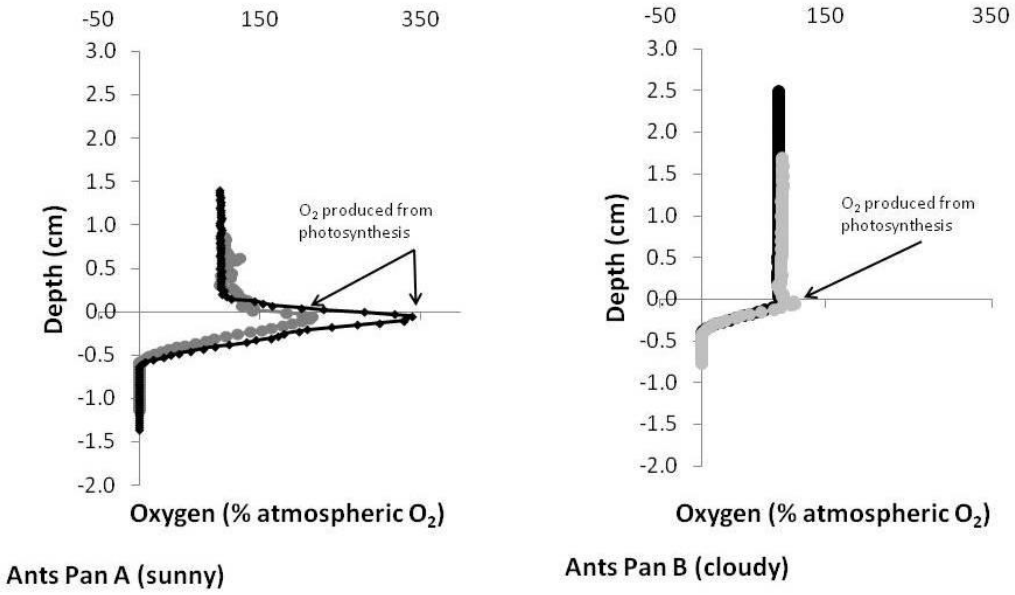

Figure 5.8 Oxygen depth profiles for Ants Pan.
Profiles on the left were recovered during the middle of the day during a sunny period; profiles on the right were taken from the early evening during a very cloudy period. O_2 is depleted below approximately 0.5 cm in both datasets.

All four O_2 profiles are from Ants Pan; two profiles were recovered during a sunny period during the middle of the day (Figure 5.8: left) and two during a cloudy part of the early evening (Figure 5.8: right). The zero line on both images represents the SWI and the peaks in O_2 coincide with this. These peaks are a product of photosynthesis and the differences between the images will be due to the change in

weather conditions whereby microphytobenthos (e.g. benthic diatoms) are more active during the sunny times, thus producing a more pronounced peak during sunlit sampling than during cloudier times. Below the SWI, and in all profiles, O_2 is rapidly used up by microbial uptake with conditions being fully anoxic by approximately 0.5 cm.

5.3.2 Pore-water geochemistry

5.3.2.1 Chloride

Chloride profiles are useful to understand evapotranspiration processes and changes of both seawater and rainwater fluxes. It also indicates how successfully the probes or cores have worked due to chloride being chemically conservative, due to plants not releasing or taking up Cl and it being unaffected by redox reactions (Bottrell et al., 2007). This is reflected well in the Cl profiles for Concretion Creek and Ants Pan (2) which show uniform concentrations with depth; Ants Pan (1) and both Lawns profiles do however, show some variation with depth. Lawns (2) and Ants Pan (1) both exhibit two large peaks, both with one data point each for the positive excursions. This is also observed in the same data point for the sulfate profiles suggesting that it is more likely to be an analytical problem, for example, the sample has been poorly sealed and evapoconcentration has occurred, or that the analysis has failed on the IC. These data points are unreliable thus they are ignored, which in Ants Pan (1), leaves a slightly scattered, yet without any big variations of Cl concentrations, profile. Removing the point from Lawns (2) leaves a similar profile trend to Lawns (1), showing a gradual increase in Cl from the surface through depth. This gentle increase in Cl concentrations throughout the profile could indicate

changes in inputs of rainwater vs. seawater over time, and Cl is diffusing upwards due to more recent rainwater input relative to seawater input.

All profiles from Warham Salt Marsh show little variation with high Cl concentrations indicating little hydrological changes (e.g. major lateral flows) and high seawater fluxes into the sediment.

5.3.2.2 Nitrate

The black dotted line in Figure 5.4 represents the detection limit for this sample run. The grass near Concretion Creek has a small amount of nitrate present in the surface decreasing until 7 cm, and below this depth the concentrations are below detection. When nitrate is plotted against chloride (Figure 5.9) it confirms that nitrate concentrations are decreasing relative to chloride in the upper part of the profile. This is most likely resulting from the reduction of nitrate in the near-surface sediments. Lawns 1 and 2 show very similar profiles with nitrate concentrations being higher at the surface than at depth; this is also in line with nitrate reduction in the near-surface.

In Ants Pan (1) there is a marked decrease in nitrate from the surface down to approximately 5 cm; the sulfate profile also shows a marked decrease in the same place. Nitrate is enriched at the surface compared with chloride (as seen in the nitrate/chloride plots; Figure 5.9); this could result from nitrification during the breakdown of OM, producing ammonium which oxidises to nitrate at the surface due to the higher levels of O_2. Below this depth there are minor fluctuations of nitrate concentrations. When removing the cores, there were large crab burrows seen close to the core retrieval locations within Ants Pan. At the same depth there is a minor increase in the corresponding Cl profile. It is speculated that some of the profiles

may be influenced by these burrows which have brought O_2 into the deeper sediment oxidising nitrite or ammonia. Ants Pan (2) is very close to detection limits throughout the profile, and any reduction of nitrate in the near surface is hard to identify. There is however, a peak in the nitrate: chloride profile at approximately 22 cm depth, which reflects an increase in chloride and not nitrate. It is unclear why there is a minor Cl decrease in this zone.

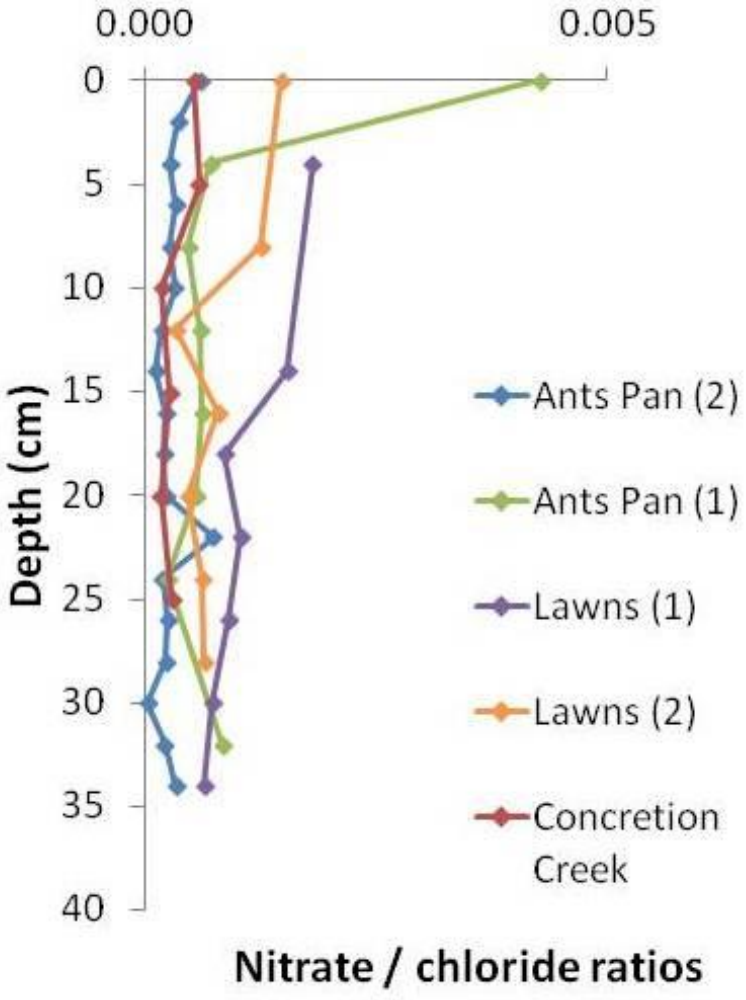

Figure 5.9 Ratio of nitrate to chloride depth pore-water depth profiles
As chloride is a conservative species it is not expected to undergo many reactions deeper in the sediment. Thus nitrate is plotted against Cl to establish the reliability of the peaks. In these datasets it is clear that nitrate is enriched to Cl in the near-surface and the gradual depletion of nitrate with depth is due to nitrate reducing bacteria.

5.3.2.3 Iron

The iron data was recovered three years after the core data, and it is assumed that these data are representative of Warham Salt Marsh (see further work section). The concentration increase from the SWI to just below the near surface could result from reductive dissolution of highly reactive Fe-minerals by iron reducing bacteria. Just below this the total iron concentrations decrease due to iron diffusing from higher concentrations to lower concentrations at about 3.5 cm. Deeper than this and down through the measured section (and in the lower Ants Pan (2) sections) concentrations fluctuate. The main process involving iron in these types of sediments is iron reduction, either biotic (usually higher in the sediment) or abiotic (usually deeper in the sediment), and removal of iron by precipitation of minerals, for instance, FeS and/or siderite. The aqueous iron concentrations is a balance between the generation of Fe(II) from iron reduction and loss of iron by mineral precipitation, and as the iron concentrations are variable throughout the profile, it suggests that iron reduction is maintained deeper in the profile rather than only being precipitated into minerals.

5.3.2.4 Sulfate

The sulfate profiles from this study show differences to idealised salt marsh profiles that are under anoxic conditions. Idealised profiles have sulfate concentrations higher in the near-surface which decline with depth (Chapter 1; Figure 1.2), consistent with bacterial sulfate reduction in the upper part of the salt marsh sediment. Instead, this study's sulfate profiles show persistent SO_4^{2-} and minor concentration variations throughout the depth sampled. This becomes even more evident when plotting sulfate against chloride (Figure 5.10). In both Ants Pan profiles (but more so in Ants Pan (1)) there is an increase of sulfate relative to chloride in the near-surface. As the major source for both sulfate and chloride is

seawater at this salt marsh, then there must be another source of sulfate. Another addition of sulfate is at depth in Ants Pan (1) which is coincident with a nitrate peak in the deepest horizon measured (as previously discussed). However, when viewing the chloride profile it becomes clear that this isn't an increase of sulfate and nitrate but a decrease in chloride; the reasons for this are unclear. Iron monosulfides have been reported at Warham (e.g. Pye et al., 1990; Mortimer et al., 2011), thus sulfate reduction does occur. The concentrations reported from this study are sensible, that is, they are in line with previously reported values and are close to initial seawater concentrations. As these sulfate profiles are for the most part, rather uniform, it suggests that there is little or no net loss of sulfate from the sulfate pool although it has been shown that S cycling occurs within these sediments.

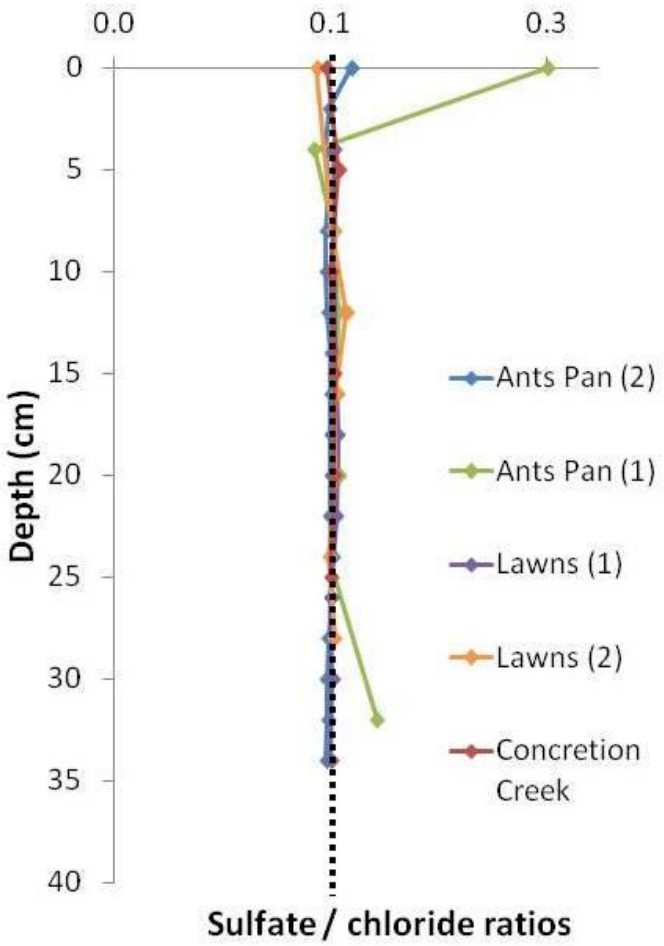

Figure 5.10 Ratio of sulfate to chloride pore-water depth profiles.
As chloride is a conservative species, it is not expected to undergo many reactions deeper in the sediment. Thus sulfate is plotted against Cl to establish the reliability of the peaks. The fact the sulfate/chloride ratios are close throughout the profile would indicate that sulfate doesn't undergo any reactions throughout the sediment, except at the very near surface. However, sulfate reducing bacteria are likely to be in this sediment and it is more likely that sulfate reduction does occur but sulfide produced is largely re-oxidised rapidly.

5.3.3 Elemental sulfur

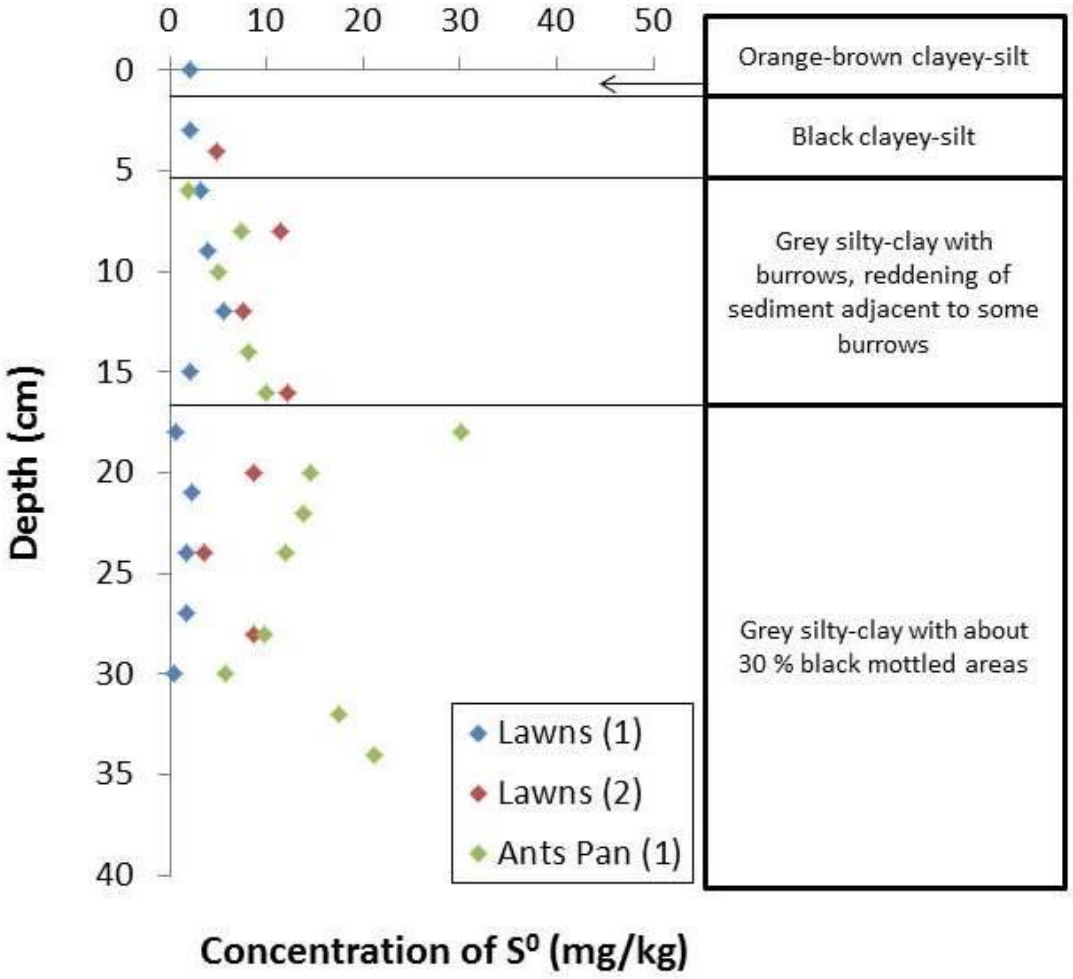

Figure 5.11 Solid-phase S^0 concentrations and sediment description against depth.

This is a 'fixed concentration depth profile' so that the variations in concentrations can be easily seen. For Ants Pan 1 the shallow values are high, between 250 and 500 mg/kg. A generalised Ants Pan sediment description is included to illustrate the redox states of the sediment. The presence of elemental sulfur at this site provides evidence for partial oxidation of sulfide at depth.

At Ants Pan site, there are high values of zerovalent sulfur in the upper 5 cm (Figure 5.11), consistent with the large amount of iridescent sheen seen on the surface of water pans and creeks. In this horizon (the upper 5 cm) in salt marsh sediments there are usually higher Fe concentrations, with Fe reduction generally restricted to this zone (Kostka et al., 2002). Microbial iron reduction does not partially oxidise sulfide to elemental sulfur or fully oxidise it to sulfate. However, any H_2S that reduces iron (as in reaction 5.4), or by the oxidation of iron monosulfides by very reactive Fe (e.g. reaction 5.3), would cause an increase in S^0. Moreover, it is possible that some of the S^0 will undergo full oxidation to SO_4^{2-} in this horizon (reaction 5.6), causing an increase in SO_4^{2-} concentrations relative to seawater (and chloride).

$$4S^0 + 4H_2O \rightarrow SO_4^{2-} + 3H_2S + 2H^+ \quad (5.6).$$

Although there will be bacterial reduction at the near-surface which uses seawater sulfate to form H_2S (which is often reoxidised to sulfate) the large increase in S^0 is more likely to be due to pore-water advection/diffusion from depth. This introduces H_2S to the near-surface where it is partially oxidised by O_2 (reaction 5.7), also explaining the excess sulfate in the sulfate:chloride profiles.

$$2HS^- + O_2 \rightarrow 2S^0 + 2OH^- \quad (5.7).$$

Concentrations of zerovalent sulfur remaining relatively high in the anoxic zone is unexpected. This is because elemental S is predominantly an intermediate product and is not normally stable under reducing conditions, often reacting with iron monosulfides to form pyrite (e.g. reaction 5.8; Berner, 1970), or with Fe^{2+} and H_2S as in reaction 5.5.

$$FeS + S^0 \rightarrow FeS_2 \quad (5.8).$$

The elemental data shows that there must be partial oxidation of sulfide throughout the sediment. The formation of iron monosulfides shows that there is reduction of sulfate to sulfide. However, the sulfate profiles show that although there is persistent sulfate throughout the depth it doesn't vary considerably in concentrations. Therefore the combined data shows that there is cycling of S species, and furthermore it must be at similar rates to provide such uniform sulfate concentration profiles.

5.3.4 Depositional and diagenetic model for Warham Salt Marsh

Oxygen is limited to the upper ½ cm of the salt marsh. In the upper part of the sediment, nitrate is reduced and concentrations remain close to detection limit, although persisting in some sites. Total iron concentrations initially increase at the near surface; this is probably reflecting an increase of Fe^{2+} in the sediments by the microbial reduction of Fe^{3+}. In Ants Pan (1) the sulfate profiles show a large input of sulfate relative to chloride and the sediments contain a large amount of S^0. The large amounts of S^0 seen in the surface (seen in the profile from Ants Pan but also known from the iridescent sheen of S^0 seen across most of Warham Salt Marsh) could be due to pore-water advection/diffusion of H_2S from the deeper sediments which is partially oxidised by iron and/or then fully oxidised by (predominantly) O_2 in the near-surface, explaining both increases seen in sulfur species. However, the other profiles and the rest of Ants Pan (1) have persistent sulfate concentrations throughout the depth measured. Indeed, when plotted against chloride, the results show minimal variation in the profiles, suggesting that sulfate is not removed or added throughout the salt marsh sediments. Yet the formation of iron monosulfides and that elemental sulfur concentrations fluctuate throughout depth prove that sulfur species in Warham Salt Marsh must undergo S cycling. As the iron profiles show variability throughout

depth, it suggests that Fe is undergoing reduction-oxidation reactions deeper in the sediment. Aplin et al. (1993) have suggested that during conditions where sedimentation rates are rapid, a proportion of reactive Fe-minerals, and the majority of the less reactive Fe-minerals, will be buried before they undergo diagenetic reactions. This provides a pool of available Fe deeper in the sediment. At Warham the sedimentation rate is known to be rapid (comparison of aerial photography); it is proposed that the pool of available Fe deeper in the sediment reacts with H_2S, reducing Fe^{3+} and partially oxidising SO_4^{2-} to S^0. Some of the S^0 can then undergo further oxidation to SO_4^{2-} at depth. It is postulated that sulfate is being reduced at a similar rate as partial oxidation of H_2S to S^0, and then full oxidation to SO_4^{2-} (Figure 5.12), explaining why it appears that sulfate reduction does not occur in the sediments when using coarse-resolution sampling. If the DET and DGT probes had been successful then these key details would have been observed.

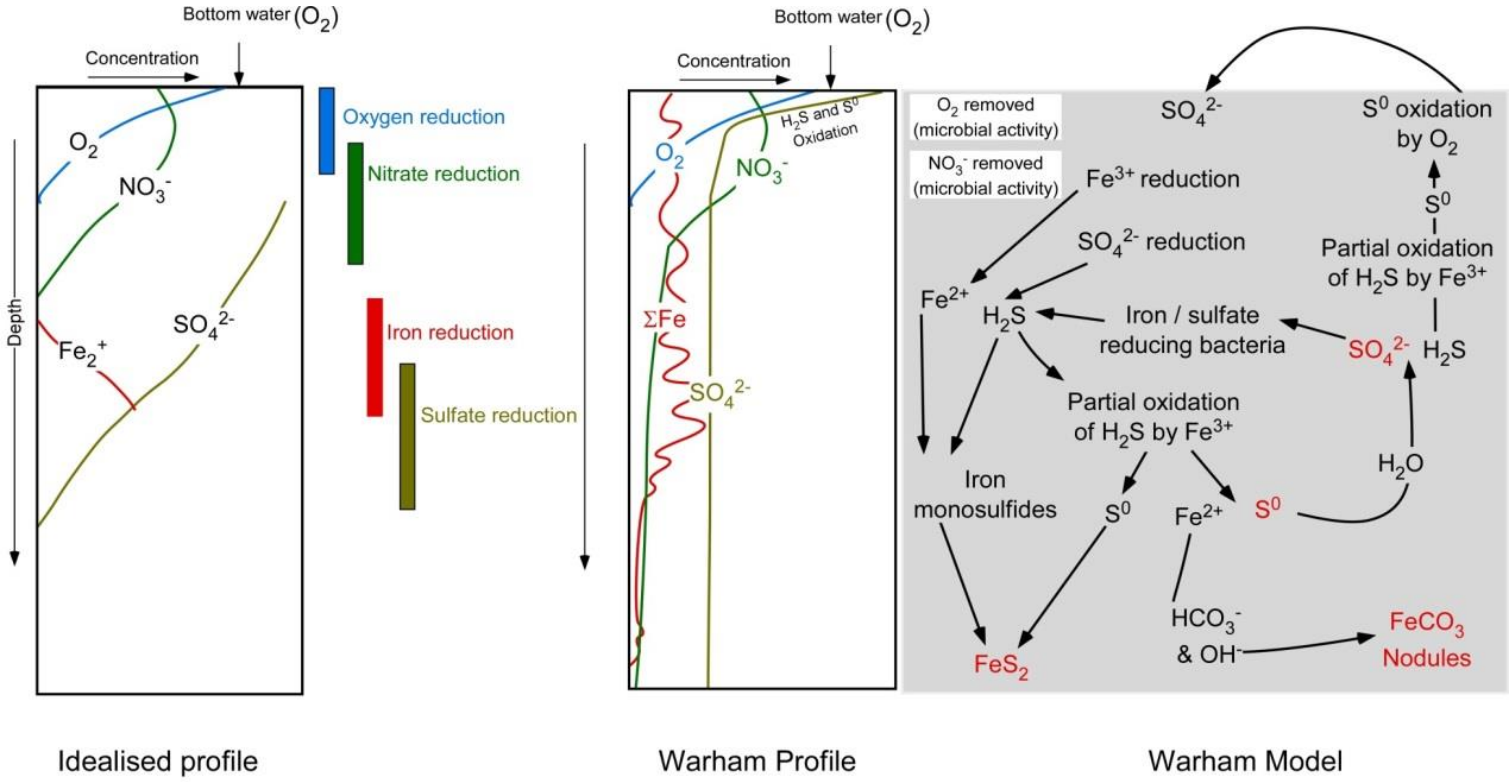

Figure 5.12 Depositional and early diagenesis model for Warham.
The image to the left shows an idealised profile for marine sediments. Salt marshes are expected to behaviour similar to this; however, Warham profiles show that sulfate is persistent throughout the measured section. The model show the key reactions for this phenomenon. Oxygen, nitrate, sulfate and iron($^{3+}$) are reduced in the upper part of the saltmarsh sediment by microbes. The reduced sulfur and iron can react to form iron monosulfides. Due to the high rates of sedimentation however, more of the highly

reactive iron($^{3+}$) is buried rapidly and later acts to oxidize sulfide, adding S^0 to the deeper parts of the sediment, some of this will then fully oxidise to sulfate. Additionally, in the near surface most of the S^0 will be fully oxidised to sulfate. Some of the reduced iron reacts with carbonate to form siderite nodules.

5.4 Conclusions

High sedimentation rates at Warham provide a mechanism to bury a proportion of reactive Fe-minerals and the majority of the less reactive Fe-minerals, without them undergoing any diagenesis, resulting in a pool of Fe^{3+} in the deeper sediment. Elemental sulfur is high in the near surface sediments in Ants Pan, but is also seen throughout the profile even though O_2 is depleted, thus it is postulated that H_2S is oxidised by the deeper buried reactive Fe^{3+} producing the partially oxidised S^0. The elemental sulfur then undergoes further reactions resulting in sulfate at depth. However, the pore-water data suggest that the sulfate does not undergo any reduction reactions (except for the very near-surface), especially when plotted against chloride. This profile is more likely to be resultant from the net effect of all sulfate reduction and sulfide oxidation. The large amounts of SO_4^{2-} and S^0 seen in the near-surface could be due to pore-water advection/diffusion of H_2S (and S^0) from the deeper sediments to the near surface where it is either partially oxidised by Fe^{3+}, producing sulfate, or O_2, producing SO_4^{2-}. The low resolution data obtained for this study misses out the key details and thus the sulfate core pore-water data are rather uniform concentration profiles due to oxidation rates being similar to reduction rates. As there is iron released deeper in the sediments from early diagenesis, it is available to react with carbonate ions (from seawater) to form siderite. Concurrently, the sulfide and reduced iron form iron monosulfides.

5.5 Further Work

The datasets used for this sub-study are not robust. This is in part, due to the assumptions associated with them, for instance, there is a supposition that the profiles are representative over time, yet the iron DET data was obtained after a significant time lapse from the other datasets. Data retrieval problems have been rife throughout field trips, and much of the further work listed below was intended to have been collected for this study. However, the method problems have been identified and the following should be successful:

- Iron and sulfate DET concentration data and iron and sulfide DGT flux data: determine the key details and elucidate the availability of species.
- Sulfur isotope analysis: identify the sulfur fractionation processes and determine if the elemental sulfur has light isotope compositions that are in line with bacterial reduction.
- Sulfate O isotopes: identify if sulfate was being cycled (reduced and reformed) as the reformed sulfate will likely contain O from different sources to the original marine sulfate.
- Solid iron speciation: this would distinguish between the Fe-minerals and would indicate how deep the highly reactive and poorly reactive minerals have been buried.
- Quantitatively determine the amount of carbonate in the pore-waters: calculate how much carbonate is available to react with the available iron.
- Isotope analysis on the carbonates: determine if the source is predominantly seawater.
- Ammonium DET analysis: identify production of nitrate by ammonium oxidation.

Chapter 6 Deposition and diagenetic model: Shales-with-Beef Member

6.1 Introduction

It is well accepted that sulfate is reduced to H_2S (reaction 1.5; Chapter 1) by bacteria using sedimentary OM as a reducing agent and energy source, increasing the alkalinity of the surrounding pore-waters (Berner, 1966; Morse et al., 1985; Walter et al., 1993; Ku et al., 1999). Most of the H_2S in marine sediments is reoxidised to sulfate or an intermediate form of S (Zopfi et al., 2004 and references therein), however, it has two other possible sinks, either binding with organic matter or metals (Francois, 1987; Zabac and Pratt, 1992; Peters et al., 2005). For the latter the H_2S usually reacts with iron minerals to produce metastable monosulfides, and in fully reduced and stable conditions, they will eventually form pyrite (e.g. Berner, 1970, 1984; Jorgensen and Fenshal, 1974; Goldhaber and Kaplan, 1980). This process will result in isotopically light pyrite as the bacteria which mediate these reactions preferentially use ^{32}S (e.g. Jones and Starkey, 1957; Harrison and Thode, 1958; Kaplan et al., 1963; Kaplan and Rittenberg, 1964; Canfield, 2001). Moreover, in marine sediments this is the most important process which affects isotopic fractionation of sulfur, thus it can help elucidate the depositional environment (e.g. Kaplan et al., 1963; Bottrell and Raiswell, 2000; Canfield, 2001). If the sedimentary depositional system does not change (isotopically light) pyrite will continue to form, however if the Fe pool is depleted then organosulfur compounds will form instead of pyrite (Kohnen et al., 1989; Bruchert and Pratt, 1996). In highly sulfidic environments, minerals such as (rare) MnS can form when reactive Fe-minerals are

depleted and as a consequence, Mn is precipitated by the high alkalinity resulting from OM degradation (Mort et al., 2010).

Changes in other parameters can also influence early diagenesis. For example, changes in sedimentation rates have long been known to change mineralogy in sedimentary formations (e.g. Raiswell, 1987), and when paused or slowed, this often results in concretions and/or cemented horizons (Majewski, 2000; Witkowska, 2012). This is clearly demonstrated by Bréhéret and Brumsack (2000), within the Marnes Bleues Formation (S.E. France). Under normal sedimentation rates barium was located within the deeper, reduced part of the sediment where sulfate was limited, but during long pauses in sedimentation, sediment winnowing occurred and sulfate and barium were located at similar horizons, leading to the precipitation of barite and subsequent growth of concretions. Similarly, Taylor et al. (1995) also found that paused or reduced sedimentation rates in the Book Cliffs Formation (sandstones) caused carbonate precipitation, however this was due to increased residence times of species within the early diagenetic zones. In the latter example, the slower sedimentation rate allowed the shallower sediments to remain longer in the biochemically active zone compared to sediments under normal sedimentation rates. Sediment remaining longer in the biochemically active zone would undergo greater evolution of pore-water chemistry leading to increased alkalinity, in turn driving more carbonate precipitation reactions, thus producing concretions. Therefore if different horizons represent the change in time-integrated effects of burial diagenesis at different sedimentation rates, then there should be systematic differences in both S and Fe cycling preserved within the rock record.

During the Lower Jurassic, the British Isles were located at a similar latitude to that of Central Spain today (Getech, 2013). The environment of deposition across most

of southern Britain was predominantly a shallow epicontinental seaway during the Sinemurian (Bradshaw et al., 1992; Evans et al., 2003; Ziegler, 1990). Although eustatic sea-level fluctuated (Hallam, 2001), the (Present Day) Dorset Coast was always in an offshore sub-aqueous environment (Figure 6.1). It is in this location, a coastal cliff on the Dorset Coast near Charmouth, that the Shales-with-Beef Member crops out; a 28-30m thick, basal member of the Charmouth Mudstone Formation. This member has been well-studied (e.g. Lang et al., 1923; Marshall, 1982; Wolff et al., 1991; Parkinson, 1996; Gallois, 2008; Paul et al., 2008; Page, 2009) and thus is a good test case to look for correlations between the change in conditions (as indicated by the formation of concretions) and any other changes within the inorganic / organic geochemistry of the surrounding host rock.

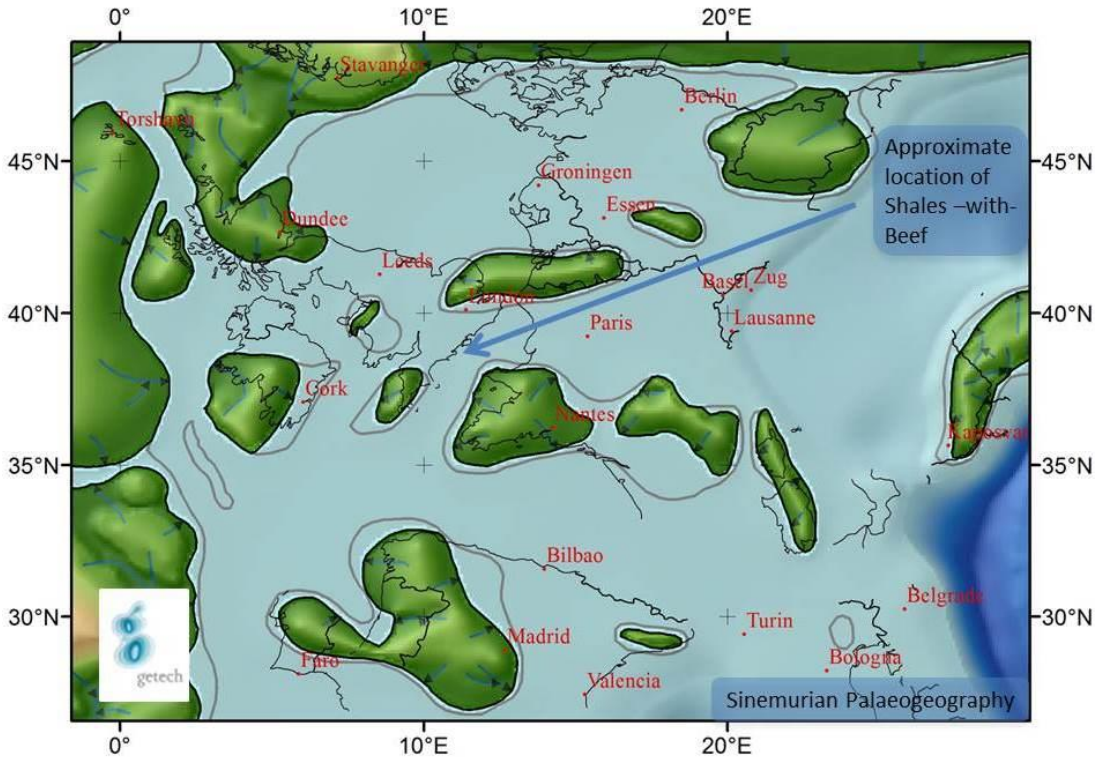

Figure 6.1 Palaeogeography of the British Isles and surrounding area.
This is the palaeotopography for (what is now) Europe during the Sinemurian (Lower Jurassic). The light blues are shallow marine and the dark blues are deeper marine; the darker greens are low lying land and the lighter greens are topographically higher. The grey line

represents low-stand coastline, showing that there are changes with the shore-line in this area; however, the Shales-with-Beef formation will always be deposited within shallow marine conditions. Image courtesy of Getech (2013).

6.1.1 Shales-with-Beef Member

The Shales-with-Beef Member is a progradational sequence (Parkinson, 1996) comprising fossiliferous marine paper shales, with limestone beds and interbedded seams of fibrous calcite separated by clay parting ("Beef") (Lang et al., 1923; Gallois, 2008; Paul et al., 2008; Page, 2009). It is highly variable laterally, but can be divided into three main stratigraphic sequences which are separated by faults (Gallois, 2008). The samples collected for this work (Figure 6.2) are from the same location as that of Lang et al. (1923). In the upper part of the Shales-with-Beef Member (Figure 6.2) there is a zone of ovoid, tabular and spheroidal calcitic concretions, with weakly pyritic margins, that are often coalesced into an irregular limestone bed; this is the Birchi Bed (no.75; Lang et al., 1923). The Birchi Beds are thought to have been deposited in an anoxic environment as the shales are finely laminated with no evidence of benthic activity, and the $\delta^{13}C$ values from the concretion core and outer rim are between -10 to -14‰, suggesting an important contribution of carbonate derived via sulfate reduction (Marshall, 1982). The latter also show that the carbonate concretions grew in the upper few cm's of the sediment (Coleman and Raiswell, 1981). The 'beef' seams are best developed around the concretions, although they do also occur in lenses throughout the shales (Marshall, 1982). Wolff et al. (1991) studied the concretions in detail and discovered that they can be broken down into three zones: a calcitic core, dolomitic zone and calcitic outer rim. These zones represent the different bacterial processes during the time of carbonate formation. The calcitic core formed during intense bacterial sulfate reduction and has suffered the most degradation. The dolomitic zone formed during

methanogenesis, and the outer rim calcites formed when there was iron and manganese reduction. This is consistent with the depositional environment remaining reduced throughout concretion formation.

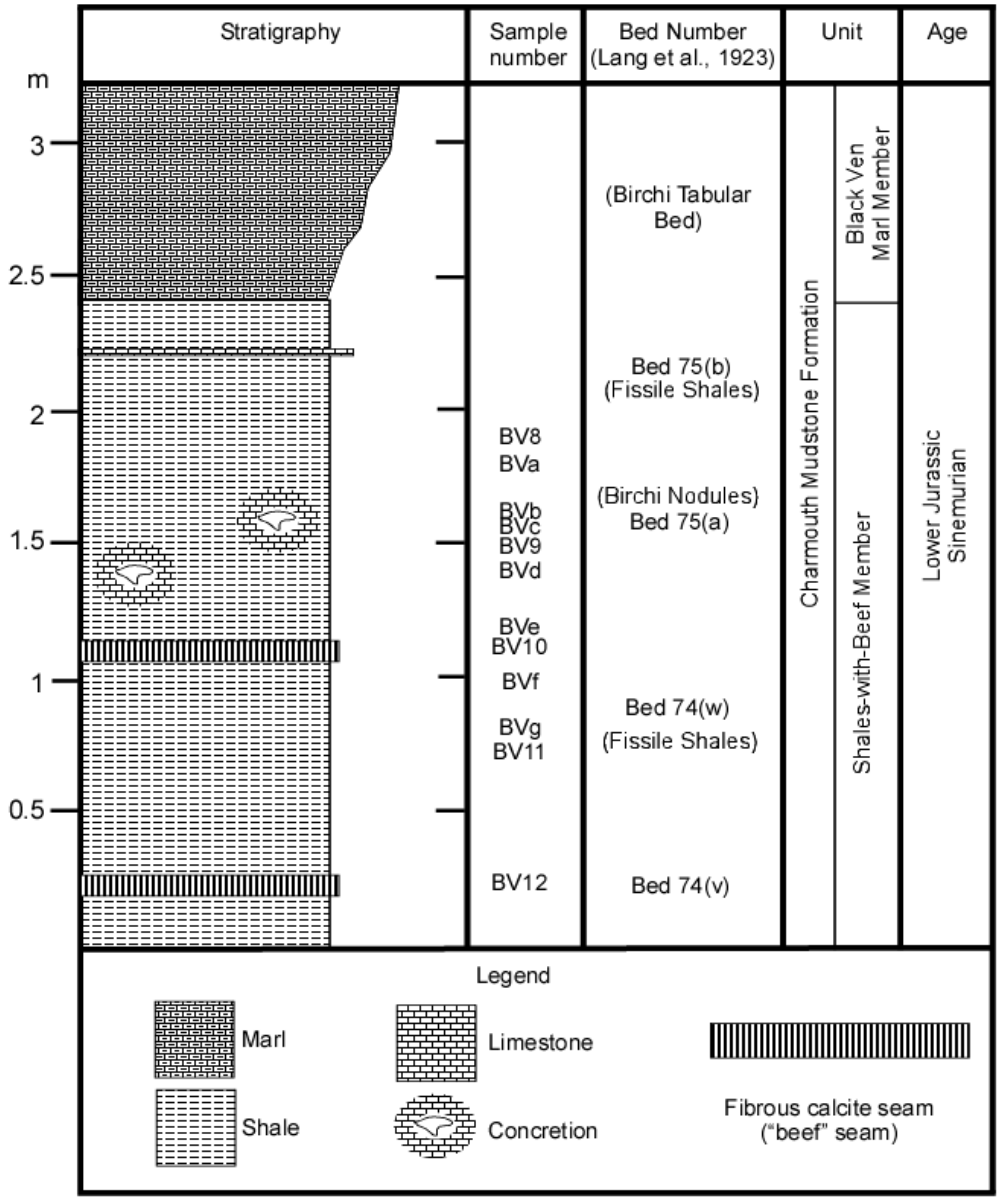

Figure 6.2 Stratigraphy of the Shales-with-Beef Member.
This shows the upper section of the Shales-with-Beef Member, part of the Charmouth Mudstone Formation. The majority of this member comprises 'paper' shales, however many concretions and 'beef' seams can be found within the unit. All samples were taken from the shales.

The large quantity of OM found in the Shales-with-Beef Member, the concretion formation, the lack of morphological changes of the shales, and lack of major uplift in this region during the Sinemurian suggests that no major changes in environment occurred during the deposition of the Shales-with-Beef Member. Therefore concretion formation is more likely to be related to sea-level variations that changed sediment supply and thus produced relatively lower sedimentation rates at times of sea-level high stand. This chapter investigates the Fe and S chemistry of the shales, comparing a concretionary horizon and the underlying concretion-free shales.

6.2 Results

Tables of analytical data can be found in the appendix section (A.3).

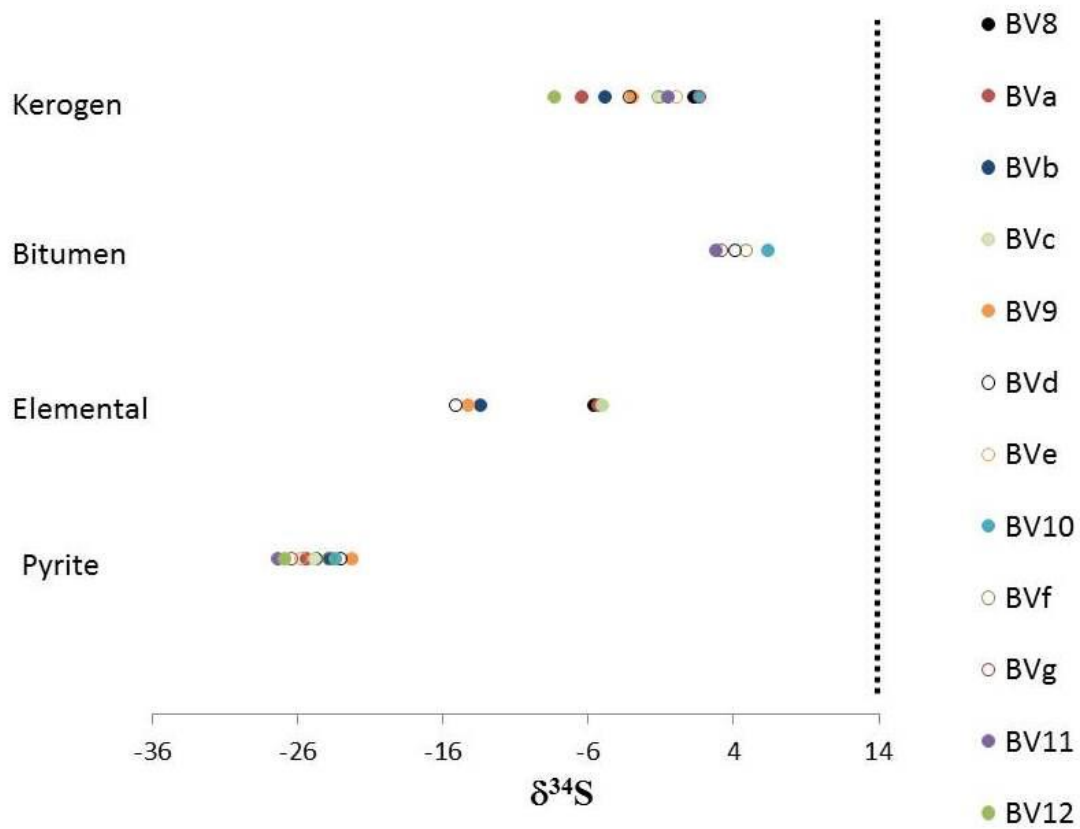

Figure 6.3 Sulfur isotopes.
The results from the kerogen, bitumen, elemental and pyrite sulfur isotopes relative to CDT. The dashed line represents the approximate

$\delta^{34}S$ of seawater during the Jurassic. Pyrite has the lowest $\delta^{34}S$ whilst kerogen and bitumen have the highest. Elemental S is between these values.

The sulfur isotopic data show that bitumen has the highest $\delta^{34}S$ values which are between 3.2 and 6.4 $\delta^{34}S$; followed by kerogen which lie within -8.3 and 1.7 $\delta^{34}S$ and the lowest values are found in pyrite at -26.9 and -22.3 $\delta^{34}S$ (Figure 6.3). Elemental sulfur has the broadest ranges with values ranging between -15.1 and -5 $\delta^{34}S$.

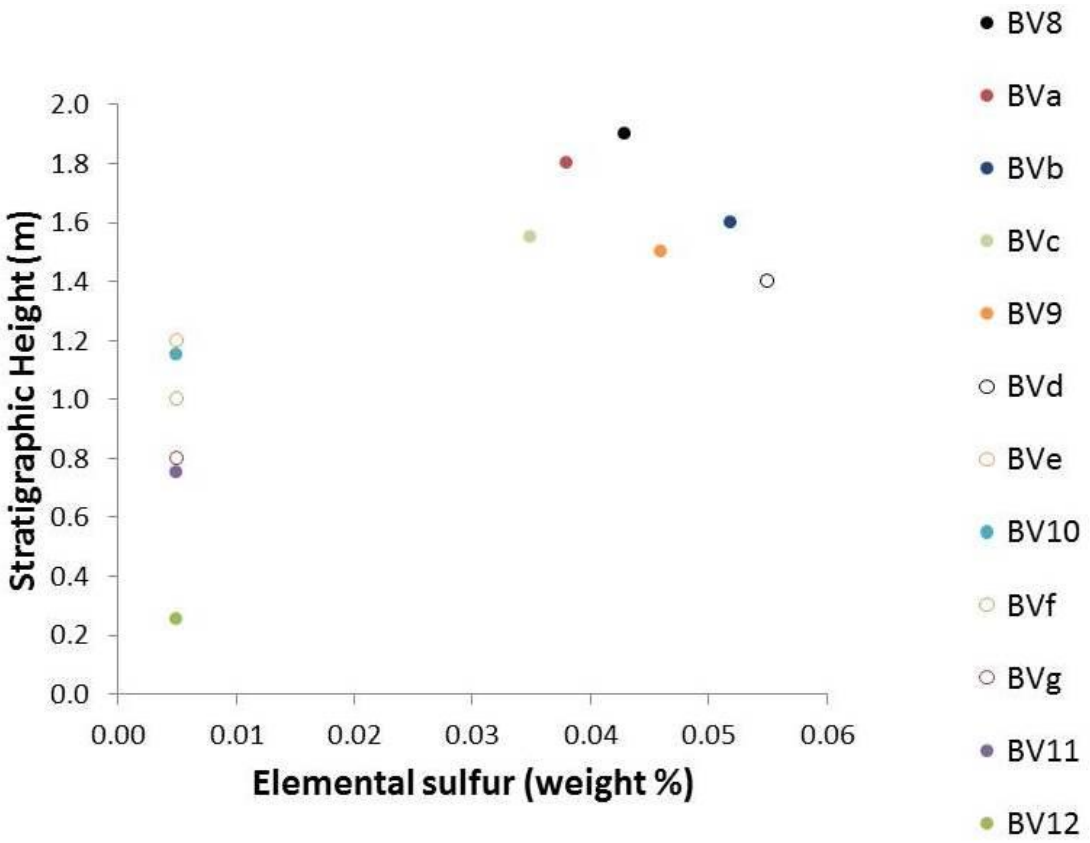

Figure 6.4 Concentration of elemental S relative to stratigraphic height.
Amount of elemental sulfur recovered from the samples. The stratigraphically lower samples do not have concentrations of S^0 above detection (i.e. <0.005 wt%). The samples recovered higher stratigraphically contain concentrations of S^0 which lie between 0.035 to 0.005 wt%.

Samples from the lowest part of the measured section until 1.2 m have elemental sulfur concentrations below detection limits (i.e. <0.005 wt% S). From 1.4 m to the top of the measured section, the concentration of elemental sulfur is scattered between 0.04 and 0.06 wt% (Figure 6.4). These data show a clear switch in the system behaviour.

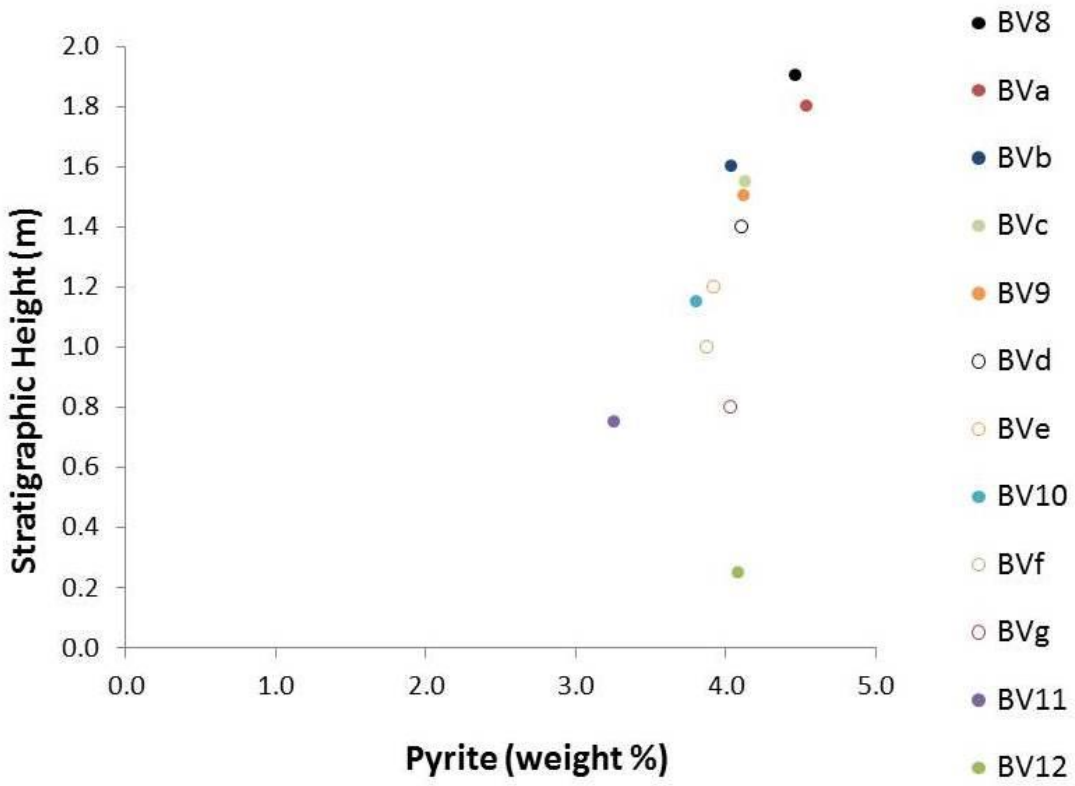

Figure 6.5 Amount of pyrite in sample.
Amount of pyrite recovered from the samples. The amount of pyrite within the samples is close to 4 wt% throughout the sample.

The amount of pyrite within the samples is close to 4 wt% throughout the profile, although BV11 is the lowest at 3.26 wt%, whilst BVa and BV8 are the highest at 4.55 and 4.47 wt% respectively (Figure 6.5).

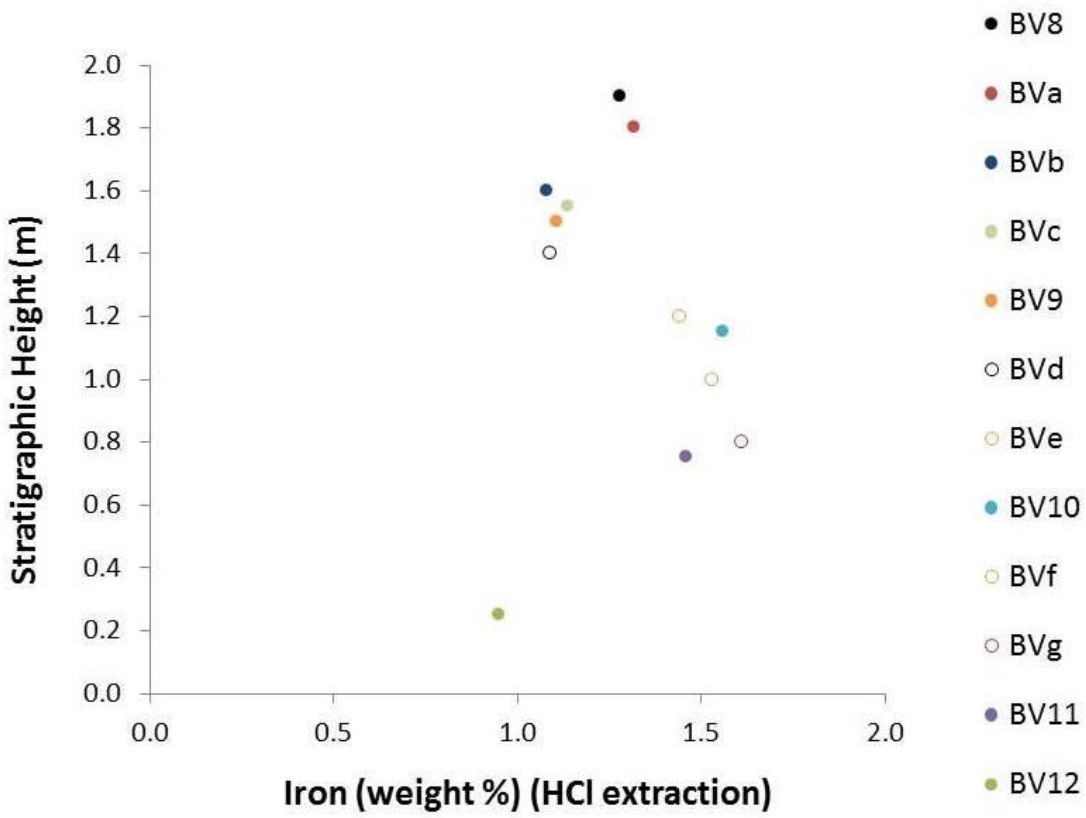

Figure 6.6 Iron extractions with HCl.
Extractable Fe (using HCl) compared against stratigraphic height. Between 0.6 and 1.2 m there are a group of data points that are between 1.44 and 1.61 wt%. Stratigraphically above and below the samples have lower iron weight at approximately 1.11.

The HCl extracted Fe shows that weight percentage ranges from 0.95 to 1.61 extractable iron using the HCl method (Figure 6.6). Lowest in the stratigraphic column for the measured section is BV12 which has the lowest value (0.95 wt%), above this, between 0.6 and 1.2 m there are a group of data points which are between 1.44 and 1.61 wt%. Between 1.4 and 1.7 m there are a group of points with a mean HCl extractable Fe of approximately 1.11 wt%. Highest data points in the measured section have values close to 1.30 wt%.

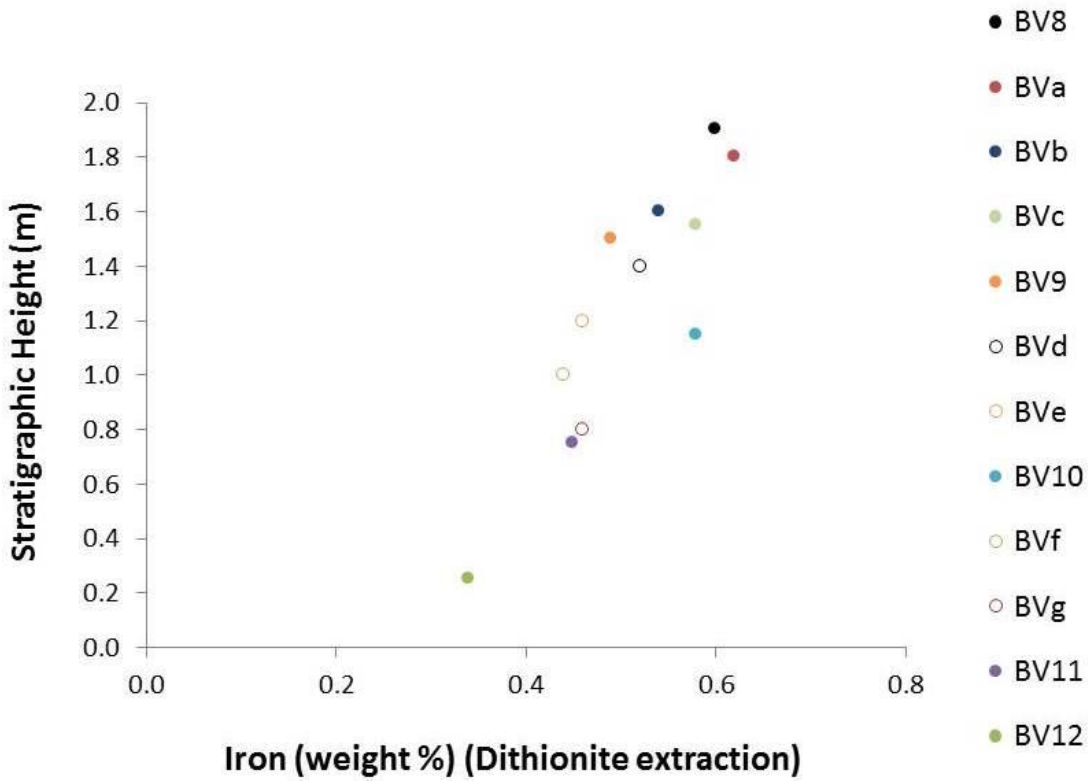

Figure 6.7 Iron extractions with dithionite.
Extractable Fe (using dithionite) compared against stratigraphic height. Overall trend is that the percentage of extractable iron increases from the lower part of the measured section up to the upper part of the measured section.

The dithionite extracted Fe (Figure 6.7) shows that weight percentage ranges from 0.3 to 0.62; the overall trend is that the percentage of dithionite extractable iron increases from the lower part of the measured section up to the upper part of the measured section.

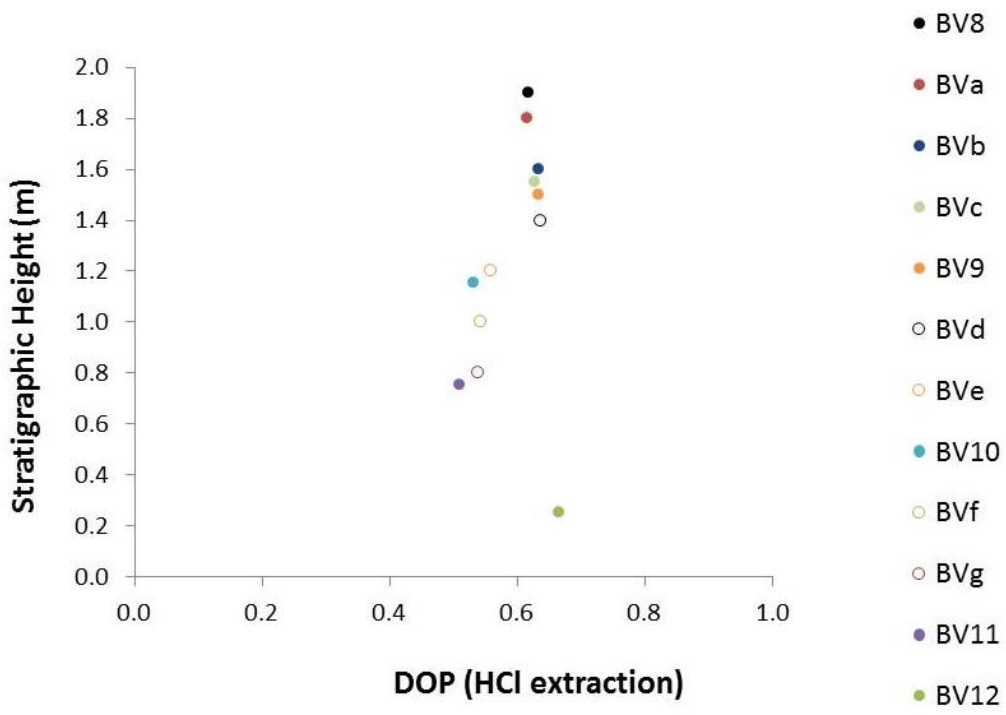

Figure 6.8 **Degree of pyritization (HCl method).**
Degree of pyritization is the ratio of pyritic Fe to pyritic Fe + acid-soluble Fe; with the acid used being HCl. Between 0.75 and 1.20 m DOP lies close to 0.51 to 0.56 and between 1.40 and 1.90 m data points lie between 0.62 and 0.64. The lowest sample stratigraphically also lies higher relative to the middle cluster of points.

There are two main trends seen within data from the degree of pyritization (DOP) using the HCl method (Figure 6.8). Between 0.75 and 1.20 m DOP lies close to 0.51 to 0.56 and between 1.40 and 1.90 m, data points lie between 0.62 and 0.64. The lowest point in the stratigraphic column however is at 0.67.

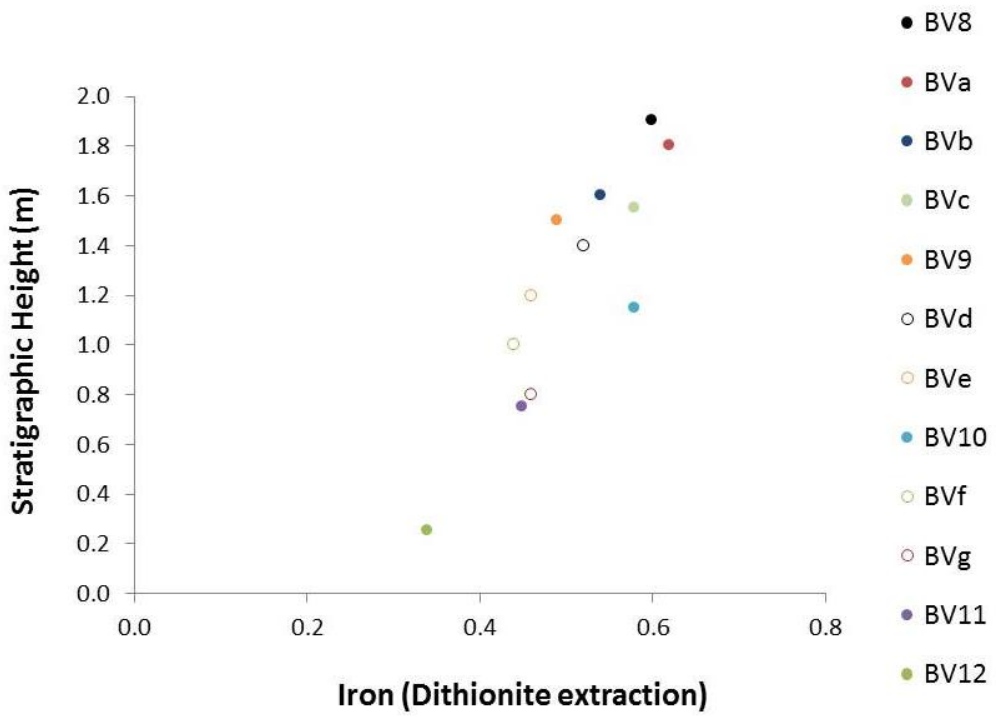

Figure 6.9 **Degree of pyritization (Dithionite method).**
Degree of pyritization is the ratio of pyritic Fe to pyritic Fe + acid-soluble Fe; with the acid using being dithionite. All samples lie close to 0.80.

The lowest point in the stratigraphic column has the highest DOP weight at 0.85; all values stratigraphically above this are slightly lower between 0.75 to 0.80, however, most values are closer to 0.80 (Figure 6.9).

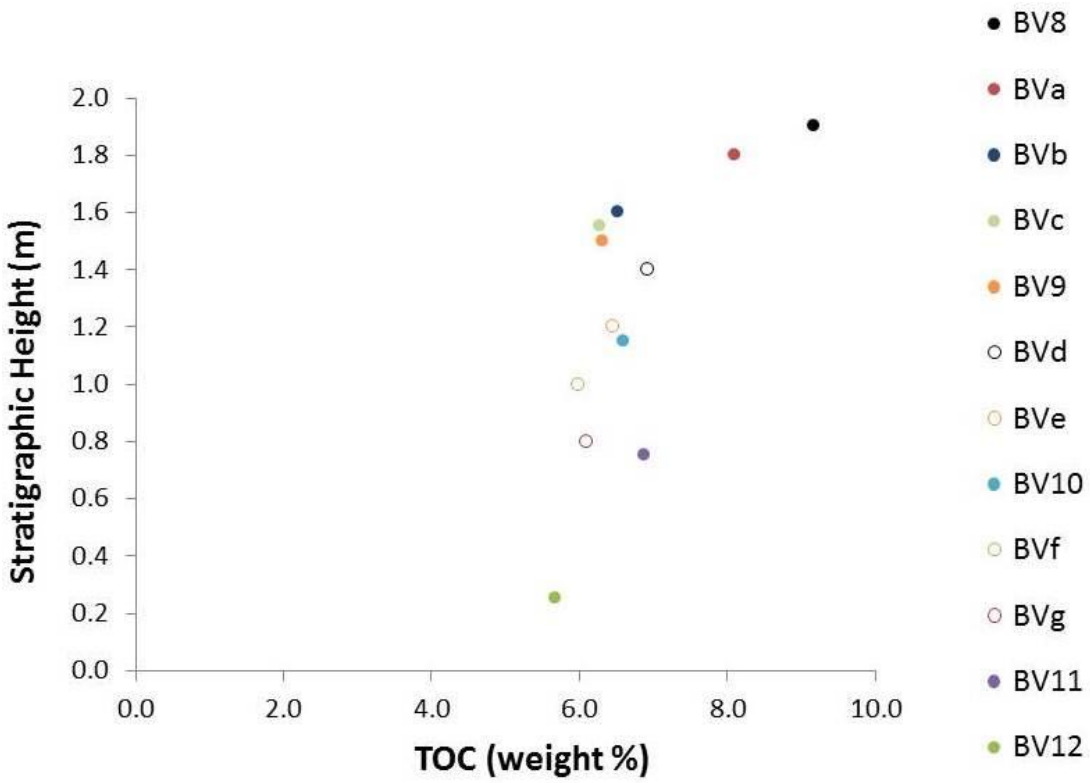

Figure 6.10 Total organic carbon (TOC) in samples.
The amount of organic carbon in the samples. TOC is generally relatively high throughout the samples at around 6%; there is higher TOC concentration in the stratigraphically highest samples.

TOC content in the samples within the first 1.65 m generally are between 5.6 to 6.9 wt%, however, most samples points lie close 6.5 wt%. The stratigraphically highest samples have higher TOC content with values at 8.1 and 9.1 wt% (Figure 6.10).

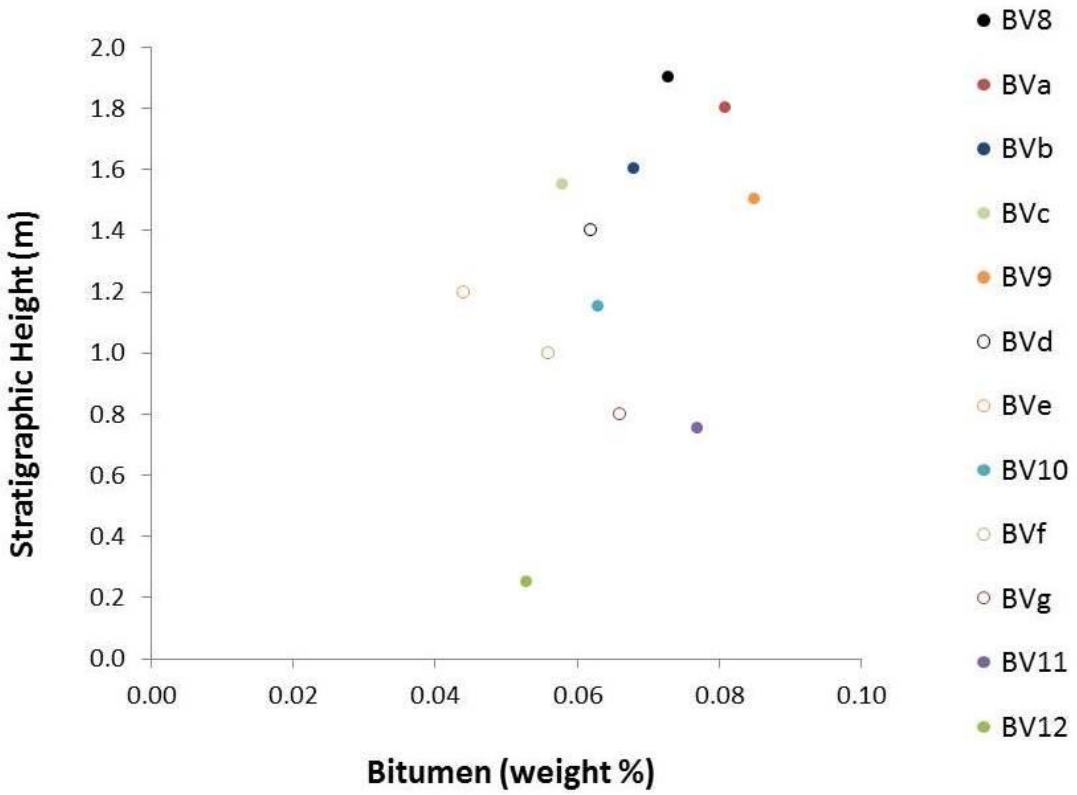

Figure 6.11 Bitumen concentrations.
Bitumen (the soluble OM) is scattered between 0.04 and 0.09 wt%.

Bitumen content in the samples varies throughout the stratigraphic column. Values are between 0.04 and 0.09 wt% bitumen (Figure 6.11).

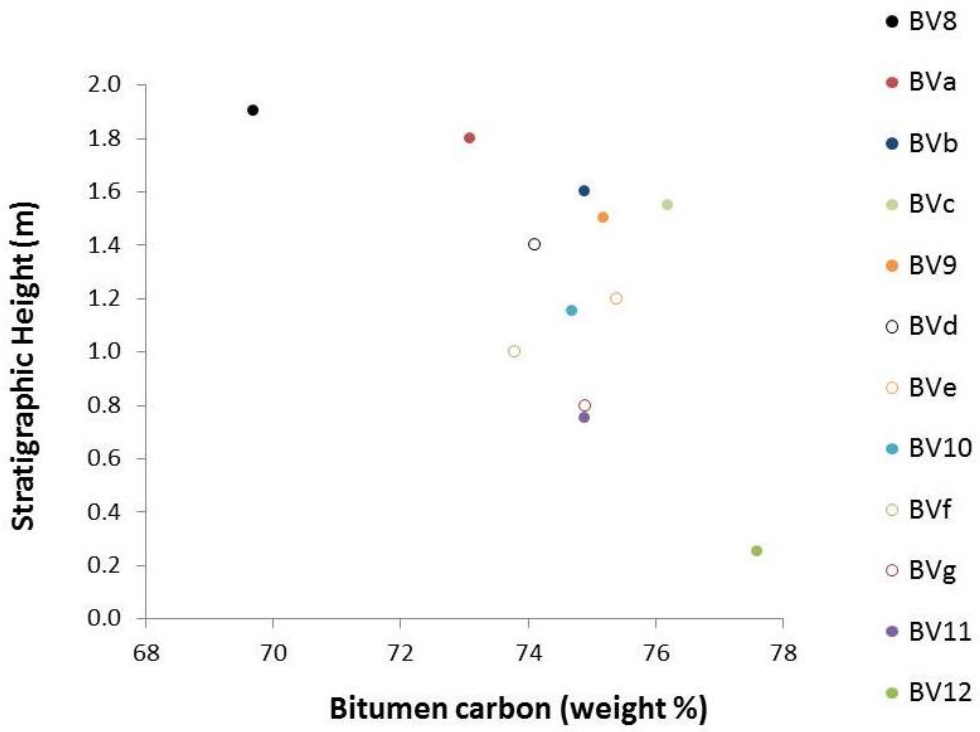

Figure 6.12 Carbon concentration in bitumen
The highest bitumen carbon concentration is stratigraphically lowest (BV12) and samples decrease in bitumen carbon concentration in the stratigraphically highest samples; however there are a group of data points which are between 1.44 and 1.61 wt% C.

The stratigraphically lowest sample (BV12) contains the highest bitumen carbon concentration at 77.6 wt% C (Figure 6.12). Stratigraphically above this, between 0.75 and 1.60 m, samples range between 73.8 and 76.2 wt% C. Samples BVa (1.80 m) and BV8 (1.90 m) have the lowest C content in the bitumen at 73.1 and 69.7 wt% respectively.

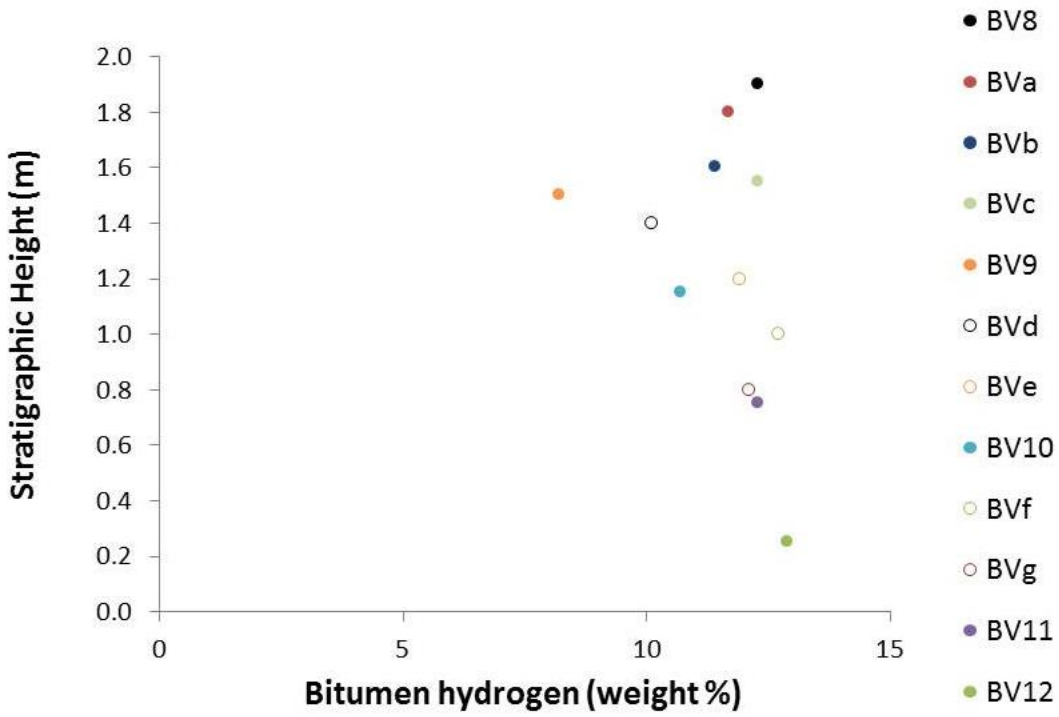

Figure 6.13 Hydrogen concentration in bitumen
The bitumen hydrogen content in the samples lie close to 12 wt% with some variation.

The bitumen hydrogen content (Figure 6.13) in the samples lie close to 12 wt% although values do go as low as 8 wt% (8.20 wt%, BV9) and the highest values are at just below 13 wt% (12.9 wt%, BV12; 12.7 wt%, BVf).

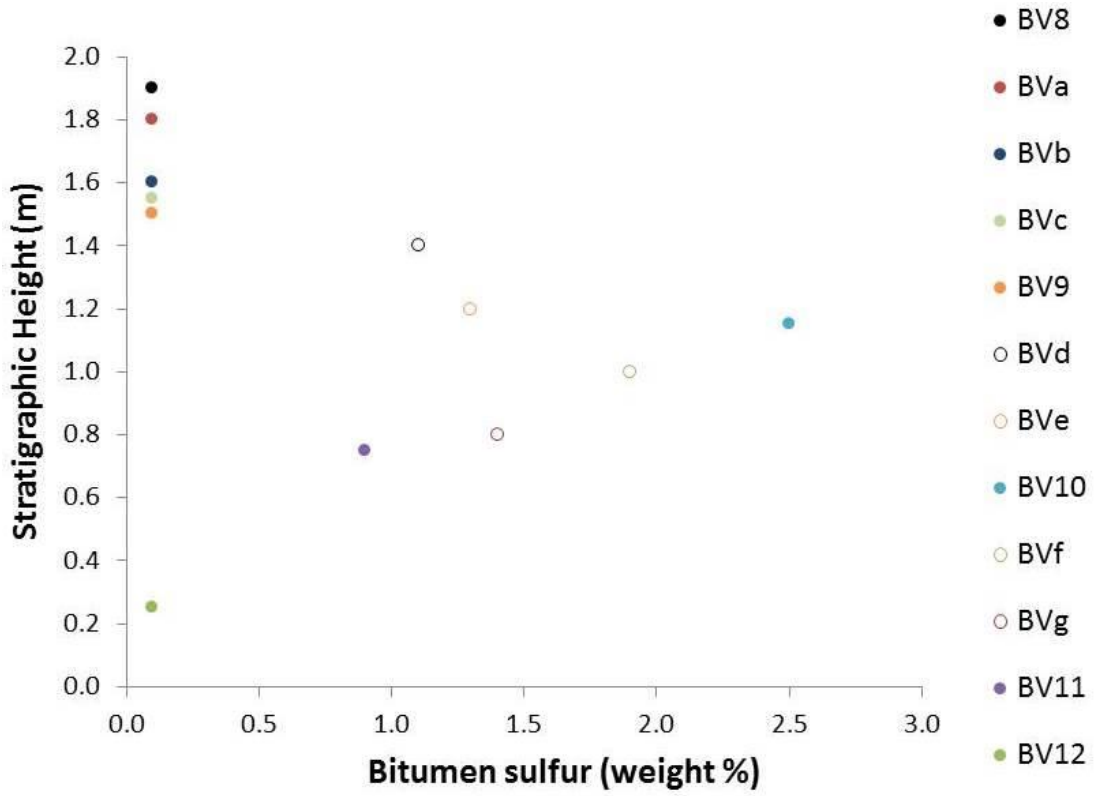

Figure 6.14 Sulfur concentration in bitumen
Above 1.5 m height (stratigraphically) the percentage of S found within the bitumen is either not present or present on very small quantities thus below detection limits; this is the same for sample BV12. The samples between 0.75 and 1.40 m, however, have values which range between 0.9 and 2.5 wt%.

The bitumen sulfur content (Figure 6.14) varies across the samples. In BV12 (lowest in the stratigraphic column) and in the stratigraphically highest samples (BV9 to BV8) the samples are <0.1%, which is below detection. The samples between 0.75 and 1.40 m have values which range between 0.9 and 2.5%. Within this range there appears to be a trend which shows an increase in bitumen sulfur content between 0.75 and 1.15 m, followed by a decrease in sulfur content.

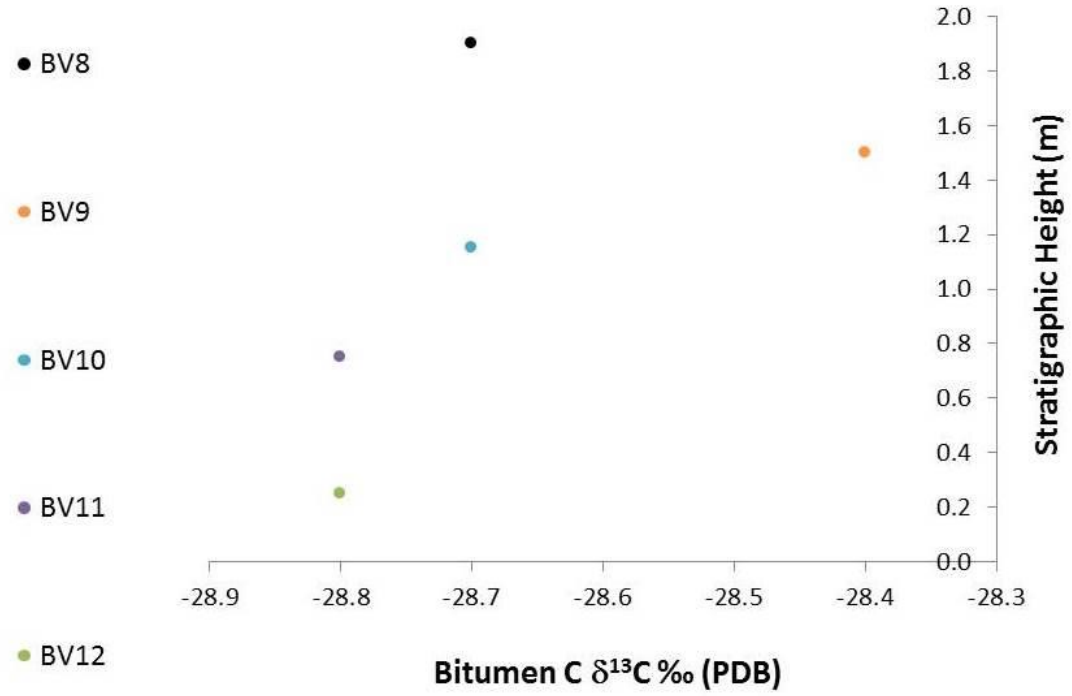

Figure 6.15 Stable carbon isotope ratio content of the bitumen.
The stable isotope carbon ratios show that there is very little variation in bitumen $\delta^{13}C$.

The bitumen carbon isotope measurements have not been measured in all samples (Figure 6.15). In the samples taken the isotopic compositions are -28.8‰ $\delta^{13}C$ (BV12 and BV11), -28.7‰ $\delta^{13}C$ (BV10 and BV8) and -28.4‰ $\delta^{13}C$ (BV9).

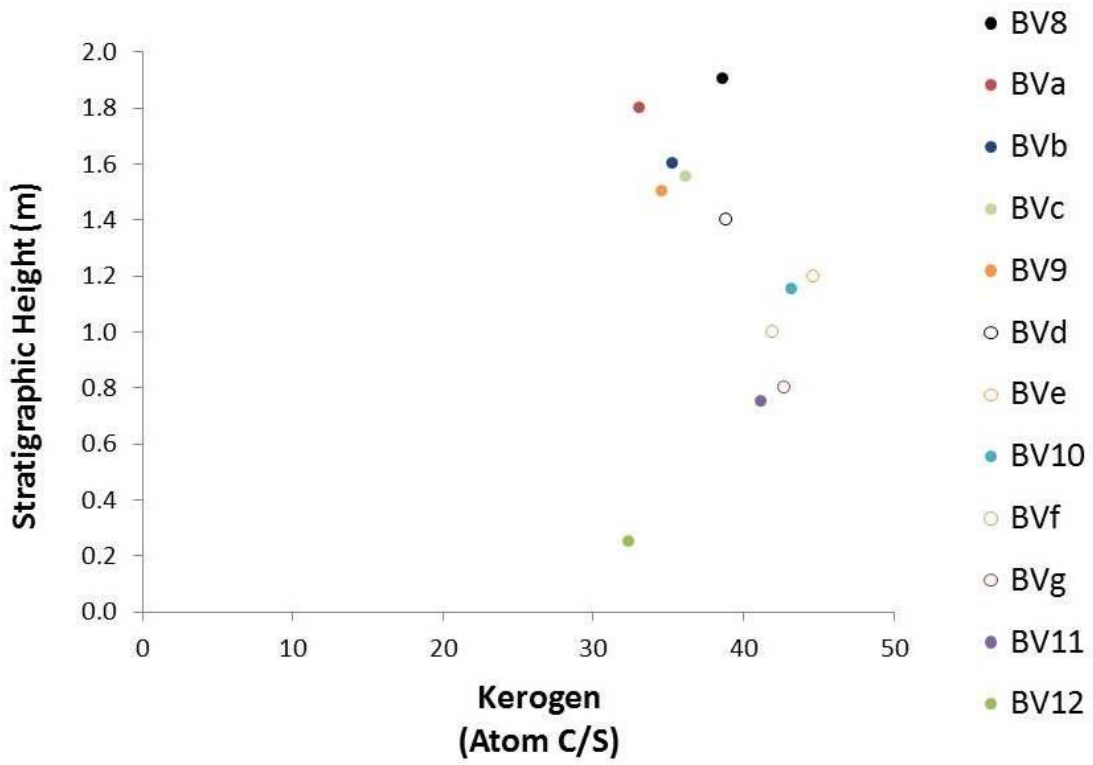

Figure 6.16 Kerogen C:S ratios.
Atomic C/S values lie between 35 and 45.

BV12 (lowest in the stratigraphic column) and BVd to BV8 (highest in the stratigraphic column: 1.40 to 1.90 m) have the lowest kerogen C/S values between ~32 and ~39. Samples that lie between 0.75 and 1.20 m have kerogen C/S values between ~41 and ~45 (Figure 6.16).

6.3 Discussion

6.3.1 Organic geochemistry

The preservation of OM can be attributed to a few key processes. The residence times of OM in oxic conditions can be reduced during times of high sedimentation rates, thus favouring the preservation of marine OM, however, if sedimentation rates remain too high then there is a dilution affect and concentration is reduced (Stein, 1990). High productivity can lead to OM preservation even in oxic basins, although

stratified water columns also lead to preservation of OM without the need for more OM as these conditions lead to anoxic and euxinic conditions, suppressing oxic degradation (e.g. Stein, 1990; Rimmer et al., 2004). Other factors include, sediment starvation, clay physically protecting OM, or a combination of any of these things (Rimmer et al., 2004). All samples show relatively high TOC, with values ranging from 5.7 to 9.2% (Figure 6.10), showing that the rock is organic rich. Wolff et al. (1991) evaluated the carbon preference index (CPI) showing that the samples had a bimodal normal alkane distribution with the highest concentrations around C17 and C27. The odd/even pattern that the Shales-with-Beef member exhibits, coupled with the bimodal distribution, indicate that it is a type II /III kerogen. Additionally, the bitumen atomic H/C value is high (average 1.86; Table 6.1). Some of the values given in Table 6.1 appear too high; this could be due to extracts being slightly contaminated with either solvents (used in the extraction process) or small amounts of clay/mica minerals containing H but no C. However, these data are consistent with the Shales-with-Beef Member being thermally immature with well-preserved kerogen, although it is unclear from this analysis alone why OM preservation is good.

Sample Number	Stratigraphic Height (m)	Atomic H/C
BV8	1.90	2.12
BVa	1.80	1.92
BVb	1.60	1.83
BVc	1.55	1.94
BV9	1.50	1.31
BVd	1.40	1.64
Be	1.20	1.89
BV10	1.15	1.72
BVf	1.00	2.07
BVg	0.80	1.94
BV11	0.75	1.97
BV12	0.25	1.99
	Average	**1.86**

Table 6.1 **Bitumen atomic H/C.**
This shows that the atomic H/C is high, probably too high; this is possibly due to analytical problems. Two possible reasons for this could be the extracts being contaminated with solvents or extracts containing small amounts of clay/mica minerals containing H but no C.

6.3.2 Sulfur geochemistry

One of the most important processes of S isotope fractionation is the reduction of sulfate by bacteria as they preferentially use ^{32}S (e.g. Jones and Starkey, 1957; Harrison and Thode, 1958; Kaplan et al., 1963; Kaplan and Rittenberg, 1964; Canfield, 2001). Initially the, shallower pore-waters will have lighter H_2S isotopic signatures compared to $\delta^{34}S$ sulfate, however the deeper the sediment pore-waters,

the heavier the H_2S becomes; Figure 6.17 (e.g. Werne et al., 2003). Additionally, the left over heavier sulfate can diffuse downwards, where it will probably be utilised by microbes and the heavier sulfide can diffuse upwards to the near-surface (and potentially be oxidised or partially oxidised) or downwards to where there is a sink, that is, where monosulfides and pyrite form. Thus there are no precisely defined zones within the sediment where particular isotopic signatures occur; rather isotopic compositions found at particular horizons can be used to give good indicators to the processes occurring. Isotopic signatures for sulfur in organic matter are much more complex; moreover the actual mechanisms that allow sulfur to be incorporated into organic matter are still not well understood (e.g. Sinninghe Damste and de Leeuw, 1990; Aplin et al., 1993; Zhu et al., 2013; Raven et al., 2015). During early diagenesis sulfur is incorporated into sedimentary OM, predominantly kerogen (Gransch and Posthuma, 1973) and organic sulfur is typically enriched in ^{34}S compared to what likely diagenetic sources (bisulfide or polysulfide) in the pore-waters (e.g. Bottrell and Raiswell, 2000; Raven et al., 2015). However, organic sulfide compounds found in kerogen form at different times during diagenesis (Raven et al., 2015 and references therein), thus the different compound sources of S and different diagenesis they will have undergone will most likely lead to diverse ^{34}S isotope signatures. Organic matter derived from the organisms inhabiting the oceans are likely to have initial isotope signatures which closely follow that of seawater sulfate as that is their source of S. When diagenesis occurs in the sediment however, the characteristically light S isotope values of diagenetic H_2S, are likely to be incorporated into the organic matter, causing lighter overall values of S within the organic matter. The more S that is incorporated into the organic matter from the H_2S the lighter the values become, therefore the incorporation of diagenetic H_2S strongly

affects the $\delta^{34}S$ values of organic matter (Figure 6.17). Additionally, there is another dimension of complexity regarding the fate of S in OM once it has been incorporated. If sulfur is added to organic matter during assimilatory sulfate reduction then it possess a component with the original seawater S isotopic signature, however, the biomolecules produced will be susceptible to biodegradation during subsequent diagenesis (e.g. Zhu et al., 2013). After burial, sulfur produced from bacterially produced sulfide, and therefore fractionated to lighter isotope compositions, may form new organic sulfur compounds, either by reaction of polysulfides or by nucleophilic attacks of sulphide (e.g. Sinninghe Damste and de Leeuw, 1990; Zhu et al., 2013; Raven et al., 2015). This is further complicated by the depths at which the sulfide is incorporated into the organic matter; deeper in the sediment the BSR sulfide isotopes will be heavier (see Figure 6.17; e.g. Bottrell and Raiswell, 1983). Sulfur, however, is predominantly thought to be incorporated into kerogen within meters of the SWI (Aplin et al., 1993). The retention of the newly formed sulfur compounds will be related to the sulfurization pathway. Thiols produced from nucleophilic attack by sulphide have stronger bounds, whilst sulphide bridges formed from polysulfides are broken down more easily (e.g. Zhu et al., 2013 and references therein; Raven et al., 2015). Thus organic matter sulfur isotopes are expected to have a mixture of isotopically light S incorporated into its chemical structure from the process of MSR and a fraction of the residual signature of seawater sulfate that was originally incorporated into the organism. If OM does lose more initial S from its structure, then it will have isotopic signatures more closely related to the bacterially produced sulphide, and if it does not lose S from its structure during diagenesis then organic matter S is expected to be lighter than seawater but heavier than the isotope values caused by fractionation. Key controls

on S being incorporated into kerogen remain unclear, however, it is not thought to be the availability of sulfide or the rate of accumulation of Fe, instead the availability of more reactive (towards OM) partially oxidised sulfur species can also exert a key control (Aplin et al., 1993; Raiswell et al., 1993).

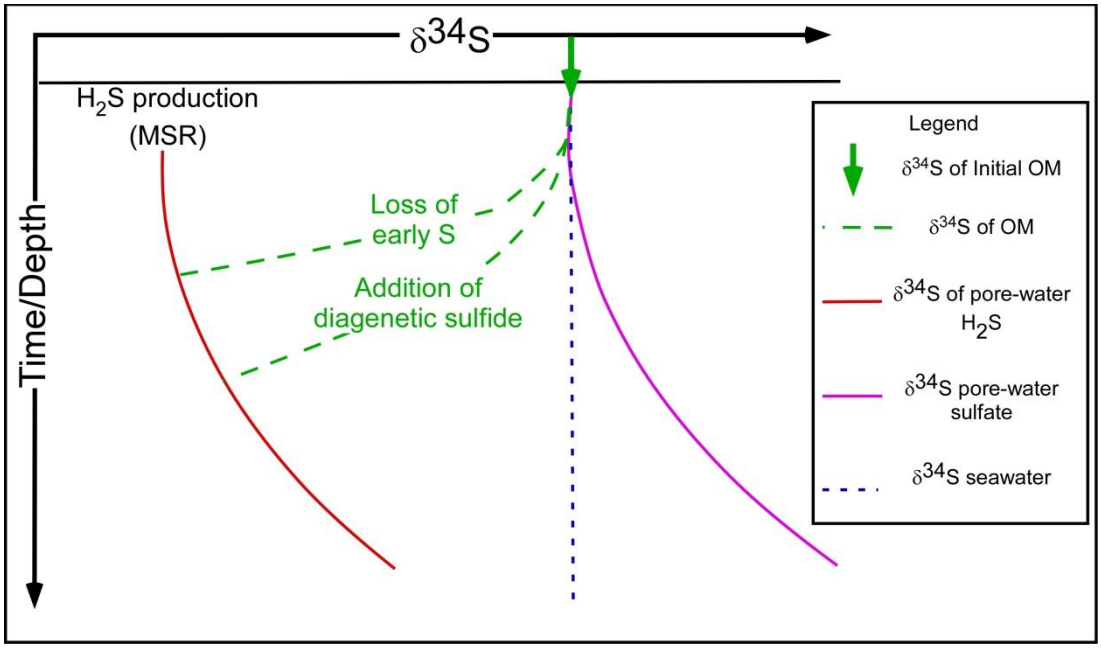

Figure 6.17 Isotope-S values model.
Seawater sulfate has high $\delta^{34}S$ and this is reflected in the primary organic matter as it is the source for S in marine OM. As the OM is buried then H_2S production will begin in anoxic zones; the bacteria preferentially choose the lightest isotopes and this is reflected in the isotopically light H_2S. The isotopically heavy sulfate (if there is plenty in the system) will be left within the pore-waters. The deeper/ older the sediment then the more isotopically heavy sulfate will be used later on in diagenesis. The organic matter left over (i.e. what will be the bitumen-S and kerogen-S) if S is not lost from its matrix, will have isotopically light microbially-produced S added to its matrix; thus it will reflect a mixture of two sources, original seawater S-isotope values and bacterially produced sulfide. However, if S is lost from the OM matrix during early diagenesis then the values would reflect more closely of that of diagenetic H_2S.

Seawater sulfate values of $\delta^{34}S$ in the Jurassic were between 14.2 and 18.0‰ (Kampschulte and Strauss, 2004), lower than present day (21‰) (e.g. Ku et al.,

1999). The kerogen-S and bitumen-S $\delta^{34}S$ from these data are lower than seawater values but higher than pyrite and elemental-S values (Figure 6.3). Bruchert and Pratt (1996) found that fulvic acid in estuarine sediments had isotopic signatures consistent with that of a mixture of ^{34}S-enriched primary biosynthetic sulfur originally assimilated from dissolved sulfate, and sulfur depleted in $\delta^{34}S$ from recycled bacterially mediated H_2S. This model assumes S is only added. If S is lost from the organic matter then it would more closely reflect diagenetic H_2S. The organically bound S within the Shales-with-Beef Member could reflect either model (Figure 6.17).

Pyrite can be found throughout the measured stratigraphic column (Figure 6.5). This shows that there must always be a supply of both sulfide and reactive iron and the conditions had remained reduced throughout the sequence measured. Additionally, the sulfur isotopes from the pyrite show the expected low $\delta^{34}S$ values (between -26.9 and -22.30‰ $\delta^{34}S$), since pyrite formation is microbially mediated by SRB which preferentially choose lighter isotopes (reaction 1.5; Chapter 1) and pyrite formation must have predominantly occurred early during diagenesis (since there must be only a small component of pyrite formed from late, more ^{34}S-enriched, sulfide).

Elemental-S is not expected to be preserved in the marine shales in high quantities as it is an intermediate product, often formed during the partial oxidation of HS^- in either reducing or oxidising conditions (reaction 6.1 and 6.2 respectively), which can then, for example, react with sulfite to form thiosulfate (reaction 6.3) (Zopfi et al., 2004 and references therein):

$$FeS + 2FeO(OH) + 2H_2O \rightarrow 3Fe^{2+} + S^0 + 6OH^- \quad (6.1),$$

$$2HS^- + O_2 \rightarrow 2S^0 + 2OH^- \quad (6.2),$$

$$S^0 + SO_3^{2-} \rightarrow S_2O_3^{2-} \quad (6.3).$$

Or if the conditions are reducing the zerovalent sulfur can react with monosulfides to form pyrite (Berner, 1970):

$$FeS + S^0 \rightarrow FeS_2 \quad (6.4).$$

The mechanism by which the zerovalent-S may be preserved is discussed later in section 6.3.3. The isotope signatures, however, eliminate the oxidation of diagenetic monosulfides and/or pyrite as a source of the elemental sulfur, and no fractionation of S isotopes occurs during the oxidation of pyrite or monosulfides (e.g. Nakai and Jensen, 1964; Thode et al., 1960); this is shown in the data by pyrite-S having substantially lower values of $\delta^{34}S$ than elemental-S. It is also noteworthy that bitumen-S and elemental-S don't appear at the same depth except for one sample at 1.4 m, which is close to the boundary of this contrast. Moreover, this boundary correlates with the formation of concretions (Figure 6.18).

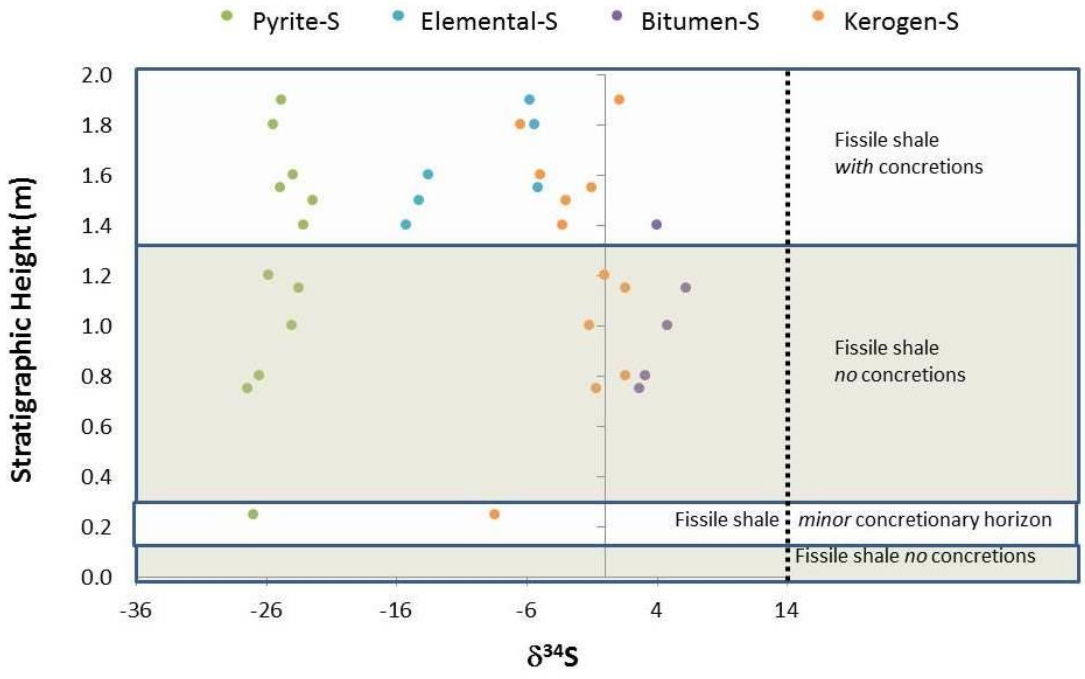

Figure 6.18 Sulfur isotopes and stratigraphy.
The results from the kerogen, bitumen, elemental and pyrite sulfur isotopes shown in relation to the concretionary horizons. Dashed line represents the approximate seawater sulfate $\delta^{34}S$ values. Elemental S is present in samples only when concretions are present and there is no bitumen-S present. Bitumen-S occurs in fissile shales with no concretions and no elemental-S is present.

Elemental-S has lower values of $\delta^{34}S$ than bitumen-S; therefore the formation of elemental-S cannot be a simple substitution from the bitumen-S. The isotopic signatures for the elemental-S suggest that there is more of an influence of recycled bacterially -produced H_2S compared to bitumen-S, but certainly not purely from this source.

C/S ratios in fine grained marine sediments have three major controls; the fraction of the OM which can be metabolised; the fraction of OM which metabolised via the process of sulfate reduction; and the fraction of reduced sulfide which is buried as pyrite (Morse and Berner, 1995). Kerogen C/S ratios will be, in part determined by similar processes, however, as previously mentioned there is the original organic matter within the OM, and there is the availability of labile Fe to react with the sulfide to produce pyrite (with that S not being able to be incorporated into the kerogen) to consider (e.g. Lyons and Severmann, 2006). Again, C/S can indicate palaeoenvironmental conditions during deposition as the availability of species and the redox conditions promote or hinder these reactions. However, C/S ratios need to be used with caution as they can be altered with increasing burial (Jones and Manning, 1994). As with the presence of kerogen-S and elemental-S not being found in the same horizons which correlate with the concretions, the kerogen C/S is in agreement that there is a marked difference in sulfur behaviour between the shales with concretions and the shales without (Figure 6.19). In the zone where the

concretions are found the kerogen is sulfur-rich in comparison to when only the fissile shales form. The reasons for this are unknown; however, it could be postulated that there is more of an influence from sulfide bridges formed from polysulfides in the pore-waters during early diagenesis. Some authors have suggested that sulfurisation of kerogen is most effective during anoxic conditions (e.g. Pearson et al., 1996); whilst others have suggested that the uptake of S into OM is favoured under weakly oxygenated bottom waters (Aplin et al., 1993).

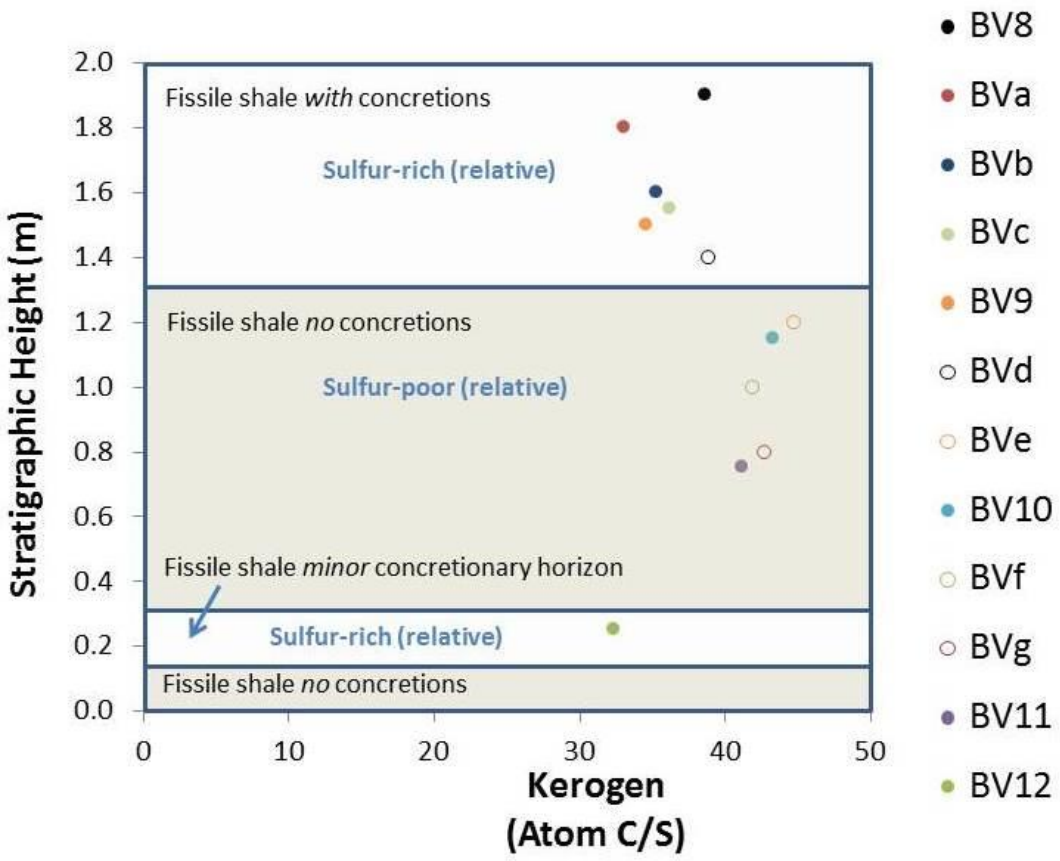

Figure 6.19 Kerogen C:S ratio vs stratigraphy.
The kerogen C/S shows that there is a marked difference in sulfur behaviour between the shales with concretions and the shales without. During the zone where the concretions are found kerogen is sulfur-rich in comparison to when only the fissile shales form.

As discussed earlier bitumen-S and S^0 do not occur in the same horizon. Bitumen-S in the samples (Table 6.2) is located within the fissile shales without the nodules, and is below detection throughout the rest of the samples. The highest ratio of bitumen atomic S/C is 0.01; therefore there is not enough sulfur in the sample for it to count as typeII/IIIS. Not only does this show that there is a behavioural difference in S cycling during times of concretion formation, it also indicates that the system was not euxinic, as the atomic S/C would be higher (≥0.04), thus there is not an excess of S in the system (Aizenshtat and Amrani, 2004 and references therein).

Sample Number	Stratigraphic Height (m)	Atomic S/C
BV8	1.90	0.0005
BVa	1.80	0.0001
BVb	1.60	0.0001
BVc	1.55	0.0000
BV9	1.50	0.0005
BVd	1.40	0.0056
BVe	1.20	0.0065
BV10	1.15	0.0126
BVf	1.00	0.0097
BVg	0.80	0.0070
BV11	0.75	0.0045
BV12	0.25	0.0000
	Average	**0.0039**

Table 6.2 **Bitumen atomic S/C.**
These values are consistent with the bottom-waters being anoxic but not euxinic.

6.3.2 Iron geochemistry

Pyrite formation relies on the availability of: bacterially metabolisable OM; reactive-Fe; and sulfate (for sulfide formation). Therefore pyrite is a good indicator of C-S-Fe chemistry, and therefore depositional regimes within the sediment undergoing diagenesis (e.g. Lyons and Berner, 1992). Iron availability is related to the form in which Fe is in when entering the marine environment, that is, some species are more reactive then others, for example, iron(oxy)hydroxides are not stable in reducing environments and break down easily forming labile Fe (e.g. Berner, 1970; Lyons and Berner, 1992; Lyons and Severmann, 2006). Iron which can break down easily during deposition and diagenesis theoretically should also break down easily as part of a rock component (Berner, 1970). Thus using HCl to extract the readily available, residual Fe, that didn't form pyrite and comparing this to the amount of pyrite in the rock elucidates some palaeoenvironmental indicators for the time of deposition (e.g. Berner, 1970; Lyons and Berner, 1992; Berner and Raiswell, 1983; Lyons and Severmann, 2006; Poulton et al., 2004). This is known as the degree of pyritization (DOP):

$$\text{Degree of Pyritization (DOP)} = \frac{\text{Pyrite-Fe}}{(\text{Pyrite-Fe} + (\text{HCl or dithionite extractable Fe}))}.$$

Distinguishing between highly reactive Fe minerals and the silicate phases can therefore identify between iron-limited or sulfur-limited conditions (e.g. Poulton and Canfield, 2005). Presently, there are a series of extractions of iron from the parent rock which can differentiate between highly reactive, poorly reactive and unreactive Fe minerals (see further work section). These data, however, were obtained in the early 1990s and extractions were obtained via dithionite (a reducing agent) and HCl.

Dithionite extracts the highly reactive Fe-minerals, as does HCl (Berner, 1970; Canfield, 1989; Raiswell et al., 1994; Poulton et al., 2004; Lyons and Severmann, 2006). However, dithionite will not extract the essentially unreactive silicate-minerals unlike HCl (Canfield, 1989; Raiswell et al., 1994; Poulton et al., 2004; Lyons and Severmann, 2006). Thus HCl will overestimate the amount of reactive Fe there is in the system (e.g. Canfield, 1989). DOP values for the differing amounts of oxygen conditions have been classified as; oxic conditions, which show low degrees of DOP (<0.42), anoxic environments, intermediate DOPs (0.46 to 0.80) and sulfidic (euxinic environments) are highest (0.55 to 0.93) (Raiswell et al., 1988). The reason why sulfidic environments yield higher DOPs is due to the time over which the less reactive Fe minerals are exposed to H_2S (Berner and Raiswell, 1983). Values for the Shales-with-Beef DOP (HCl extraction) are between 0.51 and 0.67 with a mean of 0.59. As the atomic S/C values are low, these data are in agreement that the bottom water was anoxic but not sulfide-rich. The DOP values from the dithionite extraction, however, are consistently higher; between 0.77 and 0.85, although the mean is 0.79 (Table 6.3).

Sample Number	Stratigraphic Height (m)	DOP (HCl)	DOP (Dithionite)
BV8	1.90	0.62	0.78
BVa	1.80	0.62	0.77
BVb	1.60	0.64	0.78
BVc	1.55	0.63	0.77
BV9	1.50	0.63	0.80
BVd	1.40	0.64	0.79
Be	1.20	0.56	0.80
BV10	1.15	0.53	0.75
BVf	1.00	0.54	0.80
BVg	0.80	0.54	0.80
BV11	0.75	0.51	0.77
BV12	0.25	0.67	0.85
	Average	**0.59**	**0.79**

Table 6.3 DOP for both HCl and dithionite extractions.
The DOP from the HCl extraction suggests either sulfidic bottom waters or anoxic, however the bitumen atomic S/C indicates anoxic bottom waters rather than sulfidic.

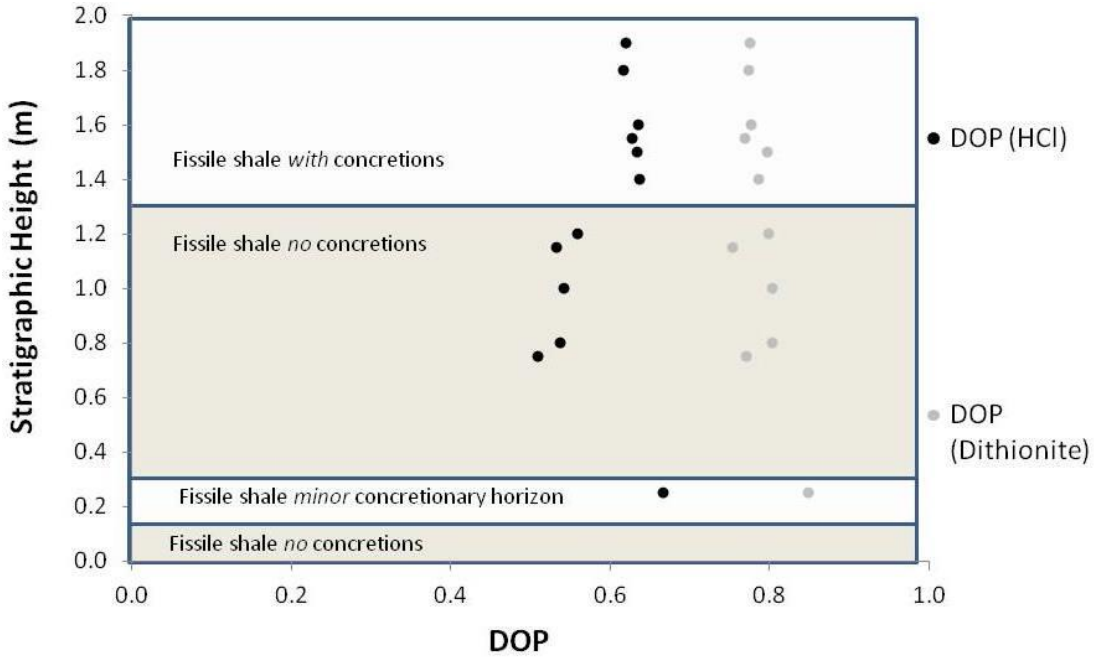

Figure 6.20 DOP in relation to concretion formation and different extractions.

During the times when concretions form, the biogeochemistry of the sediment is different to that when concretions are not present, as there is a difference in the DOP (between dithionite and HCl extractions), suggesting a difference between horizons within the less reactive silicate minerals, or clay, fraction of Fe.

The DOP from the dithionite extraction is consistent throughout the measured profile (Figure 6.20). This suggests that there isn't a strong variation of input from highly reactive Fe minerals or sulfide during deposition or diagenesis. The DOP from the HCl extraction, however, suggests that there are changes between the horizons of fissile shale with concretions and just fissile shale. The fact that DOP_{HCl} increases during times of concretion formation would indicate that there may have been more reaction between less reactive forms of Fe and H_2S in the pore-waters in the concretionary horizons than during the times when the fissile shales are deposited. As HCl extractions also take Fe from the less reactive minerals and dithionite removes only Fe from the highly reactive mineral stages, then this data suggests that the difference seen in these data are related to less reactive minerals. Thus there must

be a change with the less reactive silicate minerals, or clays. This has been suggested before as highly reactive minerals have been masked with mechanism proposed being related to clay mineral formation during diagenesis (Poulton et al., 2010).

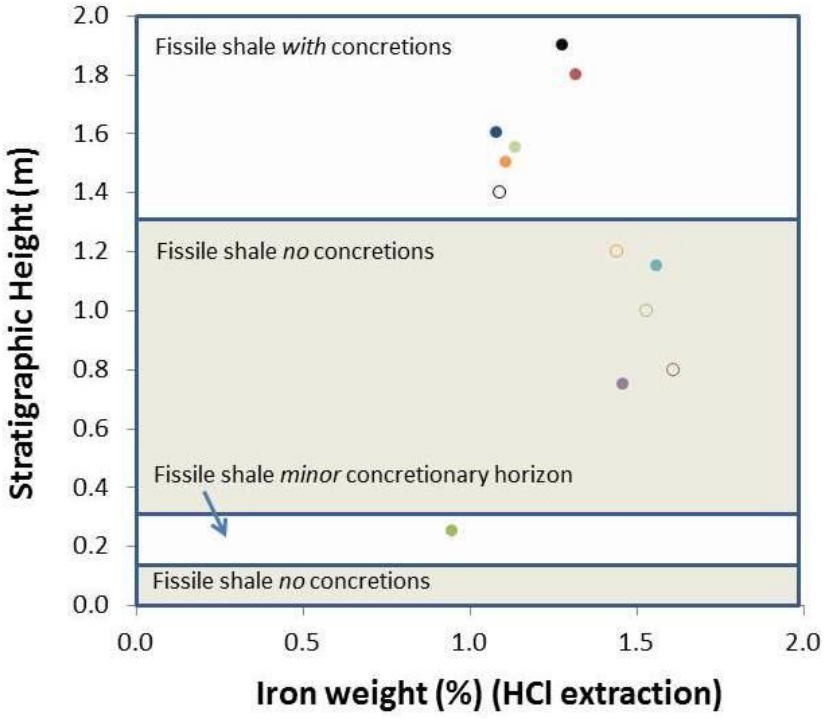

Figure 6.21 Iron weight (%) from the HCl extraction.
The zones with concretions have lower extractable Fe than those without, using the HCl method.

The iron concentration in the sample from the extraction of HCl suggests it is lower in the zones where concretions form than the zone without concretions (Figure 6.21). The iron concentration extracted from the dithionite, however, doesn't show a marked change between horizons with concretions or those without (Figure 6.22).

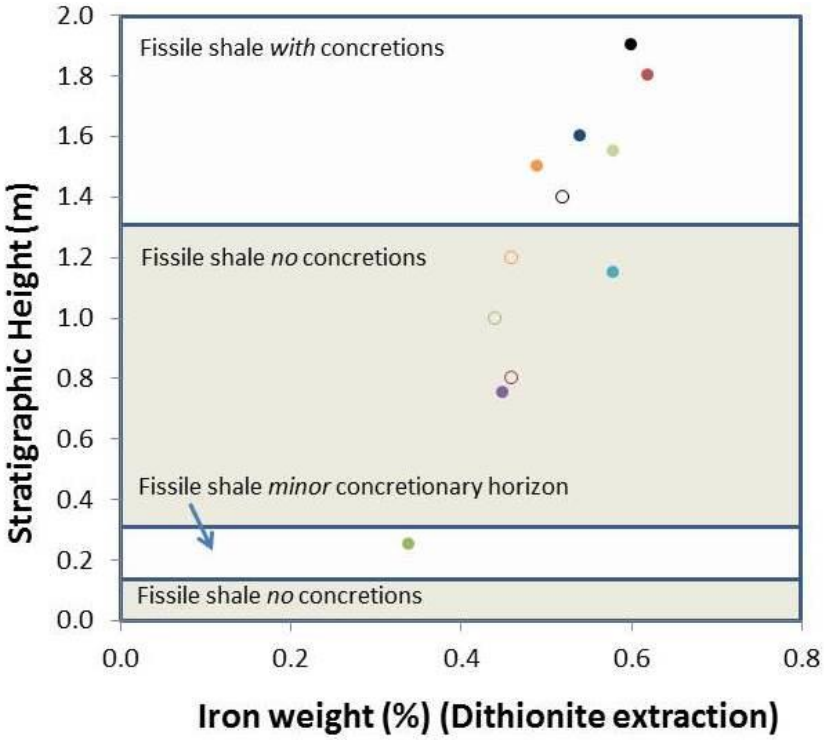

Figure 6.22 Iron weight (%) from the dithionite extraction
Unlike the iron weight percentage from the HCl extractions, the dithionite extractions do not show a marked difference between the zones with and without concretions..

The difference between the results from the iron data could be related to the formation of authigenic clay minerals during burial diagenesis or due to rapid sedimentation rates (Poulton et al., 2010; Poulton and Canfield, 2011). As high sedimentation rates are unlikely (due to the distance from the hinterland either during maximum or minimum transgression; Figure 6.1), it is proposed that during times of concretion deposition there is masking in the Fe pools due to more intense diagenesis (because of a slowdown in sedimentation rates). This mechanism allows the less reactive pool of Fe to deplete as it undergoes intense diagenesis, allowing new clay minerals to form, as HCl (but not dithionite) can extract from this pool. Additionally, this intense diagenesis which increases the labile Fe pool can also be used to partially oxidise sulfide, forming elemental sulfur for example, since a larger pool of Fe(III) will be released from the sediment. This again correlates with what is

seen in the sulfur geochemistry as the elemental S is detectable in the concretion horizon but not in the fissile shale alone.

6.3.3 Depositional model for the Shales-With-Beef Member

The difference between Fe and S chemistry in the fissile shales with concretions and fissile shales without shows that there are changes in the balance of processes taking place during diagenesis of these two lithotypes. In the zone where concretions form the kerogen is sulfur-rich in comparison to when only the fissile shales form. As sulfurisation is more effective during anoxic conditions (e.g. Pearson et al., 1996); or weakly oxygenated bottom waters (Aplin et al., 1993), this helps elucidate the palaeoenvironmental conditions during the time of deposition. The bitumen-S is in agreement that the conditions were anoxic but not euxinic. Bitumen-S was not present during times of concretions and instead S^0 was. Although the key controls on S being incorporated into OM during early diagenesis remain unclear, different biomolecules produced during early diagenesis will be susceptible to biodegradation (e.g. Zhu et al., 2013); sulfide bridges formed from polysulfides are more likely to be broken during subsequent diagenesis than thiols for example (e.g. Sinninghe Damste and de Leeuw, 1990; Zhu et al., 2013; Raven et al., 2015). The S^0 present during times of concretions is clearly not a straight substitute for the bitumen-S as indicated by the isotope signatures. Additionally, thiols produced from nucleophilic attack by sulphide have stronger bounds and are less likely to be broken during later diagenesis, whilst sulphide bridges are weaker and are expected to readily break down (e.g. Zhu et al., 2013 and references therein; Raven et al., 2015). The isotopic signature from the S^0 is heavier than pyrite because it formed in the deeper part of the system, from the persistent H_2S, and therefore H_2S was not available to be incorporated into bitumen. Instead, it is proposed that during times of concretion

formation, OM has incorporated more polysulfides, which can then break down easier during later diagenesis. The polysulfide source is not reoxidised products from diagenetic H_2S as the isotopic signatures are too heavy. The S-chemistry indicates that the palaeoenvironmental conditions were anoxic to weakly-oxygenated bottom waters, and that there was a mechanism for oxidation for the excess S^0 to form during times of concretion formation. In addition to this the DOP (from the HCl extraction) is in agreement with anoxic but not euxinic conditions. During times of concretion formation however, there are higher amounts of DOP, suggesting that there is more H_2S in the system. Data retrieved from the dithionite extractions however, is consistent throughout the measured profile. The change seen only with the HCl extraction and not dithionite suggests that there is a change with the less reactive silicate minerals or clays (Poulton et al., 2010; Poulton and Canfield, 2011). Indeed, iron concentrations from the samples extracted from HCl are lower during times of concretion suggesting that there is another sink; whilst the dithionite extractions show very little change between concretion and no concretion horizons. It is proposed that during times of concretion deposition there is masking in the Fe pools due to more intense diagenesis. Intense diagenesis can cause i) the breakdown of less reactive Fe minerals as they are in the biogeochemical zone for longer ii) the formation of new authigenic clays and iii) the partial oxidation of sulfide, forming elemental sulfur for example (e.g. Aplin et al., 1993).

The organic matter initial input variation was negligible as the TOC content does not vary much throughout much throughout the measured section (Figure 6.10). Additionally, there must always be available iron and sulfur; evidenced by the lack of changes to the amount of pyrite in the measured section (Figure 6.5). This strongly suggests that the initial inputs of organic matter, iron and sulfur are similar

throughout the deposition of the measured section, and variations in inputs are not causing the changes seen within the S and Fe chemistry during concretion formation in the Shales-with-Beef Member. Additionally, the preservation of organic-rich sediments is often thought to be because of a number of factors, including reducing conditions, high primary productivity, sediment starvation, clay physically protecting OM, or a combination of these things (Rimmer et al., 2004). This data shows that reducing conditions remained throughout the section measured, and that there is no additional TOC during times of concretion formation, indicating no major changes to the depositional system. Therefore, it is postulated that differences seen are related to changes in sedimentation rates which fluctuate due to the variations in (3^{rd} order) sea-level. Slower sedimentation rates are postulated to have occurred during times when both Fe and S cycling show systematic changes and coincide with the formation of concretions. This is consistent with other studies that have demonstrated that paused and/or slowed sedimentation rates have been the mechanism of concretion formation (e.g. Raiswell, 1987; Taylor et al., 1995; Majewski, 2000; Bréhéret and Brumsack, 2000; Witkowska, 2012). This can be due to winnowing of the sediments or increased residence times within the early diagenetic species allowing shallower sediments to remain longer in the biochemically active zone (e.g. Taylor et al., 1995; Bréhéret and Brumsack, 2000; Witkowska, 2012). The Shales-with-Beef Member is likely to have had two differing depositional environments which show subtle differences in S and Fe cycling; low stand (when there are no concretions) and high stand (during times of concretion forming). High sedimentation rates have not been postulated as the palaeogeography (Figure 6.1) shows that the hinterland did not undergo major uplift and that the deposition of the Shales-with-Beef Member was distal relative to the shoreline (as in

indicated by palaeogeographies and the shoreline; Figure 6.1) during maximum transgression or maximum regression (Getech, 2013 and references therein).

6.3.3.1 Low stand

During normal sedimentation rates (or low-stand) the normal steady state "Berner" model applies (Figure 6.23). That is, when organic matter is buried, and once O_2 is depleted, bacteria use the OM as a reducing agent and energy source to reduce sulfate to sulfide. There is available Fe in the system which reacts with the H_2S to form metastable monosulfides. The AVS/sulfide formed will probably go through many cycles of oxidation and reduction before final burial as pyrite (Berner, 1970), but there is less intense cycling than when the concretions form. H_2S can persist in the deeper part of the sediment as there are no major mechanisms of oxidation. The S-isotopic values of the H_2S will increase in the deeper/older sediment, as the bacteria will have preferentially utilised the lighter ^{32}S in the shallower part of the sediment. The heavier H_2S can either diffuse up through the sediment or be incorporated into the bitumen and kerogen during diagenesis. Although there will be carbonate minerals forming (in the very shallow parts of the sediment), they will be minor and not develop into concretions. During this time, there will be excess iron left in the system as evidenced by the Fe_{HCl} extractions (Figure 6.23).

6.3.3.2 High stand

As eustatic sea-level rises, the hinterland is further away, thus the amount of sediment reaching the (Present Day) Dorset Coast was reduced. There are clear changes within the diagenesis of the rock: i) concretions form ii) elemental S is preserved iii) iron (solid) speciation is different. The concretions forming indicate that there is increased alkalinity in the system. The overlying Birchi Beds have ^{13}C

values that are between -10 to -14‰, showing that there was an important contribution of carbonate derived from sulfate reduction (Marshall, 1982), and that they formed in the upper few cm's of the sediment (Coleman and Raiswell, 1981). The presence of elemental-S indicates a change in the dynamics of S-cycling, and the changes in Fe speciation indicate a change in the dynamics of Fe cycling. The continuation of pyrite formation, with similar isotopic values, and the fact that organic matter distribution is similar throughout the measured sections are similar, (although with a minor increase in the top of the measured section), shows that the anoxic conditions remained with plenty of sources of Fe, S and OM. Thus, it is postulated that a reduction of sedimentation rates caused the anomalies seen in this horizon. This allows the shallower sediments to remain longer in the biochemically active zone which drives more Fe-cycling, as evidenced by less Fe_{HCl} remaining. The intense cycling allows more Fe(III) to be released from minerals at a later stage, which could then oxidise the H_2S to form S^0 (e.g. reaction 6.1). The S^0 is heavier than pyrite because it formed from the persistent H_2S in the deeper part of the system. This also could explain why the bitumen has non-detectable S as the H_2S is not available for it to be incorporated into it. The kerogen has undergone diagenesis, and therefore in both horizons the values represent a mix of primary S and added H_2S during early diagenesis, thus the values are closer to seawater (assuming that kerogen doesn't lose S during early diagenesis). The higher Fe_{dith} can be explained if the recently available Fe(II) is then incorporated into clays. Although the oxidation of H_2S does cause the surrounding pore-water to be more acidic (reaction 6.1), the more intense Fe-cycling and subsequent alkalinity generation must outpace the acidity, which then induces concretion formation (Figure 6.23).

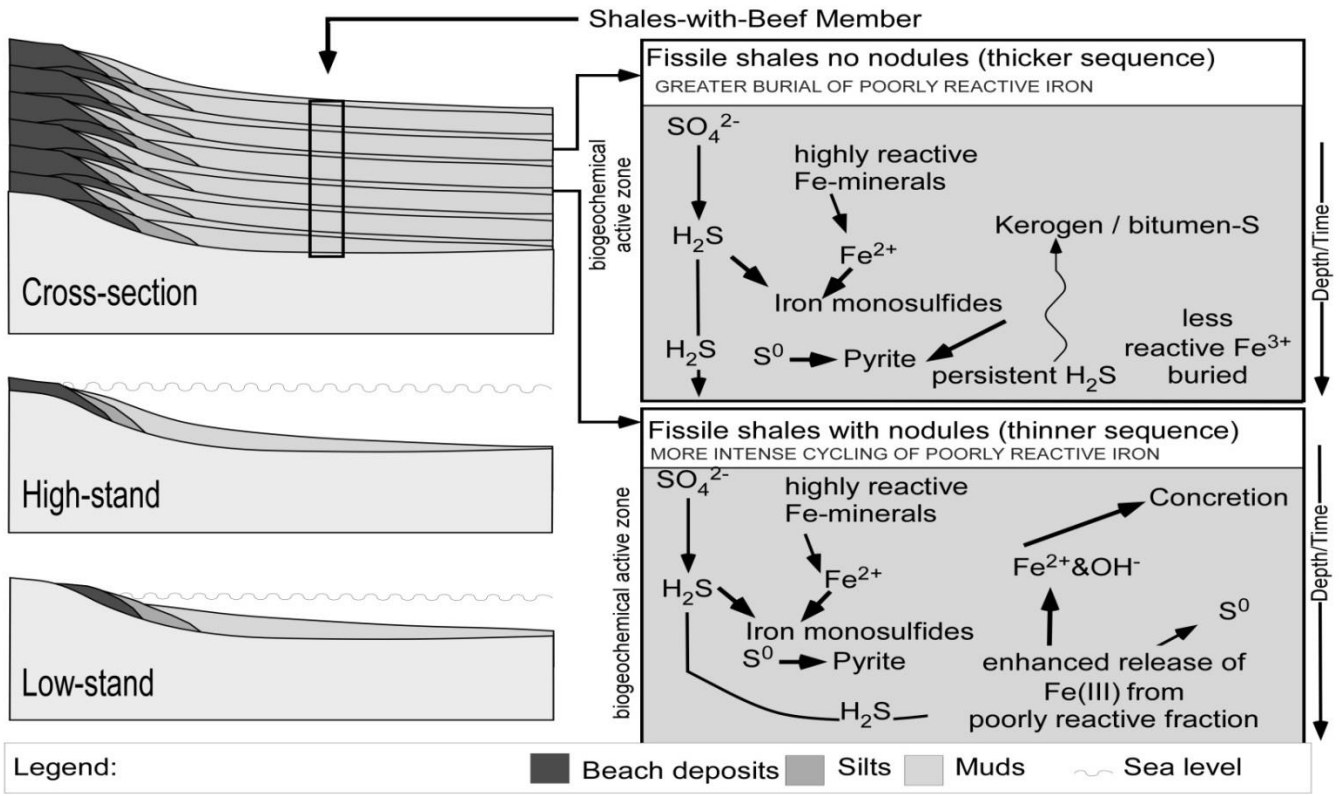

Figure 6.23 Depositional and diagenetic model for the Shales-with-Beef Member.
During normal sedimentation rates, organic matter is buried, and once O_2 is depleted, bacteria use the OM as a reducing agent and energy source to reduce sulfate to sulfide. Available Fe in the system reacts with the H_2S to form metastable monosulfides. As there are no major oxidation mechanisms, H_2S persists in the deeper part of the sediment. The S-isotopic values of the H_2S

increase in the deeper/older sediment, as the bacteria will have preferentially utilised the lighter ^{32}S in the shallower part of the sediment. The heavier H_2S can either diffuse up through the sediment or be incorporated into the bitumen and kerogen during diagenesis. As eustatic sea-level rises, the amount of sediment reaching the (Present Day) Dorset Coast was reduced. The presence of elemental-S indicates a change in the dynamics of S-cycling, and the changes in Fe speciation indicate a change in the dynamics of Fe cycling. The continuation of pyrite formation, with similar isotopic values, and the similarity of the OM distribution throughout the measured section, shows that the anoxic conditions remained with plenty of sources of Fe, S and OM. Reduced rates of sedimentation could cause the shallower sediments to remain longer in the biochemically active zone which drives more Fe-cycling. More Fe(III) is released from minerals at a later stage, which oxidises some H_2S to form S^0. The S^0 is heavier than pyrite because it formed from the persistent H_2S in the deeper part of the system. The kerogen has undergone diagenesis (in as much as it can at that temperature), and thus in both horizons the values represent a mix of primary S and added H_2S during early diagenesis. The recently available Fe(II) is then incorporated into clays. The more intense Fe-cycling and subsequent alkalinity generation induces concretion formation.

6.4 Conclusions

The data show that there was a consistent amount of organic matter (type II/III kerogen) throughout deposition of the Shales-with-Beef Member. The concentration of pyrite within all the samples signifies that there was a constant supply of both iron and sulfide; moreover this also demonstrates that the conditions remained reduced. The results of the organic matter analysis, however, indicate that the conditions were not so reducing that the basin was euxinic; this is in agreement with the DOP values which indicate that the bottom water was anoxic but not sulfide-rich, again throughout the entire section measured. However, there are marked differences with the iron and sulfur chemistry which coincide with the horizons that contain concretions. Throughout the measured section the DOP_{dith} values did not show variation, which is in contrast to times of concretion formation in the DOP_{HCl} data when there was a higher DOP, the latter suggesting that more H_2S was available to react with iron. As dithionite only extracts the more reactive Fe minerals, whilst HCl

extracts those and the less reactive minerals, this strongly suggests that there was predominantly a change in the less reactive silicate minerals (clays). This change coincides with a switch from bitumen that contains S and S^0 that remains undetectable, to bitumen lacking undetectable S to detectable S^0. The lack of change to sediment inputs, that is, the OM matter and conditions remaining reduced, coupled with the changes in iron and sulfur chemistry and forced precipitation of concretions shows that the system is no longer in a steady-state. The $\delta^{34}S$ isotope values show that the elemental sulfur is not from reoxidation of monosulfides and the source of elemental-S is less fractionated. As changes in sediment rates can heavily influence the mineralogy of the sediment, it is proposed that these changes are due to a reduction in sedimentation rates due to fluctuations in sea-level. During low-stand, the steady-state model applies with bacteria reducing sulfate to sulfide which then reacts with the available Fe to form monosulfides and eventually pyrite. The H_2S can persist in the deeper part of the sediment as there are no major mechanisms of oxidation. Heavier H_2S either diffuses up through the sediment or is incorporated into the bitumen and kerogen during diagenesis. During high-stand there is less sediment supply. Bacteria still reduce sulfate to sulfide; reacting with available Fe to form monosulfides and pyrite. However, due to the slow sedimentation rate, species remain longer in the biochemically active zone with more intense Fe cycling, allowing more Fe(III) to be released at a later stage; this then oxidises the H_2S to form S^0, thus the H_2S is not available for it to be incorporated into the bitumen. The Fe is also incorporated into clays. Although the oxidation of H_2S does increase the surrounding pore-water to be more acidic, it is outpaced by the alkalinity produced when Fe is reduced thus the conditions are generated for concretion formation.

6.5 Further work

The formation of clays is speculated, but more robust data could be obtained by correlating these data with Al/Fe ratios and Sr isotope data. Additionally, the methods for iron speciation have been updated since sampling, thus more information could be obtained. Through a series of extractions iron minerals can be differentiated between (e.g. Poulton and Canfield, 2005; Lyons and Severmann, 2006; Cumming et al., 2013):

- Highly reactive iron ($Fe_{(HR)}$). This is pyrite $Fe_{(pyr)}$, iron associated with acid volatile sulfides $Fe_{(AVS)}$, residual unsulfidised dithionite extractable Fe ($Fe_{(dith)}$), iron associated with magnetite ($Fe_{(dith)}$) and iron-rich carbonates ($Fe_{(carb)}$);
- Poorly reactive iron from silicates ($Fe_{(PR)}$);
- $Fe_{(UNR)}$ – unreactive, usually in the silicate phase;
- $Fe_{(T)}$ – total iron, is the sum of all of the above.

Distinguishing between the highly reactive minerals would help identify between iron-limited and sulfur-limited conditions (Poulton and Canfield, 2005). New samples could be taken so that the better iron extractions could be used. This would also resolve, along with obtaining Al data (for Al/Fe ratios), the hypothesis that iron clays are forming. The Al/Fe ratios should identify if non-sulfidised Fe has been used to form clay minerals by identifying enrichment of Fe to Al (Lyons and Severmann, 2006; Cumming et al., 2013).

^{86}Sr is a naturally occurring isotope whilst ^{87}Sr is radiogenic and results from the decay of ^{87}Rb, thus seawater tends to have low ^{87}Sr and therefore lower ^{87}Sr / ^{86}Sr (Capo et al., 1998). The transported clay minerals which were included into the

Shales-with-Beef Member during deposition will be much older in comparison to the authigenic clays (the latter would reflect ^{87}Sr / ^{86}Sr similar to seawater). ^{87}Rb will have been incorporated into the clay minerals as well (half-life of ^{87}Rb is 48.8 Ga). The calcium carbonates which formed in the shallower sediments also have Sr associated with their formation and they will reflect pore-water values. Pore-waters will originally contain seawater Sr but if detrital clays are weathered during diagenesis they will release more radiogenic Sr. If there is more intense diagenesis during the times of concretion formation then this will break down the (older) clays releasing Fe^{2+} and higher $^{87}Sr/ ^{86}Sr$ (because of more decay of ^{87}Rb in the transported clays) into the pore-waters. This heavier Sr is redistributed into calcium carbonate minerals, whilst the iron should form new clay minerals (or pyrite). Thus if the iron in the clay minerals are weathered, due to staying longer in the biogeochemical active zone, then the new authigenic clays and calcium carbonate minerals will too have higher $^{87}Sr/ ^{86}Sr$.

The preservation of OM is linked to sedimentation rates. If the rate is too high or too low then dilution of the source rock will occur, thus preservation will be poorer. As the horizons are relatively small, the slowing down of sedimentation has not affected the OM preservation in the samples obtained for this study. If a thicker concretionary horizon of the Shales-with-Beef Member was sampled and OM preservation is poorer than the rest of the formation, then this would also support the theory of a decrease in sedimentation rate during time of concretion formation.

Some palaeoredox workers (e.g. Turgeon and Brumsack 2006; Rimmer, 2004) have used trace metals enrichments relative to Al to help determine the conditions (e.g. anoxic versus dysoxic) within the marine system; some of these methods maybe applicable to a study of this nature. Including the use of Ti:Al to help define

fluctuations in sea-level. Results from trace metals could support the interpretation of these data.

Chapter 7 Study Discussion & Conclusion

7.1 Introduction

This thesis has been carried out as discrete studies pertaining to metal interactions with the sulfur cycle in aquatic sediments. As each chapter has already included discussion and conclusions, this chapter is designed to integrate the key findings across the sites.

7.2 Main findings

7.2.1 Thorne Moors Redox Zones main findings

Redox zones at Thorne Moors are complicated due to a series of processes interacting with one another. These include the interaction between plants, lateral water flows and bacterially mediated processes. The pore-water profiles show similarities over time and at different locations showing that these complex interactions were not transitory. Oxidised species of S and N are added to the peatbogs at the surface by atmospheric deposition which bacteria then use up as a source of energy in the near-surface leaving low concentrations of these chemical species deeper in the peat profile. It is well established that plant material decays and gradually becomes humified to form peat, releasing oxygen, sulfur and nitrogen (Novak et al., 2009; Zaccone et al., 2007, 2011). Over time the peat can be seen to decompose at the same rates, but over very short periods the peat decomposes differentially, which this study has shown adds short-lived spikes of SO_4^{2-} and $N0_3^-$ (but not Cl^-) that diffuse quickly both up and down the peat. *Eriophorum* roots exude O_2 thus creating a microenvironment whereby oxidation of both N and S occur, and is also evident in the high-resolution profiles generated in this study. Lateral water

flows (pipes) bring in O_2 from the surface, or at least differing amounts of Cl^-, SO_4^{2-} and NO_3^- from other parts of the peat, as seen in the DET pore-water profiles. Due to the nature of these processes it is hard to distinguish simplistic "redox zones" through the profile; moreover this study has shown that some of these processes are occurring within the catotelm, which is therefore not so chemically inactive as some workers have previously assumed. Additionally the complexity of the processes were found to be consistently repeated temporally and spatially, although there were some (minor) variations between sites that could be attributed to slight differences in morphology and ecology. It is therefore clear that for better peat monitoring we need to move away from the simplified two-layered model to understand the functionality of peatlands as carbon sinks or sources. This sub-study also suggests, by comparison with previous work at Thorne Moors, that the reduced sulfur loading which the site was subjected to until the early 1970s, has now been mitigated giving a recovery of approximately 40 yrs.

7.2.2 Thorne Moors trace metals main findings

Initial results suggested that long-term trace metal accumulation (except Ni) in peatbogs is controlled by dust deposition as the solid-phase trace metal profiles closely corresponded to the ash profile. However, as iron is known to be mobile in peatbogs (due to redox reactions and vegetation cycling) it showed that post-depositional processes were missing. This was investigated by examining the correlation between ash and the metals; not all correlated well. Lack of correlating, however, may be related to the source of the trace metals (i.e. from a source different to the dust input) and not because they undergo diagenetic processes. For example, Pb had a source which was not related to dust (leaded petrol emissions) and therefore was not expected to correlate well. Enrichment factors were calculated and

anthropogenic inputs to the peatbog assessed. The solid-phase datasets showed evidence of mobility for Fe, Ni and Zn; all metals which have shown evidence for mobility in previous studies. Cu and Pb appeared to be immobile, and Co, for the most part, immobile. The anthropogenic input calculations suggested that a smaller fraction of Co, which is related to anthropogenic activity and coupled with iron, is mobile. Detail from the DET and DGT gels show that there are horizons in the sediment where metal availability increases yet it is not coupled with a corresponding increase in concentration, suggesting that some trace metals are available at depth but move into the solid-phase at the same horizon. As would be expected most processes seem to occur in the shallowest part of the peat, due to live and partially decomposed organic matter, and oxygen penetration into the surface layers. As there is little or no O_2 in the deeper parts of the peat and not much live organic matter (apart from roots), only minor variations in both concentrations and fluxes are expected.

This study strongly suggests that Pb is not mobile and can reliably be used in atmospheric deposition studies and Pb^{210} dating. Moreover, this study also demonstrated that using these combined methods is a cheap and quick effective evaluation of determining if trace metal are mobile within sediments. Indeed, these combined methods can be used to screen sediments for their appropriateness of using isotope studies.

7.2.3 Warham main findings

A pool of Fe^{3+} occurs deeper in the sediment. This is due to high sedimentation rates providing a mechanism to bury a proportion of reactive Fe-minerals and the majority of the less reactive Fe-minerals, without them undergoing any diagenesis. Elemental

sulfur is found throughout the depth range sampled in relatively high concentrations at Ants Pan, even though O_2 is depleted. It is postulated that H_2S is oxidised by the deeper buried reactive Fe^{3+} producing the partially oxidised S^0. The elemental sulfur then undergoes further reactions resulting in sulfate at depth. The pore-water data did not show this, indeed, when plotted against chloride there were no major enrichments or depletions (except for the very near-surface in one profile) throughout the depth sampled. The observed profiles are more likely to result from a net balance between sulfate reduction and sulfide oxidation. The large amounts of SO_4^{2-} and S^0 seen in the near-surface could be due to pore-water advection/diffusion of H_2S from the deeper sediments to the near surface where it is oxidised by O_2.

This data did not achieve the high resolution datasets that it intended to. Therefore key details were missed and instead the sulfate core pore-water data are rather uniform concentration profiles. This dataset alone is not robust, however, work by Wilmot (2006) demonstrated that Warham sediment (under laboratory conditions) had Fe(III) reduction driven by sulfide oxidation in both abiotic and biotic conditions; both leading to an accumulation of S^0 and in the biotic experiments only, siderite precipitation. The work presented here is in agreement with the solid-phase data of S^0 found in Warham sediments. Both the laboratory experiments and data from this study were integral to providing an understanding of early diagenesis at Warham. Together these data were published in Mortimer et al. (2011).

7.2.4 Shales-with-Beef Member main findings

Data from the Shales-with-Beef Member shows that the inputs of OM, Fe and S were similar throughout the measured section (TOC and pyrite content varies little throughout). Pyrite formation also shows that the conditions must have been

reduced. DOP values and C/S support this view demonstrating that conditions were anoxic but not euxinic. There are, however, horizons in the measured section which contain concretions which coincide with marked differences with the S and Fe chemistry. Dithionite can only extract the most reactive Fe minerals and HCl can extract the reactive pool and the slightly less reactive minerals; these two differing extraction techniques showed differences between horizons with concretions and those without. DOP_{HCl} increases during times of concretion formation indicating that there is more H_2S in the pore-waters, than during the times when the fissile shales are deposited. DOP_{DITH} does not change. This strongly suggests that there was only a change in the less reactive minerals (silicates). This also coincides with a switch from bitumen that contains S and S^0 that remains undetectable, to bitumen lacking undetectable S to detectable S^0. The $\delta^{34}S$ isotope values show that the elemental sulfur is not from reoxidation of monosulfides and the source of elemental-S is less fractionated. Concretion formation has been correlated with sedimentation rates in previous studies (e.g. Raiswell, 1987; Majewski, 2000; Witkowska, 2012; Bréhéret and Brumsack, 2000), thus it is proposed that there were changes in sedimentation rates due to fluctuations in sea-level when the concretionary horizons are present in the Shales-with-Beef Member. The palaeogeographies (Chapter 6; Figure 6.1) show the location of the Shales-with-Beef Member during the Sinemurian; they were not deposited in a coastal setting, there wasn't any (significant) uplift in the area to push the formation above sea-level, thus it likely that the sedimentation rates were slowed rather than increased.

During low-stand, the steady-state model applies with bacteria reducing sulfate to sulfide which then reacts with the available Fe to form monosulfides and eventually pyrite. Isotopically heavier H_2S (with respect to S) persisted in the deeper part of the

sediment; however, it also diffused up through the sediment and/or was incorporated into the bitumen and kerogen during diagenesis. During high-stand there was less sediment supply. Bacteria still reduced sulfate to sulfide which reacted with the available Fe to form both monosulfides and pyrite. Species remained longer in the biochemically active zone, however, resulting in more intense Fe cycling. This allowed more Fe(III) to be released at a later stage which partially oxidised the H_2S to form S^0. Thus H_2S was not available for it to be incorporated into the bitumen. The available Fe was also incorporated into clays. Oxidation of H_2S did increase the surrounding pore-water to be more acidic; however, this was outpaced by the alkalinity produced by the reduction of Fe, thus conditions were generated for concretion formation.

7.3 Comparisons between the component studies in this thesis

7.3.1 Thorne Moors metals and redox correlations

The trace metal measurements were made at the same time as the anion analyses at site 1 and 2 (2011), therefore parallels can be drawn between observations made in these different studies. However, these data are hard to correlate, especially so as iron produced at depth diffuses up to a near surface sink. In general sulfate concentrations are low with sulfate reduction predominantly in the near surface, and the system is not likely to be controlled by sulfur species. Some interpretations however, can be drawn by correlating some of the short sharp excursions across these two sites. In the same horizon as high Cl^-, NO_3^- and SO_4^{2-}concentrations, which have been interpreted as lateral water flows, there are low Fe(aq) concentrations and low Fe availability. When the lateral water flows occur, oxygen is brought deeper into the peat, which increases the sulfate and nitrate concentrations,

but decreases the iron concentrations as any available iron(II) will oxidise and form iron oxy(hydroxides). An example for this horizon can be found at site 1 at approximately 16 cm. In areas where there is a sulfate and nitrate increase but not a corresponding chloride increase, it has been postulated that this is either because of root oxidation or "hotspots" of decomposition. There is evidence for the latter as, in site 2 at approximate 31 cm, there are positive excursions of sulfate, nitrate and iron availability. Additionally, this peak can be seen in the cadmium profile too.

7.3.2 Shales with Beef Member and Warham

Warham has high a sedimentation rate which provides a mechanism to bury a proportion of reactive Fe-minerals, and the majority of the less reactive Fe-minerals without them undergoing any diagenesis; resulting in a pool of Fe^{3+} in the deeper sediment. Conversely, the Shales-with-Beef Member was deposited during times of variable sedimentation rates, and Fe-minerals remain in the biochemically active zone for longer during times of concretion formation. Both scenarios lead to bacteria reducing sulfate to sulfide; reacting with available Fe to form monosulfides (and pyrite in the Shales-with-Beef Member) as would be expected in reducing sediments, but both showed an increase of S^0 in the sediment. The latter was due to abiotic reactions of sulfide and iron, where iron is reduced and sulfide is oxidised. The concretions coexist with pyrite, or monosulfides (for Warham) in the same horizons.

7.4 Contrasting sites

Some reactions are interpreted to be ubiquitous in all sites. For example all sites have the reaction of sulfate to sulfide via MSR:

$$2H^+ + SO_4^{2-} + 2CH_2O \rightarrow H_2S + 2CO_2 + 2H_2O \quad (7.1).$$

The reduced sulfide, however, has been interpreted to have differing subsequent reactions at each of the sites. This is, in part, related to the source of sulfate, the reducing conditions of the sites, the major sink for sulfide and the depth in which reactions happen. At Thorne Moors, the most important source of sulfate is from organic matter (Bottrell et al., 2010), additionally, pyrite is not a major sink for sulfate (or iron; see phase diagram in Chapter 4, Figure 4.14) and instead the major sink for the sulfide is incorporation into organic matter (Bottrell et al., 2010). It is known that iron monosulfides form at Warham, yet siderite also forms at this site which is unusual (Pye et al., 1990). The main conclusion for Warham is the interaction of sulfide with iron. Sedimentation rates at this site are fast, seen from the rapid accretion of this coastline via comparing aerial photographs (Pye, 1984). It has been interpreted that Fe^{3+} has been buried quickly and a subsequent reaction has occurred in which sulfide is partially oxidised to S^0 by Fe^{3+} which is also reduced to Fe^{2+}:

$$FeS + 2FeO(OH) + 2H_2O \rightarrow 3Fe^{2+} + S^0 + 6OH^- \quad (7.2).$$

Black Venn has DOPs which indicate anoxic conditions and sulfide has reacted with reduced iron to form pyrite. During times of concretions, however, there is a mechanism which allows iron from less reactive pools (e.g. Fe-silicates) which stays in the biogeochemical zone local than normal and results in the same processes as seen in reaction 7.2. Clearly, the behaviour of sediment diagenesis is related to numerous processes and conditions within the sediment (e.g. pH, oxygen concentrations etc.), but importantly related to the reactivity and amounts of chemical species within the sediments. For example, terrestrial sediments often are limiting in S, whilst euxinic conditions are more likely to be limited in Fe (e.g. Lyons and Severmann, 2006 and references therein). Organic matter is generally

limiting in most marine sediments (e.g. Berner and Raiswell, 1983). Additionally, there may be plenty of species in the sediment which may not be particularly reactive, e.g. Fe-silicates versus Fe-oxides. Changing conditions can juxtapose biogeochemical zones into horizons where they would not normally found, which may result in more diagenesis.

Sites used in these studies were very differing; Thorne Moors comprises of dead and alive organic matter, whilst both Warham and Shales-with-Beef have much less OM (initial inputs and preserved) in the sediment. Additionally the marine and transitional sites have more sulfate than Thorne Moors does. The diffusion of O_2 into the sediment at Warham and Shales-with-Beef Member (inferred from the data) is shallower than at Thorne Moors, which directly exerts a control on the redox potential in the sediment. Additionally, Thorne Moors has the complex interaction of vegetation, which can introduce O_2 deeper into the system; the Shales-with-Beef Member shows no evidence of burrowing. These differences are important to understand as the geochemical cycles of sulfur, iron and carbon regulate CO_2 and O_2 in the atmosphere (Holland, 1984; Berner, 1999, Canfield, 2000, Zhu et al., 2013), which in effect is the burial of pyrite.

7.5 Stages of diagenesis relating to data collection

DET and DGT gels measure the immediate products of sediment diagenesis. Additionally the profiles identify where there are diffusion gradients (by the shape of the profile from DET gels), and the immediate availability of species. However, predicting long term consequences with regards to diagenesis would lead to erroneous results, as the gels cannot identify ‘sediment storage information’, as only the pore-water concentrations and fluxes are obtained. Cores, however, can measure

pore-waters (usually at a much lower resolution) and solid-phase chemistry. This allows comparisons to be made from instantaneous chemistry, that is, the products (or lack thereof, e.g. sulfate reduction results in profiles which have decreasing sulfate with depth) and the longer term storage of the final products, that is AVS, pyrite or metals for example. However, using the solid-phase data from cores alone relies on correlating species burden and timing of inputs, thus inferring early diagenesis reactions. DET and DGT methods are independent of knowing sediment age and species burden and timing inputs. The rock record represents the integrated history of accumulation and potential subsequent loss or gain, due to multiple phases of diagenesis. Using the rock record therefore clearly relies on a good understanding of the multiple diagenetic phases by understanding the reactions and resulting products, as well as understanding, how (if at all) these differing diagenetic phases react with one another. To do this both modern day and past examples have to be understood and calibrated with one another so that the diagenetic phases are understood. In some cases these means that oversimplifications have arisen.

7.6 This study within the wider context of biogeochemical cycles

The established framework for microbial diagenesis in aquatic sediments is degradation of OM by a series of respiration reactions that yield sequentially less energy from different terminal electron acceptors (that is, aerobic respiration, denitrification, manganese reduction, iron reduction, sulfate reduction and methanogenesis). However, previous work has shown that the model of a simple progression in processes is an oversimplification. This study strongly reinforces the inadequacies of the “simple progression” model, and moreover has elucidated the details of the far more complex pattern of interactions that characterize two types of environments, which are well known to store carbon (and methane). Indeed,

peatbogs are shown to exhibit a myriad of different processes in a pattern of complex element recycling. Many sedimentary environments can be affected by changes in sedimentation rates and this study has clearly shown how this change can affect the fate of redox-sensitive elements during early diagenesis. These systems have to be well understood so that we know the consequences of changing a variable that affects aquatic systems. That is, we need to understand the detail behind the global biogeochemical models to account and/or correctly predict how changes to the global system will affect fluxes, residence times or reservoirs of key elements. This is especially so for the iron, sulfur, carbon and oxygen cycles as these four elements control the oxidation state of all Earth's surface environments (e.g. Holland, 1984; Berner, 1999; Canfield, 2000; Mortimer et al., 2011; Zhu et al., 2013).

References

Aizenshtat, Z., Amrani, A., 2004. Significance of $\delta^{34}S$ and evaluation of its imprint on sedimentary organic matter: I. The role of reduced sulfur species in the diagenetic stage: A conceptual review. *IN*: Geochemical Investigation in Earth and Space Science: A tribute to Isaac R. Kaplan. Eds: Hill, R.J., Geological society, London, Special Publications, v.9: 15- 33

Aldrich C., Feng D., 2000. Removal of heavy metals from wastewater effluents by biosorptive flotation. Miner. Eng. v.13: 1129–1138.

Allen, A.G., Nemitz, E., Shi, J.P., Harrison, R.M., Greenwood, J.C., 2001. Size distribution of trace metals in the United Kingdom. Atmospheric Environment v.35:4581-4591.

Alongi, D.M. 1998. Coastal Ecosystem Processes. CRC Press, New York.

Andrejko, M.J., Fiene, F. and Cohen, A.D., 1983. Comparison of ashing techniques for determination of the inorganic content of peats. In: P.M. Jarrett (Editor), Testing of Peats and Organic Soils. American Society for Testing and Materials, Spec. Publ. p. 820 - 241.

Armstrong, W., Justin, S.H.F.W., Beckett, P.M., Lythe, S., 1991. Root adaptation to soil waterlogging. Aquat. Bot., v.39: 47-73.

Aplin, A.C., Macquaker, J.H.S., Lovley, D.R., Meadows, P., Small, J., Lyons, T., Aargaard, P., 1993. C–S–Fe geochemistry of some modern and ancient anoxic marine muds and mudstones. Phil. Trans. R. Soc. Lond. v.344: 89–100.

Appleby, P.G. and Oldfield, F., 1992. Application of lead-210 to sedimentation studies. In: *Uranium Series Disequilibrium* (M. Ivanovich and R.S. Harmon, eds.), pp. 731–738. Oxford University Press.

Balistrieri, L.S., Foster, A.L., Gough, L.P., Gray, Floyd, Rytuba, J.J., and Stillings, L.L., 2007, Understanding metal pathways in mineralized ecosystems: U.S. Geological Survey Circular 1317.

Baralkiewicz, D., Siepak, J., 1999. Chromium, Nickel and Cobalt in Environmental Samples and Existing Legal Norms. Polish Journal of Environmental Studies v.8 (4):201-208.

Bartlett, R., Bottrell, S., Coulson, J., 2005. Behaviour of sulphur during diagenesis of a maritime ombrotrophic peat from Yell, Shetland Islands, UK. Appl. Geochem. v.20: 1597-1605.

Bartlett, R., Bottrell, S.H., Coulson, J.P., Lee, J., Forbes, L., 2009. ^{34}S tracer study of pollutant sulfate behaviour in a lowland peatland. Biogeochem. v.95: 261-275.

Belyea, L.R., Baird, A.T, 2006. Beyond "the limits to peat bog growth": cross-scale feedback in peatland development. Ecological Monographs, v.76(3): 299-322.

Bender, M.L., 1983. Pore-water chemistry of the mounds Hydrothermal Field, Galapagos Spreading Center: results from Glomar Challenger piston coring. Journal of Geophysical Research, v.88(B2): 1049-1056.

Berg, P., McGlathery, K. J., 2001. A high resolution pore water sampler for sandy sediments. Limnol. Oceanogr., v. 46(1): 203-210

Berner, R. A., 1966. Chemical diagenesis of some modern carbonate sediments. Am. J. Sci. v.264: 1–36.

Berner, R.A., 1968. Rate of concretion growth. Geochim. Cosmochim. Acta. v.32:477-483.

Berner, R.A., 1970. Sedimentary pyrite formation. Amer. J. Sci. v.268: l-23

Berner, R.A., 1981. A new geochemical classification of sedimentary environments. J. sedim. Petrol. v.51:359-365.

Berner, R.A., 1982. Burial of organic carbon and pyrite sulfur in the modern ocean: its geochemical and environmental significance. American Journal of Science, v. 282: 451-473.

Berner, R.A., 1984. Sedimentary pyrite formation: An update. Geochemica et Cosmochimica, v.48:605-615.

Berner, R.A., 1989. Biogeochemical cycles of carbon and sulfur and their effect on atmospheric oxygen over Phanerozoic time. Palaeogeogr., Palaeoclimatol., Palaeeecol., v.75: 97-122.

Berner, R.A., 1999. Atmospheric oxygen over Phanerozoic time. Proceedings of the National Academy of Sciences of the United States of America 99:10955–10957.

Berner, R. A., & Raiswell, R., 1983. Burial of organic carbon and pyrite sulfur in sediments over Phanerozoic time: a new theory. Geochimica et Cosmochimica Acta, 47(5):855-862.

Blodau, C., Mayer, B., Peiffer, S., Moore, T.R., 2007. Support for an anaerobic sulphur cycle in two Canadian peatland soils. J. Geophys. Res. 112, G02004 doi: 10.1029/2006JG000364

Blomqvist, G., 2001. De-icing salt and the roadside environment. Thesis published at the Royal Institute of Technology, Stockholm.

Blomqvist, S., 1991. Quantitative sampling of soft-bottom sediments: problems and solutions. Mar. Ecol. Prog. Ser. v.72: 295-304.

Bohlin, E., Hämäläinen, M., Sundén, T., 1989. Botanical and chemical characterization of peat using multivariate methods 1. Soil Science v.147: 252-263.

Boorman, L., 2009. The role of freshwater flows on salt marsh growth and development *IN*: Coastal Wetlands an integrated ecosystem approach Eds, Perillo, G.M.E., Wolanski, E., Cahoon, D.R., Brinson, M.M., Elsevier.

Bottrell, S.H., 1996. Organic carbon concentration profiles in Recent cave sediments: records of agricultural pollution or diagenesis? Environmental Pollution v.91: 325-332.

Bottrell, S.H., Coulson, J., Spence, M., Roworth, P., Novak, M., Forbes, L., 2004. Impacts of pollutant loading, climate variability and site management on the surface water quality of a lowland raised bog, Thorne Moors, E. England, UK. Appl. Geochem. **v.**19: 413-422.

Bottrell, S. H., Hatfield, D., Bartlett, R., Spence, M. J., Bartle, K. D., & Mortimer, R. J., 2010. Concentrations, sulfur isotopic compositions and origin of organosulfur compounds in pore waters of a highly polluted raised peatland. Organic Geochemistry, 41(1):55-62.

Bottrell, S.H., Mortimer, R.J.G., Spence, M. Krom, M.D., Clark, J.M., Chapman, P.J., 2007. Insights into redox cycling of sulfur and iron in peatlands using high-resolution diffusive equilibrium thin film (DET) gel probe sampling. Chem. Geol. *v.*244: 409-420.

Bottrell S.H., Novak M., 1997. Sulfur isotopic study of two pristine *Sphagnum* bogs in the western British Isles. J. Ecol. v.85: 125-132.

Bottrell, S.H., Raiswell, R., 2000. Sulphur isotopes and microbial sulphur cycling in sediments. *IN*: Riding, R.E., Awramik, S.M. (Eds.), Microbial Sediments. Springer-Verlag, Berlin, 96-104.

Boursiquot, S., Mullet, M., Ehrhardt, J.J., 2002. XPS study of the reaction of chromium (VI) with mackinawite. Surface and Interface Analysis v. 34:293-297.

Bowden, W.B., 1987. The biogeochemistry of nitrogen in freshwater wetlands. Biogeochemistry v.4: 313-348.

Bradl, H.B., Kim, C., Kramar, U., Stuben, D., 2005. Interactions of heavy metals, *In* Heavy metals in the environment: Origin, interaction and remediation, v.6: 126-128

Bradshaw, M. J., Cope, J. C. W., Cripps, D. W., Donovan, D. T., Howarth, M. K., Rawson, P. F., West, I. M. and Wimbledon, W. A. 1992. Jurassic. Journal of the Geological Society, London.

Brandl H., Hanselmann, K.W., 1991. Evolution and application of dialysis porewater samplers for microbiological studies at sediment-water interfaces. Aquatic Sciences, v53(1): 55-73.

Bréhéret, J.G., Brumsack, H.J., 2000.Barite concretions as evidence in sedimentation in the Marnes Bleues Formation of the Vocontian Basin (SE France). Sedimentology Geology v. 130:205-228.

Brendel, P.J.W, Luther III, G.W., 1995. Development of a gold amalgam voltammetric microelectrode for the determination of dissolved Fe, Mn, O2, and S(-II) in porewaters of marine and freshwater sediments. Environ. Sci. Technol. v.29: 751-761.

Brown, P.A., Gill, S.A., Allen, S.J., 2000. Metal removal from wastewater using peat. Water Research, v, 34(16): 3907-3916.

Bruchert, V., Pratt, L.M., 1996. Contemporaneous early diagenetic formation of organic and inorganic sulfur in estuarine sediments from St. Andrew Bay, Florida, USA. Geochemica et Cosmochimica, v.60(13): 2325-2332

Bufflap, S.E., Allen, H.E., 1995. Sediment pore water collection methods for trace metal analysis: a review. Wat.Res., v. 29(1): 165-177.

Burdige, 2006. Geochemistry of marine sediments. Princeton University Press: 97-139

Canfield, D.E., Raiswell, R., Westrich, J.T., Reaves, C.M., Berner, R.A., 1986. The use of chromium reduction in the analysis of reduced inorganic sulphur in sediments and shales. Chem. Geol. v.54:149-155.

Canfield, D., E., 1989. Reactive iron in marine sediments. Geochim. Cosmochim. Acta v.53:619–632.

Canfield, D, 2001. Isotope fractionation by natural populations of sulfate-reducing bacteria. Geochemica et Cosmochimica, v.65(7): 1117-1124.

Canfield, D.E., Habicht, K.S., Thamdrup, B., 2000. The Archean sulfur cycle and the early history of atmospheric oxygen. Science 288:658–660

Capo, R.C., Stewart, B.W., Chadwick, O.A., 1998. Strontium isotopes as tracers of ecosystem processes: theory and methods. Geoderma v.82: 197–225

Carignan, R., 1984. Interstitial water sampling by dialysis: methodological notes. Limnol. Oceanogr. v.29: 667-670.

Carignan, R., Rapin, F., Tessier, A., 1985. Sediment porewater sampling for metal analysis: A comparison of techniques. Geochim. Cosmochim. Acta, v. 49: 2493-3497.

Chapman, S.J., 2001. Sulphur forms in open and afforested areas of two Scottish peatlands. Water, Air Soil Poll. v.128: 23-39.

Chapman, P.M, Wang, F., Germano, J.D., Batley, G., 2002. Pore water testing and analysis: the good, the bad, and the ugly. Marine Pollution Bulletin, v.44: 359-366.

Chapelle, F.H., Bradley, P.M., Thomas, M.A., McMahon, P.B., 2009. Distinguishing Iron-Reducing from Sulfate-Reducing Conditions. Ground Water v.4(2):300-305.

Chesworth, W., Martinez Cortinzas, A., Garica-Rodeja, E., 2006. The redox-pH approach to the geochemistry of the earth's land surface, with application to peatlands. Martini, I. P., Cortizas, A. M., & Chesworth, W. (Eds.). (2007). Peatlands: evolution and records of environmental and climate changes (Vol. 9). Elsevier.

Chmura, G.L., Anisfeld, S.C., Cahoon, D.R., Lynch, J.C., 2003. Global carbon sequestration in tidal, saline wetland soils. Global Biogeochemical Cycles, v.17(4):(22)-1-(22)-11

Clark, J.M., Bottrell, S.H., Evans, C.D., Monteith, D.T., Bartlett, R., Rose, R., Newton, R.J., Chapman, P.J. 2010. The importance of the relationship between scale and process in understanding long-term DOC dynamics. Science of the Total Environment v.408: 2768-2775.

Clarke, L.B., Lesley L. Sloss, 1992. Trace elements-emissions from coal combustion and gasification. Vol. 49. IEA Coal Research.

Claussen, M., Mysak, L., Weaver, A., Crucifix, M., Fichefet, T., Loutre, M.F., Weber, S., Alcamo, J., Alexeev, V., Berger, A., Calov, R., Ganopolski, A., Goosse, H., Lohmann, G., Lunkeit, F., Mokhov, I., Petoukhov, V., Stone, P., Wang, Z., 2002. Earth system models of intermediate complexity: closing the gap in the spectrum of climate system models. Climate Dynamics. v18(7): 579-586

Claypool, G.E., Kaplan, I.R., 1974. The origin and distribution of methane in marine sediments. *In* I.R. Kaplan (ed.), Natural Gases in Marine Sediments. Plenum Press, 99-139

Clymo, R. S. 1984. The Limits to Peat Bog Growth. Philosophical Transactions of the Royal Society of London, Series B 303, 605-654.

Coleman, M.L., 1980. Corrections for mass spectrometer analysis of sulphur dioxide. IGS Isotope Geology Unit, Stable Isotope Report, No.45,12pp.

Coleman, M.L., Hedrick, D.B., Lovley, D.R., White, D.C., Pye, K., 1993. Reduction of Fe (III) in sediments by sulphate-reducing bacteria. Nature, v.361: 436–438.

Coleman, M.L., Raiswell, R., 1981. Carbon, oxygen and sulphur isotope variations in concretions from the Upper Lias of N.E. England. Geochim. Cosmochim. Acta, v.45:329-340.

Coleman, M.L., Raiswell, R., 1993. Microbial mineralization of organic matter: mechanisms of self-organization and inferred rates of precipitation of diagenetic minerals. Phil. Trans. R. Soc. London v.344:69-87.

Cowardin, L.M., Carter, V., Golet, F.C. and La Roe, E.T. 1979. Classification of wetlands and deepwater habitats in the United States. U.S. Dept. Interior, Fish & Wildlife Service, FWS/OBS-79/31.

Cox, P.M., Kwaitkowski, L., 2013. Assessment of the iMarNet Ocean biogeochemical Models. University of Exeter (in conjunction) with Integrated Marine Biogeochemical Modelling Network.

Craig, H., 1957. Isotopic standards for carbon and oxygen and correction factors for mass-spectrometric analyses of carbon dioxide. Geochim. Cosmochim. Acta v.12:133-149.

Crist, R.H., Martin, J.R., Chonko, J., 1996. Uptake of metals on peat moss: An ion-exchange process. Environ. Sci. Technol., v 30: 2456-2461.

Cui, Y., Kump, L.R., Ridgwell, A.J., Charles, A.J., Junium, C.K., Diefendorf, A.F., Freeman, K.H., Urban, N.M., Harding, I.C., 2011. Slow release of fossil carbon during the Palaeocene-Eocene Thermal Maximum. Nature Geoscience, v.4: 481-485.

Cumming, V.M., Poulton, S.W., Rooney, A.D., Selby, D., 2013. Anoxia in the terrestrial environment during the late Mesoproterozoic. Geology, v.41(5):583-586.

Currey, P.M., Johnson, D., Dawson, L.A., van der Wal, R., Thornton, B., Sheppard, L.J., Leith, I.D., Artz, R.R.E., 2011. Five years of simulated atmospheric nitrogen deposition have only subtle effects on the fate of newly synthesised carbon in *Calluna vulgaris* and *Eriophorum vaginatum.*Soil Biology and Biochemistry v.43(3): 494 – 502.

Curtis, C.D., 1987. Inorganic geochemistry and petroleum exploration *IN*: Brooks, J., Welte, D., (eds) Advances in Petroleum Geochemistry, 2, Academic Press, 91-140.

Curtis CD, 1972. Scandium. In: Fairbridge RW, editor. The encyclopedia of geochemistry and environmental sciences. Stroudsburg, Pennsylvania: Dowden, Hutchinson, and Ross.

Dammon W.H., 1978. Distribution and movements of elements in ombrotrophic peat bogs. Oikos, v.30(3): 480-495.

Damste, J. S. S., & De Leeuw, J. W. (1990). Analysis, structure and geochemical significance of organically-bound sulphur in the geosphere: state of the art and future research. Organic Geochemistry, 16(4), 1077-1101.

Davison, W., Grime, G.W., Morgan, J.A.W., Clarke, K., 1991. Distribution of dissolved iron in sediment pore waters at submillimetre resolution. Nature, v.352: 323-325.

Davison, W., Woof, C., Turner, D.R., 1982. Handling and measurement techniques for anoxic interstitial waters. Nature, v.295: 582-583.

Davison, W., Zhang, H., 1994. In site speciation measurements of trace components in natural waters using thin-film gels. Nature v.367: 546 – 548.

Davison, W., Zhang, H., Grime, G.W., 1994. Performance characteristics of gel probes used for measuring the chemistry of pore waters. Environ. Sci. Technol. v.28: 1623-1632.

David, D.J., and Williams, C.H., 1975. Heavy metal contents of softs and plants adjacent to the Hume Highway near Marulan, New South Wales. Aus. J. exp. Agric. Anim. Husb. 15: 414-418.

Denney, S., Sherwood, J., Leyden, J., 1999. In situ measurements of labile Cu, Cd and Mn in river waters using DGT. Sci. Total Environment, v.239:71-80.

Devries, C.R., Wang, F., 2003. In situ two dimensional high-resolution profiling of sulfide in sediment interstitial waters. Environ. Sci. Tech. v.37: 792-797.

Docekalova, H., Clarisse, O., Salomon, S., Wartel, A., 2002. Use of constrained DET probe for a high-resolution determination of metals and anions distribution in the sediment pore water. Talanta, v.57: 145-155.

English Nature, 2002. Peat bog conservation the importance of lowland raised bogs.

Evans, D., Norwegian Petroleum Society and Geological Survey of Denmark and Greenland. 2003. The millennium atlas: petroleum geology of the central and northern North Sea. The Geological Society.

Falkowski, P.G., Barber, R.T., Smetacek., V., 1998. Biogeochemical Controls and Feedbacks on Ocean Primary Production. Science v.281: 200-206

Fengxiang, H.X., Banin, A., Su, Y., Monts, D.L., Plodinec, J., Kingery, W.L., Triplett, G.E., 2002. Industrial age anthropogenic input of heavy metals into the pedosphere. Naturwissenschaften v.89: 497-504.

Fones, G.R., Davision, W., Grime, G.W., 1998. Development of constrained DET for measurements of dissolved iron in surface sediments at sub-mm resolution. Sci. Total Environment, v.221: 127-137.

Fones. G.R., Davison, W., Holby, O., Jorgensen, B.B., Thamdrup, B., 2001. High-resolution metal gradients measured by an in situ DGT/DET deployment in Black Sea sediments using an autonomous benthic lander. Limnol. Oceanogr. v. 46: 982-988.

Fourqurean, J.W., Zieman, J.C., Powell, G.V.N., 1992. Relationships between porewater nutrients and seagrasses in a subtropical carbonate environment. Marine Biology, v.114(1): 57-65.

Francois, F., 1987. A study of sulphur enrichment in the humic fraction of marine sediments during early diagenesis. Geochim. Cosmochim. Acta v.51:17-27.

Friedl, A., Wüest, G. 2002 Disrupting biogeochemical cycles - Consequences of damming. Aquatic Sciences, v.64(1):55-65.

Froelich P.N. Klinkhammer, G.P., Bender, M.L., Luedtke, N.A., Heath, G.R., Cullen, D., Daupin, P., Hammond, B., Maynard, V., 1979. Early oxidation of organic matter in pelagic sediments of the eastern equatorial Atlantic: sub-oxic diagenesis. Geochim. Cosmochim. Acta. v.43: 1075-1090.

Funnell, B.M., Pearson, J., 1984. A guide to the Holocene geology of North Norfolk. Bull. Geol. Soc. Norfolk v.34:123-148.

Fuseler, K., Krekeler, D., Sydow, U., Cypionka, H., 1996. A common pathway of sulfide oxidation by sulfate-reducing bacteria. FEMS Microbiology Letters, v.144:129-134

Gallois, R.W., 2008. The lithostratigraphy of the Shales-with-Beef member of the Charmouth Mudstone Formation, Lower Jurassic. Geoscience in South-West England, v.12: 32-40.

Galloway, J.N., Thornton, J.D., Norton, S.A., Volchok, H.L., McLean R.A.N., 1982. Trace Metals in atmospheric deposition: a review and assessment. Atmospheric Environment v.16(1): 1677-1700.

Gao, S., Tanji, K.K., Scardaci, S.C., Chow, A.T., 2002. Comparison of redox indicators in a paddy soil during rice-growing season. Soil Sci. Am. J. v.66: 805-817.

Gautier, D.L.,1986. Interpretation of early diagenesis in ancient marine sediments. Soc. Econ. Paleont. Miner, Short Course Notes, v.17:6-78.

Gaynard, T. J., Armstrong, W., 1987. Some aspects of internal aeration in amphibious habitats. In: Plant Life in Aquatic and Amphibious Habitats, British Ecological Society Special Symposium, 5 (Ed. by R. M. M. Crawford), pp. 303-320. Blackwells, Oxford.

Gebauer, R.L.E., Reynolds, J.F., Tenhunen, J.D., 1995. Growth and allocation of the arctic sedges *Eriophorum angustifolium* and *E. vaginatum*: effects of variable soil oxygen and nutrient availability. Oecologia v.104: 330-339.

Getech Group Plc, 2013. *Globe*: Atlases of Global Palaeogeographies: volume 3 Jurassic.

Geotechdata, 2010 url: http://www.geotechdata.info/geotest/vane-shear-test.html

Giblin, A.E., Likens, G.E., White, D., Howarth, R.W., 1990. Sulfur storage and alkalinity generation in New England lake sediments. Limnol. Oceanogr. v.35: 852-869.

Goldhaber, M.B., Kaplan, I.R., 1980. Mechanisms of sulfur incorporation and isotope fractionation during early diagenesis in sediments of the Gulf of California. Mar. Chem. v9: 95-143

Gorham, E., 1991. Northern Peatlands: role in the carbon cycle and probable responses to climatic warming. Ecological Applications, v.1: 182-195.

Gransch, J. A., & Posthuma, J., 1973. On the origin of sulphur in crudes. In Advances in Organic Geochemistry 1973 (pp. 727-739). Editions Technip Paris.

Grover, S.P.P., Baldock, J.A., 2013. The link between hydrology and decomposition: Beyond von Post. Journal of Hydrology, v.479: 130-138.

Gündoğan, R., Acemioğlu, B., & Alma, M. H., 2004. Copper (II) adsorption from aqueous solution by herbaceous peat. Journal of Colloid and Interface Science, 269(2):303-309.

Halas, S., Shakur, A., Krouse, H.R., 1982. A modified method of SO2 extraction from sulphates for isotopic anaylsis using NaPO3. Isotopenpraxis, v. 18:11-13.

Hallam, A., 2001. A review of the broad pattern of Jurassic sea-level changes and their possible causes in the light of current knowledge. Palaeogeography, Palaeoclimatology Palaeoecology v.167: 23-37.

Harris, S.J., Mortimer, R.J.G., 2002. Determination of nitrate in small water samples (100mL) by the cadmium-copper reduction method: A manual technique with application to the interstitial waters of marine sediments. Inter. J., Environ. Anal. Chem. v. 82(6): 369-376.

Harper, M.P., Davison, W., Tych, W., 1997. Temporal, spatial, and resolution constraints for in situ sampling devices using diffusional equilibration: dialysis and DET. Environ. Sci. Technol. v. 31: 3110-3119.

Harrison, A.G., Thode, H.G., 1958. Mechanism of the bacterial reduction of sulphate from isotope fractionation studies. Trans. Faraday Soc., London 54: 84–92.

Hatcher, P.G., Spiker, E.C. 1988. Selective degradation of plant biomolecules. In: Humic substances and their role in the environment (Eds F.H. Frimmel and R.F. Christman) John Wiley and Sons, Chichester pp. 59-74.

Hatcher, P.G., Spiker, E.C., Orem, W.E. 1986. Organic geochemical studies of the humification process in low-moor peat. In: Peat and water: aspects of water retention and dewatering in peat (Ed. C.H. Fuchsman), Elsevier Applied Science, New York pp. 195-242.

Hedges, J.I., 1992. Global biogeochemical cycles: progress and problems. Mar. Chem., v.39: 67-93.

Hesslein, R.H., 1976. An in situ sampler for close interval pore water studies. Limnol. Oceanogr. v.21(6): 912-914.

Hendry, M.J., Wassenaar, L.I., 2000. Controls on the distribution of major ions in pore waters of a thick surficial aquitard. Water Resources Research, v. 36(2): 503-513.

Holden, J, 2005. Peatland Hydrology and carbon release: why small-scale process matters. Philiosophical transactions of the Royal Society A, 363: 2891-2913

Holden, J., Burt, T. P., 2003. Hydrological studies on blanket peat: the significance of the acrotelm-catotelm model. J. Ecol. v.91: 86-102.

Holland, H.D., 1984. The Chemical Evolution of the Atmosphere and Oceans. Princeton Univ. Press, Princeton, N.J.

Hopkins., F.M., Filley, T.R., Gleixner, G., Lange, M., Top, S.M., Trumbore, S.E., 2014. Increased belowground carbon inputs and warming promote loss of soil organic carbon through complementary microbial responses. Soil Biology & Biochemistry v.76:57-69.

Howarth, R.W., Hobbie, J.E., 1982. The regulation of decomposition and heterotrophic microbial activity in salt marsh soils: a review. In: Kennedy V.S. (ed.), Estuarine Comparisons. Academic Press, NY.

Howarth, R.W., 1993. Microbial processes in salt-marsh sediments. In: Ford T.E. (ed.), Aquatic Microbiology: An Ecological Approach. Blackwell Scientific Publications, Cambridge, MA.

Howes, B.L., Howarth, R.W., Teal, J.M., Valiela, I., 1981. Oxidation-reduction potentials in a salt marsh: Spatial patterns and interactions with primary production. Limnol. Oceanogr. v.26(2):350-360.

Hungar, S., Benning, L.G., 2007. Greigite: a true intermediate on the polysulfide pathway to pyrite. Geochemical Transactions, v. 8(1):1-20

Hutton, M., Symon, C., 1986.The quantities of cadmium, lead, mercury and arsenic entering the U.K. environment from human activities. Sci. Total. Environ v.57: 129-150.

Ingram H.A.P., 1978. Soil layers in mires: function and terminology. Journal of Soil Science v.29: 224–227.

Jacobs, P.H., 2002. A new rechargeable dialysis water sampler for monitoring sub-aqueous in-situ sediment caps. Water Research, v.36: 3121-3129.

Jezequel, D., Brayner, R., Metzger, E., Viollier E., Prevot, F., Fievet, F., 2007. Two-dimensional determination of dissolved iron and sulfur species in marine sediment pore-waters by thin-film based imaging. Thau Lagoon (France). Estuarine, Coastal and Shelf Science, v.72: 420-431.

Jickells, T.D., An, Z.S., Anderson, K.K., Baker, A.R., Bergametti, G., Brooks, N., Cao, J.J., Boyd, P.W., Duce, R.A., Hunter, K.A., Kawahate, H., Kubilay, N., LaRoche, J., Liss, P.S., Mahowald, N., Prospero, J.M., Ridgwell, A.J., Tegen, I., Torres, R., 2005. Global Iron Connections between Desert Dust, Ocean Biogeochemistry, and Climate. Science v.308(5718):67-71.

Jones, J.M. and Hao, J., 1993. Ombrotrophic peat as a medium for historical monitoring of heavy metal pollution. Environmental Geochemistry and Health v.15(2/3) 67-74.

Jones, R.D., Hood, M.A., 1980. Effects of temperature, pH, salinity, and inorganic nitrogen on the rate of ammonium oxidation by nitrifiers isolated from wetland environments. Microb. Ecol. v.6: 339-347.

Jones, G. E., Starkey, R. L., 1957. Fractionation of stable isotopes of sulfur by microorganisms and their role in deposition of native sulfur. Appl. Microbiol. v.5:111-118.

Jorgensen, B. B., Fenchel, T., 1974. The sulfur cycle of a marine sediment model system. Marine Biology v.24: 189-201.

Kampschulte, A., Strauss, H., 2004.The sulfur isotopic evolution of Phanerozoic seawater based on the analysis of structurally substituted sulfate in carbonates. Chemical Geology, v.204:255-286.

Kaplan, I.R., Emery, K.O., Rittenbebg., S.C., 1963. The distribution and isotopic abundance of sulfur in recent marine sediments off southern California. Geochimica et Cosmochimic Acta, v27(4): 297-312.

Kaplan, I.R., Rittenberg, S.C., 1964. Microbiological fractionation of sulphur isotopes. Journal of General Microbiology v.34: 195–212.

Keller, C. K., van der Kamp G., Cherry, J. A., 1991. Hydrogeo-chemistry of a clayey till, 1. *Spatial variability. Water Resources Research, v. 27(*10*):* 2543–2554.

King, G.M., 1988. Patterns of sulfate reduction and the sulfur cycle in a South Carolina salt marsh. Limnol.Oceanogr. v.33: 376–390.

Knorr, K.-H., Blodau, C., 2009. Impact of experimental drought and rewetting on redox transformations and methanogenesis in mesocosms of a northern fen soil. Soil Biol. Biochem. v.41: 1187-1198.

Kohnen M. E. L., Sinninghe Damste J.S.S., ten Haven H. L., de Leeuw, J. W., 1989. Early incorporation of polysulphides in sediment organic matter. Nature v.341: 640-641.

Koretsky C.M., Haas, J.R., Ndenga, N.T., Miller, D., 2006. Seasonal variations in vertical redox stratification and potential influence on trace metal speciation in minerotrophic peat sediments. Water, Air and Soil Pollution, v.173: 373-403.

Kostka, J.E., Luther, G.W., 1994. Partitioning and speciation of solid-phase iron in salt-marsh sediments. Geochim. Cosmochim. Acta, v.58: 1701-1710.

Kostka, J.E., Roychoudhury, A., Van Cappellen, P., 2002. Rates and controls of anaerobic microbial respiration across spatial and temporal gradients in saltmarsh sediments. Biogeochemistry v.60: 49–76.

Krom, M.D., Davison, P., Zhang, H., Davison, W., 1994. High resolution pore-water sampling with a gel sampler. Limnol. Oceanogr. v.39: 1967-1973.

Ku., T.C.W., Walter, L.M., Coleman, M.L., Blake, R.E., Martini, A.M., 1999. Coupling between sulfur recycling and syndepositional carbonate dissolution: Evidence from oxygen and sulfur isotope composition of pore water sulfate, South Florida, Platform, U.S.A. Geochim. Comochim. Acta v.63(17):2529-2546.

Kumpiene, J., Ore. S., Lagerkvist, A., Maurice, C., 2007. Stabilization of Pb- and Cu-contaminated soil using coal fly ash and peat. Environmental Pollution, v145 (1): 365–373.

Kurtz A.C., Kump L.R., Arthur M.A., Zachos J.C., Paytan A., 2003. Early Cenozoic decoupling of the global carbon and sulfur cycles. Paleoceanography v.18(4), :(14-1)-(14-14)

Kylander, M.E., Weiss, D.J., Martinez Cortizas, A., Spiro, B., Garcia-Sanchez, R., Coles, B.J., 2005. Refining the pre-Industrial atmospheric Pb isotope evolution curve in Europe using an 8000 year old peat core from NW Spain. Earth and Planetary Science Letters, v.240(2): 467-485.

LaForce, M.J. Hansek, C., Fendorf, S., 1998. Constructing simple wetland sampling devices. Soil Sci. Soc. Am. J. v.64: 809-811

Lamers, L.P.M., Dolle, G.E.T., Van Den Berg, S.T.G., Van Delft, S.P.J., Roelofs, J.G.M., 2001. Differential responses of freshwater wetland soils to sulphate pollution. Biogeochemistry v.55: 87-102.

Lamers, L.P.M., Falla, S.J., Samborska, E.M., van Dulken, I.A.R., van Hengstum, G., Roelofs, J.G.M., 2002. Factors controlling the extent of eutrophication and toxicity in sulfate-polluted freshwater wetlands. Limnol. Oceanogr. v.47(2): 585-593.

Lang, W.D., Spath, L.F., Richardson, W.A., 1923. Shales-with-'beef,' a sequence in the Lower Lias of the Dorset Coast. Quarterly journal of the Geological Society, v.79: 47-66.

Lee, D.S., Garland, J.A., Fox, A.A., 1994. Atmospheric concentrations of trace elements in urban areas of the United Kingdom. Atmospheric Environment v.28(16):2691-2713.

Lee, J.A., Tallis, J.H., 1973. Regional and historical aspects of lead pollution in Britain. Nature v.245: 216-218.

Leermakers, M., Gao, Y., Gabelle, C., Lojen, S., Ouddane, B., Wartel, M., Baeyens, W., 2005. Determination of high resolution pore water profiles of trace metals in sediments of the Rupel River (Belgium) using DET (diffusive equilibrium in thin films) and DGT (diffusive gradients in thin films) techniques. Water, Air, and Soil Pollution, v.166 (1-4): 265-286.

Lefevre, N., Watson, A.J., 1999. Modelling the geochemical cycle of iron in the oceans and its impact on atmospheric CO_2 concentrations. Global Biogeochemical cycles, v.13(3):727-736.

Livens, F.R., Jones, M.J., Hynes, A.J., Charnock, J.M., Mosselmans, J.F.W., Hennig, C., Steele, H., Collison, D., Vaughan, D.J., Pattrick, R.A.D., Reed, W.A., Moyes, L.N., 2004. X-ray absorption spectroscopy studies of reactions of technetium, uranium and neptunium with mackinawite. J. Environ. Radioact. V. 74(1-3):211-219.

Lord, C.J., Church, T.M., 1983. The geochemistry of salt marshes: Sedimentary ion diffusion, sulfate reduction, and pyritization. Geochim. Cosmochim. Acta v.47:1381-1391.

Luther III, G.W., Brendel, P.J., Lewis, B.L., 1998. Simultaneous measurement of O_2, Mn, Fe, I^- and S(-II) in marine pore waters with a solid-state voltammetric microelectrode. Limnol. Oceanogr, v.43(2): 325-333.

Luther III, G.W., Glazer, B.T., Ma, S., Trouwborst, R.E., Moore, T.S., Metzger, E., Kraiya, C., Waite, T.J., Druschel, G., Sundby, B., Taillefert, M.m Nuzzio, D.B., Shank, T.M., Lewis, B.L., Brendel, P.J, 2008. Use of voltammetric solid-state (micro)electrodes for studying biogeochemical processes: Laboratory measurements to real time measurements with an in situ electrochemical analyser. Marine Chemistry, v.108(3-4): 221-235.

Lyons, T. W., & Berner, R. A., 1992. Carbon-sulfur-iron systematics of the uppermost deep-water sediments of the Black Sea. Chemical Geology, 99(1):1-27.

Lyons, T.W., Severmann, S., 2006. A critical look at iron paleoredox proxies: New insights from modern euxinic marine basins. Geochim. Cosmochim. Acta. v.70: 5698-5722.

Ma, W., Tobin, J.M., 2004. Determination and modelling of effects of Ph on peat biosorption of chromium, copper and cadmium. Biochemical Engineering Journal v.18: 33-40.

MacKenzie A.B., Farmer J.G., Sugden, CL., 1997. Isotopic evidence of the relative retention and mobility of lead and radiocaesium in Scottish ombrotrophic peats.Scie.Tot.Env, v.203: 115-127.

MacKenzie, A.,B., Logan, E.M., Cook, G.T., Pulford, I.D., 1998 a. Distributions, inventories and isotopic composition of lead in ^{210}Pb-dated peat cores from contrasting biogeochemical environments: Implications for lead mobility. Sci Total Environ. v.223: 25-35.

MacKenzie, A.,B., Logan, E.M., Cook, G.T., Pulford, I.D., 1998 b. A historical record of atmospheric depositional fluxes of containments in west central-Scotland derived from an ombrotrophic peat core. Sci. Total Environ, v.222: 157-166.

Majewski, W., 2000. Middle Jurassic concretions from Czestochowa (Poland) as indicators of sedimentation rates. Acta Geologica Polonica v.50: 431‑439.

Mankovska, B., 1977. The content of Pb, Cd and C1 in forest trees caused by the traffic of motor vehicles. Biologia, Bratisl. v. 32: 477-489.

Marshall, J.D., 1982. Isotopic composition of displasive fibrous calcite veins: reversals in pore water compositional trends during burial diagenesis. Jour. Sed. Pet., v.52: 615-630.

Martinez Cortizas, A., Pontevedra-Pombal, X., Nóvoa Muñoz, J.C., García-Rodeja, E., 1997. Four Thousand Years of Atmospheric Pb, Cd and Zn Deposition Recorded by the Ombrotrophic Peat Bog of Penido Vello (Northwestern Spain). Water, Air, and Soil Pollution, v.100(3-4): 387-403.

Martinez Cortizas, A., García-Rodeja, E., Pontevedra-Pombal, X., Novak, M., Munoz, J.C., Weiss, D., Cheburkin, A., 2002. Atmospheric Pb deposition in Spain during the last 4600 years recorded by two ombrotrophic peat bogs and implications for the use of peat as archive. Sci Total Environ v.292: 33-44.

Mighall, T.M., Timberlake, S., Foster, I.D.L., Krupp, E., Singh, S., 2009. Ancient copper and lead pollution records from a raised bog complex in central Wales, UK. Journal of Archaeological Science, v.36: 1504-1515.

Miller, J.C., Miller, J.N., 1993. Statistics for analytical chemistry (3rd edition). Ellis Horwood, Chichester, p. 115-117.

Montgomery, R.J.G., Zimmermann, C.F., Price, M.T., (1979). The collection, analysis and variation of nutrients in estuarine pore water. Estuarine and Coastal Marine Science, v.9: 203-214.

Morford, J., Kalnejais, L., Martin, W., Francois, R., Karle, I., 2003. Sampling marine pore waters for Mn, Fe, U, Re and Mo: modifications on diffusional equilibration thin film gel probes. Journal of experimental Marine Biology and Ecology, v.285-286: 85-103.

Morford, J.L., Emerson, S., 1999. The geochemistry of redox sensitive trace metals in sediments. Geochemica et Cosmochimica Acta v.63 (11-12): 1735-1750.

Morgan M.D., 1995. Modeling excess sulfur deposition on wetland soils using stable sulfur isotopes. Water Air Soil Pollut. v.79: 299-308.

Moore E.A., Kurtz A.C., 2008. Black carbon in Paleocene-Eocene boundary sediments: a test of biomass combustion as the PETM trigger. Palaeogeography. Palaeoclimatology. Palaeoecology, v. 267: 147–52.

Moore, S., Evans, C.D., Page, S.E., Garnett, M.H., Jones, T.G., Freeman, C., Hooijer, A., Wiltshire, A.J., Limin, W.H., Gauci, V., 2013. Deep instability of deforested tropical peatlands revealed by fluvial organic carbon fluxes. Nature, v.493:660-663.

Moore, T., Blodau, C., Turunen, J., Roulet, N., & Richard, P. J., 2005. Patterns of nitrogen and sulfur accumulation and retention in ombrotrophic bogs, eastern Canada. Global Change Biology, 11(2):356-367.

Morgan M.D., 1995. Modeling excess sulfur deposition on wetland soils using stable sulfur isotopes. Water Air Soil Pollut. v.79: 299-308.

Morris, P.J., Waddington, J.M., 2011. Groundwater residence time distributions in peatlands: Implications for peat decomposition and accumulation. Water Resources Research, v.47(2):1-12.

Morris, P.J., Waddington, J.M., Benscoter, B.W., Turetsky, M.R., 2011. Conceptual frameworks in peatland ecohydrology: looking beyond the two-layered (acrotelm –catotelm) model. Ecohydrology v.4: 1-11.

Morse, J.W., Zulig, J.J., Bernstein, L.D., Millero, F.J., Milne, P., Mucci, A., Choppin, G.R., 1985. Chemistry of calcium carbonate-rich shallow water sediments in the Bahamas. Am. J. Sci. v.285: 147–185

Mort, H.P., Slomp, C.P., Gustafsson, B.G., Anderson, T.J., 2010. Phosphorous recycling and burial in Baltic Sea sediments with contrasting redox conditions. Geochimica et Cosmochimica Acta, v.74(4): 1350-1362.

Mortimer, R.J.G., Galsworthy, A.M.J., Bottrell, S.H., Wilmot, L.E., Newton, R.J., 2011. Experimental evidence for rapid biotic and abiotic reduction of Fe(III) at low temperatures in salt marsh sediments: a possible mechanism for formation of modern sedimentary siderite concretions. Sedimentology v.58: 1514-1529.

Mortimer, R.J.G., Harris, S., Krom, M.D., Freitag, T.E., Proseer, J.I., Barnes, J., Anschutz, P., Haynes, P.J., Davies, I.M., 2004. Anoxic nitrification in marine sediments. Mar. Ecol. Prog. Ser. v. 276;37-51.

Mortimer, R.J.G., Krom, M.D., Hall, P.O.J., Hulth, S., Ståhl, H., 1998. Use of gel probes for the determination of high resolution solute distributions in marine and estuarine pore waters. Marine Chemistry v. 63: 119-129.

Mortimer, R.J.G. and Rae, J.E. (2000) Metal speciation (Cu,Zn, Pb, Cd) and organic matter in oxic to suboxic salt marsh sediments, Severn Estuary, Southwest Britain. Mar. Poll.Bull. v.40: 377–386.

Mullet, M., Boursiquot, S., Ehrhardt, J.J., 2004. Removal of hexavalent chromium from solutions by mackinawite, tetragonal FeS. Colloid Surf A-Physicochem Eng Asp v. 244(1-3):77-85.

Muraoka, H., Son, Y., Fang, J., 2010. The ecological process of carbon cycling in terrestrial ecosystems in East Asia. J. Plant Res. v.123: 391-392.

Nakai, N., Jensen, M.L., 1964. The kinetic isotope effect in the bacterial reduction and oxidation of sulphur. Geochim. Cosmochim. Acta, v.28:1893-912.

Natural England, 2014. Climate change adaption manual – evidence to support nature conversation in a changing climate (NE546), 129-134; 199- 204.

Ndiokwere, C.l., 1984. A study of heavy metal pollution from motor vehicle emissions and its effect on roadside soil, vegetation and crops in Nigeria. Environmental Pollution (Series B) 7: 35-42.

Neuzil, S.G., 1997. Onset and rate of peat and carbon accumulation in four domed ombrogenouspeat deposits, Indonesia. In Rieley, J.O., Page, S.E. (Eds), Biodiversity and Sustainable Management of Tropical Peatlands, Samara, Cardigan, U.K., 55-72.

Nicholson, K.W., Branson, J.R., 1990. Factors affecting resuspension by road traffic. Sci. Total. Env. v.93: 349-358.

Nieminen T.M., Ukonmaanaho L., Rausch N., Shotyk W., 2007. Biogeochemistry of nickel and its release into the environment. Met. Ion Life Sci. v.2: 1-30.

Nordstrom, D,K., Ball, J.W., 1986. The geochemical behaviour of Aluminium in acified surface waters. Science, v.232:54 -56.

Norton S.A. and Kahl J.S, 1987.A comparison of lake sediments and ombrotrophic peat deposits as long-term monitors of atmospheric pollution. New approaches to monitoring Aquatic Ecosystems, ASTM STP 940, T.P. Boyle, Ed., American Society for Testing and Materials, Philadelphia, 1987, 40-57.

Novak, M., Adamova, M., Wieder, R.K., Bottrell, S.H., 2005. Sulfur mobility in peat. Appl. Geochem. v.20: 673-681.

Novak, M., Brizova, E., Adamova, M., Erbanova, L., Bottrell, S.H., 2008. Accumulation of organic carbon over the past 150 years in five freshwater peatlands in western and central Europe. Sci. Total Env. v.390: 425-436.

Novak, M., Erel, Y., Zemanova, L., Bottrell, S.H., Adamova, M.,2008a. A comparison of lead pollution record in *Sphagnum* peat with known historical Pb emission rates in the British Isles and the Czech Republic. Atmospheric Environment v.42: 8997-9006.

Novak, M., Zemanova, L., Jackova, I., Buzek, F., Adamova, M., 2009. Isotope composition of bulk carbon in replicated Sphagnum peat cores from three Central European high-elevation wetlands. Geochemical Journal , 43(6): 5-9 e5-e9.

Novak, M., Zemanova , L., Voldrichova, P., Stepanova, M., Adamova, M., Pacherova, P., Komarek, A., Krachler, M., Prechova, E., 2011. Experimental Evidence for Mobility/Immobility of Metals in Peat. Environ. Sci. & Technol., v.45(17): 7180-7187.

Odzak, N., Kistler, D., Xue, H., Sigg, L., 2002. In situ metal speciation in a eutrophic lakes using the technique of diffusion gradients in thin films (DGT). Aquat. Sci. v.64: 292-299.

Olid, C., Garcia-Orellana, J., Martinez-Cortizas, A., Masque, P., Peiteado-Varela, E., Sanchez-Cabeza, J., 2010.Multiple site study of recent atmospheric metal (Pb, Zn and Cu) deposition in the NW Iberian Peninsula using peat core. Sci Total Environ. v.408: 5540-5549.

Olk, D.C., Brunetti, G., Senesi, N. 2000. Decrease in humification of organic matter with intensified lowland rice cropping. Soil Soc. Am. J. v.64: 1337-1347.

Pacyna, J.M., 1986. In: Nriagu, J.O., Davidson, C.I. (Eds.), Toxic Metals in the Atmosphere. Wiley, New York.

Page, K.N., 2009. High Resolution ammonite stratigraphy of the Charmouth Mudstone Formation (Lower Jurassic: Sinemurian-Lower Pliensbachian) in south-west England, UK. Volumina Jurassica v7(7):19-29.

Parkinson, D.N., 1996. Gamma-ray spectrometry as a tool for stratigraphical interpretation: examples from the western European Lower Jurassic. Geol. Soc. Special Publications v.103, 231-255.

Paul, C.R.C., Allison, P.A., Brett, C.E., 2008. The occurrence and preservation of ammonites in the Blue Lias Formation (lower Jurassic) of Devon and Dorset, England, and their palaeoecological, sedimentological and diagenetic significance. Palaeogeography, Palaeoclimatology, Palaeoecology, v.270: 258-272.

Pearson, M. J., Hill, A. F., Fallick, A. E., & Ecuvillon, S., 1996. Sulphur incorporation in Jurassic marine mudrocks and their bitumens at low thermal maturity, Cleveland Basin, England. Geochimica et cosmochimica acta, 60(21):4181-4192.

Penthick, J.S., 1980. Salt-marsh initiation during the Holocene transgression: the example of the North Norfolk marshes, England. Journal of Biogeography, v. 7: 1-9

Peters, K., Walters, C.C., Moldowan, J.M., 2005. The Biomarker Guide (vol 1). Biomarkers and Iosotopes in the Environment and Human History. Cambridge University Press: 72- 117.

Posch, M., Forsius, M., Johansson, M., Vuorenmaa, J., Kamari, J., 2003. Modelling the recovery of acid-sensitive Finnish headwater lakes under present emission reduction agreements. Hydrology and Earth System Sciences, v.7(4): 484 - 493.

Postma, 1981. Formation of siderite and vivianite and the pore-water composition of a Recent bog sediment in Denmark. Chem. Geol. v.31: 225-244.

Poulton, S., 2003. Sulphide oxidation and iron dissolution kinetics during the reaction of dissolved sulphide with ferrihydrite. Chem. Geol. v.202: 79–94.

Poulton, S.W., Canfield, D.E., 2005. Development of a sequential extraction procedure for iron: implications for iron partitioning in continentally derived particulates. Chem. Geol. v. 214: 209–221.

Poulton, S.W., Fralick, P.W., Canfield, D.E., 2010. Spatial variability in oceanic redox structure 1.8 billion years ago. Nature Geoscience, v.3: 486 – 490.

Poulton, S.W., Krom, M.D., Raiswell, R., 2004. A revised scheme for the reactivity of iron (oxyhydr)oxide minerals towards dissolved sulfide. Geochim.Cosmochim. Acta v.68(18): 3703-3715.

Powell, B., Martens, M., 2005. A review of acid sulfate soil impacts, actions and policies that impact on water quality in Great Barrier Reef catchments, including a case study on remediation at East Trinity. Mar. Poll. Bull. v.51: 149-164.

Pye, K., 1981. Marshrock formed by iron sulphide and siderite cementation in saltmarsh sediments. Nature, v.294:650-652.

Pye, K., 1984. SEM analysis of siderite cements in intertidal marsh sediments, Norfolk, England. Mar. Geol. v.56: 1–12.

Pye, K., Dickson, J.A.D., Schiavon, N., Coleman, M.L., Cox, M., 1990. Formation of siderite-Mg-calcite-iron sulphide concretions in intertidal marsh and sandflat sediments, north Norfolk, England. Sedimentology v. 37: 325-343.

Raiswell, R., Buckley, F., Berner, R.A., Anderson, T.F., 1988. Degree of pyritization of iron as a paleoenvironmental indicator of bottom-water oxygenation. J. Sediment. Petrol. v.58:812-819.

Raiswell, R., Canfield, D.E., Berner, R.A., 1994. A comparison of iron extraction methods for the determination of degree of pyritization and the recognition of iron-limited pyrite formation. Chem. Geol. v.111:101-110.

Raiswell, R. 1987. Non-steady state microbiological diagenesis and the origin of concretions and nodular limestones, *IN*: Marshall, J.D., (ed.) *Diagenesis of sedimentary sequences*. Geological society, London, Special Publications, 36, 41-54.

Rausch, N., Ukonmaanaho, L., Nieminen, T.M., Krachler, M., Shotyk, W., 2005. Porewater evidence of metal (Cu, Ni, Co, Zn, Cd) mobilization in an acidic, ombrotrophic bog impacted by a smelter, Harjavalta, Finland and comparison with reference sites. Env Sci Technol. v.39: 8207-8213.

Rausch, N., 2005. Deposition and Fate of Trace Metals in Finnish Bogs and Implications for the Use of Bogs as Geological Archives, PhD Thesis, University of Heidelberg, Heidelberg, pp. 1–203.

Raven, M.R., Adkins, J.F., Werne, J.P., Lyons, T.W., Sessions, A.L., 2015. Sulfur isotopic composition of individual organic compounds from Cariaco Basin sediments, Organic Geochemistry (Accepted Manuscript).

Remenda, V.H., van der Kamp, G., 1997. Contamination from sand-bentonite seal in monitoring wells installed in aquitards. Ground Water, v.35(1): 39-46.

Revsbech, N.P., Jorgensen, B.B., 1986. Microelectrodes: their use in microbial ecology. In Advances in Microbial Ecology, Vol 9 (ed K.C. Marshall), p 293-352.

Robertson, D., Teasdale P.R., Welsh, D.T., 2008. A novel gel-based technique for the high resolution, two-dimensional determination of iron (II) and sulfide in sediment. Limnol. Oceanogr. Methods, v.6: 502-512.

Robinson, B.W., Kusakabe, M., 1975. Quantitative preparation of sulphur dioxide for $^{32}S/^{34}S$ analysis by combustion with cuprous oxide. Anal Chem. v.47:1179-1181.

Rothwell, J.J., Taylor, K.G., Chenery, S.R.N., Cundy, A.B., Evans, M.G., Allott, T.E.H., 2010. Storage and Behavior of As, Sb, Pb, and Cu in Ombrotrophic Peat Bogs under Contrasting Water Table Conditions. Environ. Sci. Technol. v, 44: 8497–8502.

Roulet, N.T., 2000. Peatlands, carbon storage, greenhouse gases and the Kyoto Protocol: Prospects, and significance for Canada, Wetlands, v.20: 605-615.

Rowe, P.J., Richards, D.A., Atkinson, T.C. , Bottrell, S.H. and Cliff, R.A. 1997. Geochemistry and radiometric dating of a mid-Pleistocene peat. Geochim. Cosmochim. Acta v.61: 4201-4211.

Roworth, P., 2000. Managing a complex cut-over peatland – the Humberhead Peatlands NNR. In: Tantram, D., Dargie, T., Dargie, M. (Eds), Nailing the paradox: Demonstrating favourable condition on damaged raised bogs. English Nature Research Reports, No. 365.

Sanger, F., Coulson, A.R., 1978. The use of thin acrylamide gels for dna sequencing, FEBS Letters, V. 87 (1): 467-492.

Scally, S., Zhang, H., Davison, W., 2004. Measurements of lead complexation with organic ligands using DGT. Aust. J. Chem., v.57: 925-930.

Scharlemann, J.P.W., Tanner, E.V.J., Hiederer, R., Kapos, V., 2014. Global soil carbon: understanding and managing the largest terrestrial carbon pool, Carbon Management, v.5(1):81-91

Schell, W.R., Tobin, M.J. Massey, C.D., 1989. Evaluation of trace metal deposition history and potential element mobility in selected cores from peat and wetland ecosystems. Sci Total Environ.v.87-88: 19-42.

Schimel, D.S., 1995. Terrestrial ecosystems and the carbon cycle. Global Change Biology v.1(1):77-91.

Schmidt, T.M., Schaechter, M., 2012. Topics in ecological and environmental microbiology. Academic Press.

Settle, D.M., Patterson, C.C., 1980. Lead in albacore: guide to lead pollution in Americans. Science v.207: 1167-1176

Sevenson, A., Viktor, T., Remberger, M., 1997. Toxicity of elemental sulfur in sediments. Environmental toxicology, v.13(3):217-224

Shotyk , W., 1988. Review of the inorganic geochemistry of peats and peatland waters. Earth Science Review, v.25: 95-176.

Shotyk, W., 1996. Peat bog archives of atmospheric metal deposition: geochemical evaluation of peat profiles, natural variations in metal concentrations, and metal enrichment factors. Environmental reviews v.4: 149-183.

Shotyk, W, 1996(a) Natural and anthropogenic enrichments of As, Cu, Pb, Sb, and Zn in ombrotrophic versus minerotrophic peat bog profiles, Jura Mountains, Switzerland. Water, Air, and Soil Pollution, v.90(3-4): 375-405.

Shotyk W., Nesbitt H.W., Fyfe, W.S, 1992. Natural and anthropogenic enrichments of trace metals in peat profiles. International Journal of Coal Geology v.20: 49-84

Shotyk, W., Blaser, P., Grunig, A., Cheburkin, A.K., 2000. A new approach for quantifiying cumulative, anthropogenic, atmospheris lead deposition using peat cores from bogs: Pb in eight Swiss peat bog profiles. Sci.Tot.Env v.249:281-294.

Shotyk, W., Weiss, D., Kramers, J.D., Frei, R., Cheburkin, A.K., Glorr, M., Reese, S., 2001. Geochemistry of the peat bog at Etang de la Gruere, Jura Mountains, Switzerland, and its record of atmospheric Pb and lithogenic trace metals (Sc, Ti, Y, Zr and REE) since 12,370 ^{14}C yr BP. Geochim. Cosmochim.Acta v.65: 2337-2360.

Shotyk, W., Weiss, D., Heisterkamp, M., Cheburkin, A. K., Appleby, P. G., & Adams, F. C., 2002. New peat bog record of atmospheric lead pollution in Switzerland: Pb concentrations, enrichment factors, isotopic composition, and organolead species. Environmental science & technology, 36(18):3893-3900.

Shuttleworth, S.M., Davison, W., Hamilton-Taylor, J., 1999. Two dimensional and fine structure in the concentrations of iron and manganese in sediment pore-waters. Environ. Sci. Technol. v.33: 4169-4175

Silvola, J., Alm, J., Ahlhold, U., Nykanen, H., Martikaninen, P.J., 1996. CO2 fluxes from peat boreal mires under varying temperature and moisteure conditions. J. Ecol. v.84:.219-228.

Sipos, P., Nemeth, T., Kovacs Kis, V., Mohai, I., 2008. Sorption of copper, zinc and lead on soil mineral phases. Chemosphere, v.73: 461-469.

Smieja-Król, B., Fiałkiewicz-Kozieł, B., Sikorski, J., & Palowski, B., 2010. Heavy metal behaviour in peat–A mineralogical perspective. Science of the total environment, 408(23):5924-5931.

Steinmann, P., Shotyk, W., 1997. Geochemistry, mineralogy, and geochemical mass balance on major elements in two peat bog profiles (Jura Mountains, Switzerland). Chemical Geology v.138: 25-53.

Steinmann, P., & Shotyk, W., 1997. Chemical composition, pH, and redox state of sulfur and iron in complete vertical porewater profiles from two< i> Sphagnum</i> peat bogs, Jura Mountains, Switzerland. Geochimica et Cosmochimica Acta, 61(6):1143-1163.

Stewart, C., & Fergusson, J. E., 1994. The use of peat in the historical monitoring of trace metals in the atmosphere. Environmental pollution, 86(3):243-249.

Stevenson, F.J., 1994. Humus chemistry: genesis, composition, reactions (2nd Edn) John Wiley and Sons, New York 497pp.

Stevenson, F.J., Goh, K.M., 1971. Infrared spectra of humic acids and related substances. Geochim. Cosmochim. Acta v.35: 471-483.

Stockdale, A., Davison, W., Zhang, H., 2009. Micro-scale biogeochemical heterogeneity in sediments: A review of available technology and observed evidence. Earth-Science Reviews v.92: 81-97.

Stockdale, A., Davison, W., Zhang, H., 2010. Formation of iron sulfide at faecal pellets and other microniches within sub-oxic surface sediment. Geochim. Cosmochim. Acta v.74: 2665-2676.

Sugden C.L., 1993. Isotopic studies of the environmental chemistry of lead. University of Edinburgh, PhD Thesis.

Tarre, S., Beliavski M., Denekamp, N., Gieseke A., de Beer, D., Green, M., 2007. High nitrification at low pH in a fluidized bed reactor with chalk as the biofilm carrier. Water Sci. Technol., v49(11-12): 99-105.

Taylor, K.G., Gawthorpe, R.L., Van Wagoner, J.C., 1995. Stratigraphic control on laterally persistent cementation, Book Cliffs, Utah. Journal of the geological Society, v.152: 225-228.

Teal, J.M., Kanwisher, J., 1966. Gas transport in the marsh grass, Spurtina alternijlora. J. Exp. Bot. v.17: 355-361.

Teasdale, P.R., Batley, G.E., Apte, S.C., Webster, I.T., 1995. Pore water sampling with sediment peepers. Trends in analytical chemistry, v.14(6): 250 -256.

Teasdale, P.R., Hayward, S., Davison, W., 1999. In situ, high-resolution of dissolved sulfide using diffusive gradients in thin films with computer-imaging densitometry. Analytical Chemistry, v. 71: 2186-2191

Thamdrup, B., Fossing, H., Jørgensen.,1994. Manganese, iron and sulfur cycling in a coastal marine sediment, Aarhus Bay, Denmark. Geochim. Cosmochim Acta, v.58(23): 5115-5129.

Thode, H.G., Harrison, A.G., and Monster, J. (1960). Sulphur isotope fractionation in early diagenesis of recent sediments of Northeast Venezuela. AAPG Bull., v.44: 1809-17.

Tolvanen, A., Alatalo, J.M, Henry, G.H.R., 2004. Resource allocation patterns in a forb and a sedge in two arctic environments – short-term response to herbivory. Nordic Journal of Botony, v.22: 741-747.

Turunen, J., Tomppo, E., Tolonen, K., Reinikainen, A., 2002. Estimating carbon accumulation rate of undrained mires in Finland – application to boreal and subartic regions. The Holocene, v.12: 69-80.

Twardowska, I., Kyziol, J., Goldrath, T., Avnimelech, Y., 1999. Adsorption of zinc onto peat from peatlands of Poland and Israel. Journal of Geochemical Exploration, v.66: 387-405.

Ukonmaanaho, L., Nieminen, T.M., Raush, N., Cheburkin, A., Le Roux, G., Shotyk, W., 2006. Recent organic matter accumulation in relation to some climatic factors in ombrotrophic peat bogs near heavy metal emission sources in Finland. Global and Planetary Change v.53: 259-268.

Ukonmaanaho, L., Nieminen, T.M., Raush, N., Shotyk, W., 2004. Heavy Metal and arsenic profiles in ombrogenous peat cores from four differently loaded areas in Finland. Water, Air and Soil Pollution, v.158: 277-294.

Urban, N. R., Eisenreich, S.J., Grigal D.F., Schurr, K.T., 1990. Mobility and diagenesis of Pb and ^{210}Pb in peat. Geochimica et Cosmochimica Acta, v.54 (12): 3329–3346.

USACE, 1987. Wetlands Research Programme Technical Report Y-87-1 (on-line edition). Corps of Engineers Wetlands Delineation Manual.

van Oploo, P., White, I., MacDonald, B.C.T., Ford, P., Melville, M.D., 2008. The use of peepers to sample pore water in acid sulphate soils. European Journal of Soil Science, v59: 762-770.

Verhoeven, 1986. Nutrient Dynamics in minerotrophic peat mires. Aquatic Botany, v.25:117-137.

Vile, M.A., Kelman Wieder, R., Novák, M., 1999. Mobility of Pb in Sphagnum-derived peat. Biogeochemistry v.45: 35–52.

Viollier, E., Inglett, P.W., Hunter, K., Roychoudhury, A.N., Van Cappellen, P., 2000. The ferrozine method revisited: Fe(II) / Fe(III) determination in natural waters. Applied Geochemistry v.15: 785-790.

Voldrichova, P., Chrastny, V., Sipkova, A., Farkas, J., Novak, M., Stepanova, M., Krachler, M., Veselovsky, F., Blaha, V., Prechova., E., Komarek, A., Bohdalkova, L., Curik, J., Mikova., J., Erbanova., L., Pacherova, P., 2014. Zinc isotope systematics in snow and ice accretions in Central European mountains. Chemical Geology v.388:130-141.

Waldron, L.J., Dakessian, Suren, 1981. Soil Reinforcement By Roots: Calculation of Increased Soil Shear Resistance From Root Properties. Soil Science. v.132(6): 427-435.

Walter L.M., Bishoff, S.A., Patterson, W.P., Lyons, T.W., 1993. Dissolution and recrystallisation in modern shelf carbonates: evidence from pore-water and solid phase chemistry. Phil. Trans. Royal. Soc. London v.344: 7-36.

Ward, N.I., Brooks, R.R., Roberts, E., and Boswell, E., 1977. Heavy-metal pollution from automotive emissions and its effect on roadside soils and pasture species in New Zealand. Envir. Sci,. Technol. v.11: 917-920

Wassenaar L.I., Hendry M.J., 1999. Improved piezometer construction and sampling techniques to determine pore water chemistry in aquitards. Ground Water, v,37(4): 564-571.

Watts, A., 2006. The search for iron sulphides; a biological whodunit: Elucidating the cause of missing iron sulphides at depth: Combined pore-water and stable isotope analysis of salt marsh pan sediments. MSc Thesis University of Leeds.

Weiss D.J., Rausch, N., Mason, T.F.D., Coles, B.J., Wilkinson, J.J., Ukonmaanaho, L., Arnold, T., Nieminen., T.M., 2007. Atmospheric deposition and isotope biogeochemistry of zinc in ombrotrophic peat. Geochimica et Cosmochimica Acta, v.71:3498‑3517.

Werne, J., Lyons, T., Hollander, D., Formolo, M., Damsté, J., 2003. Reduced sulfur in euxinic sediments of the Cariaco Basin: sulfur isotope constrains on organic sulfur formation. Chemical Geology v.195: 159–179.

West, S., Charman, D. J., Grattan, J. P., & Cherburkin, A. K., 1997. Heavy metals in Holocene peats from south west England: detecting mining impacts and atmospheric pollution. Water, Air, and Soil Pollution, 100(3-4):343-353.

Widerlund, A., Davison, W., 2007. Size and density distribution of sulfide-producing microniches in lake sediments. Environ. Sci. Technol. v.41: 8044-8049.

Wilmot, L.E., 2007. An investigation of saltmarsh sediments - via field survey, chemical analysis and incubation experiments – to examine the cause of an oxidised zone at depth beneath water pans. MSc Thesis University of Leeds.

Williams, C.R., Harrison, R.M., 1984. Cadmium in the atmosphere. Experientia, v.40; 29 – 36**.**

Witkowska, M., 2012. Palaeoenvironmental significance of iron carbonate concretions from the Bathonian (Middle Jurassic) ore-bearing clays at Gnaszyn, Krakow-Silesia Homocline, Poland. Acta Geologica Polonica, v.62(3): 307‑324.

Wolff, G.A., Rukin, N., Marshall, J.D., 1991. Geochemistry of an early diagenetic from the Birchi Bed (L. Lias, W. Dorest, U.K.). Advances in Organic Geochemistry, v.19(4-6): 431-444.

Xia, K., Bleam, W., Helmke, P.A., 1997. Studies of the nature of Cu^{2+} and Pb^{2+} biding sites in soil humic substances using X-ray absorption spectroscopy .Geochim. Cosmochim. Acta v.61: 2211-2221.

Xu, D., Wu, W., Shiming, D., Sun, Q., Zhangm C., 2012. A high resolution dialysis technique for rapid determination of dissolved reactive phosphate and ferrous iron in pore water sediments. Sci. Total Environment, v.421-422: 245-252.

Xu, Y., Schoonen M.A.A., 1995. The stability of thiosulfate in the presence of pyrite in low-temperature aqueous solutions. Geochemica et Cosmochimica, v.59 (22): 4605-4622.

Zabac, D.A., Pratt, L.M., 1992. Isotopic composition and speciation of sulfur in the Miocene Montery Formation: Re-evalutaion of sulfur reactions during diagenesis in marine environments. Geochim. Cosmochim. Acta. v.56: 763-774.

Zaccone, C., Miano, T.M. and Shotyk, W. 2007. Qualitative comparison between raw peat and related humic acids in an ombrotrophic bog profile. Org. Geochem. v.38: 151-160.

Zaccone, C.,Sanei, H., Outridge, P.M., Miano, T.M. 2011. Studying the humification degree and evolution of peat down a Holocene bog profile (Inuvik, NW Canada): a petrological and chemical perspective. Organic Geochemistry v.42: 399-408.

Zachos, J.C., Dickens, G.R., Zeebe, R.E., 2008. An early Cenozoic perspective on greenhouse warming and carbon-cycle dynamics. Nature v.451(17):279-283.

Zhang, H., Davison W., Miller, S., Tych, W., 1995. In situ high resolution measurements of fluxes of Ni, Cu, Fe and Mn and concentrations of Zn and Cd in porewaters by DGT. Geochimica et Cosmochimica Acta, v.59 (20): 4181-4192.

Zhang, H., Davison W., Mortimer, R.J.G., Krom, M.D., Haynes, P.J., Davies, I.M., 2002. Localised remobilization of metals in a marine sediment. Sci. Tot. Env. v.296: 175- 187.

Zhang, H., Davison W., 1995. Performance characteristics od diffusion gradients in thin film for the in situ measurements of trace metals in aqueous solution. Anal. Chem. v.67: 3391-3400.

Zhang, H., Davison W., 1999. Diffusional characteristics of hydrogels used in the DGT and DET techniques. Analytica Chimica Acta v.398: 329-340.

Zhu, M.X., Shi, X.N, Yang, G.P., Hao, X.C., 2013. Formation and burial of pyrite and organic sulfur in mud sediments of the East China Sea inner shelf: Constraints from solid-phase sulfur speciation and stable sulfur isotope. Continental Shelf Research v.54:24–36.

Ziegler, P. A. 1990. Geological Atlas of Western and Central Europe. Shell Internationale Petroleum Maastschappij B.V.: The Hague, v. 2, Edition 2nd.

Zopfi, J., Ferdelman, T. G., Fossing, H,. 2004. Distribution and fate of sulfur intermediates—sulfite, tetrathionate, thiosulfate, and elemental sulfur in marine sediments. *In* Sulfur Biogeochemistry—Past and Present: Boulder Colorado (eds. J. P. Amend, K. J. Edwards and T. W. Lyons). Geological Society of America, pp. 97–116.

Appendix

A.1 Data precision

Data Precision (Warham) All sites				
	Chloride	Nitrate	Sulfate	Iron
Standard	19.01364975	0.514368417	10.12563599	0.0894337
Standard	19.03196003	0.451900614	9.855853543	0.0878767
Standard	17.77484342	0.480948064	9.943757173	0.0880918
Standard	18.05093459	0.473423441	9.885660962	0.0888042
Standard	17.75984334	0.508015548	9.969326611	0.0888317
Standard	17.71302305	0.522473866	9.679663166	0.0889335
Standard	16.95739426	0.520754968	9.564867842	0.0889519
Standard	17.90572764	0.564102713	9.920328927	0.0889233
Standard	18.37125679	0.556381902	9.971003138	-
Standard	19.10816142	0.580917592	10.08877768	-
Standard	18.90725507	0.558369032	10.48012746	-
Standard	19.0119	0.5131	10.1235	-
Average	18.30049578	0.520396346	9.967375208	0.0887309
Standard Deviation	0.707813296	0.039325611	0.232333556	0.000503507
Precision (%RSD)	**3.9**	**7.6**	**2.3**	**0.6**

Data Precision: Thorne Moors (Fe DGT) site 1 and 2		
	Site 1	**Site 2**
Standard	0.2100	0.0396
Standard	0.2000	0.0376
Standard	0.2000	0.0378
Standard	0.2100	0.0380
Standard	0.2000	0.0379
Standard	0.2000	0.0375
Standard	0.2000	0.0377
Standard	-	0.0379
Standard	-	0.0377
Standard	-	0.0374
Standard	-	0.0385
Standard	-	0.0389
Standard	-	0.0397
Average	0.2029	0.0382
Standard Deviation	0.0045	0.0007
Precision (%RSD)	**2.2270**	**1.9229**

Data Precision: Thorne Moors (Fe DET) site 1 and 2		
	Site 1	**Site 2**
Standard	0.210675429	0.204810547
Standard	0.210213497	0.204399482
Standard	0.210627329	0.205472693
Standard	0.210620343	0.208256042
Standard	0.210446462	0.208083759
Standard	0.210565343	0.208220869
Standard	0.210641595	0.204670694
Standard	0.210424537	0.206135105
Standard	0.210180042	-
Standard	0.210464515	-
Standard	0.210501084	-
Standard	0.211131216	-
Standard	0.211333251	-
Standard	0.211861756	-
Standard	0.211500316	-
Standard	0.212151784	-
Standard	0.211991663	-
Standard	0.210755342	-
Standard	0.212131038	-
Standard	0.212264731	-
Average	0.2110241	0.001685186
Standard Deviation	0.0007082	0.81703537
Precision (%RSD)	**0.3355800**	**0.81703537**

Thorne Moors Site 2 (2011)			
	Chloride	**Nitrate**	**Sulfate**
Standard	107.07	20.4103	44.13438098
Standard	106.54	20.4249	43.58627591
Standard	106.80	20.3558	43.94448777
Standard	106.17	20.2897	42.51119772
Standard	106.32	20.2698	43.39267904
Standard	106.39	20.2876	42.81414517
Standard	106.07	20.3378	43.10599261
Standard	105.85	20.2237	43.10922273
Average	106.40	20.32496425	43.32479774
Standard Deviation	0.40	0.07001146	0.55155349
Precision (%RSD)	**0.37**	**0.34446044**	**1.27306651**

Thorne Moors Site 3 (2011)			
	Chloride	**Nitrate**	**Sulfate**
Standard	52.252162	17.43366773	20.92751458
Standard	51.782035	17.33909715	21.59624142
Standard	50.947457	16.98260901	21.85915827
Standard	50.713871	16.86644891	21.87852193
Standard	51.199019	17.05740929	22.01005306
Standard	51.131498	16.94188252	22.92620339
Standard	51.006491	16.89995085	22.51102008
Average	51.29036182	17.07443792	21.95838753
Standard Deviation	0.537105349	0.22326710	0.63963706
Precision (%RSD)	**1.047185729**	**1.30761024**	**2.91295095**

Thorne Moors Site 4 (2011)			
	Chloride	**Nitrate**	**Sulfate**
Standard	99.05870215	33.23	41.03966448
Standard	98.5889229	33.32	40.88215615
Standard	98.57075197	33.32	41.11611242
Standard	98.01519434	33.02	40.65320376
Standard	97.93107232	33.02	40.64226036
Standard	97.89923343	32.86	40.54391416
Standard	98.57908773	33.11	40.59097425
Standard	98.72102041	33.14	40.8774178
Standard	98.95722791	33.16	40.93942747
Standard	99.2717	33.37	41.06154547
Average	98.48	33.13	40.81
Standard Deviation	0.43	0.15	0.21
Precision (%RSD)	**0.44**	**0.45**	**0.51**

Thorne Moors Site 5 (2011)			
	Chloride	**Nitrate**	**Sulfate**
Standard	53.144897	17.66670612	22.14006307
Standard	52.65353228	17.85675165	22.39426329
Standard	55.46929335	18.79110321	23.03676781
Standard	53.04906583	17.96312406	22.73939147
Standard	52.54744229	17.77924414	22.39344848
Standard	52.48008911	17.71893411	22.61787242
Standard	52.93487683	17.82106357	23.33167844
Average	53.18274239	17.94241812	22.66478357
Standard Deviation	1.039747205	0.38629625	0.41089812
Precision (%RSD)	**1.95504624**	**2.15297763**	**1.81293643**

Thorne Moors Site 1 (2010)			
	Chloride	**Nitrate**	**Sulfate**
Standard	38.1298	10.2124	9.1557
Standard	42.7617	9.986	9.4264
Standard	44.1943	11.1795	10.6767
Standard	44.9424	10.6946	10.5421
Standard	45.5788	11.7602	11.2108
Standard	46.91	11.2364	11.4218
Average	43.75283333	10.84485	10.40558
Standard Deviation	3.082617928	0.672808893	0.926738
Precision (%RSD)	**7.045527554**	**6.203948357**	**8.906164**

Thorne Moors Site 2 (2010)			
	Chloride	**Nitrate**	**Sulfate**
Standard	38.7682	8.6491	9.1362
Standard	39.5877	8.7204	9.2101
Standard	40.5434	9.3203	9.69
Standard	40.5149	9.4042	9.768
Standard	40.4704	9.3831	9.9099
Standard	40.2666	9.4244	9.8883
Standard	40.8931	8.8026	8.7634
Standard	42.3817	9.3713	9.5232
Average	40.42825	9.134425	9.4861375
Standard Deviation	1.038062606	0.343600157	0.411389943
Precision (%RSD)	**2.567666437**	**3.761595907**	**4.336748686**

A.2 Detection limits

Detection Limit for nitrate (Warham)	
	nitrate
Blank	0.0137
Blank	0.0403
Blank	0.0229
Blank	0.0219
Blank	0.0125
Blank	0.0346
Blank	0.0172
Blank	0.0203
Blank	0.0085
Blank	0.0239
Blank	0.0109
Average	0.020609091
Standard Deviation	0.009835289
Standard Deviation *3	**0.029505867**

Detection Limit for Thorne Moors (Site 2: 2011)		
	nitrate	**sulfate**
Blank	0.0048	0.25886
Blank	0.0091	0.154241
Blank	0.0053	0.159879
Blank	0.0102	0.217084
Blank	0.0105	0.193618
Blank	0.0097	0.218936
Blank	0.0097	0.203913
Blank	0.0052	0.172078
Blank	0.0065	0.200818
Blank	0.0072	0.195745
Blank	0.0065	0.196361
Blank	0.0073	0.181707
Blank	0.0205	0.268138
Blank	0.0198	0.248659
Blank	0.0108	0.224503
Blank	0.0081	0.18656
Average	0.0094	0.205069
Standard Deviation	0.004619574	0.033067
Standard Deviation *3	**0.013858721**	**0.099201**

Detection Limit for Thorne Moors (Site 3: 2011)		
	nitrate	**sulfate**
Blank	0.195	0.19339
Blank	0.189	0.16485
Blank	0.232	0.16082
Blank	0.206	0.17719
Blank	0.224	0.19651
Blank	0.136	0.18672
Blank	0.137	0.17137
Blank	0.140	0.18879
Blank	0.138	0.18546
Blank	0.219	0.27602
Blank	0.234	0.28977
Blank	0.136	0.19967
Blank	0.142	0.19681
Average	0.179	0.19903
Standard Deviation	0.041	0.03928
Standard Deviation *3	**0.124**	**0.11784**

Detection Limit for Thorne Moors (Site 4: 2011)		
	nitrate	**sulfate**
Blank	0.1770	0.171782
Blank	0.1438	0.227915
Blank	0.1606	0.215654
Blank	0.1494	0.206852
Blank	0.1562	0.189961
Blank	0.1591	0.196388
Blank	0.1462	0.185197
Blank	0.1585	0.173241
Blank	0.1480	0.191601
Blank	0.1979	0.175001
Blank	0.1474	0.241625
Blank	0.1487	0.200507
Blank	0.1384	0.181629
Blank	0.1460	0.152786
Blank	-	0.026795
Average	0.1555	0.18246
Standard Deviation	0.0155	0.04877
Standard Deviation *3	**0.0465**	**0.14631**

Detection Limit for Thorne Moors (Site 5: 2011)		
	nitrate	**sulfate**
Blank	0.36222	0.376947
Blank	0.34148	0.374442
Blank	0.38191	0.365835
Blank	0.38166	0.316322
Blank	0.36042	0.355601
Blank	0.35632	0.374202
Blank	0.19641	0.288179
Blank	0.18003	0.22995
Blank	0.16783	0.246242
Blank	0.16314	0.22938
Blank	0.32452	0.394043
Blank	0.31172	0.341715
Blank	0.16633	0.247693
Blank	0.16460	0.210857
Average	0.27561	0.310815
Standard Deviation	0.09435	0.06634
Standard Deviation *3	**0.28306**	**0.199021**

Detection Limit for Thorne Moors (Site 1: 2010)		
	nitrate	**sulfate**
Blank	0.4424	0.2369
Blank	0.4154	0.2692
Blank	0.4154	0.2328
Average	0.4244	0.2463
Standard Deviation	0.015588457	0.019938
Standard Deviation *3	**0.046765372**	**0.059813**

Detection Limit Thorne Moors (Site 2: 2010)		
	nitrate	**sulfate**
Blank	0.6938	1.0411
Blank	0.7071	1.04
Blank	0.6939	1.0436
Blank	0.6939	1.184
Blank	0.6978	1.1027
Blank	0.7007	1.0978
Blank	0.6931	1.0907
Average	0.697185714	1.0857
Standard Deviation	0.005176366	0.051597
Standard Deviation *3	**0.015529097**	**0.15479**

A.3 Shales-with-Beef data

Sample ID	Stratigraphic Height	Fe HCl-ex	DOP HCl	Fe Dithionite	DOP Dithionite
	m	Wt %		Wt %	
BV8	1.90	1.28	0.62	0.60	0.78
BVa	1.80	1.32	0.62	0.62	0.77
BVb	1.60	1.08	0.64	0.54	0.78
BVc	1.55	1.14	0.63	0.58	0.77
BV9	1.50	1.11	0.63	0.49	0.80
BVd	1.40	1.09	0.64	0.52	0.79
BVe	1.20	1.44	0.56	0.46	0.80
BV10	1.15	1.56	0.53	0.58	0.75
BVf	1.00	1.53	0.54	0.44	0.80
BVg	0.80	1.61	0.54	0.46	0.80
BV11	0.75	1.46	0.51	0.45	0.77
BV12	0.25	0.95	0.67	0.34	0.85

Sample ID	Stratigraphic Height	$\delta^{13}C$ Bit-C	$\delta^{34}S$ Bit-S	$\delta^{34}S$ pyrite	$\delta^{34}S$ elemental S	$\delta^{34}S$ kerogen-S
	m	per mille	per mille	per mille	per mille	per mille
BV8	1.90	-28.70	n.a.	-24.70	-5.60	1.30
BVa	1.80	n.a.	n.a.	-25.40	-5.30	-6.40
BVb	1.60	n.a.	n.a.	-23.80	-13.40	-4.80
BVc	1.55	n.a.	n.a.	-24.80	-5.00	-0.90
BV9	1.50	-28.40	n.a.	-22.30	-14.20	-2.90
BVd	1.40	n.a.	4.10	-23.00	-15.10	-3.10
BVe	1.20	n.a.	n.a.	-25.70	n.a.	0.10
BV10	1.15	-28.70	6.40	-23.40	n.a.	1.70
BVf	1.00	n.a.	4.90	-23.90	n.a.	-1.10
BVg	0.80	n.a.	3.20	-26.40	n.a.	1.70
BV11	0.75	-28.80	2.80	-27.30	n.a.	-0.50
BV12	0.25	-28.80	n.a.	-26.90	n.a.	-8.30

Sample ID	Stratigraphic Height	Pyrite	Elemental S	TOC	Bitumen S	Kerogen
	m	Wt %	Wt %	Wt %	Wt %	Atom C/S
BV8	1.90	4.47	0.04	9.17	<0.1	38.70
BVa	1.80	4.55	0.04	8.11	<0.1	33.10
BVb	1.60	4.04	0.05	6.52	<0.1	35.30
BVc	1.55	4.14	0.04	6.28	<0.1	36.20
BV9	1.50	4.13	0.05	6.32	<0.1	34.60
BVd	1.40	4.11	0.06	6.92	1.10	38.90
BVe	1.20	3.92	<0.005	6.46	1.30	44.70
BV10	1.15	3.81	<0.005	6.60	2.50	43.30
BVf	1.00	3.88	<0.005	5.98	1.90	41.90
BVg	0.80	4.03	<0.005	6.09	1.40	42.70
BV11	0.75	3.26	<0.005	6.88	0.90	41.20
BV12	0.25	4.09	<0.005	5.69	<0.1	32.40

Sample ID	Stratigraphic Height	Bitumen	Bitumen-C	Bitumen -H
	m	Wt %	Wt %	Wt %
BV8	1.90	0.07	69.70	12.3000
BVa	1.80	0.08	73.10	11.7000
BVb	1.60	0.07	74.90	11.4000
BVc	1.55	0.06	76.20	12.3000
BV9	1.50	0.09	75.20	8.2000
BVd	1.40	0.06	74.10	10.1000
BVe	1.20	0.04	75.40	11.9000
BV10	1.15	0.06	74.70	10.7000
BVf	1.00	0.06	73.80	12.7000
BVg	0.80	0.07	74.90	12.1000
BV11	0.75	0.08	74.90	12.3000
BV12	0.25	0.05	77.60	12.9000